Developing a Probabilistic Stock Turnover System Dynamics Model to Forecast Whole-life Energy of Chinese Urban Residential Building Stock

Wei Zhou

Wolfson College

Department of Engineering
University of Cambridge

This thesis is submitted for the degree of
Doctor of Philosophy

July 2021

Declaration

This thesis is the result of my own work and includes nothing which is the outcome of work done in collaboration except as declared in the Preface and specified in the text. It is not substantially the same as any that I have submitted, or, is being concurrently submitted for a degree or diploma or other qualification at the University of Cambridge or any other University or similar institution except as declared in the Preface and specified in the text. I further state that no substantial part of my thesis has already been submitted, or, is being concurrently submitted for any such degree, diploma or other qualification at the University of Cambridge or any other University or similar institution except as declared in the Preface and specified in the text. It does not exceed the prescribed word limit for the relevant Degree Committee.

Abstract

Developing a Probabilistic Stock Turnover System Dynamics Model to Forecast Whole-life Energy of Chinese Urban Residential Building Stock

Wei Zhou
Department of Engineering, University of Cambridge

China is a major driving force of the growth of the global building stock – in 2018 alone, 2.5 billion m^2 in new buildings were constructed, amounting to 34% of the global total. In the same year, the final operational energy consumption of Chinese buildings was 504 million tonnes of oil equivalent (toe). More than one third of this energy was consumed by urban residential buildings. With a growing urban population and mounting demand for energy services in the built environment, urban residential buildings play an increasingly important strategic role in China's efforts to decarbonise its building sector. Nevertheless, there is a basic lack of authoritative data on Chinese urban residential stock. Official statistics on total floor area of the stock only exist up to 2006. The historical stock growth trajectory from 2007 onwards is therefore unknown. This creates a major barrier to understanding and analysing future trends in stock evolution or energy use.

Meanwhile the embodied energy associated with the massive flow of materials consumed by the ongoing construction boom across China remains under-explored. Urban buildings in China are generally short-lived, implying a lower risk of operational energy lock-in as the stock is rapidly replenished with more efficient buildings; however, this comes at a cost of high embodied energy incurred by construction. Very limited studies have been conducted on the trade-offs between embodied and operational energy, resulting in little in the way of an evidence base to inform policymaking.

This thesis fills these key research gaps, by modelling both stock turnover dynamics and the whole-life (operational and embodied) energy of Chinese urban residential buildings over the medium to long term. Whilst the thesis excludes carbon from its scope, its outputs prepare the ground for quantifying energy-related carbon emissions of the stock.

A stock turnover model is developed using a System Dynamics methodology. The model captures the dynamic interplay between new construction, aging of existing buildings in operation, and demolition of old buildings. With survival analysis applied to building lifecycle, annual demolition of buildings is modelled as a stochastic process based on the hazard function of a Weibull

distribution. Using official statistics on annual new construction over the historical period of 1978 to 2006, the parameters of the Weibull distribution are calibrated by fitting the stock turnover model to historical data on total floor area up to 2006. Based on the calibrated lifetime distribution and annual new construction data from 2007 onwards, the stock turnover model is run to estimate the total stock size of urban residential buildings and the dynamically changing age profile of buildings in the stock for each year up to the present day. One key result finds that the average building lifetime is 34.1 years, much shorter than the design lifetime of 50 years.

The stock turnover model is then extended to forecast future stock trajectories through Bayesian Model Averaging (BMA). In addition to the Weibull distribution, another four potential distributions for the survival model are considered, including Lognormal, Loglogistic, Gamma and Gumbel distributions. For each, the probabilistic stock turnover model is simulated using Markov Chain Monte Carlo (MCMC) methods. BMA is then applied to combine model-specific predictions of the historical stock evolution based on the respective probabilities of the five survival models. Finally, by extending model structure and incorporating variables relating to urbanisation and housing demand, future stock turnover dynamics and possible trajectories over the medium to long term are forecast. These results suggest that the floor area of urban residential stock in China is likely to peak around 2065, at between 42.4 and 50.1 billion m^2.

The probabilistic stock turnover model and its results, which are core to the modelling and analysis of this thesis, lay the groundwork for estimating embodied energy, operational energy, and whole-life energy of the stock. The scope of embodied energy covers the different building lifecycle stages of material production, transportation, on-site construction, and demolition. Building materials are limited to steel, cement, aluminium and glass, the most commonly used for Chinese buildings. To assess operational energy, an improved SD model is developed which addresses some major methodological issues identified in previous SD-based models for operational energy. By adapting this generic model to the urban context in north China, where space heating requirements are most significant, and integrating it with the probabilistic stock turnover model, the operational energy is forecast. The results show that embodied and operational energy are likely to peak around 2027 and 2051, respectively.

Four realistic scenarios for the whole-life energy of urban residential stock in north China are then investigated. Under the business-as-usual (BAU) scenario, peak energy is expected to occur around 2050, with a mean value of 383.7 million tonnes of coal equivalent (tce). Extending building lifetime (Policy A) and accelerating heating energy efficiency improvement (Policy B) both reduce whole-life energy compared with the BAU scenario. Policy C integrates Policy A and Policy B and captures the endogenous dynamics of time-varying building lifetime distribution and

heating energy intensities. Compared with the BAU scenario, Policy C achieves a cumulative energy saving of 35.7 million tce on average during the period 2025-2030. While this is under 10% of the total, it exceeds the sum of operational energy of buildings in 24 out of the total 31 provinces of mainland China in 2015.

The detailed findings of model development and application provide extensive evidence, based on which a series of policy recommendations are made. Amongst them, the most fundamental is that the trade-offs across stock-level embodied and operational energy should be analysed, and a whole-life perspective taken, in designing future policies for buildings in order to move towards China's target of carbon neutrality by 2060.

This thesis makes several important contributions. The modelled lifetime of 34.1 years quantifies and substantiates the observation that Chinese buildings are generally short-lived. The model development and its application are characterised by first-of-its-kind approaches to forecast stock evolution in a Bayesian framework, which is the major contribution of this thesis. This is also a first effort at integrating stock-level embodied and operational energy in a single model, in order to draw conclusions about whole-life energy for China's urban residential building stock under a number of policy scenarios. The quantified whole-life energy, along with the characterisation of building stock turnover dynamics and the probabilistic forecasting of future stock evolution, will enable further analysis to develop insights into whole-life carbon emissions of the building stock, which is of strategic importance under China's announced climate targets. Methodologically, with high generality and flexibility, the model can now be adapted to a wide variety of geographical contexts.

List of Publications

Some of the material included in this thesis has been published in or submitted to the following academic journals.

Published journal papers

Zhou, W., Moncaster, A., Reiner, D. M. and Guthrie, P. (2019) 'Estimating lifetimes and stock turnover dynamics of urban residential buildings in China', *Sustainability* (Switzerland), 11(13). DOI: 10.3390/su11133720.

Zhou, W., O'Neill, E., Moncaster, A., Reiner, D. M. and Guthrie, P. (2020) 'Forecasting urban residential stock turnover dynamics using system dynamics and Bayesian model averaging', *Applied Energy*, 275. DOI: 10.1016/j.apenergy.2020.115388.

Zhou, W., Moncaster, A., Reiner, D.M. and Guthrie, P. (2020) 'Developing a generic System Dynamics model for building stock transformation towards energy efficiency and low-carbon development', *Energy and Buildings*, 224. DOI: 10.1016/j.enbuild.2020.110246.

Submitted journal paper (under review)

Zhou, W., Moncaster, A., O'Neill, E., Reiner, D.M., Wang, X. and Guthrie, P. (2021) 'Modelling future trends of annual embodied energy of urban residential building stock in China'. Submitted to *Energy Policy*.

Acknowledgement

First and foremost, I thank my wife and daughter, Chang and Zhuochen, for their love. Taking a career break to pursue a PhD overseas was a major decision that came at significant costs across many aspects. I am so blessed to be unconditionally understood and supported by my family. Without them joining me and always standing by my side, I would not have been able to navigate my way through this challenging journey and reach where I am now. I dedicate this thesis to them.

I express my sincere gratitude to my supervisor, Dr. Alice Moncaster, for taking me on as her student. The opportunity to pursue a PhD at Cambridge as a mid-career professional meant a lot to me. I am deeply grateful to her for sharing her ideas and knowledge as a true expert in buildings and construction, for offering enlightening guidance and invaluable advice, for always making herself available for fruitful discussions, and above all, for trusting and believing in me all the way with her unfailing support and encouragement. I have been extremely fortunate to enjoy the maximum possible degree of freedom to explore possibilities and manage my research and always receive timely and constructive feedback from her to make sure I was on the right track. Beyond my research, I also benefited hugely from her advice on and support to my professional development. It has been truly a great experience and privilege to have completed my PhD journey under her supervision.

I am very grateful to my co-supervisor, Dr. David Reiner, for all his insightful comments, constructive suggestions, and continuous encouragement. I have been immensely inspired by his knowledge and expertise in energy and climate change policies and technologies. I also sincerely thank him for his great support to my application for the extended academic visit to Massachusetts Institute of Technology in the US, which was a very rewarding experience not only benefitting my specific research work, but also broadening my horizons in general.

I feel privileged to have Prof. Peter Guthrie as my advisor. I deeply appreciate his numerous academic and professional advice and continuous encouragement throughout my PhD. I am also very grateful to him for being my professional sponsor to support my application for a registration with the Engineering Council as a chartered engineer.

I would like to sincerely thank Prof. Simon Guest, who is the Head of Division D, Department of Engineering, for his high-level comments and advice on my research. I also thank him for approving administrative matters and supporting my application for various funds for overseas

Table of Contents

List of Figures

List of Tables

List of Abbreviations

AIC	Akaike's Information Criterion
BAU	business-as-usual
BFG	blast furnace gas
BIC	Bayesian Information Criterion
BMA	Bayesian model averaging
CABEE	China Association of Building Energy Efficiency
CDF	cumulative distribution function
CDQ	coke dry quenching
CEN	European Committee for Standardization
CO_2	carbon dioxide
COG	coke oven gas
EE	embodied efficiency
EI	energy intensity
GHG	greenhouse gas
GABC	Global Alliance for Buildings and Construction
HM	Harmonic Mean
IEA	International Energy Agency
IPCC	Intergovernmental Panel on Climate Change
IPEEC	International Partnership for Energy Efficiency Cooperation
IS	Importance Sampling
LCA	Life Cycle Assessment
MCMC	Markov chain Monte Carlo
MIIT	Ministry of Industry and Information Technology
MOHURD	Ministry of Housing and Urban-Rural Development of China
NDC	Nationally Determined Contribution
NDRC	National Development and Reform Commission
OE	operational energy
OECD	Organisation for Economic Co-operation and Development
PCFA	per capita floor area
PDF	probability density function
PMP	posterior model probability
RISN	Research Institute of Standards and Norms
SAMR	State Administration for Market Regulation
SD	System Dynamics

THUBERC	Tsinghua University Building Energy Research Centre
UNDP	United Nations Development Programme
UNEP	United Nations Environment Programme
UNFCCC	United Nations Framework Convention on Climate Change

Units and Measurements

EJ	-	exajoule
GJ	-	gigajoule
kgce	-	kilogram of coal equivalent
kWh	-	kilowatt-hour
tce	-	tonne of coal equivalent
tCO_2	-	tonne of carbon-dioxide
toe	-	tonne of oil equivalent

1

Introduction

1.1 Background

The buildings sector is a major source of global emissions and, as such, has been identified as a primary target for the clean energy transition and emissions mitigation efforts (IPCC 2014; Rogelj et al. 2018). In 2019, the operation of buildings was responsible for 30% of global final energy use and 28% of direct and indirect energy-related carbon emissions (Global Alliance for Buildings and Construction and UNEP 2020). Adding the energy and emissions associated with the manufacturing of building materials and construction activities into the accounting increases these shares to 35% for energy and 38% for emissions, making buildings the largest energy-consuming and carbon-emitting sector (Global Alliance for Buildings and Construction and UNEP 2020).

China is a major driving force of the growth of global building stock, having the largest buildings market in the world (Yu et al. 2015; Global Buildings Performance Network 2019). Over the past ten years, the floor area of new buildings constructed in China each year has remained consistently above 2 billion m^2 (National Bureau of Statistics 2019). In 2018, new buildings amounting to 2.5 billion m^2 were constructed in China, accounting for 33.8% of the global total for new construction of 7.4 billion m^2 (IEA 2020b). In the same year the total floor area of Chinese buildings, including residential, commercial and public buildings, reached 60 billion m^2 (THUBERC 2020). However, authoritative data on China's building stock is limited, especially for urban residential buildings. Official statistics on total floor area of the urban residential stock only exist up to 2006. The historical stock growth trajectory from 2007 onwards is therefore unknown.

The massive construction activity in China has generated a commensurate flow of materials,

which has significantly influenced trends in building material demand. Globally, the use of steel and cement in buildings, two most commonly used building materials and also the two largest sources of building material-related CO_2 emissions (World Green Building Council 2019), increased by 4% per year from 2000 to 2015, and China's share increased from 30% to nearly 40% during this period (IEA and UNEP 2018). The use of steel, cement and other materials to meet the demand from new construction led to a significant amount of embodied energy and carbon.

The continued strong growth in new construction is closely related to the observation that Chinese buildings are generally short-lived. According to the former Vice-Minister of the Ministry of Housing and Urban-Rural Development (MOHURD), the average lifetime of buildings in urban areas of China was only 25–30 years, considerably shorter than the intended lifetime of 50 years at design stage (China Daily 2010). There are various reasons underlying the short lifetime of buildings, including design standards, quality of building materials, construction techniques and practices, maintenance and renovation, and urban renewal and expansion (Yang & Kohler 2008; Fawley & Wen 2013; Huang 2006; Hu, Bergsdal, et al. 2010; Cai et al. 2015). The short lifetime of buildings implies a fast turnover rate of the building stock in which the building stock is being constantly replenished as a result of old buildings with short lifetimes being removed and new buildings being constructed to meet demands. The complexity and uncertainty of these building-stock dynamics have significant implications for stock-level lifecycle energy and carbon performance over the medium to long term.

This level of construction also means that the relative proportions of embodied energy and carbon for the building stock of China are far higher than the global averages. In 2015, embodied energy and carbon resulting from new buildings in China accounted for 12% and 16% of China's economy-wide total energy consumption and carbon emissions respectively (THUBERC 2018). These levels are comparable to the operational energy and emissions of the total existing building stock in China in the same year. The magnitude of embodied energy and carbon, in both absolute and relative terms, demonstrates that without including these, both the immediate energy and carbon impacts of buildings, and the savings that could be achieved, will be missed (Pomponi & Moncaster 2018).

There are two seemingly conflicting arguments here. Design regulations, construction techniques and materials, building equipment, services and technologies, are all advancing, and this can lead to an argument for shorter lifetime in order for stock-level operational energy/carbon intensity to take advantage of innovations and improvements as they occur. A more rapid turn-over rate would therefore imply the stock is less prone to the risk of operational energy and carbon "lock-

in" (Hermann et al. 2013; IEA 2013b; Chalmers 2014; Thomas 2015; IPCC 2014) compared to building stocks in other countries with longer lifetimes and thus slower turnover rates. However, to avoid the evident current excessive embodied energy and carbon, a slow turnover rate would be preferred, whereby buildings should be retained for as long as possible to reduce the annualised energy impacts of construction over the lifetime of the building. These two arguments suggest there must be a strategic trade-off of embodied-versus-operational energy and carbon. For Chinese buildings, characterised by short lifetimes and fast stock turnover, a whole-life approach addressing both embodied and operational energy and carbon in an integrated manner is particularly relevant and necessary, with the view of achieving the envisioned sector-wide transformation towards low energy and decarbonisation.

Nevertheless, government strategies, plans and pilot initiatives relating to building energy and carbon have focused almost entirely on the operational phase of buildings (Hong, Shen & Tang 2018). In China's energy statistics, embodied energy of construction materials is accounted for under the various industrial subsectors, such as cement, steel, aluminium, etc., without explicit links to the building sector. Whilst this is a largely standard accounting approach which is not China-specific, it leads to embodied energy being less visible and more likely to be overlooked compared with operational energy. Sector-specific design codes for energy-efficient buildings and evaluation standards for green buildings deal almost exclusively with operational energy and carbon, leaving embodied energy and carbon largely ignored (Zhu et al. 2020).

The Chinese government has announced its overarching climate targets of peaking economy-wide emissions by 2030 (NDRC 2015) and achieving carbon neutrality by 2060 (Mallapaty 2020; Yu et al. 2020). Clearly, the magnitude of energy and environmental impacts makes buildings a key challenging sector to address. To achieve any reductions, a better understanding of current and future building lifetime and stock turnover is also essential. There is a pressing need for an updated sector-specific policy and regulatory framework targeting both embodied and operational energy and carbon, and consisting of aggressive targets, sustained and effective policy instruments and assertive actions, tailored to the broader energy and climate policy settings in China.

1.2   Research objective and method

This thesis sets out to develop a building stock turnover and whole-life energy model for application to the urban residential building stock in China.[1] It aims to contribute to filling the

---

[1] The scope of this research is limited to building stock and energy. As for carbon emissions, apart from

research gaps relating to this area and providing evidence to inform policymaking.

Methodologically, this thesis is based on extensive modelling. At the heart of model development is the choice of a modelling approach best serving the purpose of the research. To model future trajectories of a building stock, the key challenge is to represent the mechanism governing the stock's evolution and expansion. Such a mechanism is driven by a dynamic interplay between new buildings, which meet incremental demand growth as a result of economic and social development, existing buildings which remain in use but undergo an ageing process, and old buildings, which reach the end of their lifetime and physically demolished or functionally disused. This characterisation is particularly relevant to the Chinese urban context where buildings are generally short-lived, and the annual construction and demolition are massive.

The stock turnover dynamics have significant implications for energy consumption of the building stock. The inflow of new buildings built to higher energy standards, the outflow of old and inefficient buildings, and the retrofit of existing buildings in the stock collectively contribute to improving the stock-wide average operational energy efficiency. Meanwhile, construction, demolition and retrofit all come at a cost of embodied energy, which is of a significant magnitude and drives up the total energy consumption of the stock from a whole-life perspective. Changes in the underlying turnover dynamics would affect the energy performance of the building stock. For example, with an extended average lifetime of buildings and the resultant slowed stock turnover, embodied energy incurred by construction and demolition tend to decrease whereas operational energy is likely to have an increased risk of lock-in. Clearly, stock turnover, annual embodied energy, and annual operational energy are closely interlinked and together form a dynamic system. Methodologically, it is important for them to be modelled in an integrated manner. That is, embodied energy and operational energy hinge on the same building stock and its underlying turnover and evolution dynamics over time. This ensures the consistency and comparability of the modelled embodied and operational energy, as well as the rationality and interpretability of the derived whole-life energy at stock level.

Based on the above consideration, this thesis uses System Dynamics (SD) to model the building

---

some process-related emissions such as those caused by the chemical process in the production of cement, almost all embodied and operational carbon emissions of buildings are energy-related. Therefore, although the modelling and analysis of this research does not directly include carbon, the quantification of embodied and operational energy prepares a solid ground for quantifying embodied and operational carbon of buildings. Moreover, the characterisation of the underlying building stock turnover dynamics and probabilistic forecasting of future trajectories of stock evolution enable further analysis to develop insights into the strategic trade-offs across stock-level embodied and operational carbon of building, which need to be adequately recognised and analysed when designing future strategies and policies for buildings under China's overarching climate targets.

stock turnover dynamics and associated embodied and operational energy. SD is a modelling approach to policy design and analysis. It features a capacity to model and investigate dynamic complexities arising from the structure, causal relationships, feedbacks, non-linearities, and time lags of the system in question (Sterman 2000; Richardson 2001; Shepherd & Emberger 2010). SD emphasises stock-and-flow dynamic relationships. Stocks are variables that accumulate a certain quantity. Flows, including inflows to and outflows from stocks, represent stock changes. Through the process of accumulating their inflows less outflows over time, stocks provide aggregate representations of the state of a dynamic system. In addition to stocks and flows, auxiliary variables and constant values are integral to a SD model. They serve to complete the representation of the causal links and feedback loops of model structures and components, and enable experimentation with policy interventions.

Applying this SD approach to buildings, a building stock keeps evolving as it accumulates incoming newly constructed buildings and outgoing demolished buildings. Energy, either embodied or operational, is an attribute of buildings and therefore can be modelled similarly, in parallel with stock turnover dynamics. Specifically, annual embodied energy takes as inputs the annual amounts of new construction and demolition. Annual operational energy is a stock variable, which is dominated by the energy performance and potential retrofit of existing buildings in the building stock, but also substantially influenced by the operational energy of incoming new buildings and outgoing demolished buildings in the year. Policy levers can be set through certain auxiliary variables and/or constant values to examine the effects of various policies to embodied, operational, and whole-life energy at the stock level.

Therefore, SD is well placed to serve the purpose of model development and application under this thesis. It is used to develop a model of stock turnover dynamics, embodied energy and operational energy, for application to the urban residential stock in China. In deriving future possible trajectories of stock and energy, the model is operationalised probabilistically, by quantifying the uncertainties associated with key input variables and propagating them to intermediate variables and high-level outputs. A series of statistical methods are applied, such as distribution fitting, Copula, Bayesian regression, Bayesian Model Averaging, Monte Carlo simulation, etc. Details are described in subsequent chapters.

1.3   Research questions

Under the overarching research objective, a series of specific and processive research questions emerge from the literature review and research gap identification in Chapter 2. They include:

Q1: How to model building stock turnover dynamics? What was the average lifetime of Chinese urban residential buildings, and how did the residential stock evolve over the recent historical period since 2007?

Q2: How can the building stock model be extended to forecast possible future trajectories of Chinese residential stock evolution over the medium to long term?

Q3: What are the possible future trajectories of annual embodied energy of urban residential stock in China over the medium to long term?

Q4: How can existing system dynamics models of building stock operational energy be improved, for better representation of stock turnover dynamics and energy retrofit of buildings and for integration with modelling of embodied energy?

Q5: What are the possible future trajectories of annual operational energy of urban residential stock in China over the medium to long term?

Q6: What are the possible future trajectories of whole-life (embodied + operational) energy of urban residential stock in China over the medium to long term? How would they vary under different policy scenarios?

1.4   Organisation of thesis

The overarching research objective, proposed research method, and specific research questions guide the research planning and design and structure the thesis. The chapters are organised in accordance with the logical and methodological links amongst them, to answer the framed research questions in sequence. The thesis has at its heart the development of the stock turnover model (Chapters 4 and 5), the forecasted future trajectories of stock turnover dynamics of Chinese urban residential buildings (Chapter 5), and the development of a generic SD model for operational energy (Chapter 7). Based on them and additional modelling work, the future trajectories of embodied energy (Chapter 6) and operational energy (Chapter 8) are estimated, preparing the ground for exploring whole-life energy trajectories under various policy scenarios (Chapter 9).

Chapter 2 conducts a critical review of the literature. It covers Chinese building stock, SD models for building stock operational energy, embodied energy of buildings, operational energy of buildings, and whole-life energy of buildings. The review identifies a series of separate but

inherently related aspects that have not been adequately addressed by past studies. These research gaps substantiate the need for further work, justify the relevance of this thesis, and explain the formulation of specific research questions and the research design.

Chapter 3 provides a general introduction to the methodological tools for model development, implementation and statistical analysis. System Dynamics (SD), which is used to develop the stock turnover and energy model, is described in terms of its theory and principles, general model structure and components, and major characteristics including endogenous perspective, feedback loops, non-linearity, structure-driven behaviours, and emphasis on general dynamic tendencies. As R and RStudio are extensively used for statistical analysis, this chapter also briefly describes the key R packages used for developing and implementing SD models in R environment, model fitting, Bayesian Model Averaging, Copula, etc.

Chapter 4 answers research question Q1. It develops a SD model to track the continuous process of stock turnover and evolution, which is driven by the dynamic interplay between new construction, aging of existing buildings, and demolition of old buildings. Applying the concept of survival analysis, the model uses a Weibull distribution to represent building lifetime uncertainties. Annual demolition is therefore estimated using the hazard function derived from the Weibull distribution. Using official statistics on stock size up to 2006, which was the last year this data was available, and official statistics on annual new construction from 1978 to 2006, the shape and scale parameters of the Weibull distribution are calibrated. This specified Weibull distribution represents building lifetime distribution. Its mean value is the average building lifetime. With the calibrated Weibull distribution and the official statistics on annual new construction from 2007 onwards, the stock turnover model is run to obtain the trajectory of Chinese urban residential stock over the recent historical period.

Chapter 5 forecasts possible future trajectories of the stock evolution, thereby answering Q2. This is approached using Bayesian Model Averaging (BMA), which essentially takes into account uncertainties at two levels. The first level refers to the uncertainties associated with the parameters of a chosen survival model, e.g. the shape and scale parameters of the Weibull distribution in Chapter 4. The second level refers to the uncertainties associated with the survival model itself. That is, along with the Weibull distribution, there may be other distributions which can serve as the survival model to provide similarly adequate description of the stock turnover dynamics generating the observed empirical data and subsequently making sensible forecasts. The BMA is operationalised through the following steps. (1) The stock turnover model in Chapter 4 is turned into a probabilistic one in a Bayesian framework. (2) The probabilistic stock turnover model is simulated through Markov Chain Monte Carlo method to obtain the posterior predictive

distribution of total historical stock. This process also obtains the marginal likelihood, which quantifies the posterior model probability of the Weibull distribution. (3) For each of the other four distributions (Lognormal, Loglogistic, Gamma and Gumbel) included as candidate survival models, the first and second steps are repeated. (4) BMA is applied to create a model ensemble to combine model-specific predictions of the historical stock evolution pathway based on the respective model probabilities of the five survival models. (5) By extending the model structure and incorporating variables relating to possible trends in urbanisation and housing demand, future stock turnover dynamics over the medium to long term are forecasted using each survival model and then combined based on model probabilities. The probabilistic stock turnover model and its results in this chapter are core to the modelling and analysis throughout the thesis.

Chapter 6 answers Q3 about embodied energy. The probabilistic forecasts of the annual new construction and annual demolition over the medium to long term, obtained in Chapter 5, provide key inputs to this chapter. The building lifecycle stages covered by this chapter include building material production, transportation, on-site construction, and demolition. The building materials are steel, cement, aluminium and glass, which are the most commonly used materials and account for the dominant share of total energy consumed by building materials production in Chinese context. Empirical data of material intensities are fitted to probability distributions. Moreover, as the material intensities are not independently distributed, their dependence structure is captured through Copula, to establish the joint distribution for generating random samples of material intensities. The energy intensities of producing different building materials are modelled using Bayesian non-linear regression. A similar approach is applied to construction and demolition energy intensity. For materials transportation, default values are taken from a standard due to limited empirical data. Based on these input variables, the annual embodied energy of Chinese urban residential buildings is modelled for the medium to long term. Its probability distribution is obtained through propagating the input variables using Monte Carlo simulations. In addition to the business-as-usual scenario, the impacts of lifetime extension and lifetime shortening are also examined.

Chapter 7 answers Q4 by developing an enhanced building stock operational energy model, which addresses structural and behavioural limitations found in previous SD-based models. The model loosens the strong assumptions made by previous models, including perfect mixing in a first-order delay in a single stock model, and perfect mixing in each delay of a third-order delay in three-vintage models. Stock disaggregation into age-specific sub-stocks enables explicit representations of the uncertainties associated with age-specific risks of demolition. As a major improvement, the model avoids the unreasonable situations where a building is allowed to undergo multiple rounds of retrofits within a very short period of time, or a building is demolished

soon after being retrofitted. The model is characterised by high structural and functional flexibility for either extensions or reductions depending upon needs, and high generality and adaptability in diverse applications. It can be used as a stand-alone model or as part of a larger model for policy evaluation and scenario analysis exploring building stock transformation. In this thesis, this generic model is adapted to the specific context of Chinese urban residential stock for modelling stock-level operational energy.

Chapter 8 is dedicated to modelling the stock-level operational energy as needed to respond to Q5. The geographical scope is north China, where space heating during winter has significant energy and environmental impacts. The generic model in Chapter 7 is extended to cover dynamic building stock evolution. The modelling takes as inputs the outputs of the probabilistic stock turnover model from Chapter 5. The operational energy consists of heating and non-heating energy, which are modelled separately. On heating energy, an average heating energy intensity is applied to the existing stock in the initial year of modelling. For new buildings, reference performance indicators of heating energy intensity established by a government standard are used to model the trend of decreasing intensity level. Randomness is added to take account of the uncertainties across various provinces. Retrofits for heating energy efficiency improvement is modelled based on what is considered realistic in the Chinese urban context. On non-heating energy, the energy intensity in the initial year is set to increase towards saturation in 2040, with randomness added. Through Monte Carlo simulations, the input uncertainties are propagated through the emergent behaviour of the model to obtain the probability distribution of its outputs, including stock-level operational energy and stock-wide average operational energy intensity.

The whole-life energy results and scenario analysis carried out in response to Q6 are presented in Chapter 9. The modelling results on embodied energy (Chapter 6) and operational energy (Chapter 8) are integrated to produce an estimate of whole-life energy. Since the operational energy analysis focuses on north China, the embodied energy result obtained in Chapter 6 is scaled down accordingly. Thus, Chapter 9 describes whole-life energy in north China. For the purpose of comparing embodied energy and operational energy, focusing on north China is a more 'conservative' approach as it may downplay the magnitude of embodied energy relative to operational energy. This way, the results will provide a stronger argument about the importance of embodied energy and the necessity of a whole-life cycle perspective for building energy. Other than the business-as-usual scenario results, this chapter also attempts to explore various policy scenarios, including extension of building lifetime, acceleration of heating energy efficiency improvement of new buildings, and the combination. Experimentation with these policy scenarios requires the models in preceding chapters to be rerun under different settings.

Chapter 10 concludes by summarising the key findings and describing the contributions to domain knowledge as well as methodological development. A series of policy implications are discussed, with a view to informing policies for transforming the Chinese building stock towards greater energy efficiency and low carbon development. The final chapter ends by acknowledging the study's limitations and offers an outlook on future research that could take forward the work described in this thesis.

The thesis structure is presented diagrammatically in Figure 1.1.

Chapter 2 Literature review

Chapter 3 Modelling and analysis tools

Chapter 4

Building lifetime and historical stock turnover dynamics

- Stock turnover model
- Calibration of Weibull distribution parameters
- Estimate of building lifetime
- Stock evolution over recent historical period

Chapter 7

Generic SD model for operational energy

- Addresses methodological limitations of previous models
- Structural and functional flexibility for extensions or reductions
- Generality and adaptability in diverse applications

Chapter 5

Forecasting future trajectories stock evolution

- Probabilistic stock turnover model
- Five candidate survival models
- Posterior predictive distribution of historical stock
- Future trajectories of stock turnover dynamics
- Bayesian model averaging

Chapter 6

Embodied energy trajectories

- Uncertainties of building material intensities
- Interdependence and joint distribution
- Energy intensities of material production, transportation, construction, and demolition
- Uncertainty propagation to annual embodied energy

Chapter 8

Operational energy trajectories

- Heating energy intensity trend and uncertainty
- Energy efficiency retrofit dynamics
- Non-heating energy intensity trend and uncertainty
- Uncertainty propagation to annual operational energy

Chapter 9

Whole-life energy trajectories

- Embodied energy versus operational energy
- Whole-life energy under BAU and policy scenarios

Chapter 10 Conclusions

Figure 1.1: Structure of thesis

2

Literature review

2.1 Chapter introduction

The overarching research objective of this thesis is to develop a building stock turnover and whole-life energy system dynamics model for application to the urban residential building stock in China. This objective guides the scope and direction of the literature review in this chapter, which covers models of the Chinese building stock, System Dynamics models for building stock operational energy, embodied energy of buildings, operational energy of buildings, and whole-life energy of buildings. The review identifies a series of research gaps and explains how the research questions presented in Chapter 1 have been derived.

2.2 Modelling Chinese building stock

To model future trends of building stock turnover dynamics, it is essential to have a holistic and in-depth understanding of the current status of the existing building stock. This is challenging in the Chinese context not only because of the magnitude of the stock but also because of the lack of authoritative official statistics (THUBERC 2015; RISN 2016; CABEE 2018; Huo et al. 2019). The latest publicly accessible statistics on urban residential building stock were published in the China Statistical Yearbook in 2007 (National Bureau of Statistics 2007). Therefore, forecasting

possible trajectories of building stock expansion and the associated energy and emissions for the future will first and foremost require estimating how the building stock has evolved since 2007. Key to this task is to capture and understand the dynamics underlying the building stock.

2.2.1 Models of building stock

Despite the fundamental importance of building stock, studies investigating the complexities and dynamics of building lifetime and building stock turnover appear to be rather limited.

One of the first simplified models of the Chinese building and infrastructure stock was developed by Yang and Kohler (2008), who set 2005 as the base year. The existing stock in 2005 was set as the initial stock, which included buildings built between 1978 and 2005, and was assumed to be composed of several age cohorts. For buildings built from 2005 onwards, a cohort-based approach was applied to define average age of buildings to model the stock evolution during the period of 2005 to 2050 on a five-year basis. Whilst their model did not explicitly represent the dynamically aging process of buildings, Yang and Kohler (2008) pointed out the considerable influence of the probable lifespan of buildings on future mass flows and environmental impacts. Similar to Yang and Kohler (2008), a static approach was taken by the High Efficiency Buildings model developed by the Centre for Climate Change and Sustainable Energy Policy, known as the 3CSEP-HEB model (Urge-Vorsatz et al. 2012). Their model assumed the Chinese building stock had an annual demolition rate of 0.5% and a retrofit rate of 1.4%, which implied homogeneity of Chinese buildings in terms of lifetime.

Taking a more dynamic perspective, Hu et al. (2010) analysed the Chinese building stock by assuming a normal distribution function for building lifetime. The size of building stock was estimated using population and per capita floor area sourced from China Statistical Yearbooks. Applying this approach, they explored various scenarios of future demand for building materials such as steel and concrete for Chinese residential buildings, both at the national level (Hu, Pauliuk, et al. 2010) and at the city level (Hu, Voet, et al. 2010). The study by Hu et al. (2010) appears to have been the first attempt to apply the concept of lifetime distribution to the Chinese building stock. For example, drawing on the work by Hu et al. (2010), Huang et al. (2013) carried out a similar study investigating materials demand and environmental impact of buildings, where it was assumed that the lifetime of concrete buildings is normally distributed, assuming an average lifetime of 30 years for brick-concrete buildings and 40 years for reinforced concrete buildings. In Hong et al. (2016), the same methodological approach was applied to develop the building stock turnover model underlying the projected trajectories of demand for building materials and the corresponding embodied energy, over the period of 2010 to 2050. Both

residential and commercial buildings were assumed to following normal distributions in terms of their lifetimes, with the standard deviation being set to be 1/3 of the average lifetime. Similarly, investigating the impact of technical progress and the use of renewable energy in building sector over the period of 2010 to 2050, Shi et al. (2016) applied the China TIMES model and represented the lifetime distribution of buildings using a normal distribution. Referring to Hong et al. (2016), the model developed by Huo et al. (2019) also used a normal distribution for lifetime distribution of residential buildings in China to estimate building floor area, energy consumption and energy intensity. In these studies, historical per capita floor area was sourced from China Statistical Yearbooks to derive possible future trajectories of per capita floor area and overall floor area.

The use of historical per capita floor area published in past China Statistical Yearbooks for building stock and energy modelling has also been common in previous studies that were less "explicit" or "dynamic", often where buildings are one component of a much larger model. For example, the residential building sector in the China End-Use Energy Model developed by Lawrence Berkeley National Laboratory used per capita floor area from the Yearbooks to estimate the overall stock size and develop a 2050 outlook for energy and emissions (Zhou et al. 2011; Fridley et al. 2012; Zhou et al. 2013; McNeil et al. 2016). Yu et al. (2014) studied the potential impacts of alternative building energy code scenarios on building energy use and associated emissions in China. In their model, Yearbook data on per capita floor area was used to calibrate the modelling of floor area expansion before 2010, and it was assumed that buildings would retire at an annual rate of 1/30 of the remaining stock. Delmastro et al. (2015) developed the Energy for Buildings (EfB) model, as part of the Energy Demand Projection Model for China (EDPM-CN), to analyse the residential energy consumption trends up to 2030 under various technological and policy scenarios. Along with other drivers of energy demand in their model, the historical per capita floor area published in the Yearbooks was a key variable. Similarly, to explore various scenarios of carbon emissions from Chinese buildings through 2050, Yang et al. (2017) applied a grey modelling technique based on the historical per capita floor area data published in past China Statistical Yearbooks to forecast the future trend of building stock size for the period up to 2020 and scenario analysis for the period beyond 2020.

2.2.2   Critique of models

There are three main methodological concerns associated with previous research: (i) arbitrary choice of mean and standard deviation; (ii) ambiguity associated with existing building stock size and age profile in the start year for the modelling; and (iii) use of per capita floor area data leading to inflated estimates. Firstly, the few studies using a distribution to represent the lifetime of

buildings assumed that building lifetime is normally distributed (Hu, Bergsdal, et al. 2010; Huang et al. 2013; Hong et al. 2016; Shi et al. 2016; Huo et al. 2019). For a substantially under-researched area, there will inevitably be multiple approaches that could be taken, and a normal distribution is not unreasonable. However, what is more critical and potentially questionable is the approach of defining the parameters of the normal distribution without validation or calibration using empirical data. In these studies, the mean, representing the average building lifetime, was assumed to take the values in the range of 30 to 50 years. Furthermore, the standard deviation was commonly assumed to be 30% of the mean. The range of values for the mean was based on anecdotal evidence drawn from limited or individual cases. Moreover, the assumption used for the standard deviation was purely arbitrary. Taken together, these parameters specify inadequately substantiated shapes of the distributions that govern the lifecycle of buildings, thereby rendering high uncertainties of the building stock turnover and calling into question the calculations of energy consumption and carbon emissions that build on the stock turnover dynamics.

Secondly, in addition to the somewhat arbitrary parameters used in the distributions, there is a general absence of detail on how the initial stock in the start year of the observation period is treated in the models. Regardless of which specific year is chosen as the start year for modelling, the size of the existing stock in that year and especially the age profile of the buildings are key determinants of the subsequent evolution of the stock. For a given stock size with a pre-defined normal distribution governing the lifetime distribution, e.g. a mean value of 50 and a standard deviation of 15, the age profile of the existing buildings in the stock makes a significant difference to the remaining lifetime of buildings and overall size of the stock. As an extreme example, an age profile with over 90% of buildings younger than 30 years means the stock will remain standing much longer than an age profile with over 90% of buildings older than 70 years. Moreover, the removal of buildings from the stock to a large extent determines the incoming new buildings which will then be subject to various probabilities of demolition over time. Hence, technically the age profile in the initial stock has a knock-on effect on stock evolution over time. Of course, such effects may be marginal for a very small initial stock in a start year over several decades ago if the modelling focus is on current status or future trend. But for an initial stock in a fairly recent year, such as 2010 in the case of (Shi et al. 2016; Hong et al. 2016), its overall size is large and comparable with the stock size for the modelling period. The composition of the stock in terms of age profiles of the buildings cannot be overlooked. In fact, the simplified model by Yang and Kohler (2008) was the only one which explicitly but briefly introduced how the initial stock in the base year was treated in the modelling. However, the lack of sufficient quantitative detail makes it difficult to gain a full understanding of their considerations and therefore evaluate the implications to modelling results relating to not only stock itself but also energy. In summary,

a review of these studies suggests that there has been a general inadequacy of robustness and transparency with regard to applying a normal distribution to building stock.

Finally, directly using the per capita floor area for urban residential buildings as published in the China Statistical Yearbooks leads to substantially inflated estimates of building stock size. The annual data reported in the Yearbooks, supplied by the Ministry of Housing and Urban-Rural Development (MOHURD), was collected through sampling that targeted urban family households with a registered permanent residence. The sampling excluded urban dwellers without permanent residence status, such as university students and young professionals recently graduated from universities who usually have so-called 'collectively registered' status, as well as a large number of unregistered rural migrant workers living in cities. As opposed to the registered family households, they are not "permanent" but "floating" in that most are not homeowners and instead rent their accommodations. The per capita floor area of the floating population is substantially less than that of registered family households and their accommodation conditions were not reflected in the sampling (Shen 2013; Liang 2014; Ren et al. 2019). This means the Yearbook data on per capita floor area for urban residential buildings has been over-estimated (Li & Xu 2013; THUBERC 2017). Accordingly, multiplying the over-estimated per capita data by actual urban population data to derive the total stock size will in no way reflect the real situation. In fact, the real situation in terms of total stock size of urban residential buildings in China is unknown, at least for the most recent historical period starting from 2007. MOHURD stopped publishing official statistics after 2006. The absence of official statistics makes calibration of model estimates impossible and therefore at least partially explains the considerable variation in estimated building stock size over this period as found in literature. For example, estimates of the urban residential building stock size in 2010 ranged from 14 billion m^2 (Yang et al. 2017), to 17 billion m^2 (Huang et al. 2013), 20 billion m^2 (Yang & Kohler 2008; Hu, Bergsdal, et al. 2010), and 21 billion m^2 (Hong et al. 2016). To obtain a reasonably accurate estimate of overall stock size of urban residential buildings, either the Yearbook data should be adjusted downwards by taking into account urban population who rent, or some alternative method of avoiding the use of per capita floor area should be explored.

2.2.3   Summary

Clearly, the problems discussed above suggest a research gap that needs to be adequately addressed. Building lifetime and stock turnover dynamics are both key determinants in modelling building energy, both embodied and operational. There is a pressing need for more research efforts in methodological development and knowledge generation for this substantially under-researched but fundamentally and strategically important area.

2.3   System Dynamics models for operational energy

2.3.1   Model categorisation

Energy models can be broadly grouped into two categories, "top-down" and "bottom-up" (van Vuuren et al. 2009; Herbst et al. 2012; Scrieciu et al. 2013; Hall & Buckley 2016). Energy models for buildings, a major energy end use sector, can be similarly categorised (Swan & Ugursal 2009; Kavgic et al. 2010; Fazeli & Davidsdottir 2017). Top-down building energy models treat the target building stock (such as the residential sector of a country or city) as an energy sink, without differentiating between individual end-uses. Using historical aggregated data on building energy consumption, top-down building energy models regress the energy consumption of building stock as a function of high-level demographic, macroeconomic, and climate related variables. Energy consumption can therefore be attributed to the characteristics of the entire building stock. This makes top-down models generally well positioned to conduct long-term energy demand and supply analysis, but not in the presence of discontinuities, such as paradigm shifts of the target building stock, energy-related technological advances or breakthroughs, etc (Swan & Ugursal 2009; Hall & Buckley 2016).

Bottom-up building energy models, by contrast, are based on detailed samples of individual buildings instead of the entire building stock. Estimated energy consumption of samples of buildings is then extrapolated to represent the building stock, based on weights that reflect the representativeness of the samples. Bottom-up building energy models can be broadly divided into two subcategories, namely, statistical methods and engineering methods. Statistical methods utilise data from energy bills and surveys of a sample of buildings to establish statistical relationships between energy consumption and a range of potential explanatory variables through regression. A notable advantage of statistical methods is the ability to discern the effect of occupant behaviour, which can vary significantly. Engineering methods, on the other hand, explicitly calculate energy consumption of end-uses based on detailed descriptions of the sampled buildings' properties, such as geometry and envelope, and the energy end uses' characteristics such as capacity ratings and use patterns of equipment and appliances, indoor temperatures, etc. Such a high level of detail, as well as a high degree of flexibility, enable engineering methods to model technological options and the impacts of new technologies which have no historical consumption data (Swan & Ugursal 2009; Kavgic et al. 2010; Lopes et al. 2012; Wilson et al. 2016).

A more detailed discussion of top-down and bottom-up building energy models is beyond the

scope of this review. It is, however, useful to highlight that, according to the IPCC AR5 (Lucon et al. 2014), top-down/integrated models and bottom-up/sectoral models do not fully agree with regard to the extent of the mitigation potential of buildings and the key mitigation strategies. Top-down models place a greater focus on energy supply-side measures for decarbonisation (e.g. fuel switching) than on final energy use reduction opportunities in buildings. By contrast, bottom-up models emphasise the reduction of energy demand for both primary fuels and electricity through technologies for energy efficiency improvement, which is supplemented by further measures such as the shift towards low or zero carbon electricity.

2.3.2   System Dynamics models for operational energy

System Dynamics is a modelling approach to policy design and analysis, featuring a capacity to model and investigate dynamic complexities arising from the model structures, causal relationships, feedback loops, non-linearities and time lags of the system in question (Sterman 2000; Richardson 2001; Shepherd & Emberger 2010; Kelly et al. 2013). Its emphasis on stock-and-flow dynamic relationships makes System Dynamics particularly well placed as a tool to model both stock-level operational energy and embodied energy incurred by annual new construction as the inflow to the stock. This integrated modelling ensures the consistency and comparability with the modelled embodied energy and operational energy. However, all existing System Dynamics based building energy models focused on operational energy only, without looking at embodied energy.

While usually addressing regional or national building stocks, existing System Dynamics based models take the common approach of extrapolating the operational energy use of a representative set of buildings to the total operational energy use of regional or national building stock and not quantitatively involving the interrelations between building sector operational energy use and economic variables such as economic growth, income, fuel prices and so on. Therefore, these models may be classified as bottom-up models (Swan & Ugursal 2009; Kavgic et al. 2010; Fazeli & Davidsdottir 2017).

Previously, such System Dynamics based building energy models have been applied in various national or regional contexts. One such model was developed by Müller and Ulli-Beer (2010) to analyse the transformation of Switzerland's stock of residential buildings towards high energy efficiency. The same model was also used by the authors as part of a larger model to explore how the market, technology, civil society and the state govern the diffusion dynamics of energy efficiency retrofits and the carbon emissions of building stock in Switzerland (Müller & Ulli-Beer 2012). With a high level of aggregation, the model defines buildings in the stock as being in one

of three conditions, new, good or bad. Over time, buildings move from being in a new condition to a good condition and later from a good condition to a bad condition. The shifts are modelled as first-order delays, with the assumptions that new buildings remain 'new' for 10 years on average, buildings in a good condition remain 'good' for 30 years on average, and buildings in a bad condition remain 'bad' and are not retrofitted, for 15 years on average. The authors used first-order delay in order to take account of variations in building-specific situations. However, mathematically this results in unrealistic extremities where some buildings move from new to bad condition in just a few years, while some other buildings remain in new or good condition for very long periods. Meanwhile, the model does not consider the removal of buildings, despite the high share of buildings in a bad condition in the total stock. This implies a very long building lifetime which is not further discussed in the study. The model further assumes that buildings in a bad condition are either retrofitted to reach the energy efficiency level of buildings in a good condition, or are reconstructed to become buildings in a new condition. The use of first-order delays for retrofit or reconstruction, together with the first-order delays used for the building aging process create a closed loop. This results in unrealistic scenarios where a new building can become old, get retrofitted and return again to a bad condition, within a very short timeframe, and unrealistically keep going through such cycles.

A similar but expanded model structure was developed by Schmidt, Jäger and Karl (2012) to study the German residential heat market. Compared to Müller and Ulli-Beer (2010), this model applied a demolition quota to model demolition of buildings in poor condition, which reflects reality more closely. However, the same three-vintage first-order structure is used to represent the aging process of buildings. As for retrofit, buildings in a poor condition, according to a defined retrofit quota, will undergo either non-energy-related retrofit or energy-related retrofit, and subsequently be converted to buildings in good condition. Again, this retrofit dynamic is modelled using first-order delay resulting in the same problem of a potential rapid cycle of condition deterioration and retrofit as observed in the previous model. Inevitably, this has implications for the modelled heat demand of buildings and the evolution of heating systems on the supply-side, which are interlinked in their model through heating demand reduction. The three-vintage first-order structure was also used by Yücel (2013) to investigate the extent of inertia caused by the existing building stock in the Netherlands. The first stock is for newly constructed buildings for 20 years on average, the second stock for medium-stage buildings for the next 20 years of life on average, and eventually the third stock for older buildings for the rest of their lifetimes. Demolition occurs to buildings in the third stock only. As in previous cases, this three-vintage first-order setup inevitably allows unrealistically short lifetimes of some buildings in the stock – some buildings will go through the three vintages in a few years and subsequently get demolished. The retrofit structure of this model is different from previous models in that there is no movement of retrofitted

buildings from old to medium-aged or new buildings. Instead, each of the three vintages (new, medium and old) undergoes a quota-based energy retrofit. However, as an implicit result, some buildings may undergo a very fast aging process, be retrofitted three times, and get demolished shortly after the last retrofit. Fazeli and Davidsdottir (2015) used largely the same three-vintage first-order delay structure to model the housing stock in Denmark, and to study the impact of various policies on the energy performance of residential stock in Iceland (Fazeli & Davidsdottir 2017). Despite their claim that their study improved the model of Yücel (2013), the energy demand of each vintage of buildings is modelled to reduce as a result of retrofit, thereby resulting inevitably in the same methodological issues as found in (Yücel 2013), with newly constructed buildings potentially experiencing multiple rounds of retrofits over very short lifetimes.

Onat, Egilmez and Tatari (2014) studied the mid- and long-term impacts of green building related policies on the possible 2050 trajectories of GHG emissions from the residential buildings in the US. They claimed that their study was the first attempt to quantify and outline the relative importance of retrofitting compared with constructing new green buildings or net zero buildings in the US, modelling a total of 19 policy strategies. Structurally, their model has a lower degree of granularity compared with the 3-vintage models discussed above, with just two stocks: existing traditional buildings are represented by a single stock, as is the stock representing green buildings. The transformation of traditional buildings to green buildings through retrofitting is modelled through a first-order delay. Likewise, the demolition of traditional buildings is modelled as a first-order delay. This structure unavoidably makes their model subject to the same methodological problems as those discussed above. In addition, the model assumes that green buildings are never demolished, despite the fact that the model is designed to study long-term impacts.

Kleemann (2016) examined the potential self-attenuation of a residential building energy retrofit quota under various energy policy scenarios. The author developed and compared five models, including a non-dynamic model of retrofit, a simple dynamic retrofit model, a retrofit cycle model, a renovation-retrofit cycle model, and a retrofit chain model. The development from the first to the fifth model involved an increasing level of granularity of structural details, greater sophistication of logical and mathematical representations, and more plausible and less ad-hoc assumptions, which collectively lead to enhanced methodological robustness. However, similar to the other models mentioned above, there is a fundamental issue inherent in even the fifth and most elaborate version of Kleemann's models. The first-order delay mechanism used to link a stock of buildings retrofitted n times with a stock of building retrofitted n+1 times implies that there always exist buildings that can be retrofitted on a continuous basis with very short intervals between two consecutive retrofits. Clearly this is not reasonable in reality, either technically or

economically.

A related issue is the way in which Kleemann's model handles the demolition of buildings. Compared to previous models, demolition is tracked on an age-specific basis, with the 'age' of a building being relative to the time elapsed since its last retrofit; this is therefore a methodological advance compared to previous models. However, it sets the annual demolition fraction of buildings, which are either unretrofitted or have been retrofitted for multiple times, as a proportion of the annual retrofit fraction, applied to the same buildings. Kleemann's justification for taking this approach is that demolition is an alternative option to retrofit that reacts to the fact that a building has an accumulated 'retrofit potential' (which may also therefore be a 'demolition potential'). However, this treatment tends to correlate demolition with retrofit and consequently downplays the impact of demolition, which may play a much more significant role in situations where building turnover rate is high. In addition, Kleemann's model does not include structures or components relating directly to energy, e.g. energy demand or energy consumption of buildings, energy savings due to retrofit, etc. What is modelled is indeed simply the "status" of buildings being retrofitted.

Nachtrieb et al. (2017) presented a modelling framework for building energy consumption at national level, known as the CERC-BEE (Clean Energy Research Center – Building Energy Efficiency) Impact Model. Compared to Kleemann's model, the CERC-BEE model is a fuller framework where not only building construction and retrofit but also energy end use technology adoption are included. However, the way in which building retrofit is modelled by the CERC-BEE model is essentially the same as Kleemann's model, namely, periodic retrofit is assumed. The flow of retrofitted buildings, from the stock of buildings retrofitted x times to the stock of buildings retrofitted x+1 times, is modelled through dividing the stock of buildings retrofitted x times by a fixed time between retrofits. Since this again is a first-order delay, it does not rule out the possibility that a building retrofitted in a given year is retrofitted again in the immediately following year. Also, similar to Kleemann's model, this model assumes that buildings that remain in use for over 50 years will undergo energy retrofit five times. As the model's structure contains five cycles of retrofit, the five cascading first-order delays technically form a fifth-order delay. Hence, if t_0 is the initial year when a cohort of new buildings are constructed, the stock representing buildings having been retrofitted x times starts to build up from year t_0+x+1, implying a certain non-negligible amount of buildings will undergo energy retrofit once every year, from year t_0+1 to year t_0+x+1. For example, a portion of the new buildings that are constructed and put into use in 2019 will therefore have been retrofitted five times by 2025. Moreover, while the model uses a hazard function to model demolition, an approach more reasonable than Kleemann's method, its setup results in the same problem – some buildings will still be demolished immediately after their

retrofits.

2.3.3 Summary

In summary, previous System Dynamics based models for stock-level building energy performance share some common structural setups and behavioural characteristics with respect to building aging dynamics and energy-related retrofits. From a methodological perspective, these are, either explicitly or implicitly, based on assumptions that appear to be questionable or implausible in the real world. The 3-vintage structure pre-defines a fixed profile of building lifetime distribution which may be significantly different from the reality. A related issue is that buildings within a vintage (a stock) are implicitly assumed to be subject to the same risk of being demolished regardless of their actual age and physical conditions. Regarding retrofit as a key measure to improve building energy efficiency, it is also unrealistic to see a building undergo multiple rounds of retrofits within a short timeframe. Similarly, retrofitting a building soon after it is built, or demolishing a building soon after it is retrofitted, makes little economic or technological sense in the real world. Although these studies have begun to address some of the stock-flow dynamics in the building sector, the identified shortcomings call into question the robustness and fidelity of the models, the resultant emergent behaviours in terms of stock dynamics and energy performance, and the subsequent analysis of policies based on these models.

From this detailed review, it is concluded that although there has been substantial progress in developing a first wave of System Dynamics models of building stock energy, important research gaps remain. An improved model is needed which will better capture and model building stock and energy dynamics, which will, in turn, generate more reasonable and meaningful modelling outputs that can inform policy design and evaluation. In addition, what none of these models has offered to date is a way of including embodied energy of buildings, which can account for a considerable share of lifecycle energy consumption of buildings, particularly those buildings that are short-lived.

2.4 Embodied energy of buildings

2.4.1 Overview of international studies

In 2019, the manufacturing of building materials and construction activities were responsible for 5% of global final energy use and 10% of global energy-related carbon emissions (Global Alliance for Buildings and Construction and UNEP 2020). Internationally, the significance of embodied energy and carbon of buildings has received increasing attention of researchers (Moncaster et

al. 2019; Cabeza et al. 2021), as evidenced by a large number of literature at building materials level (Harris 1999; Venkatarama Reddy & Jagadish 2003; Gustavsson & Sathre 2006; Upton et al. 2008; Abeysundara et al. 2009; Bribián et al. 2011; Aye et al. 2012; May et al. 2012; Bansal et al. 2014; Praseeda et al. 2015; Dixit 2017a; Morini et al. 2019; Zeitz et al. 2019), building component level (Cole 1999; T. . Chen et al. 2001; Emmanuel 2004; Crawford et al. 2006; Abeysundra et al. 2007; Utama & Gheewala 2009; Goggins et al. 2010; Broun & Menzies 2011; Chau et al. 2017; Moncaster et al. 2018; Kyriakidis et al. 2018; Anuradha et al. 2019), building level (Thormark 2002; Mithraratne & Vale 2004; Karlsson & Moshfegh 2007; Hacker et al. 2008; Mahdavi & Doppelbauer 2010; Verbeeck & Hens 2010a; Verbeeck & Hens 2010b; Rossi et al. 2012; Ramesh et al. 2012; Dodoo & Gustavsson 2013; Giordano et al. 2017; Hu 2019), and building stock level (Brown et al. 2014; Koezjakov et al. 2018; Seo et al. 2018).

The large number of case studies prompted a series of comprehensive reviews in this field with the view of widening and deepening the understanding of the significant impacts of embodied energy and carbon, as well as streamlining the quantification of embodied energy and carbon for transparency, consistency and comparability, to better inform policymaking and practice. Moncaster and Song (2012) reviewed in detail existing data and methodologies for calculating embodied energy and carbon of buildings and identified a range of issues such as variability and unreliability of data, incomparability of results, and the need for consistent and transparent databases and methodologies. Similar observations were also made by Cabeza et al. (2013), although their focus was placed upon building materials rather than whole buildings.

Pomponi and Moncaster (2016) systematically reviewed 102 articles to identify a series of strategies for mitigating embodied carbon in the built environment. A meta-analysis revealed that no single strategy would be effective in embodied carbon reduction. Instead, a pluralistic and multidisciplinary approach needs to be taken to achieve a substantial change. Based on a subset of the reviewed articles, which had adequate information about embodied carbon coefficients, data sources, system boundaries, and life cycle stages, Pomponi and Moncaster (2018) further looked into the data used and methodological assumptions made in those studies. Given the remarkable variation in results and issues of incompleteness, low transparency, and low comparability, the authors suggested immediate action to be taken to avoid the risk of embodied carbon becoming a second wave of performance gap in environmental assessment of buildings.

The IEA's Energy in Buildings and Communities Programme (IEA-EBC) Annex 57 on the evaluation of embodied energy and carbon for building construction was implemented from 2011 to 2016, with the objective of developing a detailed understanding of the multiple calculation methods and the interpretation of their results. A total of 80 international case studies collected

under Annex 57 revealed the extent of methodological differences and demonstrated the need for basic principles, data and planning recommendations to improve transparency and traceability (Birgisdottir et al. 2017). Based on the cases, Rasmussen et al. (2018) systematically explained and analysed the methodological implications of the quantitative results of the cases and provided a framework for reinterpretation and comparison. Malmqvist et al. (2018) identified and characterised a wide array of design and construction strategies for new and refurbished buildings to reduce embodied energy and carbon at the building level. Complementing the findings of Rasmussen et al. (2018) and Malmqvist et al. (2018), a research synthesis and meta-analysis was conducted by Moncaster et al. (2019) to develop further insights into the methodological choices and quantitative results of the 80 cases and analyse the impacts of contextual factors at both policy and project level in reducing the embodied energy and carbon of buildings.

To investigate the status quo of embodied energy parameters, Dixit (2017b) conducted an extensive review of embodied energy literature from 1975 through 2016, covering Asia, Europe, North America and Oceania. Based on the reviewed case studies, the author examined the variations of a series of methodological and data quality parameters, including system boundary, method of embodied energy calculation, energy inputs, primary and secondary data, data incompleteness and accuracy, and data representativeness. The author recommended a combination of establishing a set of guidelines and performing a detailed uncertainty analysis to address these parameters. Focusing on recurrent embodied energy (REE) used in maintenance, repair and replacement over a building's life cycle, Dixit (2019) conducted a systematic review of literature to identify and analyse key parameters affecting its calculation. The author categorized REE parameters into controllable parameters, which include design and facility management parameters, and uncontrollable parameters, which are dynamic and uncertain. The review pointed out the need for further research to identify and quantify the uncertainties of REE parameters.

Through a literature map analysis, Cabeza et al. (2021) conducted a comprehensive overview of the global progress of and barriers to quantifying embodied energy and carbon of structural materials of buildings. Based on 70 articles reviewed, the authors found that cradle-to-gate was the mostly used boundary system, data source was rarely articulated, and there was a gap regarding embodied energy and carbon coefficients of materials. Minunno et al. (2021) conducted a systematic literature review and a meta-analysis of 181 articles to collect and analyse the life cycle assessments of construction materials and buildings. They established a benchmark of embodied energy and carbon of construction materials through descriptive and inferential statistical tools and then developed a two-step procedural guideline for ranking and

comparing results and adopting strategies to reduce the adverse environmental impact of buildings.

2.4.2   Studies in Chinese context

Research relating to embodied energy and carbon of buildings in Chinese context has lagged behind the international progress, as largely evidenced by the fact that there were very few Chinese cases in those comprehensive reviews. Whilst there has been a trend of gradually increasing interest of academics in embodied impacts of Chinese buildings in recent years, the amount of reported research work is far less than being commensurate with the magnitude of Chinese building stock and its significant implications for energy and carbon.

2.4.2.1   Micro-level

Chen et al. (2001) studied the energy embodied in the building envelope of two typical high-rise residential buildings in Hong Kong and found that energy embodied in steel and aluminium together accounted for over three quarters of the total embodied energy of both buildings. Zhong (2005) compared the embodied energy of two residential buildings in Beijing and found the embodied energy per m^2 of the building with a frame-shear structure substantially exceeded that of the building with a brick-concrete structure. With a larger scale survey in Beijing, Gu et al. (2007) investigated over 100 residential buildings covering various structural types and 13 office buildings. They found the average embodied energy intensity was 3850 MJ/m^2 for residential buildings, 5500 MJ/m^2 for conventional office buildings, and 7300 MJ/m^2 for large office buildings. Aden, Qin and Fridley (2010) conducted an assessment of embodied energy and carbon emissions of residential and commercial buildings in Beijing. The ten buildings used as cases demonstrated a wide range of energy and material intensity values suggesting a high case specificity. Yan (2011) surveyed 44 buildings in Zhejiang province, all of which were constructed after 2005. For the four samples of residential buildings, the energy consumption of producing building materials required by one square metre of constructed floor area was found to range from 1587 to 7062 MJ/m^2.

Using a cluster of six commercial buildings in the Beijing economic development area as a case study, Han et al. (2013) applied a hybrid method to quantify the embodied energy of building construction. Structure and façade system were found to contribute 58% of the total embodied energy. Li et al. (2013) applied a process-based method to estimate the embodied carbon of a 1459 m2 five-storey brick-concrete residential building in Nanjing. The embodied carbon, including material production, construction, demolition, and waste disposal, would be 614 tCO_2. Li et al. (2014) developed an assessment framework for analysing the embodied carbon impacts

of buildings based on the concept of work breakdown structure, and demonstrated its applicability using three residential buildings in Jiangsu province in eastern China. Focusing specifically on steel-construction buildings that have been developing rapidly in China in recent years, Su and Zhang (2016) used a process-based method to analyse embodied energy and carbon of three steel-construction residential buildings constructed after the Wenchuan earthquake in 2008 in southwestern China.

Zhang and Wang (2015) conducted life-cycle carbon assessment of three buildings in Harbin city, Heilongjiang province, which represented typical residential and office buildings in urban and rural areas of China. Their results showed that carbon emissions during the materialization stage, which consisted of material production, transportation and on-site construction, were of considerable importance in alleviating environmental pressure. Using three different cases in the same city, Zhang and Wang (2016) conducted a comparative study of the process-based method and input-output method and found that material production accounted for 80-90% of total building embodied emissions. Of the three cases, the 17-storey residential building was used as the target to further investigate the importance of embodied emissions relative to total building life-cycle impacts (Zhang & Wang 2017).

Gan, Cheng, et al. (2017) presented a process-based method for quantifying embodied carbon of high-rise buildings using composite core-outrigger structure and applied it to a reference building in Hong Kong. Using the same quantification method and the same reference building, Gan, Chan, et al. (2017) evaluated the embodied carbon as a function of different design parameters, including choice of construction materials, structural forms, use of recycled materials, and building heights.

Yang et al. (2018) presented a building-information-modelling enabled life cycle assessment method and applied it to a residential building of brick-concrete structure located in Chongqing city in southwestern China. Building material production was found to contribute 24% of the life cycle carbon emissions of the studied building. Hong et al. (2018) used multi-regional input-output (MRIO) and process-based LCA to develop an integrated framework to incorporate technological difference and regional disparities into embodied energy quantification at project level. The framework was validated using case-specific data of six buildings in Beijing, Hebei and Jiangsu. Most recently, Su et al. (2020) evaluated a passive building located near Shanghai and found that the embodied energy and carbon of the building were respectively 37.6% and 16.2% higher than a hypothetical conventional building in the same climate zone.

Detailed assessment of individual buildings provides valuable knowledge about and insight into

the drivers of embodied energy and carbon. However, due to case-specific factors across technological, economic, environmental and social dimensions, as well as differences in methodological and dataset choices, there exist large disparities in assessed levels of embodied energy and carbon per unit of floor area and its importance relative to the operational energy and carbon. Moreover, individual cases cannot be generalized to represent the macro-level characteristics of a sizeable building stock. Furthermore, studies based on individual cases are mostly cross-sectional, thus they cannot capture the temporal dynamics of building embodied energy and carbon as a result of trends in structural forms and material choices, advancement in technologies and practices, evolving building standards and regulations, and mounting climate impacts. Therefore, case studies have inherent limitations in providing a macro-level view needed to formulate policies targeting stock-level transition towards green buildings.

2.4.2.2 Macro-level

Compared to micro-level cases, studies of stock-level embodied energy and carbon of buildings in China are quite rare. At city level, Liu and Hu (2006) sampled 100 residential buildings in Beijing built in different years and of different structure types. The city-wide material consumption, energy consumption by material production, and environmental impacts attributable to residential buildings were estimated based on the samples for the historical period of 1949 to 2003. Guo and Wang (2018) used data from various national and local statistical yearbooks to calculate annual energy consumption by building material production and construction activities in Shanghai in 2015, which was found to account for 12.85% of total energy consumption of Shanghai.

At the national level, Lin *et al*. (2015) estimated the aggregated energy consumption of steel, cement and aluminium production meeting the demand of constructing buildings and infrastructure across China, which increased from 0.36 billion tce in 2004 to 0.85 billion tce in 2012. Applying a similar method, Zhang et al. (2015) estimated the energy consumption of building material production and construction of Chinese building sector over the period of 2001 to 2013. Extending Lin's method, Zhang *et al*. (2019) applied a process-based model to estimate the historical embodied energy and carbon of the Chinese building stock by considering the impact of different building structural types on material intensities. The total embodied energy of urban residential, rural residential, and public and commercial buildings in 2016 was found to reach 410 million tce, accounting for approximately 9% of China's economy-wide energy consumption. Chen *et al*. (2017) used an input-output model to estimate the carbon emissions of the Chinese construction industry from 1995 to 2011 and found industry's carbon emissions increased by nearly 400% over this period. Indirect emissions, which were incurred by upstream activities such as material production, remained the major component of total emissions and

consistently accounted for over 95%. Huo *et al*. (2019) developed a building stock turnover model to estimate the embodied energy of urban residential buildings in China. The embodied energy, estimated using an approach highly similar to Zhang *et al*. (2019), was found to have increased moderately from 86 million tce in 2000 to 97.5 million tce in 2015, accompanied by generally decreasing trends of material production energy intensity and construction energy intensity.

Only a very few studies have gone beyond the historical evaluation and explored the possible outlook over the next few decades. Huang *et al*. (2013) used a material flow analysis model to estimate the long-term materials demand and environmental impact from the entire Chinese building sector. They found the total embodied carbon from Chinese buildings from 2011 to 2050 would reach 56.7 billion tonnes, with a peak annual contribution of 1.49 billion tonnes reached around 2030. Employing a similar approach, Hong *et al*. (2016) modelled the stock turnover of residential and commercial buildings in China and forecast that building materials demand and the associated embodied energy would reduce by 73% and 77% respectively, from 2010 to 2050. However, both Huang *et al.* (2013) and Hong *et al*. (2016) have an inherent methodological limitation in their use of a normal distribution with pre-defined parameters to represent building lifetime distribution. This approach calls into question their forecasting results that built on the modelled building stock turnover.

As a noteworthy common feature of macro-level studies, the large variance in material intensity, as demonstrated by micro-level studies based on individual buildings, appears to have been overlooked in their models. The common approach taken by these macro-level studies was to apply a single average value to the intensity of a particular material in a given year. Various data sources were referred to by these studies to determine the single average values used in their calculations. The implication of this approach is strong, as evidenced by the substantial variation in the stock-level results of these macro-level studies, even for the historical period with known quantity of annual new construction. For example, the embodied energy of the national building stock in 2012 was estimated to be 330 million tce by Zhang *et al*. (2019), almost double the estimate of 170 million tce by Hong *et al*. (2016). As for urban residential stock, its embodied energy in 2015 was estimated by Zhang *et al*. (2019) and Huo *et al*. (2019) to be 150 million tce and 97.5 million tce, respectively.

2.4.3   Summary

On the whole, the existing literature suggests three substantial research gaps in embodied energy of Chinese buildings. Firstly, there is a dearth of regional or national level quantification of embodied energy of the Chinese building sector. Secondly, amongst the limited national-level studies, most focus on estimating the historical amounts of embodied energy, with very few

exploring future scenarios and trajectories. Thirdly, despite their importance, uncertainties associated with the material intensity, energy intensity, and future annual new construction and their propagation into stock-level embodied energy have remained largely under-researched.

2.5 Operational energy of buildings

2.5.1 Global situation

Globally, over the period of 2010 to 2019, owing to continued efficiency improvements in building envelopes, systems and equipment, the operational energy intensity of buildings decreased by 9.8%, in final energy consumption per m^2 (IEA 2019a). However, this progress was not sufficient to offset the combined effect of improved access to energy, increased ownership of energy-consuming devices and rapid growth in building floor area. These factors collectively drove up the total final energy demand from buildings. In 2019, the global final energy consumption in buildings increased by 8.5% compared to its 2010 level, amounting to 128 exajoules (EJ), or 4.367 billion tce, and accounting for 30% of global total final energy consumption (Global Alliance for Buildings and Construction and UNEP 2020). The increasing trend of energy consumption has rendered the buildings sector off-track from the pathway required to realise the IEA's Sustainable Development Scenario (IEA 2020c).

China is a major driving force of the growth of the global building sector. The total floor area of the new buildings constructed in China in 2018 was 2.5 billion m^2 (National Bureau of Statistics 2019), accounting for over a third (33.8%) of the global total of new buildings of 7.4 billion m^2 (IEA 2020b). According to the World Energy Outlook 2019 (IEA 2019b), the final energy consumption by buildings in China, as the world's largest building energy consumer, was 0.504 billion tonnes of oil equivalent (toe), or 0.72 billion tce, in 2018. China's share in final energy consumption by global buildings increased to 16.3% in 2018, from its 2010 level of 13.1%.

2.5.2 Studies in Chinese context

2.5.2.1 Estimating historical operational energy

In the China Energy Statistical Yearbook, operational energy consumption by buildings is not directly and explicitly recorded. It is implicitly disaggregated into and counted under various energy end-use sectors (Wang 2014). To estimate historical data for building energy consumption based on the yearbooks, Huo et al. (2018) proposed a method to identify and extract building-related energy consumption from various sectors in the composition of the Energy Balance Sheet. For example, for urban residential buildings, transportation-related fuel consumption, i.e. gasoline and diesel, was taken out from the urban sub-category of the "household consumption"

sector of the Energy Balance Sheet. Fuel consumption by heating, as part of urban household energy consumption, was found to have been under-estimated and thus adjusted by using centralised heating data in the China Statistical Yearbook. Using this method, the energy consumption of urban residential buildings in China was estimated to increase from 0.639 billion tce in 2010 to 0.814 billion tce in 2014 (Huo et al. 2018).

The overall development of Chinese buildings and operational energy performance was reported by the Annual Report on China Building Energy Efficiency. The annual report was developed by Tsinghua University Building Energy Research Centre (THUBERC) and widely recognised as an authoritative source on building energy in China. The building energy consumption in the annual reports was calculated based on a bottom-up model, with real data from large-scale surveys and long-time monitoring of a large number of cases as fundamental inputs (Peng et al. 2015; THUBERC 2019b). According to recent annual reports, the total operational energy of Chinese buildings increased from 0.816 billion tce in 2010 to 0.858 billion tce in 2015, and further to 1.0 billion tce in 2018 (THUBERC 2012; THUBERC 2013; THUBERC 2014; THUBERC 2015; THUBERC 2016; THUBERC 2017; THUBERC 2018; THUBERC 2019a; THUBERC 2020). For urban residential buildings, the operational energy consumption, include space heating, space cooling, home appliances, cooking, lighting, and water heating, reached 0.379 billion tce in 2018 (THUBERC 2020).

2.5.2.2 Modelling future scenarios of operational energy

Compared to understanding the historical situation, there were significantly more research interests in exploring future scenarios against the backdrop of climate targets, as evidenced by a number of modelling-based studies on medium- to long-term operational energy performance of Chinese building stock and policy implications.

Eom et al (2012) presented a technologically detailed, service-based model of China's building energy demand, which was nested in the well-established Global Change Assessment Model (GCAM). In the model, key drivers of the evolution of building sector included economic growth, urbanization, building floorspace, demand for building energy services, fuel and technology competition within the services. The modelling results suggested that China's building energy growth would not wane anytime soon, and technology improvements would put downwards pressure on the growth but not be sufficient to halt it. The analysis also highlighted the trade-offs between economy-wide carbon prices and sectoral regulatory policies, the increased electrification of building sector in response to carbon policy, the implication of CHP expansion to climate policy, and the challenge of addressing traditional biomass consumption.

Yu, Eom, Zhou et al. (2014) extended and adapted Eom's model by disaggregating China into four climate regions with each of them having three building types (urban residential, rural residential, and commercial) while taking into consideration regional heterogeneities in socioeconomic development, energy service requirements, and fuel choices. On aggregate, the total operational energy consumption of all buildings in all climate regions was projected to reach 1.21 billion tce in 2050. Using the same model, Yu, Eom, Evans et al. (2014) found that applying mandatory energy codes to new buildings as well as mandatory codes to retrofitting existing buildings would have the potential of bringing down the total energy consumption in 2050 by 19%, to 0.98 billion tce.

The Centre for Climate Change and Sustainable Policy (3CSEP) and Global Buildings Performance Network (GBPN) presented a bottom-up model to examine the energy saving potential trends of space heating and cooling under various efficiency retrofit scenarios (Urge-Vorsatz et al. 2012; Urge-Vorsatz et al. 2013). Focusing on US, EU-27, China and India which collectively were responsible for over 60% of 2005 global final building energy use, the model, was an engineering-economic model with a rich characterization of the targeted regions' building stock based on climate typology, building type and vintage, and the application of a number of demographic and macroeconomic factors. The results showed that the lock-in effect of Chinese buildings, defined as the difference in final energy use for space heating and cooling between moderate and deep efficiency scenario in 2050, would be as much as 63%. The study suggested that policies to limit stock growth, such as progressive property taxes, zoning and building size restrictions, should be pursued.

The Lawrence Berkeley National Laboratory (LBNL) conducted a series of studies relating to energy and emissions of Chinese building sector, including economy-wide energy and emissions outlook wherein buildings were examined as one of the key sectors (Zhou et al. 2007; Zhou et al. 2011; Fridley et al. 2012; Zhou et al. 2013), and those focusing specifically on buildings (Fridley et al. 2008; Zhou et al. 2012; Zhou et al. 2014; McNeil et al. 2016; Zhou et al. 2016). Core to their studies was the LBNL China 2050 Demand Resources Energy Analysis Model (DREAM) which was a bottom-up model developed using the Long-range Energy Alternative Planning (LEAP) modelling platform. DREAM was used as the model to characterise past and future energy consumption in China, evaluate the energy and emissions impact of specific policies in various sectors, analyse environmental impacts of CO_2 and SO_2 co-controls, and perform policy and technical efficiency scenario analysis (LBNL 2017).

In LBNL's study on China energy and emissions paths to 2030 (Fridley et al. 2012), the energy saving potential and remaining gap for improvements through 2030 were identified for residential

and commercial buildings by comparing a reference scenario with a maximum technology scenario, under which the highest technically feasible efficiencies and advanced technologies would be adopted irrespective of costs or deployment barriers. Both scenarios shared the same demographic and macroeconomic parameters as drivers of the sectoral energy demand. The total primary energy consumption by residential and commercial buildings under the reference scenario would reach 1.17 billion tce by 2030. By contrast, the more aggressive efficiency improvements and technology switching under the maximum technology scenario would lead to the residential primary energy consumption peaking at 0.494 billion tce in 2020 and the commercial primary energy consumption peaking at 0.405 billion tce in 2030, respectively.

Using the same model but setting scenarios and assumptions different from (Fridley et al. 2012), Zhou et al. (2013) presented a 2050 energy outlook of China. For building sector, they concluded that residential primary energy consumption would keep rising till 2050 under the continued improvement scenario but would experience a plateauing period from 2020 to 2050 under the scenario of accelerated implementation of more aggressive efficiency policies. As for commercial buildings, the model claimed that the energy consumption growth would be largely dominated by end-use energy intensity rather than overall floor area.

The DREAM model was updated to disaggregate the building sector by building type, climate zones, new versus existing buildings, and efficiency retrofits versus new efficiency designs (Zhou et al. 2014). A transformative pathway scenario characterised by accelerated implementation of key strategies, such as passive and integrative building design, super-efficient equipment, retrofitting, prefabricated buildings, smart controls, and renewable and clean energy for on-site equipment and power generation, was expected to keep the building sector on track to achieve over 50% reduction in primary energy consumption by 2050 (Zhou et al. 2016). Similarly, based on the DREAM model, McNeil et al (2016) quantified and compared potential energy savings and emission reduction impacts from various policies and programs relating to building codes, district heating metering, energy efficiency labelling, and retrofitting.

In IEA's Energy Technology Perspective (ETP) model, the building sector was modelled using a global simulation stock accounting model, split into residential and non-residential (commercial and public service) subsectors across different countries and regions. For both subsectors, the model uses socio-economic drivers, such as population, GDP, income, urbanisation, etc., to project major building energy demand drivers, including floor area, number of households and residential appliance ownership. Applying the demand drivers to energy intensities of end-uses (space heating, cooling, water heating, cooking, lighting, appliances, equipment, and others) and related technology and fuel options produced the final energy consumption and CO_2 emissions

(IEA 2013a; IEA and THUBERC 2015). By 2050, the final energy consumption of Chinese buildings was expected to reach 31 EJ (1.057 billion tce) under the business-as-usual scenario and 22 EJ (0.75 billion tce) under the 2 degree scenario (IEA 2015; IEA and THUBERC 2015). This was updated in World Energy Outlook 2019 (IEA 2019b) to be 0.648 billion toe (0.926 billion tce) in 2040 under the Stated Policies Scenario and 0.495 billion toe (0.707 billion tce) in 2040 under the Sustainable Development Scenario in 2040, respectively.

The Research Institute of Standards and Norms (RISN) under the MOHURD studied the future possible trends of building energy consumption in the context of China's overall energy supply capacity and economy-wide climate targets (RISN 2016). Under the baseline scenario and three policy scenarios characterised by different levels of urbanisation, floor area per capita, and operational energy intensity, the total operational energy of Chinese building stock in 2050 was estimated to range from 0.862 to 1.587 billion tce. The authors argued that the total operational energy should be controlled at no more than 1.2 billion tce in 2030, which should account for no more than 25% of China's total energy consumption in 2030. This was expected to be achieved through curbing the increase of stock size, applying more stringent energy standards of new buildings, promoting low-energy buildings, and accelerating retrofits.

Whilst the aforementioned CEBM was mainly used to estimate the historical building energy consumption published in the annual reports, it also formed the basis for analysing future trends and making policy recommendations by researchers from THUBERC. Several versions of future peak values of total building stock and energy consumption were proposed over the past few years. Peng, Yan and Jiang (2013) claimed that it would be possible to control the total stock size and energy consumption to not exceed 60 billion m^2 and 0.84 billion tce in the future. This long-term target was slightly adjusted to 60.8 billion m^2 and 0.85 billion tce in Peng (2014), and 60.8 billion m^2 and 0.83 billion tce in Peng et al. (2015). In the 2017 Annual Report of THUBERC, the target increased significantly to 72 billion m^2 and 1.1 billion tce (THUBERC 2017). No methodological details about the target setting were provided. It is, however, noteworthy that the total stock and energy consumption in 2018, as reported in their 2020 Annual Report, already reached 60.1 billion m^2 and 1 billion tce (THUBERC 2020). These numbers tend to suggest that the long-term target of peak values was likely to have been set unrealistically and there is a need to update it again.

Tan et al. (2018) developed a bottom-up model to forecast the future trend of operational energy and carbon emissions of Chinese buildings up to 2050. They categorized the Chinese buildings into four subcategories, in the same way as the THUBERC model. In addition to the baseline scenario, they defined a policy scenario with 18 energy-saving policies involving design

strategies, energy efficiency of equipment and appliance, and renewable energy applications. Under either scenario, their model suggested that the energy consumption of Chinese buildings would not peak by 2050, but continue to increase, although the rate of increase would slow down over time. In 2050, the energy consumption was projected to reach 1.045 billion tce under the baseline and 0.823 billion tce under the policy scenario, respectively.

Reinventing Fire China was a detailed, bottom-up assessment of China's future energy demand based on primary demographic, economic and technical drivers (Energy Research Institute/Lawrence Berkeley National Laboratory/Rocky Mountain Institute 2019). Buildings was one of the three key energy end-use sectors covered by the model. The results showed that the operational energy consumption of Chinese buildings would reach its peak of 2.29 billion tce in 2045 under the reference scenario. In contrast, under the Reinventing Fire scenario, the peak would be 14 years earlier and 40% lower, i.e. 1.36 billion tce in 2031. By 2050, the energy consumption of Chinese buildings would be 2.27 and 1.0 billion tce under the two scenarios. The large amount of savings under the Reinventing Fire scenario was expected to be achieved primarily through integrative and passive design, supper-efficient equipment and appliances, building retrofits, smart systems, and building prefabrication.

2.5.3   Summary

From the above studies, it can be observed that the projection of future operational energy of Chinese building stock varied significantly. This is understandable and as expected, as the setting of scenarios involved a range of factors and assumptions, many of which were at the discretion of modellers. However, it is clear that the building stock itself, in terms of size and composition, was not adequately addressed, despite that it is a fundamental determinant in assessing energy use of a building stock. Whilst some studies provided details about their assumptions and modelling results relating to building stock, such as the Reinventing Fire China model, most of them did not do so. In general, in most studies the methodological description and analytical discussion about stock were disproportionately brief as compared to building design strategies, technology applications, and policy options.

However, in these studies, the wide ranges of stock size in typical future years clearly demonstrate the need for placing more emphasis on the dynamics and uncertainties of future stock growth. For example, for 2050, which perhaps is the most commonly chosen target year, the total stock size of Chinese buildings, in billion m^2, was estimated to be 70 in (Urge-Vorsatz et al. 2012), 78 in (Yu, Eom, Zhou, et al. 2014), 81.1 in (Tan et al. 2018), 82.7 in (Zhou et al. 2014), 83.6 in (IEA and THUBERC 2015), 85.8 in (Energy Research Institute/Lawrence Berkeley National Laboratory/Rocky Mountain Institute 2019), and 88.9 in (RISN 2016). The estimate by

THUBERC (2017) was 72 billion m^2, although they used the term 'future' instead of a specific year. In addition, underlying the total stock size, the composition of buildings in terms of vintage, is equally important, if not more, because it provides the important linkages between the increasingly stringent building design codes and the stock-average building energy intensity, with particular regard to heating and cooling (IEA 2020a).

In summary, the significant impact of building stock on operational energy warrants more in-depth investigation into its future growth and turnover dynamics.

2.6 Whole-life energy of buildings

Given the energy and environmental impacts of buildings throughout their life cycles, it is important for sustainable building design and policy-making aiming for decarbonisation to take a holistic and integrated perspective by focusing on both operational and embodied energy together, namely the whole-life energy.

2.6.1 International studies

Internationally, topics relating to whole-life energy and carbon of buildings have been researched extensively. A study on Swedish low-energy buildings found that the initial embodied energy accounted for 45% of total energy need over a 50 years lifespan (Thormark 2002). Crawford and Treloar (2003) suggested that embodied energy represented 20 to 50 times the annual operational energy of most buildings in Australia. Rawlinson and Weight (2007) pointed out that in the UK the embodied energy in complex commercial buildings was equivalent to 30 times annual operational energy use. A case study in Portugal showed that operational energy was an average of 187.2 MJ/m^2/year and the embodied energy accounted for approximately 2372 MJ/m^2, representing 25.3% of the former for a service life of 50 years. This ratio was expected to rise substantially with the improvement of operational energy efficiency mandated by building regulations (Pacheco-Torgal et al. 2012).

Stephan et al. (2012) investigated the whole-life energy of a single-family passive house in Brussels, Belgium and a house in Melbourne built to high national energy efficiency standards in Australia. Based on a 50-year building lifetime, the whole-life energy was 14,428 GJ for the Belgian case, with 59.1% attributable to embodied energy, and 15,537 GJ for the Australian case, with 44.7% embodied energy, respectively. As emphasised by the authors, these results clearly proved the need to integrate embodied energy requirements for a more comprehensive evaluation of life cycle energy at both building and city scales.

Devi and Palaniappan (2014) presented a life cycle energy analysis of a residential building consisting of 96 identical apartment-type homes in Chennai, India. For a building lifetime of 50 years, the embodied energy, consisting of material production, on-site construction and demolition, represented 37% and the operational energy represented 73% of life cycle energy, respectively. Increasing the building lifetime from 50 to 75 years would reduce the life cycle energy intensity from 0.66 to 0.58 GJ/m^2 per year. In addition, reducing the operational energy intensity by 25%-50% would raise the share of embodied energy in life cycle energy to 50%-70%.

Crawford et al. (2016) quantified the life cycle energy of a three-bedroom single family house in Melbourne, which was a representative sample of new Australian houses for costing purposes. Over a 50-year lifetime, the life cycle embodied energy and life cycle operational energy of the house would be 4729 GJ (44%) and 6124 GJ (56%), respectively. They also found that thermal operational energy savings achieved through improving envelope thermal performance could be offset by the additional embodied energy required for supplementary insulation materials and thermally efficient windows. These results demonstrated the need for more comprehensive building regulations to reduce life cycle energy.

Based on a review of 90 case studies in European countries such as Belgium, Finland, Spain, Sweden, etc., Chastas et al. (2016) identified an increasing significance of embodied energy in the transition from conventional to passive, low-energy, and nearly zero-energy residential buildings. Specifically, they found that the share of embodied energy in whole-life energy was 11%-33% for passive, 26%-57% for low-energy, and 74%-100% for nearly zero-energy buildings, whereas this share was only 6% to 20% for conventional buildings. The authors argued that a whole-life energy cycle analysis is needed in the methodological framework of current energy efficiency regulations.

A similar recommendation was made by Giordano et al. (Giordano et al. 2017), who assessed the whole-life energy of an office building in Turin, Italy. Eight design scenarios were defined to compare the impacts of structure of the building, energy sources for material production, and U-value limits of wall, roof and floor systems. The results showed that, with the design scenarios featuring more elements towards a nearly zero energy building, the share of embodied energy in whole-life energy increased from 32% to 67%.

A 977 m^2 building in the United States was used by Hu (2019) as a case to investigate its life cycle impacts across energy, water, environment, and human health. Other than the original design, three alternative design options of the buildings were also explored. The alternative options involved changes in building materials, internal wall, floor, foundation, roof, mechanical

system and ventilation system. It was found that the ratio of lifecycle embodied energy to lifecycle operational energy ranged from 89% to 107% across the four scenarios.

2.6.2 Studies in Chinese context

For Chinese buildings, the large amount of studies focusing on operational energy and carbon excluded embodied energy and carbon from their boundaries. Studies on whole-life energy and carbon of buildings were just a small subset of those on embodied energy and carbon, and therefore were limited.

Zhong (2005) estimated the whole-life energy of two residential buildings in Beijing, over an assumed lifetime of 50 years. The result showed that the share of embodied energy in whole-life energy was 17% for the building with a brick-concrete structure and 24% for that with a frame-shear structure. Despite the difference in structure, the whole-life energy intensities of the two buildings were almost the same, being 30.9 GJ/m^2 and 30.7 GJ/m^2, respectively. The survey by Gu et al. (2007) involving more than 100 residential buildings and 13 office buildings in Beijing revealed that the embodied energy of residential buildings was equivalent to 8 years of annual operational energy. For office buildings, this ratio was 13 for conventional ones and 8 for large-scale ones, respectively. In the study by Li et al. (2013) on a residential building in Nanjing, operational carbon incurred by electricity and gas consumption for heating, cooling, cooking, lighting and appliances was estimated using a simplified method. With a design building lifetime of 50 years, the whole-life energy of the building during the 50 years would be 1466 tCO_2, with embodied energy accounting for 42%. Extending the lifetime to 70 years or shortening it to 30 years would lead to the share of embodied energy being 34% or 55%, respectively.

At stock level, the study by Zhang et al. (2015) extended to cover operational energy of residential buildings in both urban and rural areas and public buildings. By combining embodied energy and operational energy, whole-life energy of the entire building stock was obtained. The share of embodied energy gradually increased over time and reached 53% in 2013. However, the share was inflated because the authors erroneously included infrastructure in the embodied energy of buildings. The share should have been lower. For example, 37% for 2013. In Huo et al (2019), along with the embodied energy of Chinese urban residential stock, the annual operational energy was estimated by using the statistical yearbook-based method reported by the authors in a separate study (Huo et al. 2018). In a year, the whole-life energy of the stock was the sum of embodied energy and operational energy. For the studied period of 2000 to 2015, the share of embodied energy in whole-life energy varied in the range of 26% to 45%.

2.6.3 Summary

The observations from Chinese buildings were largely in line with the consensus on whole-life energy/carbon importance emerging from literature in the wider international context. The magnitude of whole-life energy of Chinese buildings, as already demonstrated by previous studies on operational energy or embodied energy, has significant implications for achieving China's announced climate targets in 2030 and 2060 (Kejun et al. 2021; Li et al. 2020; Zhou et al. 2021). However, the small amount of studies in Chinese context, particularly those at stock level, strongly suggests a pressing need for further work to develop a holistic understanding of and in-depth insight into this strategically important but under-researched area. Moreover, extensive searching of literature has shown a scarcity of studies exploring future trajectories of whole-life energy of Chinese building stock at a regional or national level. This critical research gap needs to be addressed to produce more evidence to inform the formulation and implementation of policies on Chinese buildings, and those on energy and climate in a broader context.

2.7 Research gaps and research questions

The review identifies a series of separate but inherently related aspects that have not been adequately addressed by past studies relating to Chinese building stock. These research gaps provide strong evidence for further research work and justify the relevance of this thesis.

On **building stock**, official statistics on total size of Chinese urban residential building stock only exist up to 2006. Studies on building stock turnover dynamics in China are limited and have several methodological issues. To represent the building lifetime uncertainty, researchers commonly use a normal distribution and arbitrarily assume its mean and standard deviation without appropriate calibration or validation. There is a general ambiguity associated with the initial stock size and age profile in the start year for modelling, whose impact on stock evolution is not negligible. Direct use of per-capita floor area data published in statistical yearbooks leads to substantially inflated estimates of building stock size. Taken together, these methodological issues call into question the stock turnover modelled by previous studies and point to the need for an improved model.

On **embodied energy**, there is a dearth of regional or national level quantification of embodied energy of the building sector in China. Amongst the limited national-level studies, most have focused on estimating the historical amounts of embodied energy, with very few exploring future scenarios and trajectories. Moreover, despite their importance, uncertainties associated with the

material intensity, energy intensity, and future annual new construction and their propagation into stock-level embodied energy have remained largely under-researched.

On **SD models for operational energy**, it is necessary to model future operational energy of the urban residential stock in the same modelling framework as the embodied energy. The review of previous SD models reveals some common fundamental structural and behavioural limitations that call into question their robustness. An improved model is needed to address these methodological issues.

On **operational energy**, in studies in the Chinese context, methodological description and analytical discussion about stock were disproportionately brief compared to building design strategies, technology applications, and policy options for operational energy efficiency improvement. The significant impact of building stock on operational energy warrants more in-depth investigation into future stock growth and turnover dynamics.

On **whole-life energy**, there are limited studies in the Chinese context, either at individual buildings level or at a stock level. Searching of literature has found no studies exploring future trajectories of stock-level whole-life energy of Chinese buildings.

Through the above extensive review of literature and the identification of research gaps, specific research questions were formulated as described in Chapter 1, to guide the research design and implementation. Table 2.1 lists the chapters (Ch. 4 to 9) and the specific research questions and sub-questions answered by each chapter. As shown, most questions are answered by more than chapters, reflecting the strong logical and methodological links amongst the chapters. It is evident that chapter 5, as the core part of this thesis, not only forecasts future trajectories of stock evolution (Q2), but also lays the groundwork for estimating annual embodied energy (Q3), annual operational energy (Q5), and whole-life energy under various scenarios (Q6). First the following Chapter 3 will explain the methodological tools for model development, implementation and statistical analysis in Chapters 4 to 9.

Table 2.1: Research questions and thesis chapters

Ch.	RQs	Specific questions / sub-questions answered
4	Q1	How to model building stock turnover dynamics?
		What was the average lifetime of Chinese urban residential buildings?
		How did the residential stock evolve over the recent historical period since 2007?
	Q2	How can the building stock model be extended to forecast possible future trajectories of Chinese residential stock evolution over the medium to long term?
	Q4	How can existing system dynamics models of building stock operational energy be improved, for better representation of stock turnover dynamics and energy retrofit of buildings and for integration with modelling of embodied energy?
5	Q2	How can the building stock model be extended to forecast possible future trajectories of Chinese residential stock evolution over the medium to long term?
	Q3	What are the possible future trajectories of annual embodied energy of urban residential stock in China over the medium to long term?
	Q5	What are the possible future trajectories of annual operational energy of urban residential stock in China over the medium to long term?
	Q6	What are the possible future trajectories of whole-life (embodied + operational) energy of urban residential stock in China over the medium to long term?
		How would they vary under different policy scenarios?
6	Q3	What are the possible future trajectories of annual embodied energy of urban residential stock in China over the medium to long term?
	Q6	What are the possible future trajectories of whole-life (embodied + operational) energy of urban residential stock in China over the medium to long term?
		How would they vary under different policy scenarios?
7	Q4	How can existing system dynamics models of building stock operational energy be improved, for better representation of stock turnover dynamics and energy retrofit of buildings and for integration with modelling of embodied energy?
	Q5	What are the possible future trajectories of annual operational energy of urban residential stock in China over the medium to long term?
8	Q5	What are the possible future trajectories of annual operational energy of urban residential stock in China over the medium to long term?
	Q6	What are the possible future trajectories of whole-life (embodied + operational) energy of urban residential stock in China over the medium to long term?
		How would they vary under different policy scenarios?
9	Q6	What are the possible future trajectories of whole-life (embodied + operational) energy of urban residential stock in China over the medium to long term?
		How would they vary under different policy scenarios?

3

Modelling and analysis tools

3.1 Chapter introduction

This chapter provides a general introduction of the methodological tools for model development, implementation and statistical analysis in subsequent chapters, including the modelling method System Dynamics (SD) and its software, and the statistical computing and graphics environment R and key packages used for this thesis.

3.2 System Dynamics

System dynamics (SD) is a modelling approach to policy design and analysis, which focuses on dynamic complexity arising from the structure, feedbacks and time lags of the system in question (Sterman 2000; Richardson 2001; Shepherd & Emberger 2010). SD was first developed during the late 1950s by Jay Forrester at MIT, and applied to supply chains, industrial dynamics and urban development (Forrester 1958; Forrester 1961; Forrester 1969). Since then, the applications of SD have been progressively expanding to cover a wide range of sectors and areas, including commodity cycles, ecology, economics, environmental studies, management, public policy, social science, etc. SD is generally applicable to any dynamic systems characterised by interdependence, information feedback, mutual interaction, and circular causality (Sterman 2000; Richardson 2001).

SD applies *systems thinking* to develop models to describe and simulate relationships amongst variables and therefore enhance the understanding of complex systems. *Systems thinking* is the ability to see the world as a complex system (Sterman 2000). It is a recognition that organizations may be seen as a complex and integrated system in which a change made to a component at a given time will create a disturbance to the system and thus impact other components of the system instantaneously or over time since they are connected in some way (Tedeschi et al. 2011). However, *systems thinking* is generally conceptual and not the kind of quantitative and dynamic simulation analysis leading to understanding behaviours (Forrester 2007), whereas SD is the method to emphasize the understanding of complexity and the design of policies for guiding changes in systems and informing decisions.

The SD approach aims to take an endogenous behavioural view of the significant dynamics of a system and place the focus inward on the characteristics of a system that themselves generate or exacerbate the perceived problem (Richardson 2001). The specific categories of modelling tasks that SD is well positioned to perform include, amongst others, a dynamically complex problem with possible unintended consequences or responses, a recurring or persistent problem, and a problem for which it is possible to generate a reference mode behaviour over time that describes its intertemporal nature (Vennix 1996; Vennix 1999). Lyneis and Ford (2007) pointed out that one of the most successful areas for SD applications had been project management. Typical model structures underlying project dynamics in this area included modelling features found in actual systems (development processes, resources, managerial mental models, and decision making), analysing and improving the control of dynamic systems, and identifying policy resistance and unintended consequences to explain adverse project behaviours and performance.

3.2.1   Major components of SD models

The building blocks of a SD model are stocks, flows, auxiliaries and constants. Stocks are variables that accumulate a certain quantity. Through the process of accumulating their inflows less outflows over time, stocks provide aggregate representations of the memory and state of a dynamic system, and are the source of its disequilibrium and dynamic behaviours. Without memory, flows represent stock changes. Flows are the sole quantities that stocks directly accumulate. Mathematically, the stock and flow structure can be represented using the following integral equation and differential equation.

$$S_t = \int_{t0}^{t} [F_{in} - F_{out}]dt + S_{t-1} \qquad\qquad (3\text{-}1)$$

$$\frac{dS}{dt} = F_{in}(t) - F_{out}(t) \qquad\qquad (3\text{-}2)$$

where S_t is the value of the stock at time t, F_{in} and F_{out} are inflow rates and outflow rates respectively, and dt is the time step.

The solution of these equations describing stocks and flows represents the aggregated state of the system being modelled. The system state changes continuously over time and depends on the previous state of the system. In addition to stocks and flows, a SD model often includes a number of auxiliary variables and constant values. They serve as intermediary variables to provide a fuller representation of the causal relationships between stocks and flows in the system.

3.2.2 Endogenous perspective

The SD approach is characterized by a focus on endogenous explanations for dynamic behaviours and phenomena. Dynamics are explained as arising primarily endogenously within the boundary of a model, i.e. from the system's internal causal structure in which elements of the system interact amongst each other, rather than from external exogenous disturbances. Exogenous disturbances are seen as triggers of system behaviours, whereas the causes are contained with the structure of the system itself. Corrective responses are dependent on conditions within the system (Richardson 2001). Hence, major efforts of SD modelling are to uncover the sources of system behaviours and look for explanations of recurring long-term problems within the internal structure rather than in external disturbances, small maladjustments, or random events (Meadows & Robinson 1985; Richardson 2001; Bajaj & Wrycza 2009).

3.2.3 Feedback loops

Feedback is one of the central concepts in SD. A feedback is present if an element influences itself indirectly through closed chains of causal relationships with other elements in the system being modelled through SD approach. Each closed chain of such causal relationships forms a feedback loop. Diagrams of loops of feedback and circular causality are instrumental in conceptualizing the structure of and developing insights into a complex system.

There are two types of feedback loops. A positive (reinforcing) loop tends to reinforce the disturbance of the initial action and generate exponential growth, whereas a negative (balancing) loop tends to counteract any disturbance of the initial action and drive the system towards an equilibrium status or goal. Usually, a SD model is composed of multiple positive and negative feedback loops which are linked in a non-linear manner to produce a wide variety of complex dynamic behaviour patterns.

In a SD model, feedback only affects future values of an element, as any feedback loop must involve at least a stock and a flow, and the stock accumulates the flow change gradually over time rather than instantaneously. As afore-mentioned, the concept of endogenous change is fundamental to SD. Without feedback, it is not possible for a SD model to generate dynamic behaviours endogenously. In other words, a SD model without feedback loops can only be driven by its exogenous variables, thus having no meaningfulness and usefulness for explanation of dynamics.

3.2.4   Non-linearity and loop dominance

As a key feature in SD model, non-linearity plays an important role in creating and explaining system behaviours and complexities (Meadows & Robinson 1985; Sterman 2000; Swinerd & McNaught 2012). Non-linear relationships cause changes of the strengths of influences of feedback loops in the system. This leads to the formation of patterns of shifting loop dominance - the system structure is active and different parts of the system may become dominant when conditions change, and consequently the overall system behaviour is shifted (Meadows & Robinson 1985). The ability to endogenously alter active or dominant structure and shift loop dominance arises from non-linearities in the equation-based model (Richardson 2001). Such ability enables a SD model to produce a wide variety of behaviour patterns and represent evolving or adapting system structures (Meadows & Robinson 1985).

3.2.5   Structure-driven behaviours

A core principle of SD approach is that system structure drives its behaviours (Meadows & Robinson 1985; Sterman 2000; Richardson 2001; Qudrat-Ullah 2016; Guerrero et al. 2016). System behaviours are determined by causal structure rather than specific events (Tedeschi et al. 2011). While discrete events and decisions can be compatible with SD's perspective of endogenous feedback (Sweetser 1999; Richardson 2001), SD takes the modelled systems as continuous processes (Qudrat-Ullah 2013) and aims to look beyond the events and decisions to focus on the policy structure and dynamic patterns underlying them (Richardson 2001). As described by Richardson (Richardson 2011), events and decisions are "deliberated blurred" into dynamic behaviour and perceived policy structures, and insights into the connections between system structure and dynamic behaviour are the goal of the SD approach.

3.2.6   Emphasis on general dynamic tendencies

According to Lyneis (1998; 2000), SD models can provide more reliable short to mid-term forecasts than statistical models and allow the determination of reasonable scenarios as inputs to decisions and policies. SD places emphasis on examining the general behaviour

characteristics and dynamic tendencies of a modelled system (Meadows & Robinson 1985; Bajaj & Wrycza 2009). One of the key objectives is to identify and understand the patterns of adjustments in response to various policy or technological interventions in the context of dynamic problems arising in complex business and socio-economic systems (Saeed 2003; Tedeschi et al. 2011).

3.2.7   Steps of SD modelling process

SD approach has been applied to a wide range of research areas. Despite the variety of applications, the major steps involved in SD modelling process generally include problem articulation and conceptualization, formulation of dynamic hypothesis, model formulation, model testing, and policy design and evaluation. As the modelling per se is an iterative process, iterations can take place between any steps (Figure 3.1).
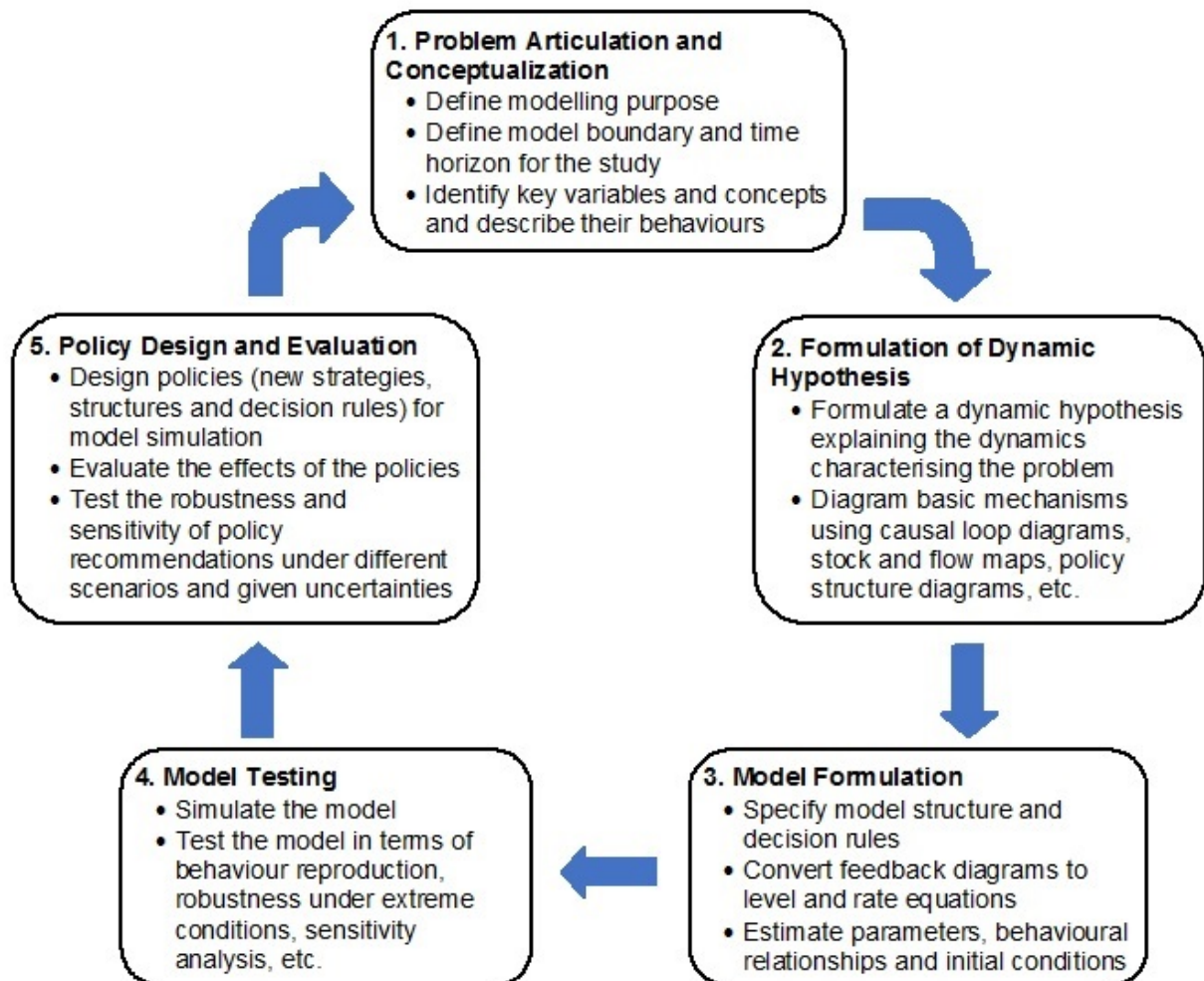
Figure 3.1: SD modelling process. Adapted from (MIT 1997; Sterman 2000)

3.2.8 Software

This thesis uses Vensim, a commercial software for System Dynamics modelling (Ventana Systems Inc. 2019).

3.3 R and RStudio

R is a high-level language and an environment for data analysis and graphics (Crawley 2013). It provides a wide variety of statistical and graphical techniques, and is highly extensible through user-created packages, which allow specialised statistical techniques, graphical devices, import/export capabilities, etc. (R Core Team 2019). Amongst the available integrated development environments (IDEs) for R, RStudio is used for model development and data analysis for this thesis.

Key R packages used by this thesis are briefly introduced below.

- Package "deSolve" (Soetaert et al. 2010), for providing an ordinary differential equation (ODE) solver to develop and implement System Dynamics models in R environment, for further statistical analysis and visualisation.

- Package "FME" (Soetaert & Petzoldt 2010a), for fitting the stock turnover model to historical data on stock size so as to estimate the average building lifetime.

- Package "BayesianTools" (Hartig et al. 2018), for performing Markov chain Monte Carlo (MCMC) to simulate posterior distribution of parameters of parametric survival models used for stock turnover dynamics in a Bayesian framework.

- Package "bridgesampling" (Gronau & Singmann 2018), for estimating marginal likelihoods to perform Bayesian Model Averaging for the stock turnover dynamics.

- Package "fitdistrplus" (Delignette-Muller & Dutang 2015), for fitting univariate distributions to empirical data of building material intensities, e.g. steel, cement, aluminum, etc.

- Package "VineCopula" (Nagler et al. 2019), for capturing the underlying dependence structure of the marginal distributions of building material intensities and establishing the joint distribution for generating random samples of vectors of material intensities.

3.4   Chapter summary

This chapter introduces System Dynamics and R, which are used for detailed modelling and analysis of stock turnover dynamics, stock evolution, embodied energy, operational energy and whole-life energy in subsequent chapters.

4

Building lifetime and historical stock turnover dynamics

4.1 Chapter introduction

This chapter examines research question Q1 about building lifetime and recent historical stock evolution. It develops a System Dynamics model in which survival analysis is applied to characterise the dynamic interplay between new construction, aging, and demolition of residential buildings in urban China. A Weibull distribution is used to represent building lifetime uncertainty. The model calibrates the Weibull distribution to derive building lifetime distribution and estimate the stock turnover dynamics during the recent historical period.

4.2 Model Development

4.2.1 Dynamics in building demolition

A fundamental consideration of the dynamic building stock is that future development is strongly influenced by past activities. In particular, building demolition activities are likely to be a function of construction activities in previous years and the expected lifetimes of buildings in use. By the end of a year, the total volume of demolition will be the sum of all existing buildings constructed in previous years that have reached the end of their lifetimes, for whatever reasons, in this particular year. Similarly, the buildings remaining in the stock are those which are either newly constructed in this particular year or those which were previously constructed but have not reached the end of their lifetime. It is acknowledged that a building may be disused functionally but still not demolished physically. Since the ultimate interest of modelling building stock turnover

is in energy consumed by buildings, a functionally disused building does not consume energy anymore and therefore is considered equivalent to a physically demolished building from an energy perspective. Hence, in the rest of this thesis, demolition and disuse are used interchangeably.

There could be various factors which accelerate demolition, including quality of building materials, design standards, construction techniques and practices, maintenance and renovation, inappropriately accelerated demolition as a result of rapid urbanisation, and so on. Whilst the degrees to which different factors play out are context-specific and therefore may differ significantly, the explicit, direct result is a fast turn-over of building stock. The implicit, indirect result, which could be more critical from a policy perspective, is the increased dynamic complexity and uncertainty associated with the building characteristics in the stock, as opposed to a more stable building stock. As key metrics for building performance, the stock-wide energy consumption and carbon emissions are inevitably subject to the turn-over of the underlying building stock itself. Therefore, the impact of a building stock's dynamic composition over time on its trajectories of energy use and carbon emissions must be well understood when developing and evaluating targets, strategies and policies that are aimed at addressing building energy and emissions from a national level.

Therefore, critical to the turn-over dynamics of building stock is building lifetime. Often there is a lack of authoritative statistics relating to building lifetime, particularly in developing countries. At a country level, given the huge volume of buildings and significant heterogeneity in terms of their physical characteristics and socio-economic contexts, it would be highly unrealistic to expect that buildings constructed and put into use in various cities across a country in a given year would be in service for exactly the same period and then demolished/disused simultaneously. Hence, using a constant to represent building lifetime would be inappropriate. As an intuitive and reasonable alternative, a profile in some form of probability density function (PDF) can be used to approximate the likely lifetime distribution of buildings constructed in a given year, so as to recognise and represent the uncertainties associated with those factors collectively influencing lifetime of buildings.

Mathematically, for any year t, the amount of demolition is the integral of the new construction in year s weighted by the probability of the new construction in year s having a lifetime equal to *(t-s)* years. That is to say, those buildings constructed in year s with a lifetime of *(t-s)* years will have reached the end of their lifetime and therefore will have been demolished or disused in year t. Interpreted in another way, the curve, expressed by (1 - the cumulative distribution function (CDF) of the lifetime profile), represents the probability that a building, constructed and put into use in

year *s*, remains in use in year *t*.

$$Demolition(t) = \int_{t_0}^{t} p(t - s) Construction(s) ds \qquad (4\text{-}1)$$

In year *s*, the building stock accumulates the difference between new construction as input and demolition as output. The accumulated difference is the buildings that remain in use in year *t*. In the most simplistic situation where the stock is initially empty and new buildings are constructed in base year t_0 only and not in any following years, the stock in year *t* is a mix of buildings belonging to this same cohort, which is the group of buildings built in the same year, but with different remaining lifetimes. If new buildings are built every year, then the stock in year t has (*t – t₀ + 1*) cohorts of buildings. In a more general situation where new buildings are constructed every year and the initial stock includes existing buildings constructed previously, e.g. for each of the past 10 years before year t_0, then the stock in year *t* has (*t – t₀ + 1 + 10*) cohorts of buildings. The stock composition of buildings by age is not obvious, but can be computed based on the lifetime distribution.

4.2.2   Building Survival Analysis

The dynamic lifecycle of buildings suggests the suitability of applying the general framework and key features of survival analysis to this research. Survival is used to describe a lifespan or a living process involving sequential occurrences of events or changes of status. Survival analysis emphasises describing, measuring and analysing the events of interest for making predictions about not only survival itself but also the so-called "time-to-event", which refers to the length of time until the occurrence of an event or the change of status (Allison 2010; Liu 2012).

There is a wide spectrum of contexts in which survival analysis is being applied. Taking as an example engineering or manufacturing which is closely relevant to the subject of this research, survival analysis usually concerns performing lifetime tests on mechanical or electrical products using certain metrics and subsequently making prediction on their durability and reliability (Kleinbaum & Klein 2012; ReliaSoft 2018). As a formal definition (International Electrotechnical Commission 2015), reliability of an item refers to the ability to perform as required, without failure, for a given time interval, under given conditions which include aspects that affect reliability, such as mode of operation, stress levels, environmental conditions, and maintenance. In practice, the interest of analysis often centres on the time period over which an item or a system functions at or above a specified standard. From this perspective, survival analysis or reliability analysis can

also be described as life data, lifetime, or failure time analysis (ReliaSoft 2018). For buildings, depending upon the granularity of analysis, either a building itself or the components thereof, such as its structure, envelope, mechanical and electrical system, and so on, can be viewed as an engineering item, each of which is characterised by its survivability or reliability under its respective conditions of operation and maintenance.

As this research targets the Chinese urban residential building stock, which is on a scale of billions of square meters, it is worth clarifying that a 'building' in this context is taken as a flexible and continuous aggregation of floor area (measured in square meters) that can be "partially" demolished or disused, mathematically. It is considered analytically inappropriate to differentiate a building itself from its components in this context. A building and its components are taken as whole to undergo its lifecycle, which technically is a survival process. Therefore, the physical demolition or functional disuse of a building designates the particular "event" of interest, whose time at occurrence is the "time-to-event" in the survival analysis framework. At a given time, for a building in use, a predicted time in the future at which the building will be physically demolished or functionally disused means the termination of the survival process of the building, namely the end of the building's life. The corresponding time interval is the expected remaining lifetime of the building. If the time at which the building was originally constructed and put into use is taken as the beginning of the time interval, then the time interval is the expected entire lifetime of the building. In this context, the expiry of building lifetime due to physical demolition or functional disuse is modelled as a stochastic process based on a hazard function. Conceptually, the hazard function represents the conditional probability that a building will expire in year t+1, provided that it has successfully survived to year t. Mathematically, the hazard function, denoted by $h(t)$, is the ratio of the lifetime PDF, denoted by $f(t)$, to the survival function, denoted by $R(t)$. The survival function is the complement of lifetime CDF, denoted by $F(t)$. This mathematical relationship is given in equation (4-2).

$$h(t) = \frac{f(t)}{R(t)} = \frac{f(t)}{1 - F(t)} \tag{4-2}$$

In general, a range of parametric survival distribution functions are available to describe the survival process in various fields. However, there is extremely limited literature on survival analysis or lifetime data analysis of buildings. Probably the most relevant studies, Miatto et al. (2017) tested various PDFs and found that lognormal distribution offered the best fit to a large volume of real data on lifespans of buildings in Nagoya and Wakayama, Japan, where buildings were short-lived, with average lifespans shorter than 30 years. The same study also conducted a smaller scale study on buildings in Salford, UK, where buildings were much older, and a

Gompertz distribution turned out to best fit the lifespan data. They pointed out that the lack of proper building cohort datasets was a fundamental issue facing building material stock accounting, such as building demolition wastes. From an economic perspective, buildings can be regarded as a type of capital asset, hence building stock can be regarded as capital stock (OECD 2001; OECD 2009). A range of PDFs have been used as proxies to approximately represent service lives and retirement/discard patterns of capital stocks in different countries, including normal, log-normal, Gompertz, Weibull, and Winfrey distributions (Johnstone 2001; OECD 2001; Bohne et al. 2006; Müller 2006; OECD 2009; Aksözen et al. 2016). For example, in the Dutch survey, information on capital stocks and capital discards was used to compute empirical survival probabilities of various types of asset and industry. Amongst them, buildings were found to be well approximated by two-parameter Weibull distributions with a shape parameter ranging from 0.97 to 2.21 and a scale parameter ranging from 20 to 47.6 (OECD 2009).

In this chapter, the Weibull distribution is used to approximate the lifetime distribution of urban residential buildings in China. The Weibull distribution has been widely used as the functional form for lifetime distribution in mortality and reliability applications (OECD 2009; Forbes et al. 2011; McLaren & Stapenhurst 2015). It is defined through a shape parameter α ($\alpha > 0$) and a scale parameter λ ($\lambda > 0$). Table 4.1 summarises the key representations of the Weibull distribution. Specifying any one of the four representations allows the other three to be ascertained.

Table 4.1: Weibull distribution (PDF, CDF, survival function, hazard function)

PDF	$f(x) = \left(\dfrac{\alpha x^{\alpha-1}}{\lambda^{\alpha}}\right) e^{\left(-\left(\frac{x}{\lambda}\right)^{\alpha}\right)}$
CDF	$F(x) = 1 - e^{\left(-\left(\frac{x}{\lambda}\right)^{\alpha}\right)}$
Survival function	$R(x) = e^{\left(-\left(\frac{x}{\lambda}\right)^{\alpha}\right)}$
Hazard function	$h(x) = \dfrac{\alpha}{\lambda}\left(\dfrac{x}{\lambda}\right)^{\alpha-1}$

In the above table, if x is used to represent "time-to-failure", the Weibull distribution is characterised by the fact that the hazard function is proportional to a power of time. Hence, the shape parameter α can be interpreted as a measure of change in the risk of an asset, e.g. a building, failing and therefore being discarded, e.g. a building being demolished/disused. For $0 < \alpha < 1$, the risk decreases over time, suggesting significant "infant mortality". For $\alpha = 1$, the risk remains constant throughout an asset's lifetime. For $\alpha > 1$, the Weibull distribution exhibits

characteristics of decay, where the older the asset is, the more likely it will fail in the near future. This indicates an "aging" process in which the value of α determines the shape of the hazard function curve, i.e. the change of failure rate over time (Rinne 2008; OECD 2009; Forbes et al. 2011; Liu 2012; Palisade 2016; Zaiontz 2018). In practice, it would be more reasonable to expect buildings to have an α above 1 than below 1.

4.2.3   Model structure and components

Ideally, the shape and scale parameters of the Weibull distribution could be determined through calibration, which is to fit the PDF of the Weibull distribution to the empirically observed data on building lifetime. This would be the direct way. However, there are no official statistics on building ages in China and past studies related to building lifetime in China are limited, as discussed above. Therefore, the calibration was performed 'indirectly'. This is done through achieving the best possible fit of the modelled annual aggregated floor area to the corresponding historical data on floor area, using the emergent behaviour of the building stock turnover model. To do so, the building stock in the turnover model is disaggregated into a series of cascading sub-stocks of buildings forming an "aging chain", with each sub-stock representing a particular age group of buildings. The basic mechanism is that, on the aging chain, sub-stock *j* receives the outflow of sub-stock *j-1* as its inflow, undergoes an aging process, and subsequently sends its outflow to sub-stock *j+1* (Figure 4.1).
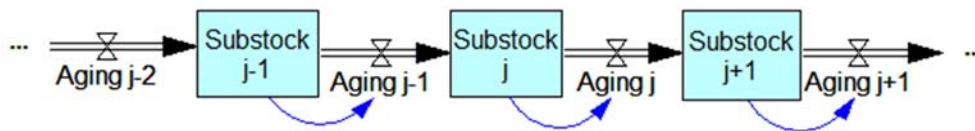
Figure 4.1: Basic mechanism of a simple aging chain.

The removal of demolished/disused buildings from each sub-stock is subject to its age-specific hazard rate, which is determined by the shape and scale parameters of the Weibull distribution. The age group duration represents the length of time that buildings in use reside in a sub-stock before shifting to the next sub-stock in the chain (Figure 4.2). With age group duration set to 1 year, the chronological aging process is discretised, i.e., each sub-stock represents buildings within a one-year age group – for instance 30-year-old buildings are in a different sub-stock to 31-year-old buildings. This level of granularity offers a detailed representation of sub-stocks characterised by heterogeneity with respect to age (and energy-related properties, provided that additional layers are added to the model). In so doing, the aging process of buildings can be separately tracking and allowing experimentation with policy interventions targeting buildings of

specific age groups.
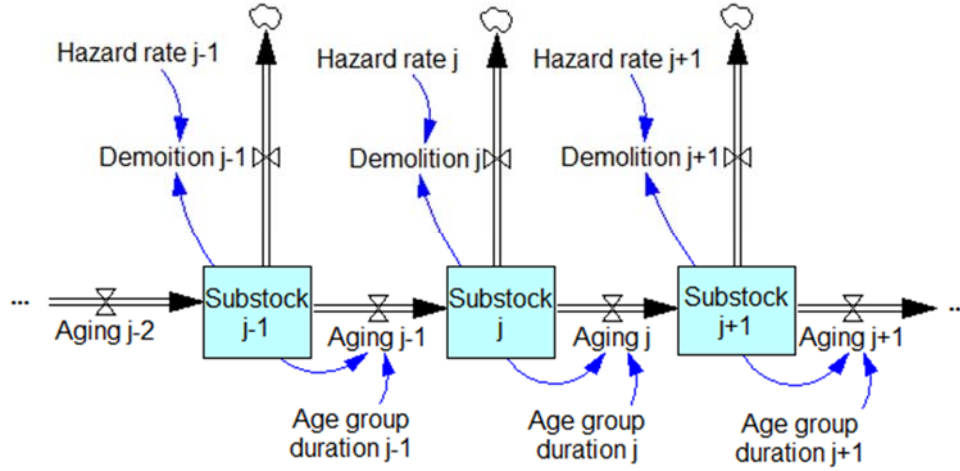
Figure 4.2: Aging chain with explicit modelling of sub-stock specific demolition.

Given that building lifetime in China is generally short, the model uses 101 sub-stocks to respectively represent 0-year-old buildings, 1-year-old buildings, 2-year-old buildings, and so on. The 101st sub-stock represents all buildings that are 100 years old or older, but such buildings account for a negligible percentage of the overall stock of urban buildings in China. Indeed, buildings aged below 40 years accounted for more than 95% in the total stock of urban residential buildings in 2010 (Liu et al. 2013).

For any given year, the mathematical relationships between (i) Building Sub-stock[j], which represents the size of j-year-old buildings, (ii) demolition[j], which represents the demolition and removal of old buildings from Building Sub-stock[j], and (iii) Aging[j] represents the shift of existing buildings from Building Sub-stock[j] to Building Sub-stock[j+1], are expressed as follows:

$$Aging[j] = \frac{Building\ Substock[j] - Demolition[j] * Time\ Step}{Age\ group\ duration} \tag{4-3}$$

$$Demolition[j] = Building\ Substock[j] * Hazard\ rate[j] \tag{4-4}$$

$$Building\ Substock[j] = \begin{cases} New\ construction - Demolition[j] - Aging[j], & for\ j = 0 \\ Aging[j-1] - Aging[j] - Demolition[j], & for\ j = 1,2,\dots 100 \end{cases} \tag{4-5}$$

In the above equation (4-4), the age-specific hazard rate[j] is calculated from the hazard function of the Weibull distribution in Table 4.1. With the age group duration and time step both set to be equal to 1 year, the aging equation can be re-written as follows.

$$
\begin{aligned}
Aging[j] &= \frac{Building\ Substock[j] - Demolition[j] * Time\ Step}{Age\ group\ duration} \\
&= \frac{Building\ Substock[j]}{Age\ group\ duration} - Demolition[j] \\
&= Building\ Substock[j] - Demolition[j]
\end{aligned}
\tag{4-6}
$$

This simplified equation, together with the previous equations for building sub-stocks, clearly show that the aging process is effectively the discrete shift of a group of buildings from age *j* to age *j+1*, duly taking into account time-varying annual demolition applicable to age *j*. At the stock level, the total stock of buildings in use is the sum of the age-specific building sub-stocks, and the total demolition of buildings is the sum of the age-specific demolitions.

Figure 4.3 illustrates the dynamics of the building aging process. In any year, the entire stock is composed of 101 age groups of buildings. The flow of buildings through the age groups forms the aging chain. Year by year, a building gets older and thus "relocates" itself between age groups along the chain, on the condition that it remains alive. For example, the highlighted blocks show a particular cohort of buildings constructed in 2019 moving up through the age groups/sub-stocks. Initially, the cohort stays in age group 0 in 2019, and then moves to age group 1 in 2020, age group 2 in 2021, age group 3 in 2022, and so on. Every year, new buildings are constructed, put in use, and therefore become part of the total stock, although the rates vary, subject to demand driven by socio-economic development and rates at which old buildings are demolished/disused and consequently removed from the stock. These new buildings keep flowing into the stock, starting from 0-year-old age group in any year. Hence, the result is, even though buildings constructed in 2019 shift from 0-year-old age group to 1-year-old age group in 2020, the 0-year-old age group in 2020 will not be empty because it will be "replenished" by new buildings constructed in 2020. Note that demolition from each of the 101 age groups is not explicitly shown in the figure to avoid visual clutter.
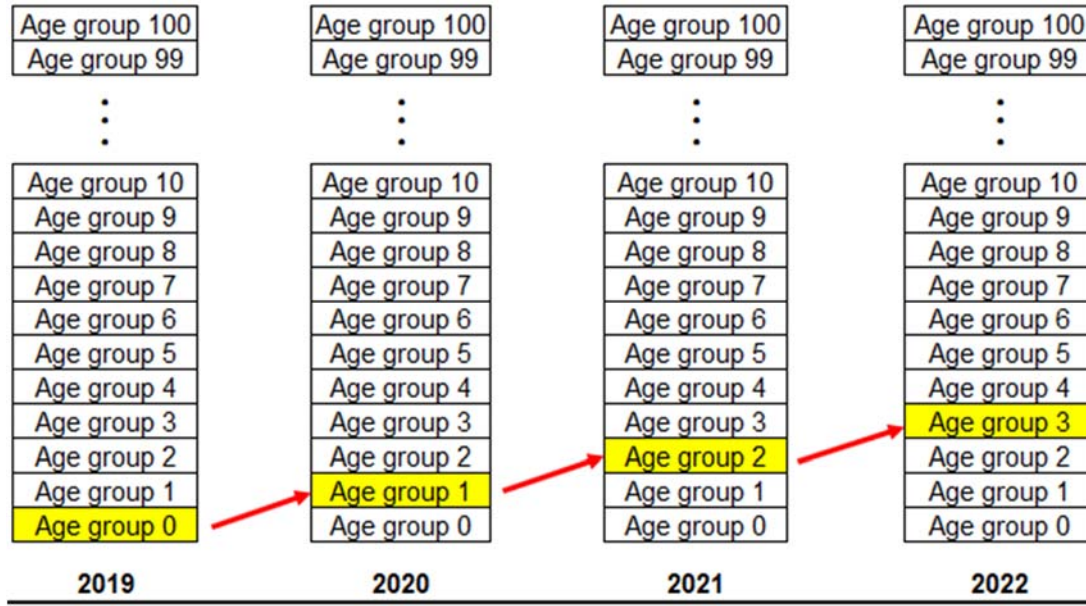
Figure 4.3: Dynamics of building aging process

4.2.4 Data sources

Historical data on total floor area of building stock from authoritative sources is limited. The latest official statistics on total floor area of urban residential buildings across China was 11.29 billion m^2 for 2006, published in the China Statistical Yearbook 2007. The source of data was MOHURD. From 2007 onwards, these statistics were no longer published. Prior to 2006, data was provided in the annual China Statistical Yearbooks and in the Statistical Communique on Urban Housing released by MOHURD from 2002 to 2005. The earliest year for which data is available is 1978. Data on annual new construction of urban residential buildings is taken from China Statistical Yearbooks.

The calibration of the shape and scale parameters of the Weibull distribution for building lifetime is realised by comparing and minimising the difference between the estimated annual total floor area of urban residential buildings, which is the emergent behaviour of the building stock resulting from the dynamic process of new construction, aging and age-specific demolition, with the official statistical data over the historical period through 2006. This method allows parameters governing building lifetime to be calibrated rather than arbitrarily defined, thereby avoiding relying on the over-estimated per capita floor area. Accordingly, the stock turnover dynamics and the resultant annual total floor area over the period of 2007 to 2017 are estimated using the officially published annual new construction data over that period and the calibrated Weibull distribution.

4.3 Results

Using the historical data and stock turnover model, the Weibull distribution is calibrated to have a shape parameter of 1.47 and a scale parameter of 37.64. Its PDF, CDF and hazard function are shown in Figure 4.4.

The resultant building lifetime distribution is found to have a mean value of 34.1 years and a standard deviation of 23.5. This confirms the general observation that urban residential buildings in China have an average lifetime much shorter than the design lifetime of 50 years. The average lifetime estimate of 34.1 years is consistent with the assumptions made by previous studies that employed a normal distribution, which commonly set the average lifetime in the range of 30 to 50 years.[2]

(a)

PDF of Calibrated Weibull Distribution
(Shape = 1.47, Scale = 37.64)

---
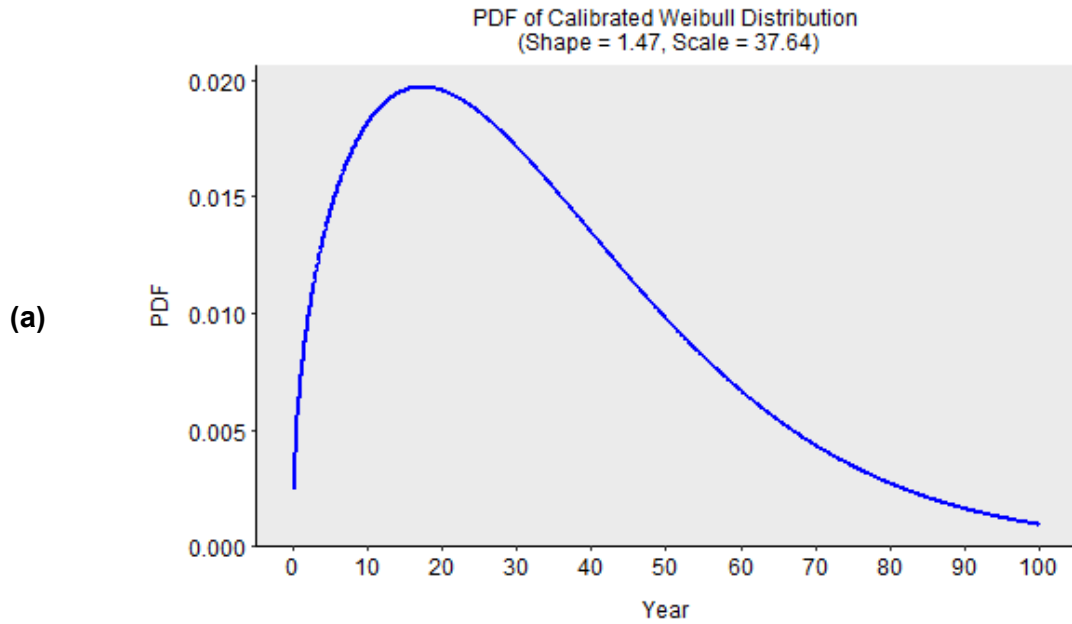
[2] It should be noted that the estimated short mean lifetime and the underlying lifetime distribution are based on data from the specific historical period of 1978 to 2006. Going forward, the mean lifetime of urban residential buildings is expected to become longer over time, as the result of more reasonably planned and implemented urban renewal and expansion, more stringent design standards and effective enforcement, higher quality of building materials, improved construction techniques and practices, and adequate maintenance and renovation.
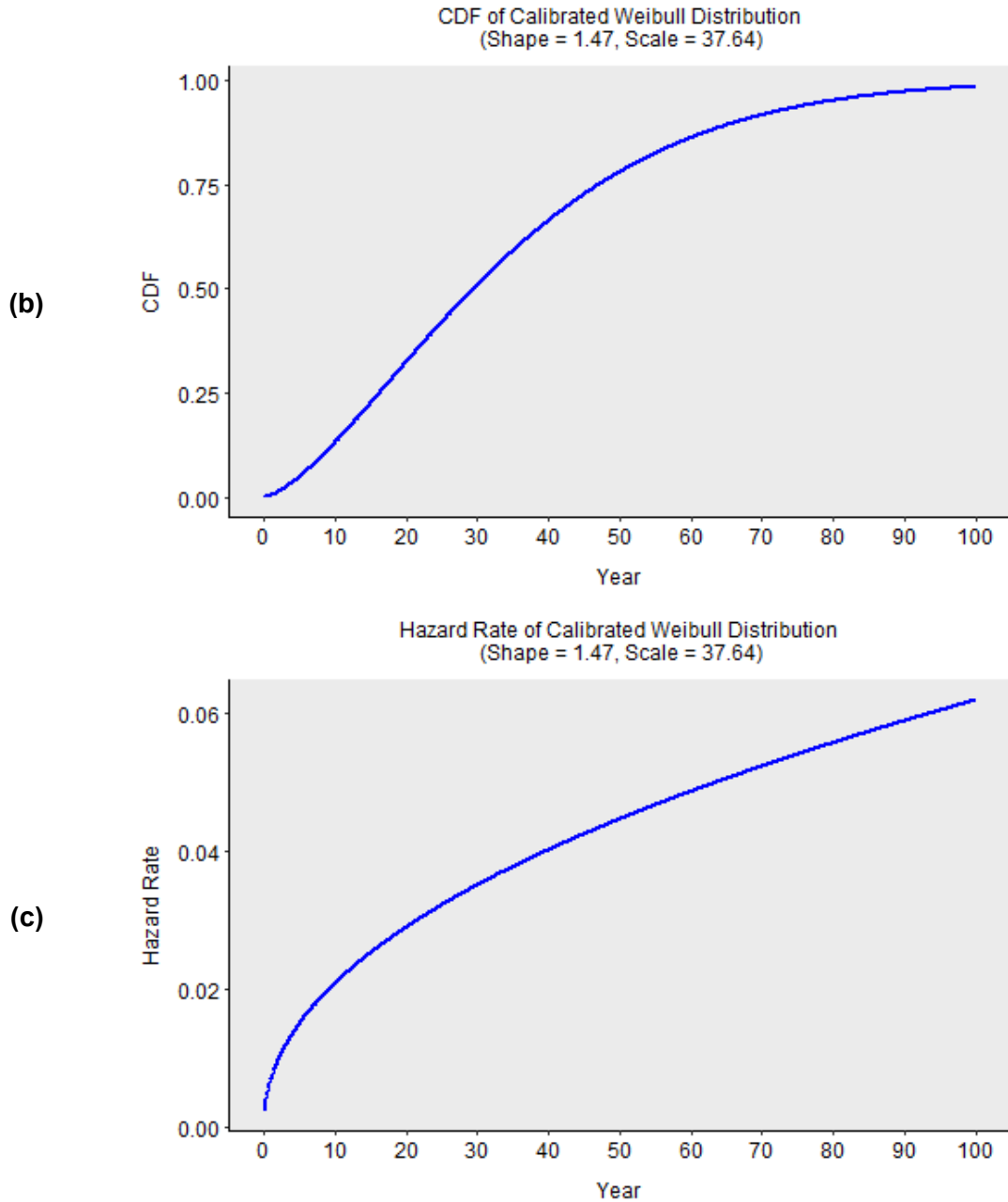
Figure 4.4: Weibull distribution calibrated using historical data: (**a**) PDF; (**b**) CDF; (**c**) Hazard Rate

Due to the lack of official statistics on annual demolition of residential buildings, it is not possible to directly cross-validate the modelling result using historical annual demolition data. In an indirect way, though, comparing the estimated demolition with previous studies provides an alternative basis for evaluating the robustness of the modelling approach and the calibrated building lifetime. According to THUBERC (2012), the ratio of aggregated demolished buildings to aggregated newly constructed buildings over China's 11th Five-Year Plan Period (2006 to 2010) was approximately 34%. Using the calibrated Weibull parameters in the stock turnover model of this study, this ratio was found to be 32%, very close to the THUBERC (2012) estimate. In

absolute terms, the annual demolition level is of the same order of magnitude as previous studies. For example, for 2010, the annual demolition is estimated by this study to be 1.49 billion m², approximately 1.3 billion m² by (Hu, Bergsdal, et al. 2010), and approximately 1.7 billion m² by (Huang et al. 2013). The difference is due primarily to different settings of lifetime distribution parameters.
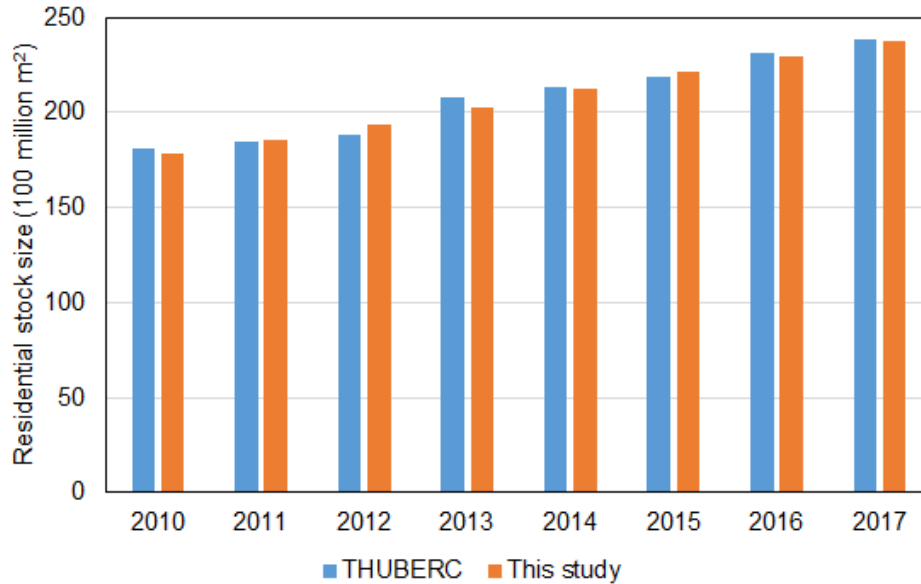
Figure 4.5: Comparison of residential stock size between this study and THUBERC (2019a).

Using the calibrated Weibull distribution and the officially published annual new construction data, the stock turnover model also produces the annual total floor area over the period of 2007 to 2017. The results suggest a continuously increasing trend of overall stock size of urban residential buildings, increasing by 33.1% over 8 years from 17.8 billion m² in 2010 to 23.7 billion m² in 2017. Figure 4.5 compares the stock size of residential buildings of this study and that of the Annual Report on China Building Energy Efficiency (THUBERC 2019a), for 2010 to 2017. The annual report was developed by the leading research institution, the Tsinghua University Building Energy Research Centre (THUBERC), as part of a larger consultancy project funded by the Chinese Academy of Engineering and is widely recognised as an authoritative report on building energy in China. As shown in Figure 4.5, the difference remains consistently marginal, which supports the validity of the assumptions that have been fed into the stock turnover model developed in this chapter.

However, compared to the annual reports which only give the total stock size, the model developed in this chapter offers additional insights into the residential buildings in the form of the explicitly modelled building aging process. The total stock of residential buildings in each year is disaggregated into age-specific sub-stocks, each of which goes through an aging process subject

to age-specific demolition probability estimated by the Weibull lifetime distribution (Figure 4.6). For each year, new buildings constructed in this year and existing buildings that remain in use in this year are spread across the age range, collectively creating the age profile of all buildings in this year. For subsequent years, the age profile changes due to new construction, aging and demolition. These on-going dynamics, which result in the turnover of the overall residential stock, are fully captured in the model. In addition, whereas the annual reports provided an overview up to that given year, the Weibull lifetime distribution in this model serves as an avenue through which possible future stock turnover trajectories can be modelled. For example, given the total size and age profile of the 2017 stock, the 2018 stock can be estimated using the new construction in 2018 and the removal of existing buildings based on their respective age-specific demolition probabilities. The same logic applies going forward, where the interaction between new construction and demolition and trends in per capita floor area will drive the growth dynamics of the stock and allow for reasonable forecasts of future growth.
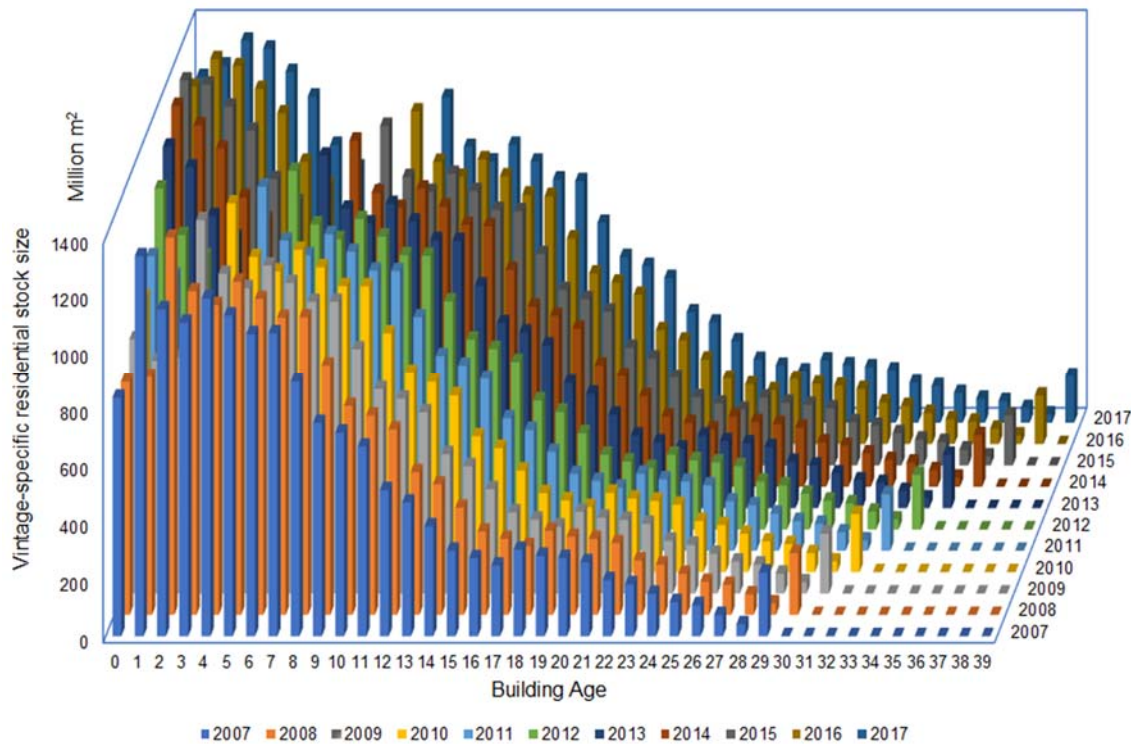
Figure 4.6: Aging process of age-specific sub-stocks of residential buildings

As shown in Figure 4.6, for the building age profile in each year, the oldest sub-stock of buildings is greater than the immediately preceding younger sub-stocks. For example, for 2007, the column representing the oldest sub-stock, which is 29-years-old, is much taller than the several preceding ones which exhibit a generally descending trend due to aging and demolition. This is because the 29-year-old sub-stock in 2007 represents all those buildings already existing in 1978 (the first year of the model) that survived to 2007. The sub-stock includes all existing buildings of

various ages in 1978. Likewise, the 30-year-old sub-stock in 2008 also represents older buildings already in use in 1978 and remaining in use in 2008. So, the x-axis in Figure 4.6 is building age for all buildings other than for this particular set, i.e. buildings in existence in 1978. It is not possible to differentiate those old buildings by their ages in the initial stock in 1978 because no statistics are available for the age profile before 1978. Therefore, without a known composition of buildings by age, the 1978 stock is treated in the model as a mixed one, in which buildings are assumed to be subject to the same probability of demolition. Mathematically, this means these buildings' lifetimes are assumed to follow an exponential distribution whose hazard function is a constant equal to the reciprocal of their average lifetime, which is taken into account in the calibration process. This is a very minor methodological limitation due to data availability constraints, but given its small overall size, the impact of the age profile of buildings in the initial stock in 1978 on more recent stock is largely negligible. Over time, this initial stock will only keep shrinking due to demolition and its impact will further diminish accordingly.

4.4   Chapter summary

This chapter develops a residential stock turnover model using a System Dynamics approach. The model applies survival analysis to represent building lifecycle, from being newly constructed to being eventually demolished. Demolition is modelled as a stochastic process based on a hazard function derived from a Weibull distribution representing the uncertainties associated with building lifetime. Using historical data starting with 1978, the first year official building stock statistics are available, the Weibull distribution's shape and scale parameters are calibrated. The specified Weibull distribution has a mean value of 34.1, which represents the average building lifetime. This result substantiates the general observation that urban residential buildings in China have an average lifetime much shorter than the design lifetime of 50 years. In the absence of official statistics on building lifetime, this estimate can assist policy-makers in characterising existing building stock. Based on the calibrated lifetime distribution, the total stock size of urban residential buildings is estimated to have increased from 17.8 billion m^2 in 2010 to 23.7 billion m^2 in 2017, with a dynamically changing age profile.

In summary, this chapter answers the research question Q1 about lifetime uncertainties and stock turnover dynamics of urban residential stock in China. The model and results prepare the ground for forecasting future trajectories of the stock in Chapter 5.

5

Future trajectories and uncertainties of stock evolution

5.1 Chapter introduction

This chapter investigates possible future evolution trajectories of the Chinese urban residential stock. It extends the stock turnover model in Chapter 4 by turning it into a probabilistic one in a Bayesian framework and applying additional model structure and variables relating to future urbanisation rate and demand for floor area. As key outputs of this thesis, the resultant posterior distributions of future stock and annual new construction answer the research question Q2 and provide key inputs to subsequent chapters. Core to the entire thesis, this chapter also explains why this model development is necessary for considering and comparing policy approaches for reducing whole-life energy, as is considered in later chapters.

5.2 Drivers of future stock turnover dynamics

Conceptually, the possible building stock evolution trajectories in the future are assumed to be subject to the same turnover process as described in Chapter 4, i.e. a dynamic interplay between construction of new buildings, aging of existing buildings in the stock, and demolition of old buildings reaching the end of their lifetimes. The key difference is that annual construction is an exogenous variable in the stock turnover model when predicting the recent stock evolution from 2007 to 2017, whereas it has to be taken as an endogenous variable in the model when forecasting future stock evolution, since future construction is unknown. Methodologically, since

the annual construction of new buildings, existing stock and annual demolition are related to each other, there is a need for some exogenous variables to be included in the model to play the role of driving the evolution of the stock. Here the future trajectories of urban population and per capita floor area (PCFA) are used to establish expected demands of total urban residential building stock. The demands will be met by the net effect of construction and demolition. The mathematical relationships are given by the equations below, which, together with the equations in Chapter 4, set up the mechanism driving the future stock evolution.

$$ExpectedTotalStock_t = UrbanPopulation_t \cdot PCFA_t \qquad (5\text{-}1)$$

$$NewConstruction_t = (ExpectedTotalStock_t - Stock_t) + Demolition_t \qquad (5\text{-}2)$$

where the new construction in year t is 0 years old and therefore equivalent to $substock_t[0]$, which is the youngest substock amongst all substocks in $Stock_t$.
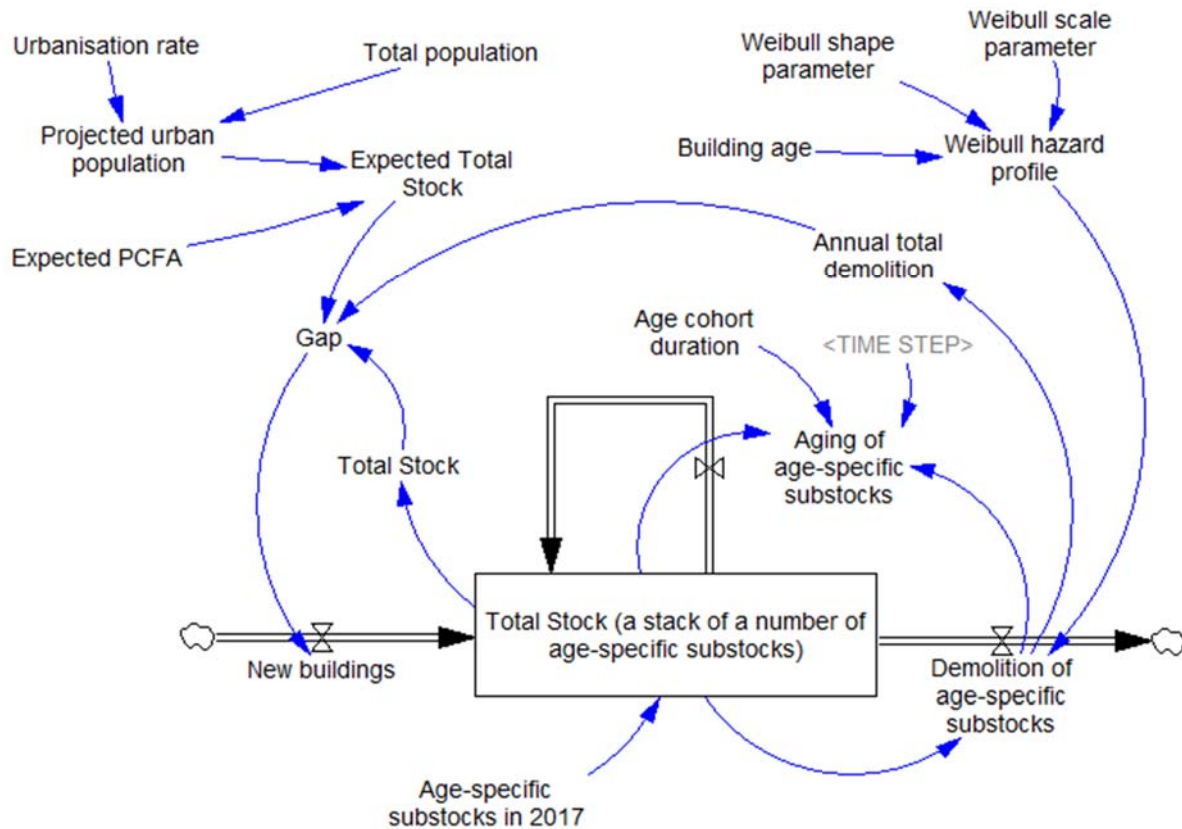
Figure 5.1: Extended building stock turnover model using Weibull distribution

A graphical representation of the above described future stock dynamic turnover model is shown

in Figure 5.1. The building stock is a stack of a number of age-specific substocks that are implicitly represented. Each substock is subject to an age-specific demolition rate determined by the hazard profile derived from the Weibull distribution. Additional feedback loops that drive future stock turnover and growth are added to the extended model.

5.3   Necessity for quantifying uncertainties

In estimating building lifetime and stock turnover dynamics, the model in Chapter 4 follows a Frequentist approach, which takes the survival model (Weibull distribution) parameters as deterministic but unknown. By fitting the modelled annual total floor area to the corresponding historical data, it produces single point estimates of the Weibull distribution's shape and scale parameters leading to the specification of building lifetime profile. The hazard function of the calibrated Weibull distribution, the total stock size and composition of age-specific substocks in 2006, and the annual new construction since 2007, together determine the stock turnover dynamics and obtain a single deterministic estimate of the total stock growth curve for the historical period from 2007 onwards.

This has implications (Burnham & Anderson 2002; Li & Shi 2010; Zhang & Yang 2015; Osgood & Liu 2013; Osgood & Liu 2015; Struben et al. 2015). The point estimate is local in nature. It does not offer an overall picture of the global shape of the parameter across its parameter space. There may be other values of the parameters that are nearly as likely as the calibrated best-fit value, in terms of generating the emergent behaviour of the model that is nearly well consistent with the empirical observations. For example, the parameter may have multiple peaks or valleys across its space. Such possibilities cannot be captured by point estimate. However, they may have substantial implications for policy intervention.

Similarly, in many cases, point estimate does not investigate the covariance between the calibrated values of parameters in the case of a model involving multiple parameters. This makes it difficult to explore the variability of model output, namely the emergent behavior, with respect to various combinations of the parameters for calibration. For example, a combination of high parameter A and low parameter B and a combination of low parameter A and high parameter B may lead to very similarly good fit of model output to empirical data. This may be translated to policy tradeoffs. This provides a useful perspective to modelers and policy-makers, but cannot be enabled by point estimate. Moreover, the point estimate of model parameters is undertaken based on a given System Dynamics model, and the resultant best-fit parameters are in fact model-specific and conditional on the implicit but strong assumption that the underlying structure and characteristics of the model itself are certain and fixed. In other words, a particular model is

chosen as it is considered 'best' based on some criteria. This ignores the uncertainty associated with the model itself and the possibility that there could be multiple plausible hypotheses with regard to the model structure, which could have been compared, selected or even combined using the empirical observations.

Therefore, neglecting the inherent uncertainties at the parameter level (shape and scale parameters) and model level (Weibull distribution as the parametric survival model, which is part of the stock turnover model), coupled with having a limited amount of empirical data on historical floor area for calibration, is likely to have material impact on the robustness and reliability of the modelling of stock turnover dynamics and the forecasting of future trends of stock growth.

To address this issue, this chapter extends the deterministic building stock turnover model to a probabilistic one, and models the stock evolution pathway of Chinese urban residential stock in a Bayesian framework. The Bayesian approach treats the parameters of a candidate parametric survival model, which is used to describe building lifetime profile in the stock turnover model, as random variables. It then derives posterior distributions of the parameters by taking account of both prior knowledge about parameter values and the likelihood of observing empirical data given certain parameter values. For a given candidate parametric survival model, this posterior distribution presents a full picture of the likely parameter space, thus enabling a good understanding of the global shape of the distribution of the parameters. Based on the posterior distribution, the credibility interval for the parameter can provide a direct probability statement about the parameter, whereas this is not the case of the confidence interval in point estimate situation, i.e. the Frequentist approach (Hamada et al. 2008; Rinne 2008; Osgood & Liu 2013). Moreover, the posterior distribution allows parameter uncertainties to be propagated through to the emergent behaviours of model outputs (Hamada et al. 2008; Osgood & Liu 2015), such as the total building stock size. This way, the uncertainty of the model output is quantified.

In addition to model-specific parameter uncertainties, a Bayesian approach allows the uncertainty of a candidate survival model itself to be estimated. In practice, it is not uncommon that there may be several models that are potentially comparably positioned to provide adequate descriptions of the distributions generating the observed data and subsequently make sensible predictions. The existence of these plausible "competing" candidate models gives rise to the uncertainty associated with the model itself. Such uncertainty may take various forms. For example, there may be uncertainty in how to model part of the model (Gibbons et al. 2008). This is the case of the building stock turnover model, in which the survival model as its core part may be a Weibull distribution or a different one. Therefore, in order to produce more accurate and reliable predictions, it is necessary to address uncertainties and make inferences at both levels,

65

i.e. parameter and model. Through Bayesian Model Averaging (BMA), predictions made by individual stock turnover models, each of which uses a specific candidate survival model in the model space, are combined in proportion to posterior model probabilities. This means the creation of a BMA model ensemble, which involves a weighted average of the predictions from a number of models, with the weights being equal to the probabilities that the models are the true model given the observed data. An advantage of BMA is that it accommodates flexibility with respect to model structures. No common structure is required for the candidate models in the model space under consideration, which can be developed based on different principles and mechanisms and operate differently. The only requirement is that these models predict the same quantity of interest (Gibbons et al. 2008). BMA can avoid the situation where inferences based on an individual candidate model are overstated, and decision-making based on predictions is subject to higher risk than expected (Li & Shi 2010; Fragoso et al. 2018).

From a policy-making perspective, a probabilistic model offers the ability to generate probability distributions of different potential outcomes of policy scenarios. This is important in the context of analysing the whole-life energy performance and decarbonisation of the generally short-lived Chinese buildings, where there is likely to be a strategic trade-off between operational and embodied energy due to factors such as massive construction and demolition, strengthening design codes for improved energy efficiency, scaled-up energy-related retrofits, technological advances, and so on. Taking a Bayesian approach, a probabilistic model incorporating building stock turnover, energy and carbon will enable future research into the probability that one policy, e.g., extending building lifetime to avoid embodied energy, would yield a more favourable outcome of stock-level whole-life energy improvement or decarbonisation as compared to another policy, e.g. accelerating stringency of new building design standards for energy efficiency. Improving the understanding of these trade-offs is the overarching objective that motivates the development and application of this probabilistic stock turnover model as an integral part of this thesis.

Based on the above consideration, the forecasting of future trajectories of the urban residential stock growth is conducted in a Bayesian framework. Details of the probabilistic model development, application and results are presented in the following sections of this chapter.

5.4 Bayesian modelling of stock turnover dynamics

5.4.1 Statistical model for historical stock

To model the stock turnover dynamics in a Bayesian framework, it is necessary to re-write the

System Dynamics model equations in Chapter 4 in more general mathematical expressions for implementation in the R statistical computing and graphics environment.

Applying the survival analysis concept, the total stock in year *t* consists of a series of substocks of different ages:

$$Stock_t = \sum_{j=t_0}^{t} substock_t[t-j] \tag{5-3}$$

Where $substock_t[t-j]$ represents buildings surviving in year *t* that are (t-j) years old. For new buildings constructed in year *t*, they are 0 years old and therefore denoted by $substock_t[0]$.

The aging process undergone by any cohort of buildings is accompanied with annual demolition determined by age-specific hazard rates, *H(age)*. Therefore, the annual total amount of demolition in year *t* is the sum of age-specific demolition of substocks at all ages.

$$Demolition_t = \sum_{j=t_0}^{t} H(t-j)substock_t[t-j] \tag{5-4}$$

For a (t-j)-year-old substock in year t, its volume is determined by the aging process that it has undergone since it was constructed in year j.

$$substock_t[t-j] = \left[\prod_{k=0}^{t-j} \left(1 - H(k)\right) \right] substock_j[0] \tag{5-5}$$

Therefore, equation (5-3) can be re-written as:

$$Stock_t = \sum_{j=t_0}^{t} substock_t[t-j]$$
$$= \sum_{j=t_0}^{t} \left\{ \left[\prod_{k=0}^{t-j} \left(1 - H(k)\right) \right] substock_j[0] \right\} \tag{5-6}$$

In the above equation (5-6), the age-specific hazard rate *H(k)* is determined by the parametric survival model chosen. Depending upon the specification, the hazard function of a survival model may or may not have a closed form expression.

As described by equation (5-6), the deterministic component of the overall statistical model is the total building stock as the function of unknown parameters θ of a chosen parametric survival model, e.g. Weibull distribution, and the known annual new cohort of buildings constructed over the historical period. This can be denoted by a function $f(\theta, t)$. The probabilistic component of the model is represented by an error term ε_t, which is assumed to be normally distributed with mean zero and unknown variance σ^2, i.e. $\varepsilon_t \sim N(0, \sigma^2)$. $f(\theta, t)$ describes the expectation of modelled building stock. Therefore, in the Bayesian framework, the total stock can be described by the overall probabilistic model as follows:

$$Stock_t = f(\theta, t) + \varepsilon_t \qquad (5-7)$$

5.4.2 Bayesian model inference

In the context of the statistical model, let *D* represent empirically observed data of total stock, y, and annual new buildings, x, for the period of 1978 to 2006, i.e. $D = \{(x_i, y_i), i = 1978, 1979, \dots, 2006\}$. According to Bayes' theorem, the posterior probability density $p(\theta|D)$, given the data *D*, is calculated as follows:

$$
\begin{aligned}
p(\theta|D) &= \frac{p(D|\theta)p(\theta)}{p(D)} \\
&= \frac{p(D|\theta)p(\theta)}{\int p(D|\theta)p(\theta)d\theta}
\end{aligned}
\qquad (5-8)
$$

where $p(\theta)$ is the prior distribution of *θ*, representing subjective prior knowledge about *θ*. $p(D|\theta)$ is the likelihood function, which can be viewed as a function of *θ* given the empirically observed data *D* which is considered fixed. It represents the likelihood that the given set of empirically observed data *D* is explained by the model with possible parameter values. $p(D)$ is the marginal likelihood, which is an integration of $p(D|\theta)$ over all possible values of *θ* across its space and therefore is not a function of *θ*, but a constant. This proportionality constant plays the role of normalizing the posterior density to ensure it integrates to 1. $p(D)$ is also known as model evidence, because it provides evidence for a candidate model, which is critical in selecting and averaging models as discussed later.

The posterior distribution $p(\theta|D)$ fully describes the uncertainty associated with the parameters. Essentially it updates the prior knowledge about the parameters in light of the empirical data. Generally, it is difficult or not possible to analytically express the posterior distribution. The solution is to instead simulate sample draws from the posterior distribution, such that the values

of these samples are distributed approximately according to the posterior distribution of the parameters of interest. The samples enable calculation of point estimates of the parameters, such as mean, median, or mode. More importantly, the samples of parameters enable drawing samples from predictive distributions associated with model outputs, e.g. the annual total building stock as the high-level emergent behavior of the dynamic building stock model, thus facilitating policy scenario analysis. Methodologically, this is realised using Markov chain Monte Carlo (MCMC) algorithm, as introduced later.

5.4.3 Posterior predictive distribution

With the posterior distribution $p(\theta|D)$, it is possible to make inferences about the total stock for a given year during the period of 2007 to 2017, an unknown observable denoted as $\tilde{y}$, given the known annual new buildings for the same year, denoted as x^* . This leads to the posterior predictive distribution of $\tilde{y}$:

$$p(\tilde{y}|x^*, D) = \int p(\tilde{y}|x^*, \theta)p(\theta|D)d\theta \qquad (5\text{-}9)$$

This equation suggests that the posterior predictive distribution is derived by marginalising the likelihood function $p(\tilde{y}|x^*, \theta)$ over the entire set of parameters, with each point in the space of parameters weighted according to its posterior probability given the empirically observed data.

5.4.4 Bayesian Model Averaging

The above posterior predictive distribution is conditional upon a choice of model M, i.e. a building stock model employing a particular parametric survival model, e.g. Weibull distribution. The equation can be written more explicitly as:

$$p(\tilde{y}|x^*, M, D) = \int p(\tilde{y}|x^*, \theta, M)p(\theta|D, M)d\theta \qquad (5\text{-}10)$$

There are multiple choices of parametric survival model, each of which may characterise the dynamics of building stock turnover. Candidates include Weibull, Lognormal, Gamma, etc. Let M_k denote a building stock turnover model using a plausible survival model k specified by parameter vector θ_k, and let $M = \{M_1, M_2, …., M_k\}$ denote the model space under consideration. This creates a model ensemble, which, when making predictions, takes into account the uncertainties associated with not only model-specific parameters but also the models per se. Now, the posterior predictive distribution of total building stock for the period of 2007 to 2017, $\tilde{y}$,

is calculated as:

$$p(\tilde{y}|x^*, D) = \sum_{k=1}^{K} p(\tilde{y}|x^*, M_k, D)p(M_k|D) \tag{5-11}$$

Where $p(\tilde{y}|x^*, M_k, D)$ is the posterior predictive distribution under model M_k given data D, and $p(M_k|D)$ is the posterior model probability (*PMP*), which is also referred to as model weight. Hence, the posterior distribution of $\tilde{y}$ predicted by the model ensemble, $p(\tilde{y}|x^*, D)$, is effectively the average of the posterior predictive distribution under each of the candidate models in the model space, weighted by their respective *PMPs*.

The *PMP* of model M_k can be interpreted as the probability of model M_k being the true model predicting $\tilde{y}$, given the observed data D, thus reflecting the extent to which M_k fits the observations as compared to other candidate models in the model space. *PMP* is given by:

$$p(M_k|D) = \frac{p(D|M_k)p(M_k)}{\sum_{j=1}^{K} p(D|M_j)p(M_j)} \tag{5-12}$$

Where $p(M_k)$ is the prior probability of model M_k being the true model, allowing the existing prior knowledge about the plausibility of model M_k to be specified explicitly, and $p(D|M_k)$ is the marginal likelihood (or model evidence) of model M_k, which is given by

$$p(D|M_k) = \int p(D|\theta_k, M_k)p(\theta_k|M_k)\mathrm{d}\theta_k \tag{5-13}$$

Where $p(D|\theta_k, M_k)$ is the likelihood of model M_k given observed data D, and $p(\theta_k|M_k)$ is the prior probability density of the parameters θ_k under model M_k. In fact, $p(D|M_k)$ is the denominator in the above equation (6) for calculating the posterior probability density of parameters θ_k under model M_k, as given by

$$p(\theta_k|D, M_k) = \frac{p(D|\theta_k, M_k)p(\theta_k|M_k)}{\int p(D|\theta_k, M_k)p(\theta_k|M_k)\mathrm{d}\theta_k} = \frac{p(D|\theta_k, M_k)p(\theta_k|M_k)}{p(D|M_k)} \tag{5-14}$$

Compared with equation (6), the above equation (12) explicitly applies subscript k to reflect that both the priors of model-specific parameters θ_k and the likelihood function of the observed data D are conditional on the particular model M_k in the model space.

Based on the above, the posterior mean of $\tilde{y}$, as predicted by the model ensemble, can be calculated as follows:

$$E[\tilde{y}|x^*, D] = \sum_{k=1}^{K} E[\tilde{y}|x^*, M_k, D]p(M_k|D) \qquad (5\text{-}15)$$

Clearly the BMA model ensemble prediction is the average of individual predictions weighted by the probability that an individual candidate model is true given the observed data. BMA model ensemble leads to a more spread posterior distribution of *y* than an individual candidate model does. This avoids the situation where inferences made based on an individual candidate model are overstated and decision-making based on predictions is much riskier than expected (Hoeting et al. 1999; Hoeting 2002; Li & Shi 2010; Fragoso et al. 2018).

5.4.5 Model space

In general, a range of parametric survival distribution functions are available to describe the survival process in various fields (Forbes et al. 2011; Liu 2012; Palisade 2016). However, literature on survival analysis or lifetime data analysis on buildings is limited. A survey on buildings in the Netherlands found that empirical survival probabilities of buildings were well approximated by Weibull distribution (OECD 2009). Miatto *et al.* (2017) tested various PDFs and found that the lognormal distribution offered the best fit to lifespans of buildings in Nagoya and Wakayama, Japan, where buildings were short-lived, with average lifespans shorter than 30 years. Zhou *et al.* (2019) applied the Weibull distribution to approximate lifetime uncertainties of Chinese urban residential buildings. From an economic perspective, buildings can be regarded as a type of capital asset, and accordingly building stock can be regarded as a type of capital asset, and accordingly building stock can be regarded as capital stock (OECD 2001; OECD 2009). Hence, a range of PDFs that have been used as a proxy for service lives and retirement/discard patterns of capital stocks may be applied to buildings, such as log-normal, Weibull, Gamma, and so on (Johnstone 2001; OECD 2001; Bohne et al. 2006; Müller 2006; OECD 2009; Aksözen et al. 2016; McLaren & Stapenhurst 2015).

In this chapter, the distribution functions used for approximating the lifetime distribution of Chinese urban residential buildings are Weibull, Lognormal, Loglogistic, Gamma and Gumbel distributions. Each distribution can characterise the turnover dynamics of the building stock, thereby representing a candidate model M_k in the model space *M*. The PDFs of these distributions are given in Table 5.1. Specifying the PDF of a distribution allows the CDF, survival function and hazard function of the distribution to be ascertained.

Table 5.1: Five candidate survival distribution functions

Distribution	Probability density function	Parameters	Priors
Weibull	$f(x) = \left(\dfrac{\alpha x^{\alpha-1}}{\lambda^\alpha}\right) e^{\left(-\left(\frac{x}{\lambda}\right)^\alpha\right)}$	Shape $\alpha > 0$ Scale $\lambda > 0$	$\alpha \sim \text{uniform}(1,10)$ $\lambda \sim \text{uniform}(1,100)$
Lognormal	$f(x) = \dfrac{1}{x\sqrt{2\pi}\sigma'} e^{-\frac{1}{2}\left[\frac{lnx-\mu'}{\sigma'}\right]^2}$ $\mu' = ln\left[\dfrac{\mu^2}{\sqrt{\sigma^2+\mu^2}}\right],$ $\sigma' = \sqrt{\ln\left[1 + \left(\dfrac{\sigma}{\mu}\right)^2\right]}$	Mean $\mu > 0$ Standard deviation $\sigma > 0$	$\mu \sim \text{uniform}(1,100)$ $\sigma \sim \text{uniform}(1,100)$
Loglogistic	$f(x) = \dfrac{e^{\frac{\ln(x)-\mu}{\sigma}}}{\sigma x (1 + e^{\frac{\ln(x)-\mu}{\sigma}})^2}$	Scale $\mu > 0$ Shape $\sigma > 0$	$\mu \sim \text{uniform}(1,100)$ $\sigma \sim \text{uniform}(1,100)$
Gamma	$f(x) = \dfrac{1}{\lambda \Gamma(\alpha)} \left(\dfrac{x}{\lambda}\right)^{\alpha-1} e^{-\frac{x}{\lambda}}$	Scale $\lambda > 0$ Shape $\alpha > 0$	$\lambda \sim \text{uniform}(1,100)$ $\sigma \sim \text{uniform}(1,100)$
Gumbel	$f(x) = \dfrac{1}{\sigma} e^{-\left(\frac{x-\mu}{\sigma}\right)} e^{-e^{-\left(\frac{x-\mu}{\sigma}\right)}}$	Scale $\mu > 0$ Shape $\sigma > 0$	$\mu \sim \text{uniform}(1,100)$ $\sigma \sim \text{uniform}(1,100)$

5.4.6   Model priors and model parameter priors

Prior probabilities of models reflect the prior knowledge, or belief, that a specific model is the true model in the domain concerned. Eliciting an appropriate prior is a non-trivial task in any Bayesian setting, and such difficulties are compounded in BMA because a probability measure for the model space, which is a more abstract parametric space, is not obvious in principle (Fragoso et al. 2018).

Whilst informative priors are expected to benefit model development and improve predictive performance, often non-informative priors have to be used due to little prior knowledge about the relative plausibility of the models considered. As a simple but reasonable neutral choice, it can be assumed that all candidate models in the model space are equally likely *a priori* (Hoeting et al. 1999; Li & Shi 2010). This means applying an uniform distribution over the model space, so that $p(M_j) = \frac{1}{K}, for\ j = 1, 2, \dots, K$. No model is considered more likely *a priori* than any other one. The consideration is to let the observed data carry all the information. This is the most commonly adopted practice in defining model priors in BMA settings (Fragoso et al. 2018). On this basis, the afore-mentioned five distributions of this chapter are assumed to have the equal prior probability equal to 0.2. This leads to the prior model probabilities being cancelled out and the *PMP* of a candidate model being proportional to its model evidence, namely, marginal likelihood.

The same consideration is applied to defining prior distributions of model-specific parameters. For any of the five candidate models, there is little prior information about its model-specific parameters. Hence it is straightforward to specify non-informative priors so as to allow the posteriors to be informed by data. As shown in Table 5.1, the priors of the model-specific parameters are all assumed to be uniformly distributed over their reasonable ranges in the context of generally short lifetimes of urban residential buildings in China.

5.4.7   MCMC sampling and posterior distribution calculation

MCMC is used to simulate the posterior distribution of a model-specific parameters. The principle is to draw values of a parameter vector θ from approximate distribution and then correct those draws to better approximate the target posterior distribution. Sampling is performed iteratively in such a way that at each step of the process it is expected that draws are made from a distribution that becomes closer to the target posterior distribution (Gelman et al. 2014). The sampling process is sequential, and the draws create an ergodic Markov chain, which, after a large number of iteration steps, evolves through the parameter space, becomes stationary and converges to the target posterior distribution. Subsequent model inference can be made based on samples from this process much as based on samples from the target posterior distribution (Hamada et al. 2008).

This study uses the Metropolis-Hastings algorithm, which is well established amongst available MCMC algorithms. At the start of iteration t, a candidate vector θ^* is generated from $\theta^{(t-1)}$ through a proposal distribution $f\left(\theta^* \middle| \theta^{(t-1)}\right)$, which is also known as a jumping distribution. The probability of θ^* being accepted to become $\theta^{(t)}$ is:

$$r = min \left\{ 1, \frac{p(\theta^*|data) \Big/ f(\theta^*|\theta^{(t-1)})}{p(\theta^{(t-1)}|data) \Big/ f(\theta^{(t-1)}|\theta^*)} \right\}$$ (5-16)

The acceptance probability r means that if the result is higher than 1, r is set to 1, the candidate θ^* is accepted and the transition from θ^* to θ^t is made. Otherwise, if the result is lower than 1, the candidate θ^* is accepted with probability equal to r and rejected with probability equal to 1-r. When accepted, the transition from θ^* to $\theta^{(t)}$ is made. When rejected, no move at iteration t is made, hence $\theta^{(t)} = \theta^{(t-1)}$, meaning that the chain is updated using the current value.

The proposal distribution $f(\cdot)$ is chosen to be a random walk proposal, where θ^* is selected by taking a random perturbation ε around the current value $\theta^{(t)}$, i.e. $\theta^* = \theta^{(t)} + \varepsilon$. The random vector ε is drawn independently of $\theta^{(t)}$ and centered on zero. As a common setting, ε is a normal distribution with mean zero and variance set to obtain efficient jumping algorithm (Jackman 2009; Gelman et al. 2014). In this regard, this study tunes the algorithm by using adaptive sampling, which generates new candidate parameters with a proposal covariance matrix that is estimated from the covariance matrix of the parameters generated so far, with a scaling factor of $2.4^2/d$, where d is the number of parameters (Soetaert & Petzoldt 2010b; Hartig et al. 2018).

5.4.8   Marginal likelihood calculation

Generally, the marginal likelihood is not analytically tractable and therefore has to be approximated using numerical methods. Typical Monte Carlo sampling methods include naïve Monte Carlo, Importance Sampling (IS), Harmonic Mean (HM), Generalised HM, and Bridge Sampling. The Naïve Monte Carlo is straightforward and in principle unbiased, but numerically inefficient and unstable if the posterior distribution is peaked relative to the prior method (Schöniger et al. 2014; Gronau et al. 2017; Fragoso et al. 2018). IS may overcome these issues by having an importance density with fatter tails than the posterior distribution (Ionides 2008; Gronau et al. 2017). HM uses the posterior distribution as the importance density. This results in the marginal likelihood being equal to the posterior harmonic mean of the likelihood. Despite its convenience and popularity, HM has been criticised extensively due to numerical instabilities and overestimation of the marginal likelihood (Xie et al. 2011; Schöniger et al. 2014; Pajor 2017). Generalised HM, a more stable version of HM, can be viewed as the reciprocal IS (Frühwirth-Schnatter 2004). Thus, for the reason analogous to IS, this method also requires the importance density to be finetuned to avoid unbounded variance. Specifically, it requires importance density to have thinner tails than the posterior distribution (Gronau et al. 2017; Wang et al. 2018; Fragoso

et al. 2018). Bridge Sampling is a general case of the afore-mentioned methods. Compared to IS and Generalised HM, it is more robust to tail behaviours of the proposal distribution (conceptually similar to importance density) relative to posterior distribution and thus avoids large or even infinite variances of estimators (Meng & Wong 1996; Frühwirth-Schnatter 2004; Gronau et al. 2017; Gronau et al. 2018). This study uses Bridge Sampling to approximate the marginal likelihood of each of the five candidate models.

5.5 Urbanisation rate and per capita floor area

The first of the two underlying driving factors, urban population, is determined in turn by total population and urbanisation rate. The historical data and future projection of China's total population are sourced from the official statistics of the Chinese government (National Bureau of Statistics 2018) and the World Population Prospects by the United Nations (United Nations Population Division 2017). As for the urbanisation rate, China has been experiencing consistently rapid urbanisation over the past few decades (National Bureau of Statistics 2018) and such a trend is anticipated to continue in the future (Asian Development Bank 2013; UNDP 2016). The projection by World Urbanization Prospects 2014 indicated that China would reach a urbanisation rate of 68.7% by 2030, 72.8% by 2040 and 75.8% by 2050 (United Nations Population Division 2014). Joint research by the World Bank and the Development Research Centre of China's State Council pointed out that the inflection of China's urbanization rate, namely the highest annual rate of urbanization rate change, already occurred in 2008 and the rate would surpass 62% in 2020, 70% in 2030 and 76% in 2050 respectively (World Bank 2014). It is therefore considered reasonable to project the future development trend of urbanisation rate based on historical trajectory and the expected saturation level over the long term. The generally S-shaped curve of the overall trend justifies the use of a logistic growth model.

$$Urbanisation_t = \frac{Urbanisation_{Peak}}{1 + e^{a+b(t-BaseYear)}} + \varepsilon_t \tag{5-17}$$

In the above equation, BaseYear is taken as 1978, the milestone year marking the beginning of nation-wide reform and opening-up policy. Urbanisation$_{Peak}$ is the upper asymptote, representing the expected saturation level of urbanisation over the long term. ε_t is the error term, which is assumed to be normally distributed with mean zero and unknown variance σ^2, i.e. $\varepsilon_t \sim N(0, \sigma^2)$. In addition, a and b are parameters determining the shape of the Logistic curve. Using urbanisation rate data available from the official statistics of Chinese government (National Bureau of Statistics 2018) and the World Urbanisation Prospects 2014 (United Nations

Population Division 2014), the vector of unknown parameters of the urbanisation model, including Urbanisation$_{Peak}$, a, b and σ, can be estimated through MCMC.

The other driving factor, PCFA, is modelled by applying a Gompertz growth model. Both Gompertz and Logistic belong to the Richards family of sigmoidal growth models. Different from Logistic function, the curve of Gompertz function is not symmetric about its point of inflection, which is reached early in the growth trend. The future value asymptote on the right hand is approached much more gradually by the curve than the lower value asymptote on the left side (Trappey & Wu 2008; Shukla et al. 2015; Tjørve & Tjørve 2017). Both Logistic and Gompertz models have been used to model PCFA (Huang et al. 2013; Li & Xu 2013; Hong et al. 2014; IEA 2017; Xu & Liu 2018). Li and Xu (2013) and Xu and Liu (2018) argued that a Logistic model is more suitable for describing growth at economy take-off stage whereas a Gompertz, showing a more apparent increasing trend at a later stage, can better reflect the development of rising demand for urban housing along with the increase of per capita income. This study uses a Gompertz model, which can be defined as follows:

$$PCFA_t = PCFA_{peak}e^{-e^{a(t-BaseYear)+b}} + \varepsilon_t \qquad (5\text{-}18)$$

where PCFA$_{peak}$ is the expected saturation level of PCFA over the long term; a and b are parameters determining the shape of the Gompertz curve; and $\varepsilon_t \sim N(0, \sigma^2)$ is the error term.

In estimating the vector of parameters of the Gompertz model, a challenge is the lack of reliable PCFA data. The historical PCFA data published by various official sources have been found to be over-estimated due to sampling representativeness issues (Shen 2013; Liang 2014; Ren et al. 2019; Li & Xu 2013; THUBERC 2017). This research takes an alternative approach. Samples are drawn from the posterior predictive distribution of the total stock for the period of 2006 to 2017 and each sample, comprising 12 data points, is divided by official data on annual urban population to get a sample of PCFA (12 data points) of the same period. This way, a number of samples of PCFA are obtained. In addition, to increase the number of data points and also to take into account the importance of possible future policy targets, additional data points for future years are added to each sample of PCFA.

The literature suggests that there is a considerably large variation in possible future PCFA levels, ranging from 24 to 60 m^2 per capita. Peng, Yan and Jiang (2013) indicated that residential building floor area in urban China should remain at 24m^2 per capita in order to control total building energy use. The Energy Research Institute (ERI) under China's National Development and Research Commission predicted that total floor area of urban residential buildings in China would reach

43.953 billion m^2 by 2030, corresponding to 42.7 m^2 per capita, a level similar to those in developed countries in 2007 (ERI 2014). IEA's Energy Technology Perspectives 2015 forecasted that residential floor area in China would reach 52m^2 per capita in the timeframe of 2030 to 2050 (IEA 2015). A joint report by IEA and THUBERC estimated that average floor area per person could increase to 58m^2 by 2050, although this level was considered unrealistic given high density levels in China (IEA and THUBERC 2015). THUBERC (2017) argued that urban residential floor area over the medium to long term should not exceed 35 m^2, thereby curbing total floor area of urban residential buildings below 35 billion m^2. According to a recent study on China's deep decarbonization led by China's National Centre for Climate Change Strategy and International Cooperation (2018), residential floor area per capita in China should be kept at the level of approximately 36 to 37 m^2 from 2030 to 2050. Such a large variation suggests high uncertainties associated with PCFA and therefore justifies the forecast of future trajectories in a Bayesian framework.

Taking these estimates from the existing literature into consideration, four additional data points reflecting possible future PCFA levels, 35m^2 for 2030, 40m^2 for 2040, 45m^2 for 2050 and 50m^2 for 2080, are added to the 12 data points of each PCFA sample to estimate the posterior distributions of the four parameters of Gompertz model (PCFA$_{Peak}$, a, b and σ) through MCMC. Samples are drawn from the results from each MCMC, which is based on each sample of PCFA comprising 16 data points, and then are combined to obtain the posterior distributions of the four parameters.

5.6   Results and discussion

5.6.1   Posterior model probabilities (*PMPs*)

Based on the methodology elucidated above, the posterior distributions of model-specific parameters of each candidate model, $p(\theta_k|D, M_k)$, were obtained using official statistics on total stock of urban residential buildings up to 2006. The primary data sources included China Statistical Yearbook and MOHURD's Statistical Communique on Urban Housing. Then, the evidence of each candidate model, i.e. the marginal likelihood, was numerically estimated using bridge sampling technique, and the PMP was calculated (Table 5.2).

Table 5.2: Prior and posterior probabilities of the five candidate models

Model	Prior	PMP
Weibull	0.2	0.219
Lognormal	0.2	0.25
Loglogistic	0.2	0.096
Gumbel	0.2	0.42
Gamma	0.2	0.015

5.6.2 Prediction of historical stock

With each candidate model, the posterior predictive distribution of total stock over the period of 2007 to 2017, $\tilde{y}$, was obtained through running the probabilistic stock turnover model using the posterior distributions of model-specific parameters, i.e. $p(\theta_k|D, M_k)$, and official statistics on annual new construction from 2007 to 2017. The posterior distribution of $\tilde{y}$ predicted by the BMA model ensemble is the PMP-weighted average of the posterior predictive distribution of $\tilde{y}$ under each candidate model in the model space. Operationally this was obtained by drawing samples from model-specific predictions with probabilities equal to the PMPs and then combining the samples. Figure 5.2 shows the 95% credible interval of posterior prediction of total stock by the BMA model ensemble. As expected, the total stock size was characterised by a continuously ascending pattern over time. The mean of the credible interval increased by 33% over eight years from 17.7 billion m^2 in 2010 to 23.6 billion m^2 in 2017.

Clearly the line representing the mean of credible interval exhibits a good fit with the estimate by the Annual Report on China Building Energy Efficiency (THUBERC 2019a), which was developed by Tsinghua University Building Energy Research Centre (THUBERC) and is widely recognised as an authoritative report on the overall situation of building energy in China.
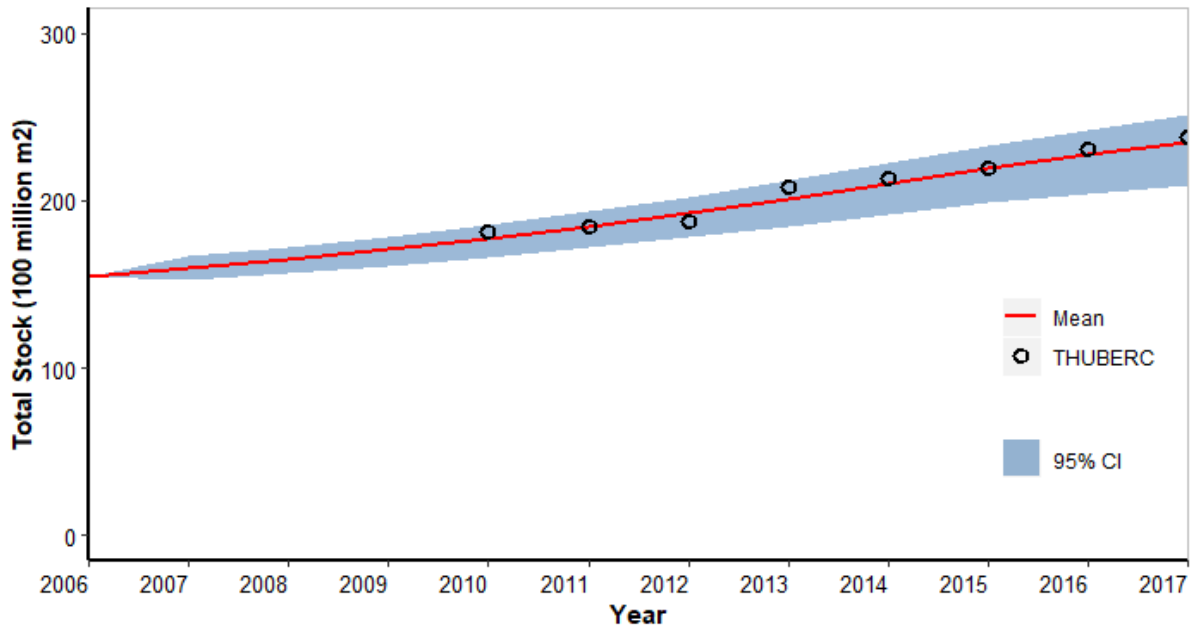
Figure 5.2: 95% Credible interval of BMA ensemble's posterior prediction of total building stock

Due to the lack of official statistics on annual demolition, it is not possible to directly cross-validate the modelling result using historical annual demolition data. In an indirect way, though, comparing the demolition estimated in this study with previous studies provides an alternative basis for evaluating the robustness of the modelling approach and results. According to THUBERC (2012), the ratio of aggregated demolished buildings to aggregated newly constructed buildings over China's 11th Five-Year Plan Period (2006 to 2010) was approximately 34%. In this study, using the mean of the posterior predictive distribution of the aggregated demolished buildings modelled over this period, this ratio is calculated to be 32%, very close to the THUBERC (2012) estimate. In absolute terms, the mean of posterior predictive distribution of annual demolition of this study is of the same order of magnitude as previous studies. For example, for 2010, the annual demolition was estimated by this study to be 1.47 billion m^2, somewhere between the approximately 1.3 billion m^2 by (Hu, Bergsdal, et al. 2010), and the approximately 1.7 billion m^2 by (Huang et al. 2013).

Compared with a single point, deterministic estimate of annual stock size, the BMA approach taken by this study produces a profile for annual stock size, i.e. the posterior predictive distribution (Figure 5.3). This probabilistic estimate of annual stock size captures both models' and the model-specific parameters' uncertainties. Having depicted all possible pathways of stock evolution, it provides a full distribution of existing stock size per year and therefore helps to improve the reliability and robustness of not only the estimate of existing stock, but also the forecasting of future total stock which, as explained in previous sections, is a function of the existing stock, the underlying survival models and parameters, and expected future demand for

housing area. The results of forecasting future stock are given in the next section.
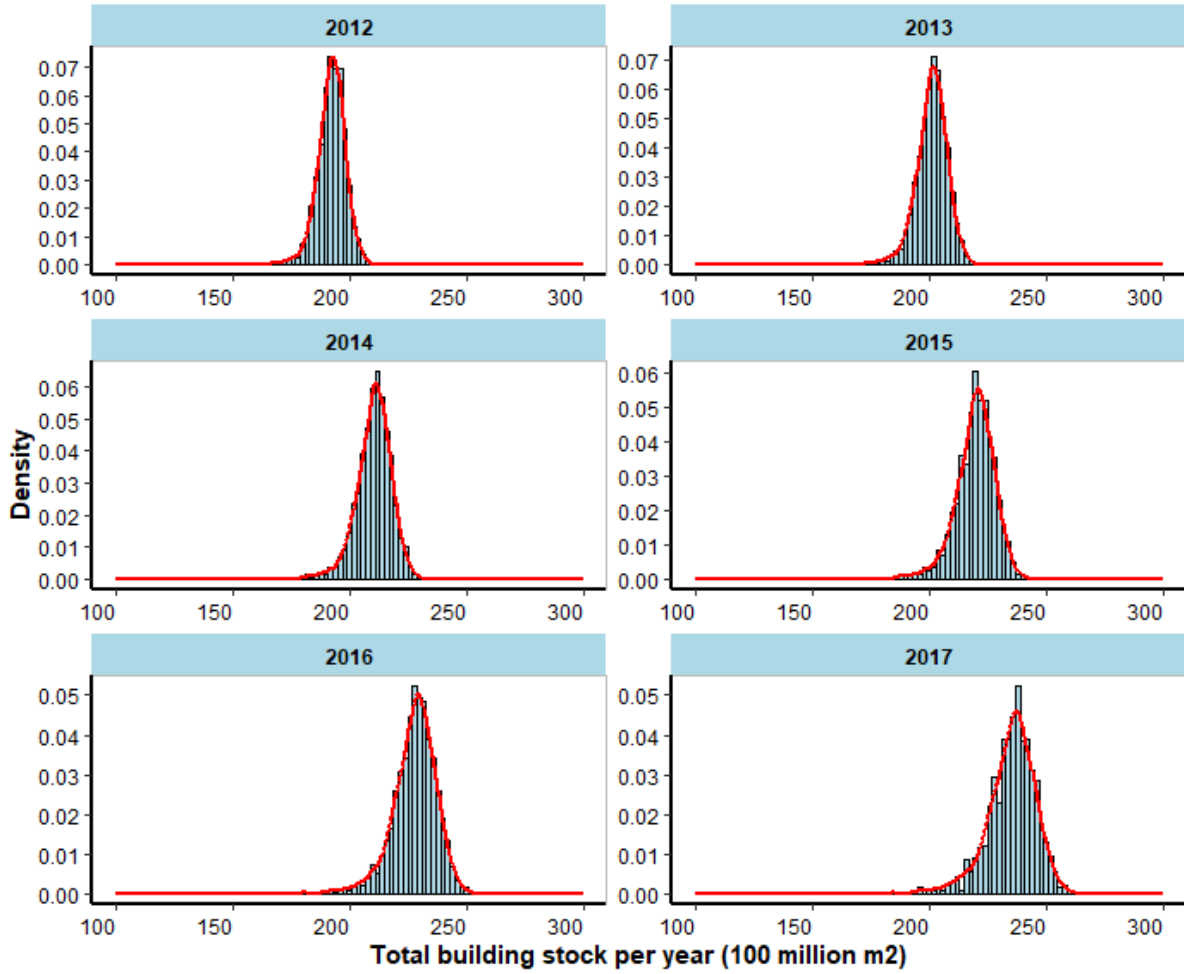
Figure 5.3: Posterior predictive distribution of total stock (2012-2017)

5.6.3   Forecast of future stock

The forecasts of future stock turnover dynamics are based on posterior predictive distribution of total stock in 2017 and the interplay between new construction, demolition, existing stock and expected stock. Operationally, the System-Dynamics-based future stock turnover model has five versions, each of which is based on one of the five candidate survival models (Weibull, Lognormal, Loglogistic, Gumbel, Gamma). For each version, such as Weibull, a large number of combined samples are drawn from the posterior distributions of survival model-specific parameters, posterior distributions of vector of parameters of PCFA model, and posterior distributions of vector of parameters of urbanisation model. Using each sample of combined parameters, that particular

version of stock turnover model is run to obtain a distinct trajectory of future stock evolution up to 2100. The trajectory reflects the stock's underlying composition of age-specific substocks in each year. Upon completing running that particular version of stock turnover model using all the samples of combined parameters, the family of trajectories of future stock evolution together produce the distribution of the total stock size per year corresponding to that particular version of the stock turnover model. By repeating this process for each version of the stock turnover model and then combining the version-specific family of trajectories in proportion to posterior model probabilities, the distribution of the total stock size corresponding to the BMA model ensemble is obtained.

As shown in Figure 5.4, driven by rising urbanisation rate and expected demand for PCFA, the total stock steadily increases over the next two decades. From around 2040 onwards, while the total stock remains the general ascending trend, its growth starts to decelerate as the inflection point is being approached. The peak of the curve occurs around 2065, when the mean of the distribution of total stock size reaches 46.3 billion m^2 and the 95% credible interval is in the range of 42.4 to 50.1 billion m^2. After 2065, the total stock starts to shrink slowly. This is due to the projected decrease of total population around the same period, the effect of which outweighs the continuous (but decelerating) increase in urbanisation rate and PCFA. By 2100, the total stock is estimated to have a 95% credible interval of 39.1 to 47.3 billion m^2. The probability distribution of annual total stock size in various years in presented in Figure 5.5. This figure offers a full picture of the probability distribution of the total stock size per year, as the uncertainties associated with not only model-specific parameter vector, but also the models in the model space are propagated through the emergent behaviours of the model outputs, namely, the dynamic evolution of the stock and the associated substocks.
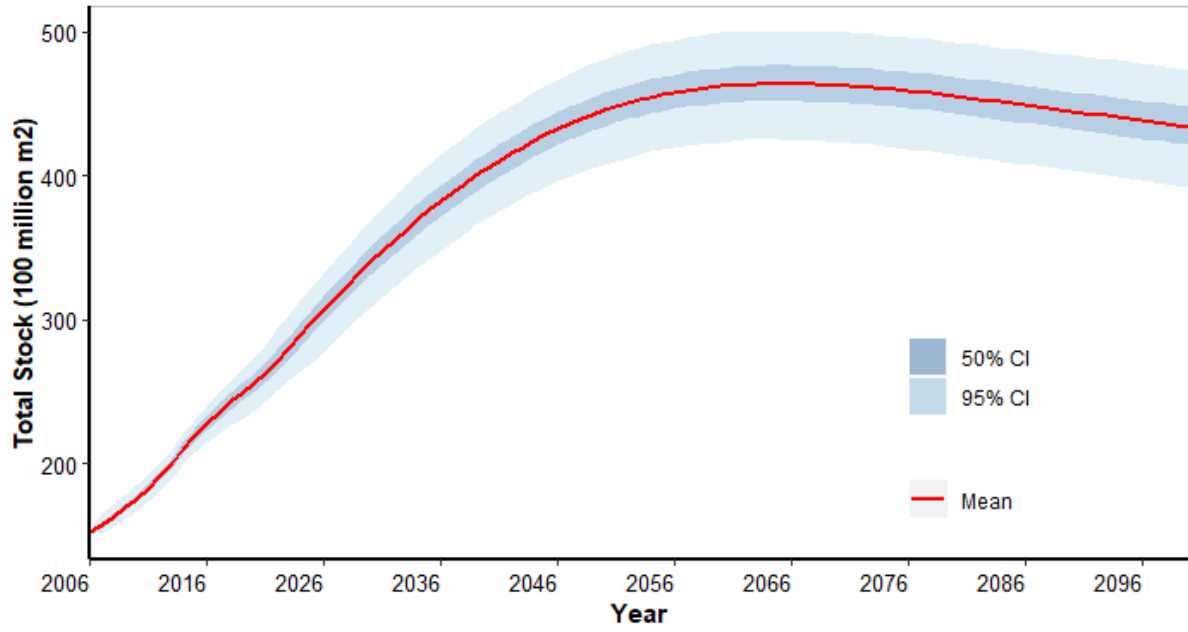
Figure 5.4: Posterior predictive distribution of stock trajectories from 2006 to 2100
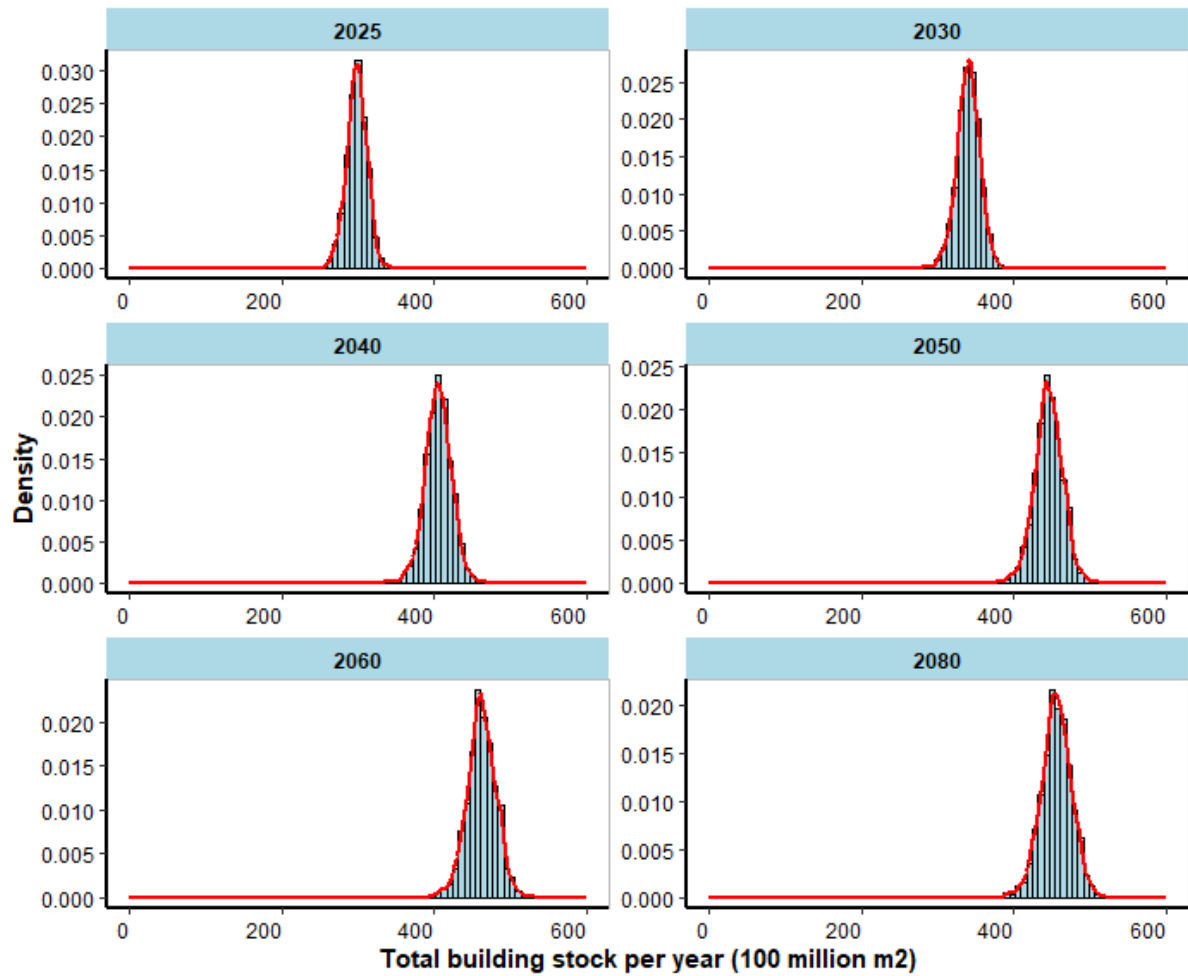
Figure 5.5: Posterior predictive distribution of total stock in various years

Underlying total stock is the dynamic evolution of the underlying age-specific substocks, which collectively form the total stock. The highly granular building stock turnover model developed through System Dynamics modelling offers additional insights into the composition of building stock through explicitly modelled building aging process. For each parameter vector in the parameter space of a candidate model in the mode space, the annual total stock is disaggregated into age-specific substocks, each of which goes through an aging process subject to age-specific demolition rate determined by the hazard function specified by this particular parameter vector of this particular candidate model. For each year, the substock of new buildings constructed in this year and the substocks of existing buildings at various ages that remain in use collectively create the age profile of the entire stock. For the year after, the stock's age profile is updated due to new construction, aging and demolition. These on-going dynamics, which result in the turnover of the overall stock and detailed representation of age-specific substocks, are fully captured in the dynamic model and, more importantly, are further characterised probabilistically by the BMA model ensemble through the posterior distributions of model-specific parameters and PMPs of candidate models. This allows us to obtain the full distribution of each age-specific substock in any given year and makes possible tracking and analysis of specific substocks. Figure 5.6 shows the posterior predictive distributions of substocks aged 10, 20, 30, 40, 50 and 60 years within the total stock in 2060.
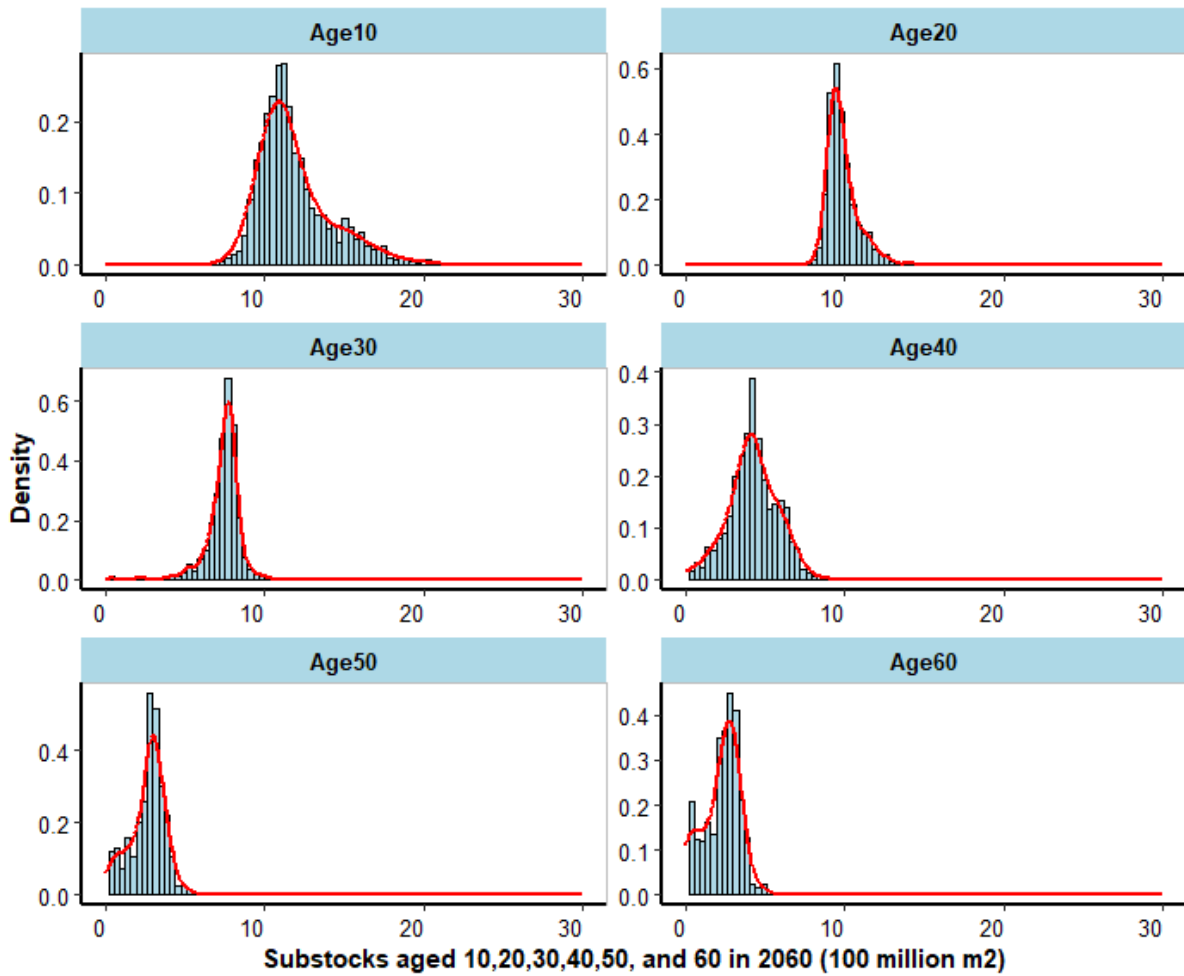
Figure 5.6: Posterior predictive distribution of substocks at various ages in 2060

Figure 5.7 and Figure 5.8 respectively show the distributions of annual construction of new buildings and annual demolition of old buildings obtained from the BMA model ensemble. Overall, future new buildings constructed per year are not expected to vary significantly from the recent historic levels. After experiencing a gradual increase from 2018 to 2025, the mean of annual new buildings maintains a generally stable level at approximately 1.5 billion m^2 for two decades and then starts to progressively decrease and eventually approach 1 billion m^2 by 2100. Such a general trend is as expected, because annual new buildings, serving as the incremental part of the total stock, is predominantly influenced by the expected demand of total stock whose increase rate slows down over time.[3] As for annual demolition, its curve shows a smoothly slowly

___

[3] A kink in year 2018 can be observed on the red line as the mean of the distribution which represents a large number of possibilities. Each possibility is the result of stock evolution process modelled using a particular combination of random samples from the urbanisation rate, PCFA, survival model-specific parameters, the survival model itself, and the stock size and age profile in 2017. Due to this random sampling, there are, inevitably, a substantial share of the possible results where incremental housing demand in 2018 would be high and thus would need to be met by an annual new construction in 2018 much higher than the actual amount in 2017. Meanwhile, there are also many possible results where the momentum of housing demand growth in 2018 would not be very strong and thus the annual new

ascending trend because a stock that builds up over time comes with an increasing aggregate of various amounts of demolished buildings at various ages. From 2053 to 2100, the mean of annual demolition remains being in a relatively narrow range of 1.1 to 1.2 billion m^2 for nearly 50 years. The peak of annual demolition occurs around 2073 and 2074, several years later than that of the total stock. The reason is that, from a stock-and-flow perspective, the demolition is an outflow from the stock with a time lag relative to the inflow. Whilst the annual demolition is made up of a large number of age-specific demolition quantities corresponding to age-specific substocks, such a mathematical complexity does not change the fundamental mechanism but only the extent of time lag, which is dependent upon building lifetime distribution. For both annual new buildings and annual demolition, their predictive distributions, as characterised by 50% and 95% credible intervals, reflect the uncertainties associated with the parameters of the Logistic model for urbanisation, the parameters of the Gompertz model for PCFA, the parameters of each of the five survival models for lifetime distribution and demolition probability, and the survival models themselves.
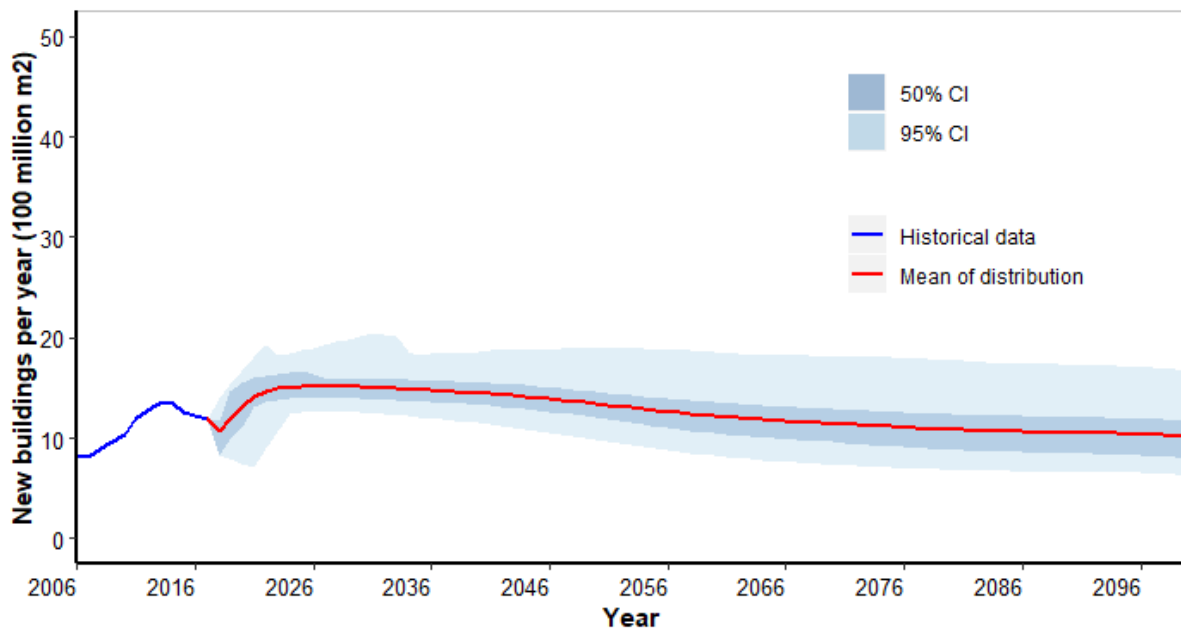
Figure 5.7: Posterior predictive distribution of annual new buildings

---

construction in 2018 would be lower than the actual amount in 2017. The same logic applies to year 2019, 2020, and so on. Averaging all these possibilities for each year produces the mean line as an indication of the general trend.
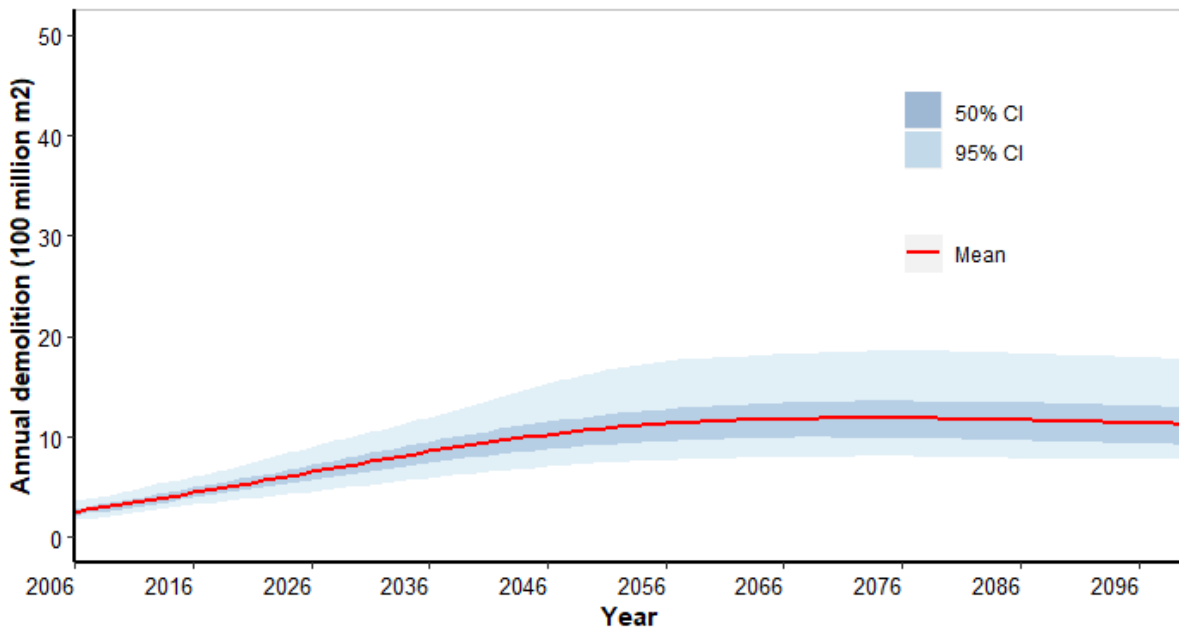
Figure 5.8: Posterior predictive distribution of annual demolition

5.6.4 Implications for building stock energy modelling

The value of establishing the BMA model ensemble and obtaining posterior predictive distributions of stock, sub-stocks, annual construction and annual demolition goes beyond forecasting the turnover dynamics of the residential stock per se. It has significant implications for further modelling and analysis of building energy consumption at stock level.

Firstly, the possible lifetime distribution profile specified by a parameter vector in the parameter space of a candidate model enables explicit estimate of annual construction of new buildings and demolition of old buildings, which are fundamental to quantifying the initial and demolition embodied energy incurred every year. The lifetime distribution enables a closer look at annualised embodied energy converted from the capital cost in embodied energy associated with future cohorts of new buildings, in the context of changing building materials and construction techniques and the resultant changing embodied energy intensities. The impact of potentially varying lifetime distribution on embodied energy, such as longer average lifetime, via planning policy or as a result of economic and environmental factors, can be examined. This is examined in Chapter 6.

Secondly, model granularity at the level of age-specific building sub-stocks offers a detailed representation of the building stocks heterogeneity with respect to operational energy performance. With buildings identified as a key sector for energy savings, it is reasonable to expect that new buildings, particularly those in urban areas, will be built to higher standards of

operational energy performance due to increasingly stringent design codes, on-going technological advances and improving operation and management practices. Separately tracking the aging process of different cohorts of buildings enables a holistic and in-depth understanding the dynamics of the stock composition of buildings with different operational performance and a detailed evaluation of the trajectories of stock-wide average operational energy intensity per m^2. This is examined in Chapter 8.

Thirdly, more importantly, the ability to model the temporal stock dynamics enables the integration of embodied and operational dimensions of building energy, as presented in Chapter 9. By simultaneously investigating both dimensions, it is possible to explore their relative importance in the context of future building sectoral developments in increasingly extensive production and use of green building materials, improving construction practice and building quality, strengthening design codes for new buildings, scaling up energy-related retrofits of existing buildings, possible policy considerations to manage aged buildings, etc. In so doing, a fuller understanding of stock-level lifecycle energy of urban residential buildings can be reached so as to better assist policy-makers in formulating policies aiming to promote energy savings and decarbonisation of buildings.

Across the three dimensions, the uncertainties associated with model-specific parameter vectors and candidate models, as fully captured by the BMA model ensemble, along with uncertainties of other parameters and input variables needed for modelling energy and carbon, can be propagated into the emergent stock-level outputs, such as annual total embodied energy and annual total operational energy of total stock. The full Bayesian approach and the resultant probabilistic distributions of stock-level outputs can mitigate the risk of potential over- or under-estimate that would otherwise be more likely to be produced by deterministic models. From a policy-making perspective, probability distributions of different potential outcomes of policy scenarios can be generated. This is particularly important in the context of analysing the decarbonisation of the generally short-lived Chinese buildings, where there is likely to be a strategic trade-off between operational and embodied energy due to the above-mentioned factors. For example, as presented in Chapter 9, it would be useful to explore the probability that one policy, e.g. extending building lifetime to avoid embodied energy, would yield a more favourable outcome of stock-level whole-life building energy consumption as compared to another policy, e.g. accelerating stringency of new building design codes to reduce operational energy. In this sense, this chapter creates a powerful modelling framework with enhanced robustness and reliability, thereby preparing a solid ground for more effectively experimenting and analysing policies aiming to decarbonise buildings in the broader context of curbing China's economy-wide emissions. This is a major contribution of this thesis.

5.6.5 Wider applicability of the modelling approach

It is useful to accentuate the value of this study in a broader international context. This study contributes an innovative methodological approach to the general field of building stock modelling. The generality, flexibility and transparency of the approach enables its application in a wide variety of geographical contexts. It is particularly relevant and useful to countries experiencing rapid urbanisation and massive construction, such as developing countries in South and Southeast Asia (World Bank 2015; Ellis & Roberts 2016; ASEAN Secretariat 2018). Addressing building energy and carbon emissions has been emphasized as a key climate change mitigation strategy in the Nationally Determined Contributions (NDCs) of these countries (IEA and UNEP 2018; UNFCCC 2020). Correspondingly, building energy is also amongst the focus areas on the development agenda of multilateral and bilateral donor agencies providing loans, grants and technical assistance to these countries. The modelling approach and its application in the Chinese context as elaborated in this chapter is well placed to provide a useful reference for these countries and donor agencies to take stock of their existing buildings, forecast possible stock evolution pathways and evaluate stock-level energy consumption and carbon emissions under different policy and intervention scenarios.

5.7 Chapter summary

A good understanding of building stock turnover dynamics is a fundamental prerequisite to sensible modelling of stock-level building energy consumption to better inform policy-making. This chapter presents a novel modelling approach to estimating recent historical total stock of urban residential buildings in China and also to forecasting future trajectories of the stock evolution. A disaggregated build stock model is developed using System Dynamics to characterise the building aging process and stock turnover dynamics. This model is then operationalised by separately investigating five candidate parametric survival models to represent the uncertainties associated with building lifetime. With each survival model, the stock turnover is simulated through Markov Chain Monte Carlo methods to obtain the posterior predictive distribution of total historical stock and the marginal likelihood used to estimate the posterior model probability. Bayesian Model Averaging is applied to create a model ensemble to combine model-specific predictions of the historical stock evolution pathway based on model probabilities. By extending the model structure and incorporating variables relating to possible trends in urbanisation and demand for per capita floor area, future stock turnover dynamics through 2100 are forecasted using each survival model and then combined through model averaging. In so doing, the model produces not only forecasts of total stock, age-specific

substocks, annual new construction and annual demolition, but also their posterior predictive distributions which fully characterise their uncertainties.

In summary, this chapter, as the core of this thesis, offers a first-of-a-kind analysis that employs a full Bayesian approach to investigate the uncertainties associated with modelling Chinese building stock. Critically addressing this highly policy-relevant but substantially under-researched area is a major contribution of this thesis. The modelling approach adopted here is well suited to carry out studies of stock-level energy and carbon impacts. In particular, the model's ability to explicitly track the aging process of substocks and fully represent probability distributions at both the stock and substock level is critical to analysing policy trade-offs facing Chinese residential buildings regarding embodied versus operational energy consumption and carbon emissions in the context of sector-wide decarbonisation. The results of this chapter answer research question Q2 and also prepare the foundation for further modelling on embodied energy in Chapter 6 and operational energy in Chapter 8.

6

Historical and future embodied energy

6.1 Chapter introduction

This chapter aims to estimate historical embodied energy and forecast future trajectories, as posed in research question Q3. The probabilistic forecasts of the annual new construction and annual demolition over the medium to long term, obtained in Chapter 5, provide key inputs to this chapter. Additional modelling on building material intensity, energy intensity of building material production, energy intensity of construction and demolition, and energy intensity of materials transportation is conduced. The resultant business-as-usual scenario of future embodied energy trends is compared with two policy scenarios involving building lifetime variation.

6.2 Methodology

This section presents the probabilistic stock-level model for tracking embodied energy and estimating its future evolution.[4] The embodied energy modelled in this thesis refers to the

---

[4] The embodied energy calculated in this chapter, operational energy in Chapter 8, and whole-life energy in Chapter 9 refer to primary energy, either in the unit of tonne of coal equivalent (tce) for absolute amount, or in the unit of kilogram of coal equivalent per square metre (kgce/m^2) for intensity. The consumption of electricity and gas is converted to coal equivalent. This is in line with the established practice in energy quantification and statistics in China. For example, primary energy is used in the China Energy Statistical Yearbook published by National Bureau of Statistics, the Standard for Energy Consumption of Building issued by MOHURD, and the Annual Report on China Building Energy Efficiency prepared by THUBERC.

aggregate of energy consumption incurred by building material production, transportation, on-site construction, and demolition. This boundary covers the product stage (A3), construction process stage (A4-5) and part of the end-of-life stage (C1) according to the building lifecycle stages defined in European Committee for Standardization CEN 15978 (CEN 2012). The probabilistic model consists of a series of components: forecasting the possible future annual new construction in stock turnover dynamics (section 6.2.1); establishing probability distributions of building material intensities (6.2.2); estimating the trajectories of the energy intensities of producing building materials (6.2.3); construction and demolition of buildings (6.2.4); and transportation of materials (6.2.5). The uncertainties of these input variables are propagated using Monte Carlo simulations to obtain the probabilistic distribution of the embodied energy of new construction per year.

6.2.1   Annual new construction

In official statistics up to the present, annual new construction of urban residential buildings is a known statistic and therefore can be directly used to estimate annual embodied energy. For the future, it is an unknown variable which is estimated through modelling the evolution of the building stock over time. This has been described in detail in Chapter 5. The results of forecasted annual new construction in Chapter 5 are used in this chapter.

6.2.2   Building material intensity

Building material intensity, defined as the quantity of a given building material (kg or ton) per unit of constructed floor area (m^2), varies substantially with building characteristics as a synthesis of cost, architectural design, structural type, heights, geological condition, climatic condition, environmental performance, etc. Such variability reflects the uncertainties of material intensity which can potentially be characterised by a probability distribution for material intensity. Provided that there exists a reasonable amount of empirical data on material intensity, the probability distribution can be approximated by fitting the data to a chosen distribution function. Whilst a normal distribution is a plausible choice, it does not necessarily offer a good fit with the empirical data, as there could be considerable skewness of data distribution that cannot be neglected (Laner et al. 2014; Heeren & Fishman 2019). Skewed distributions such as Weibull or Gamma might fit the data better than a symmetrical normal distribution (Cao et al. 2016; Roh et al. 2019). Thus, these distributions should be explored and the one offering the best fit with the data, as measured by relevant goodness-of-fit criteria such as Akaike's Information Criterion (AIC) and Bayesian Information Criterion (BIC), should be used to generate random samples of material intensity for Monte Carlo simulation.

Despite its importance for various types of assessments, material intensity data is only sparsely available for limited regions in the world (Heeren & Fishman 2019). In China, no official statistics on building material use intensity exist (Zhang et al. 2019). Limited empirical data has been based primarily on individual case studies. There is a dearth of large-scale survey and statistics. Although some previous studies referred to surveys conducted by other parties (Gu 2009; Zhang et al. 2019), detailed data is not publicly accessible. This thesis refers to Zhao et al. (2014) for material intensity data. Their data was collected through surveying over 150 urban residential buildings in different Chinese cities. These samples covered major structural types of residential buildings in the Chinese urban context, including brick-concrete, shear wall, frame-shear and steel (Zhang et al. 2019).

Table 6.1 shows the surveyed intensities of typical building materials, which are categorised into low-rise, mid-rise and high-rise residential buildings (Zhao et al. 2014). Amongst these materials, steel and cement are the most extensively used (Zhang et al. 2019), and their production also consumes significantly more energy than other materials (Zhao et al. 2014). Aluminium and glass are also energy-intensive in their production process (Hong et al. 2016). For the entire Chinese building construction sector, the energy consumption of steel, cement, aluminium and glass production combined account for 92% of the total energy consumption of all building materials production (THUBERC 2019a; Zhang et al. 2019). Therefore, this thesis focuses on steel, cement, aluminium and glass in its modelling.

Table 6.1: Average material intensity of residential buildings

Type of residential buildings / Materials	Low-rise residential buildings	Mid-rise residential buildings	High-rise residential buildings
Steel (kg/m^2)	59.00	65.69	84.90
Cement (kg/m^2)	306.10	182.59	167.71
Aluminium (kg/m^2)	0.00	0.04	0.91
Sand and gravel (kg/m^2)	705.11	27.48	336.32
Ready-mixed concrete (m^3/m^2)	0.12	0.23	0.33
Brick (unit/m^2)	266.70	22.44	5.16
Non-load-bearing block masonry (m^3/m^2)	0.00	0.11	0.03
Glass (kg/m^2)	0.75	0.35	1.13
Ceramics (kg/m^2)	11.11	1.04	7.49
Wood (m^3/m^2)	0.01	0.00	0.00
Building stone (kg/m^2)	16.18	0.00	0.00

During the model selection process, for steel and cement, the empirical intensity data from the building samples was fitted to the following candidate distributions: Gamma, Lognormal, Normal and Weibull. The best-fit distribution was Weibull for steel and Gamma for cement, respectively. For glass, intensity data was available for less than half of the samples. Combining this data with the data given by other studies (Yu & Li 1999; Zhu et al. 2020) and performing distribution-fitting found that glass intensity was best approximated by a Lognormal distribution. Compared to glass, there were substantially fewer samples of buildings reporting their consumption of aluminium. The sparse building-specific data on aluminium intensity did not allow the candidate distributions to be fit informatively. Thus, this study assumed that aluminium intensity would follow a normal distribution, with its mean value set based on the samples as well as limited data given in other studies (Hong et al. 2016; Zhu et al. 2020). The standard deviation of the normal distribution is assumed to be 0.5.

The univariate distributions obtained from data-fitting, namely the Weibull distribution for steel, Gamma distribution for cement, Lognormal distribution for glass, and Normal distribution for aluminium, are all marginal distributions. In reality, the intensities of these major materials are correlated to some extent, because the use of these materials in residential buildings largely follows some general pattern reflecting the typical choices of building structures and common practices of design and construction in urban context. This means the material intensities are not independent but dependent random variables. This has an important implication since drawing random samples from the fitted marginal distributions of the material intensities and then combining them to represent the materials use of a simulated building sample will likely result in a practically unrealistic combination of materials. For example, the simulated sample might have some unreasonable combination of very high cement intensity and very low steel, or vice versa. It is therefore necessary to capture the underlying dependence structure between the material intensities by finding the multivariate joint distribution.

The dependence structure of material intensities is modelled through a copula, which by definition is a d-dimensional distribution function on the hypercube $[0,1]^d$ with standard uniform univariate margins (Schmidt 2007; Killiches et al. 2017). According to Sklar's theorem, which is fundamental to the copula concept and application, any multivariate joint distribution can be written in terms of univariate marginal distributions and a copula which describes the dependence structure between random variables. Conversely, given a copula and univariate marginal distributions, a multivariate joint distribution can be defined. That is, a copula serves as the link of a multivariate joint distribution to its univariate margins (McNeil et al. 2015; Hofert et al. 2018; Zhang & Singh

2019). Putting this into the context of this study, a copula can be applied to form the multivariate joint distribution of steel, cement, glass and aluminium intensities based on their respective empirically obtained marginal distributions. The constructed multivariate joint distribution can then be used to generate random samples of vectors of material intensities.

As compared to steel and cement, the marginal distribution of glass intensity was fit using much less available data and that of aluminium intensity was estimated even more arbitrarily. Taking this into consideration, this study focuses on the dependence between steel intensity and cement intensity, thereby reducing the potentially 4-dimensional multivariate distribution to a bivariate distribution. Operationally, this means random samples of glass intensity and aluminium intensity are drawn from their respective marginal distributions, independently of the bivariate joint distribution of steel and cement intensities. Such a simplification has very limited impact on materials production energy consumption, which has been found to be dominated by steel and cement in most previous studies in the above literature review section.

This study also takes into consideration the longitudinal variation of steel and cement intensities over time. There has been an observed trend over the past two decades that the share of brick concrete structure in new residential buildings constructed every year has been declining steadily, whereas frame-shear and shear wall structures have become the mainstream, especially in large cities (Zhang et al. 2019). Such a transition in structural types has increased the average steel intensity of new buildings (Zhao et al. 2014). Buildings employing a steel structure have been particularly promoted by government policies, such as China's 13th Five-Year Plan for Building Energy Conservation and Green Building Development (MOHURD 2017). Meanwhile, the fact that residential buildings in cities have been becoming taller on average means more cement has been required for structural support (Hong et al. 2016). Consequently, residential buildings have been becoming increasingly material intensive, with particular regard to steel and cement (Zhang et al. 2019). Such a trend is expected to continue over the next decades, with a gradually lowering rate of intensity increase. This is modelled in this study by gradually increasing the mean values of the marginal distributions of steel and cement intensities, while keeping their variance unchanged to reflect the substantial uncertainties associated with individual building characteristics. In other words, the marginal distributions are shifted without changing their shapes. In this process, the original dependence structure as captured by the constructed copula function remains unchanged due to copula's property of invariance under monotonous transformation (Hofert et al. 2018). This enables the generation of random samples from the time-variant bivariate joint distribution of steel and cement intensities (Figure 6.1).
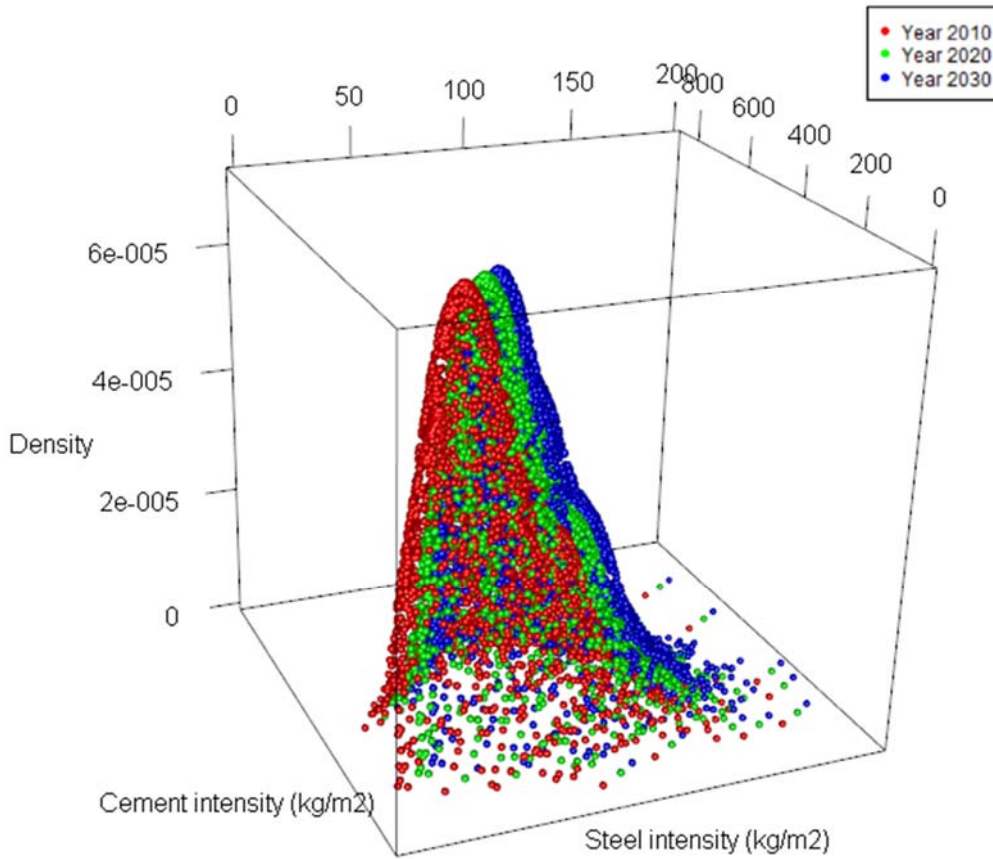
Figure 6.1: Joint distribution of steel and cement intensities in 2010, 2020 and 2030.

6.2.3   Energy intensity of building material production

The energy intensity of building material production refers to the energy consumed in producing a tonne of a given building material. Data from various sources shows a generally decreasing trend of energy intensities of steel, cement, aluminium and glass production driven by technological advancement and evolving sectoral policy requirements. Based on available historical statistics, this study models the possible trajectories of energy intensities in the short to medium term through Bayesian non-linear regression. This assumes a business-as-usual scenario under which the energy intensities of materials production, in the absence of disruptive technologies and/or drastic changes of policy orientation and intensity, are expected to follow the descending trends, but with diminishing potential for improvement over time.

The steel industry is one of the major energy-intensive industries in China that have been strictly regulated for improving energy efficiency and mitigating environmental impact (NDRC 2004). Eliminating outdated production capacity, increasing the rate of pellets in blast furnaces, improving scrap steel utilization and promoting new energy applications have been key measures

in structural adjustment and optimisation leading to substantial energy savings in the industry (China Iron and Steel Industry Association 2019; He et al. 2020). Meanwhile, a wide spectrum of energy-saving technologies have been widely applied in the industry, including coke dry quenching (CDQ), blast furnace top pressure recovery turbine (TRT), sintering waste heat recovery, recovery of blast furnace gas (BFG), coke oven gas (COG) and Lindz-Donawitz gas (LDG), slag washing water waste heat recovery, etc (NDRC 2004; Center for Industrial Energy Efficiency 2014; MIIT 2016; China Iron and Steel Industry Association 2019). With these measures, the industry-wide energy performance has realised continued improvement. The average energy intensity of steel production was 1.44 tce/t in 1995. By 2010, it dropped by 34%, to 0.95 tce/t in 2010 (Wang 2001; Wang 2013; Wang 2016). From 2010 to 2018, the decreasing trend remained but the rate slowed down (Wang 2018; Wang 2019). The generally smooth and slowing down decreasing trend of the historical values suggests a profile that could be reasonably well approximated by an exponential decay curve with a non-zero lower asymptote. Thus, a three-parameter exponential decay function, as shown in equation (6-1), is applied to model the possible future trends of energy intensity of steel production.

$$EI_{steel} = a + (b - a)e^{c(Year - Year_0)} + \varepsilon_t \qquad (6\text{-}1)$$

where *b* is the value of energy intensity of steel production in the initial year *Year₀*, which is 1995 in this case; *a* is the lower asymptote that the curve approaches over time, suggesting that energy saving potential will become increasingly limited and is unlikely to drop down to 0; *c* represents the relative decrease of energy intensity for a unit increase of *Year*; ε_t is the random error term assumed to be normally distributed with mean zero and unknown variance σ^2, i.e. $\varepsilon_t \sim N(0, \sigma^2)$.

Similar to the steel industry, the cement industry has made significant progress in energy saving through various policy and technological measures. The industry has undergone structural transformation characterised by the elimination of outdated production capacity and increased industry concentration ratio (NRDC 2019). New dry process has become the mainstream in cement production across the country. Kiln waste heat recovery for power generation and energy efficient grinding systems have been widely adopted (Center for Industrial Energy Efficiency 2014; NRDC 2019). Since 2016, tiered electricity tariffs have been introduced to cement production as a policy measure to eliminate inefficient capacity (NDRC and MIIT 2016). All these measures have contributed directly to bringing down the energy intensity of cement production. From 1980 to 1995, the industry-wide average energy intensity decreased by 9.1%, from 0.219 tce/t to 0.199 tce/t. This was then followed by a period of accelerated decrease till 2010, when the energy intensity dropped to 0.143 tce/t. After 2010, the decrease started to slow down (Wang 2001; Wang 2013; National Bureau of Statistics 2017; Wang 2016; Wang 2019). Given such a largely

reverse S-shaped pattern, a four-parameter logistic decay model is used to analytically express the developing trend of energy intensity of cement production, as shown in equation (6-2).

$$EI_{cement} = a + \frac{(b-a)}{1 + e^{(c(Year-Year_0)-d)}} + \varepsilon_t \qquad (6\text{-}2)$$

where $Year_0$ is the initial year, which is 1980 in this case; b is the higher asymptote; a is the lower asymptote representing the lowest possible energy intensity under the business-as-usual scenario; c is the slope around the inflection point; d, together with c and $Year_0$, determines the $Year$ value producing an energy intensity equal to the mean of b and a; and $\varepsilon_t \sim N(0, \sigma^2)$ is the random error term.

The same four-parameter logistic decay model was applied to aluminium and glass, with their respective parameters estimated using available historical data. For aluminium, owing to the phasing-out of old plants using Söderberg cell, adoption of large-sized pre-baked cell, promotion of new technologies such as low-temperature and low-voltage electrolysis and innovative cathode collector bar, as well as the implementation of tiered electricity tariff (NDRC 2004; Ding et al. 2012; NDRC and MIIT 2013; Center for Industrial Energy Efficiency 2014), the electricity intensity of aluminium electrolysis decreased substantially, from 17,100 kWh per ton (kWh/t) in 1990 to 13,555 kWh/t in 2018 (National Bureau of Statistics 2017; Wang 2019). Converted to the unit of tce/t using the annual gross coal consumption rate of electricity generation, this corresponds to a decrease from 6.7 tce/t in 1990 to 4.36 tce/t in 2010, and further to 3.93 tce/t in 2018.

Similarly, the flat glass industry has become more energy efficient. With strong policy inventions, glass production capacities using inefficient methods such as vertical drawing and Colburn sheet process have been eliminated in an accelerated manner and replaced with the state-of-the-art float glass production process (NDRC 2004). Technologies such as kiln insulation, oxy-fuel combustion, flue gas waste heat recovery and utilisation have been gradually adopted to save energy and reduce emissions during the production process (Center for Industrial Energy Efficiency 2014; Yan et al. 2017). All these measures have brought down the energy intensity of flat glass production from 0.5 tce/t in 2000 to 0.28 tce/t in 2018 (Center for Industrial Energy Efficiency 2014; Wang 2019; Wang 2016).

6.2.4   Energy intensity of building construction and demolition

On-site building construction and demolition activities incur energy consumption that is not trivial. As found by Malmqvist et al. (2018) based on European cases reviewed under the IEA's Annex

57 project '*Evaluation of Embodied Energy and Carbon Dioxide Emissions for Building Construction*', embodied energy from the construction stage could vary between 6% and 38% of total embodied energy. However, compared to materials production, few studies have focused specifically on the construction and/or demolition stage, and empirical data on individual cases is limited (Moncaster et al. 2019; Zhu et al. 2019).

Given the interest of this thesis in stock-level embodied energy incurred by annual construction and demolition, an alternative approach is taken, which is to investigate key metrics of the Chinese construction industry as a whole. Firstly, historical statistics on annual total energy consumption of the Chinese construction industry are taken from the energy balance sheet provided in the Chinese Energy Statistical Yearbook (National Bureau of Statistics 2017). Since this annual data is not further disaggregated into specific categories, it is used as a proxy to represent the total energy consumed by construction and demolition activities undertaken by construction enterprises. Secondly, industry-wide average energy intensity in a given year is obtained by dividing the annual total energy consumption by the total floor area under construction in the same year taken from China Statistical Yearbook (National Bureau of Statistics 2019). Thirdly, using the pattern found in the estimated energy intensity data over the historical period of 1990 to 2017, an exponential decay function as specified by the above equation (6-1) is applied to model possible future trends of construction and demolition energy intensity. The parameters of the function are estimated through Bayesian inference, similar to the approach used for energy intensity for material production.

6.2.5 Energy intensity of materials transportation

Similar to construction and demolition energy, materials transport is an under-researched aspect of building embodied energy that needs more attention (Pomponi and Moncaster, 2018; Moncaster *et al.*, 2019). Malmqvist et al. (2018) pointed out that transportation should not be neglected in calculating embodied energy, as long-distance transportation of large volumes of materials, such as pre-fabricated modular building components, can have a substantial impact on life cycle embodied energy and carbon of buildings. The energy intensity of materials transportation is a function of transportation mode, vehicle loads, fuel type, and transportation distance. A common understanding in literature is that medium-duty and heavy-duty diesel trucks are the major way of transporting building materials in China (Yan 2011; Zhang et al. 2019; Hao et al. 2020; Zhu et al. 2020). As for transportation distance, there is a lack of adequate empirical data. This study refers to default values for material-specific transportation distance as given in the Standard for Building Carbon Emission calculation issued by the Ministry of Housing and Urban-Rural Development (MOHURD)(MOHURD 2019b). In this study, the estimated energy

intensities of materials transportation are assumed to be constant over the modelled period.

6.3 Results

6.3.1 Historical and future embodied energy

Based on the methodology elucidated above, the possible trajectories of the embodied energy incurred by annual new construction of urban residential buildings were modelled for the period of 2010 to 2060 (Figure 6.2). In each year, the embodied energy is a distribution, which quantifies its uncertainty. For the historical period, the annual new construction, the energy intensities of materials production, and the construction and demolition energy intensity are all known and therefore take fixed values. The distribution reflects the uncertainty associated with building material intensities, namely, the consumption of steel, cement, aluminium and glass per m^2 of floor area constructed. For future decades, the annual new construction is a random variable characterized by its posterior predictive distribution, which is determined by the stock turnover dynamics. Similarly, the materials production energy intensities and construction and demolition energy intensity are subject to quantified uncertainties in their respective developing trends. The uncertainties of these variables, along with those of material intensities, are propagated through the model to inform the distribution of embodied energy.
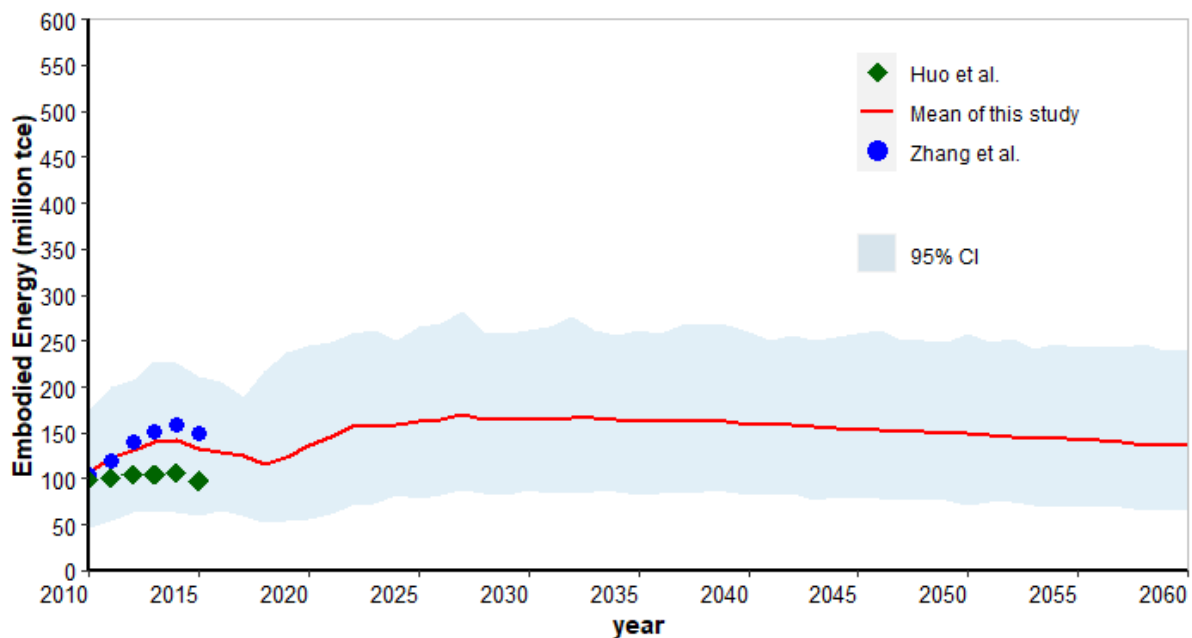

Figure 6.2: Possible trajectories of embodied energy of annual new construction

In Figure 6.2, the light blue belt is the 95% credible interval for embodied energy, and the red line

99

is the mean value. The embodied energy is found to have started to increase from 2010 to 2014. It then declines gradually as a result of the decrease in annual new construction. From 2019 onwards, it starts to pick up due to expected increase in annual new construction in response to expected incremental housing demand growth (Zhou et al. 2020). The trend continues but the rate slows down gradually. The peak is expected to be reached around 2027, when the 95% credible interval ranges from 87 million tce to 283 million tce and the mean value is 170 million tce. Following the peak, the embodied energy largely plateaus until 2034, when it starts to slowly decline. By 2050, the mean value decreases to 150 million tce. Underlying the bending of the belt is primarily the combined effect of the possible trajectories of annual new construction and the material intensities. As explained above, the energy intensities of materials production and those of construction and demolition activities are expected to have minor impacts due to the limited potential of energy efficiency improvement over time. This reflects the observed trend of decelerating energy intensity decrease implying that the 'low-hanging fruit' have been picked, as well as the assumed baseline scenario where no disruptive technologies and/or policies would emerge and improve energy efficiency significantly.

It is useful to compare the results with previous studies. As shown in Figure 6.2, the credible interval of embodied energy for the historical period of 2010 to 2015 presents a pattern fairly similar to the deterministic estimates of Zhang *et al*. (2019) and Huo *et al*. (2019). This pattern, featuring a continuous increase until 2014 and then a drop in 2015, is well aligned with the variation of the actual amount of annual new construction of urban residential buildings in this period. This alignment is as expected, because the annual new construction is the fundamental determinant of the demand for materials. The curve of mean value of the distribution lies between the other two studies, which referred to different sources of sample data on material intensities. As the difference between Zhang *et al*. (2019) and Huo *et al*. (2019) gets larger over time, the mean curve is consistently much closer to Zhang *et al*. (2019) than to Huo *et al*. (2019). This clearly demonstrates that, with other factors being the same or similar, the material intensities can have a significant impact on the embodied energy.
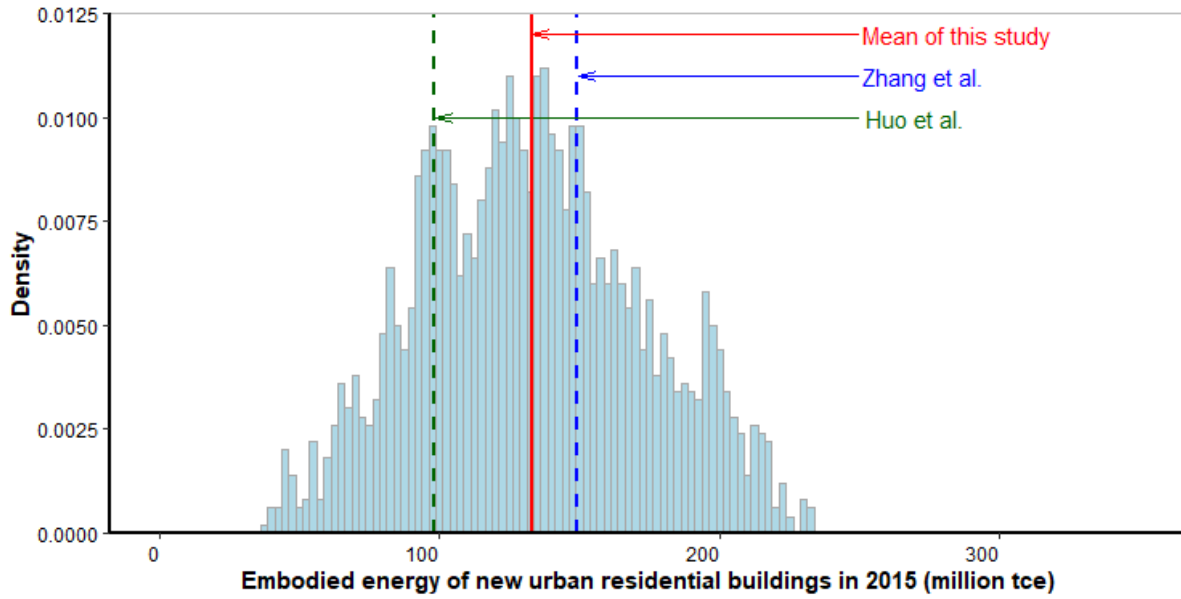
Figure 6.3: Estimated embodied energy in 2015 - comparison with other studies

Figure 6.3 takes a closer look at the situation in 2015. The minimum and maximum values of the full distribution are 37.3 million tce and 232.4 million tce, respectively. The 95% credible interval is in the range of 60.3 and 211.7 million tce. Falling into this credible interval, the estimates by Huo *et al*. (2019) and Zhang *et al*. (2019) are 98 and 149 million tce respectively. Using the empirical cumulative distribution function informed by the distribution in this figure, the probability of the estimated embodied energy being higher than 98 million tce and lower than 149 million tce is 45.9%. This suggests a considerable probability of over- or under-estimation by taking a deterministic approach based on limited data. There is, therefore, a material risk of inaccurately interpreting the results and making less informed decisions about policy measures. In contrast, probability distributions obtained from a stochastic approach enable the quantification and communication of uncertainties, which help to mitigate the risk of over- or under-estimation and improve the robustness and reliability of the results.

6.3.2   Impact of building lifetime

As pointed out in previous studies, Chinese urban buildings are generally short-lived. A number of studies relating to materials demand and environmental impact of Chinese buildings take the same approach to building lifetime by representing it as a normal distribution with an assumed mean value of between 30 and 45 years (Hu, Bergsdal, et al. 2010; Hu, Pauliuk, et al. 2010; Hu, Voet, et al. 2010; Shi et al. 2012; Huang et al. 2013; Shi et al. 2016; Hong et al. 2016; Huo et al. 2019). Some recent studies took a step forward by estimating the lifetime. For example, Cai *et al*. (2015) found that Chinese buildings had an average lifetime of 23.2 years. Zhou *et al*. (2019)

used a Weibull distribution to quantify the lifetime uncertainty of urban residential buildings and found the average lifetime was 34 years. As a critical factor in the stock turnover dynamics, the short building lifetime makes it necessary to investigate how the variation in average lifetime affects the annual new construction and the associated embodied energy.

Two scenarios are modelled for comparison with the baseline scenario. The first scenario progressively extends the average lifetime by 10 years over the period of 2021 to 2040. This is modelled by shifting the lifetime distribution profile towards higher values. As specifying any one of the four representations (PDF, CDF, survival function, hazard function) allows the other three to be ascertained, shifting the lifetime distribution (PDF) results in an adjusted hazard function, which decelerates the amount of annual demolition of existing old buildings. The second scenario examines the effect of shortened lifetimes. As the reverse of the first scenario, this scenario progressively shortens the average lifetime by 10 years over the period of 2021 to 2040. Whilst less likely in practice than the lifetime extension scenario, it helps to demonstrate the effect of lifetime extension from the opposite perspective and the implications for stock turnover and stock-level operational energy performance justify its usefulness. Since Bayesian Model Averaging (BMA) was used to obtain the original forecast under the baseline scenario, re-modelling stock turnover dynamics under adjusted hazard functions was repeated for each of the five candidate survival models and combined through BMA.
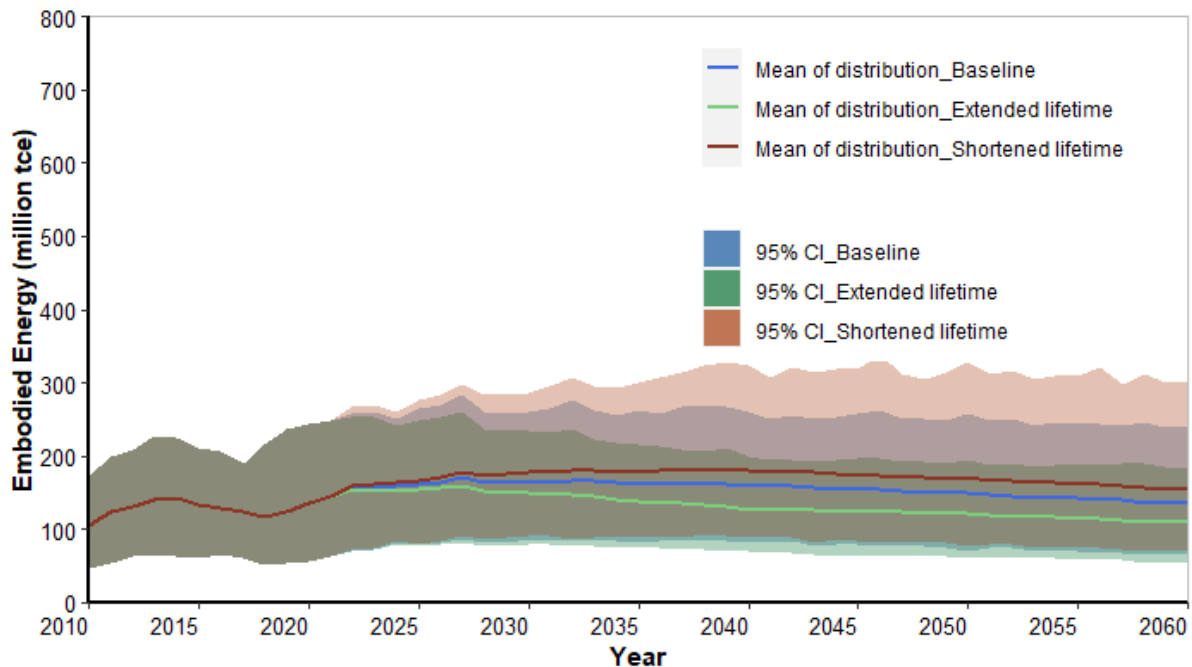

Figure 6.4: Impact of building lifetime on embodied energy of annual new construction

As shown in Figure 6.4, the effect of extending or shortening building lifetime is minor in the first

few years since any extension or shortening is gradual, but grows over time. The belt of the extension scenario starts to bend shortly after the introduction of adjusted hazard function in 2021. It reaches a peak in 2027, when its 95% credible interval ranges from 82.9 million tce to 259.7 million tce and the mean value is 159.2 million tce. After peaking, unlike the baseline scenario which remains stable for seven years, the extension scenario immediately starts to shift downwards. It increasingly diverges from the baseline scenario over time, because the progressively extended lifetime results in fewer existing buildings being demolished and accordingly fewer new buildings constructed. The declining trend of the extension scenario decelerates in 2040 when the extension ends. As for the shortened lifetime scenario, it keeps increasing once lifetime begins to shorten. Accelerated demolition means more new buildings need to be constructed to meet demand. This trend continues until 2039 when the peak is reached.
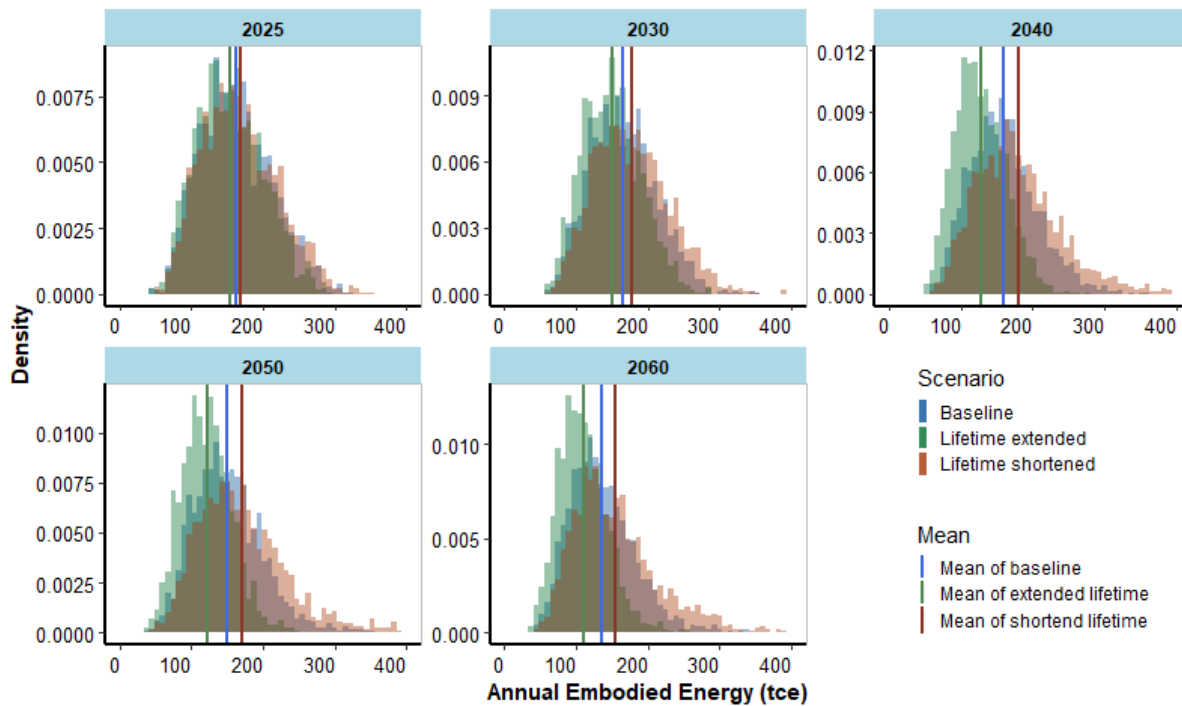
Figure 6.5: Distribution of embodied energy under three lifetime scenarios in typical years

The comparison of the three scenarios in typical years is presented in Figure 6.5 which overlays the three distributions. In 2025, the three distributions overlap almost entirely and are hardly discernible from one another. Their mean values are very close to each other. The difference between the three distributions is more notable in 2030. By 2040, when the average lifetime is no longer extended or shortened, the three distributions are most separate and so are their mean values: 127.5 million tce for the extension, 159.3 million tce for the baseline, and 179.2 million tce for the shortening scenarios, respectively. From 2041 onwards, all three belts slowly shift

downwards, as the incremental demand for housing that drives the stock turnover keeps decreasing gradually towards reaching a saturation level. During this period, the difference in the three distributions remains substantial due to the 10-year difference in average building lifetime. Apart from visual inspection, the difference between scenarios can be quantitatively evaluated using the empirical CDFs. In 2030, the probability of the baseline scenario embodied energy being higher than the lifetime extension scenario is 61%, whereas the probability of the lifetime shortening scenario being higher than the baseline scenario is 54%. In 2040, these two probabilities are 71% and 60%, respectively. These numbers substantiate the effect of changing lifetime dynamics in a probabilistic setting. The above findings clearly demonstrate that increasing building lifetime will effectively reduce embodied energy in the future.

6.3.3   Comparison between embodied energy and operational energy

Adopting a whole lifecycle perspective enables a comparison of embodied energy (EE) and operational energy (OE) at the total stock and per m^2 levels. In practice, however, developing such estimates can be very challenging. Energy consumption by buildings is not directly recorded in the China Energy Statistical Yearbook (Wang 2014). Overall operational energy performance of Chinese buildings is reported by the Annual Report on China Building Energy Efficiency, developed by Tsinghua University Building Energy Research Centre (THUBERC). Real data from large-scale surveys and long-time monitoring of a large number of cases are the most fundamental inputs to their model (Peng et al. 2015; THUBERC 2019b). According to recent annual reports, the operational energy consumption of urban residential buildings, including centralised heating, increased from 257 million tce in 2010 to 324.4 million tce in 2015, and further to 378.8 million tce in 2018 (THUBERC 2012; THUBERC 2013; THUBERC 2014; THUBERC 2015; THUBERC 2016; THUBERC 2017; THUBERC 2018; THUBERC 2019a; THUBERC 2020).
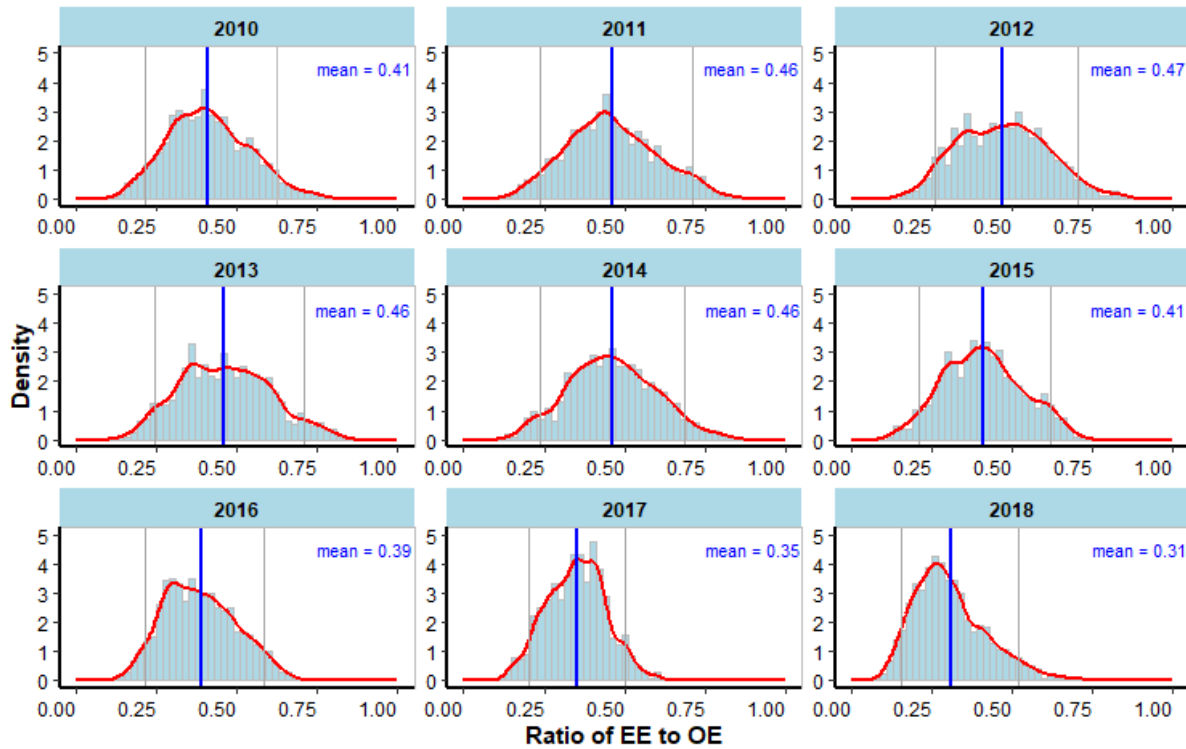
Figure 6.6: Distribution of the ratio of embodied energy of annual new buildings to annual operational energy of the urban residential stock

Using the THUBERC data and the estimated EE under the baseline scenario, the ratio of EE to OE in the same year is obtained for 2010 to 2018 (Figure 6.6). For each year, the ratio is represented by a distribution because the embodied energy follows a distribution capturing the uncertainties of material intensities. The distribution of the ratio in each year, as depicted by a histogram overlaid with a density curve, is largely bell-shaped, with some skewness. The blue line represents the mean value of distribution and the two grey lines represent the 5th percentile and 95th percentile, respectively. From 2010 to 2015, the mean value of EE to OE is in the range of 0.41 to 0.47. From 2016 to 2018, it drops but still remains above 0.3. This slightly downward trend is caused by two factors. On the one hand, there was a slight drop in annual new construction. This was accompanied by further improvement of material production energy intensities and a slight increase in average material intensity due to the evolving landscape of new building structures, which are characterised by higher shares of frame-shear and shear wall structures. The combined effect is a marginal decrease in embodied energy of new buildings. On the other hand, the overall residential stock kept growing due to continuous incoming new buildings, which far outweighed the effect of the old buildings reaching the end of their lifetime and being removed from the stock. The net increase in stock more than offset the effects of higher energy efficiency of new buildings and energy retrofit of existing buildings, thereby driving up stock-wide operational energy. However, going forward, given China's overarching climate

objectives of peaking economy-wide emissions by 2030 (NDRC 2015; Guan et al. 2018) and achieving carbon neutrality by 2060 (Mallapaty 2020; Yu et al. 2020), strengthening policies on new and existing buildings will be needed to curb the increase of stock-level operational energy and emissions.

Table 6.2: Ratio of embodied energy intensity to annual operational energy intensity

Year	Average embodied energy intensity (kgce/m^2)	Annual operational energy intensity (kgce/m^2)	Ratio
2010	103.3	14.2	7.3
2011	105.0	14.6	7.2
2012	103.7	14.7	7.0
2013	104.6	14.6	7.2
2014	107.1	14.5	7.4
2015	106.2	14.8	7.2
2016	107.5	14.6	7.4
2017	107.4	15.0	7.2
2018	106.0	15.5	6.8

Source for annual operational energy intensity: (THUBERC 2020)

In addition to the stock-level comparison, it is useful to compare embodied energy with operational energy per unit of building floor area, i.e., embodied versus operational energy intensity of buildings. As summarised in Table 6.2, the average embodied energy intensity remained stable in the narrow range of 103 to 107 kgce/m^2. In 2015, the value was 106, close to the average figures of 81 kgce/m^2 provided by Huo *et al*. (2019) and 126 kgce/m^2 by Zhang *et al*. (2019). Between 2010-2018, therefore, embodied energy intensity (of new stock) was around 7 times that of operational energy intensity (of existing stock). This result is largely consistent with Gu *et al*. (2007), who found the ratio to be 8 for urban residential buildings in Beijing. A study by the China Building Materials Academy reported that the ratio was 3, 6, and 30 respectively for steel, brick, and concrete structures (Zhao et al. 2014). Overall, the comparison between embodied energy and operational energy, whether in terms of overall stock or intensity, provides strong evidence of the importance of embodied energy.

6.4   Discussion

This section extends the above findings to a more general discussion, with a view to identifying and analysing sector-specific and cross-cutting policy measures closely relating to building

embodied energy and highlighting the strategic importance of integrating embodied energy into policies addressing building energy.

6.4.1 Property market and new construction

Annual new construction is the fundamental determinant of the consumption of materials. Construction activities are driven by market demand, which includes not only basic housing, but also upgraded housing conditions such as luxurious apartments, houses, second homes, etc. Over the past two decades, a series of policies were issued by the central and local governments to regulate the overheated real estate sector and curb the rising demand for high-end housing. Typical examples included implementing a restriction on the proportion of apartments with sizes above a certain benchmark that property developers are allowed to develop per year, imposing surcharges on transactions involving oversized properties, and restricting second and third home purchases (Asia Green Real Estate 2019). The effects of these policies were mixed. Meanwhile, in a large number of cities across the country, high property vacancy rates have become a widely observed phenomenon. Whilst there existed various factors underlying this situation such as speculative investment, the existence of large amount of empty properties means serious overbuilding and oversupply of residential properties, which could have been avoided, at least partially, to free resources that could be used more efficiently in other parts of the economy (Chivakul et al. 2015; Glaeser et al. 2017). Analysis on real estate policy measures is beyond the scope of this study, which has taken an engineering approach to model the stock turnover dynamics. However, it is fully acknowledged that the future evolvement of the property market regulated by government policies is the fundamental driving force of new property development in the pipeline. Policy measures putting an effective rein on overheated real estimate will not only generate a series of economic and social benefits, but also contribute indirectly to environmental benefits, e.g. reduced consumption of building materials and the underlying energy use and carbon emissions.

6.4.2 Material intensity

For a given quantity of new construction, material intensities directly determine the magnitude of materials consumption and therefore are a decisive factor of the associated embodied energy. Material intensities are largely dependent upon building classification and structural types. In the Chinese urban context, residential buildings have been experiencing a transition in structural type, with frame-shear and shear wall structures replacing brick concrete structure to become the mainstream (Zhao et al. 2014; Zhang et al. 2019). Promoted by a series of policies (MIIT and MOHURD 2015; MOHURD 2017), the share of steel structure residential buildings has also been

increasing (Zhang et al. 2019). These changes have led to new buildings becoming gradually more material intensive.

In parallel with the evolution of structural types for urban residential buildings, increasingly greater emphasis has been placed upon developing green buildings. The MOHURD and State Administration for Market Regulation (SAMR) jointly issued the Assessment Standard for Green Building in 2006, which was the first ever national standard specifically targeting green buildings (MOHURD 2019a). Subsequently updated in 2014 and 2019, this standard sets the overall evaluation framework and specific criteria for rating potential green buildings. Whilst the standard has particular criteria concerning material saving and the use of green materials, there are no quantitative targets or indicators relating to material intensity. Likewise, the Code for Green Design of Civil Buildings, issued by MOHURD in 2010, sets a guiding principle of controlling building volume and reducing material consumption (MOHURD 2010). It does not set any quantitative design requirements on material intensities but encourages the use of materials consuming less energy for production. On the whole, in the absence of mandatory and specific requirements, it is unlikely that material intensities of urban residential buildings would achieve substantial decrease in the short to medium term.

As previously mentioned, there are no official statistics on building material intensities in China. Empirical data is limited, and mostly focused on individual building cases. A small number of studies based their calculations on some surveys whose details were not publicly accessible. Therefore, availability of data has been a major barrier to quantification and modelling work, including this study. A sample size much larger than the one used in this study would have produced more robust modelling results.

6.4.3 Materials production energy intensity

Owing to continued policy intervention and technological advance, significant progress has been achieved in improving the production efficiency of building materials. As a key metric of production efficiency, the average energy intensities of key enterprises in relevant industries in China have been improving rapidly, with the gap between China and internationally advanced levels shrinking continuously (National Bureau of Statistics 2017; Wang 2019). Going forward, it would be increasingly technologically challenging and economically costly to improve further, as the 'low-hanging fruits' have been picked (Wang et al. 2015; Voïta 2018). However, it shall be noted that the industry concentration of these energy-intensive industries, such as steel and cement, remains generally low (China Iron and Steel Industry Association 2019; NRDC 2019). A considerable share of products is supplied by small and medium sized enterprises which usually

have energy intensities more than 30% higher than the average of large enterprises leading industrial development (Wang 2019). This has kept industry-wide energy intensities high. For example, the industry-wide average energy intensity of steel production was 861 kgce/t, whereas the average energy intensity of large enterprises was 634 kgce/t. From this perspective, there exist huge opportunities for upgrading the industries and bringing down the high energy intensities of small and medium sized enterprises and therefore the industry average. To realise this immense potential, it is important to keep up and strengthen the momentum of industry integration and transformation to eliminate excessive and outdated production capacity and mainstream state-of-the-art production processes and energy efficient technologies. The continuity and consistency of policy measures will be key in this process.

6.4.4 Addressing embodied, as well as operational, energy

Over the past few decades, there has been a continuous improvement in the energy efficiency of Chinese buildings owing to the enforcement of a series of design codes and technical standards. These codes and standards are mostly prescriptive and design process-oriented. More often than not, code compliance does not necessarily translate to actual energy efficiency of a building in real operation. With the view of achieving more progress and controlling actual energy consumption of buildings, MOHURD issued the Standard for Energy Consumption of Building in 2016, which set specific quantitative energy consumption indicators by building type and climate zones (MOHURD 2016). Whilst this standard is not yet mandatory or time-bound, it sends a strong signal of an envisaged transition of the design and evaluation of building energy efficiency, from focusing only on prescriptive design and ex-ante compliance to placing a parallel emphasis on performance-based and result-driven design and ex-post monitoring and evaluation of actual energy performance of buildings. It therefore can be reasonably expected that buildings will be progressively more energy efficient and 'greener' over time.

Meanwhile, due to the absence of any quantitative limits on building material intensities in existing regulations, as well as given the observed trend of residential building structural type evolution, it is unlikely that embodied energy intensity of new buildings would decrease over the short to medium term. Rather it is more likely to increase. In fact, it has been found that the desired operational performance of green buildings was often obtained at the cost of much higher embodied energy and carbon than conventional buildings (Zhao et al. 2014). With new buildings becoming more operationally efficient, the capital cost of embodied energy and carbon will be more significant and shall be fully taken into consideration in the decision-making process for sustainable design, construction and use of buildings. Setting quantitative indicators for embodied energy intensity in codes or standards, similar to the above-mentioned standard for

operational energy, would be a useful approach before mandatory requirements can be introduced and enforced.

At a higher level, a lifecycle perspective addressing stock-wide operational and embodied energy in an integrated manner should be considered by policymakers in formulating strategies and action plans. Given that building is one of the major energy end-use sectors, this will have strong implications for achieving China's pledge of peaking its economy-wide emissions by 2030 (NDRC 2015; Guan et al. 2018) and achieving carbon neutrality by 2060 (Mallapaty 2020; Yu et al. 2020).

6.5   Chapter summary

This chapter models possible future trajectories of embodied energy of Chinese urban residential building stock. Empirical data of building material intensities are fitted to probability distribution functions, with the joint distribution of steel and cement intensities captured using a copula function. Energy intensities of material production, building construction and demolition are modelled using Bayesian non-linear regression. As for the annual construction of new buildings, the modelling results from Chapter 5 are used. The uncertainties of these input variables are propagated to the embodied energy of new buildings through Monte Carlo simulation.

It is found that the embodied energy of Chinese urban residential buildings is likely to peak around 2027, with a 95% credible interval ranging from 87 to 283 million tce and a mean of 170 million tce. Under the current trajectory, the embodied energy is forecast to remain high at around 150 million tce per year through the end of the forecast period, a very substantial fraction of China's total annual energy consumption. Obvious methods towards reducing this energy in the future include reducing annual construction, or reducing material energy intensity, either through reducing the energy intensity of key materials, or moving to using materials with lower embodied energy. However, a further route which is explored and quantified here is by increasing building lifetime, which is very short in the current urban context in China. Gradually increasing this lifetime is shown to reduce embodied energy by 20% (31.8 million tce) by 2040. This chapter also shows that over 2010-2018, annual embodied energy of new construction was between 31% and 47% of total operational energy of existing buildings. The ratio of embodied energy intensity to operational energy intensity remained around 7 throughout this period. These findings therefore provide strong evidence of the importance of considering embodied as well as operational energy.

In summary, this chapter answers research question Q3 on embodied energy. The results will be used for calculating the whole-life energy consumption in Chapter 9.

7

A generic System Dynamics model for building stock operational energy

7.1 Chapter introduction

Answering research question Q4, this chapter develops an enhanced System Dynamics model for operational energy performance of a building stock. It describes in detail how the model is conceptualised and developed to address the methodological limitations of previous models as discussed in the literature review in Chapter 2.

7.2 Level of stock disaggregation

The collective salient features of the previous building stock models can be represented using the model in Figure 7.1. Essentially the building stock is composed of 3 vintages (sub-stocks) representing buildings that are newly constructed and in their early stage, buildings that are relatively aged and in their medium stage, and buildings that are old and in their late stage leading to final demolition. Outflows from each sub-stock are modelled using first-order delays.
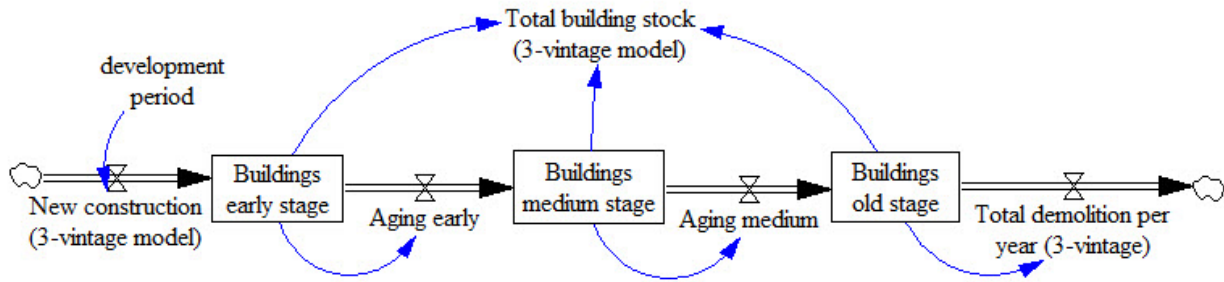
Figure 7.1: Commonly used 3-vintage structure in previous models

Assuming the delay time for each stage is equal, e.g. 10 years, the setup of cascading the 3 first-order delays in series creates a third-order delay. Mathematically, the final outflow representing building demolition is the convolution of the sequence of first-order delays (Fadali & Visioli 2013). Statistically, the distribution of the final outflow is equivalent to the Erlang distribution specified by a shape parameter equal to 3 and a scale parameter equal to 10 (Forbes et al. 2011). These two parameters suggest that the average lifetime of buildings in the stock is 30 years and the standard deviation is 17.3. Such a model setup implicitly pre-defines a fixed lifetime distribution of a cohort of new buildings, without considering that it is highly likely to be different from the situation in reality. Even if the delay time for each stage is not set to be identical, as with some models, the cascaded third-order delay leads to a unique pre-defined and fixed lifetime distribution. Therefore, the problem that the assumed lifetime distribution substantially differs from reality remains.

More fundamentally and critically, the first-order delay mechanism for outflow from a stock, as commonly seen in the above-mentioned models, implies perfect mixing of the individual elements in the stock (Eberlein et al. 2012). Once an individual item flows into the stock, it immediately gets mixed up with (and becomes indistinguishable from) all other items that flow into the stock at the same time and also those existing items that have already been in the stock for some time. All items in the stock have the same average residence time in the stock and therefore are subject to the same probability of exiting the stock, which is equal to the reciprocal of the average residence time, regardless of their age. The same feature is also described by statisticians as an exponential distribution having a "lack of memory" or being "memoryless", suggesting that the hazard rate is constant and independent of time and past survival experience (Forbes et al. 2011; Liu 2012). This feature results in an undesired consequence that is referred to as "cohort blending" in some contexts. Cohort blending leads to, for example, large distortions in simulated mortality and morbidity in chronological aging processes in demographic dynamics (Eberlein & Thompson 2013).

Analogously, in the context of building stock, perfect mixing implies that all buildings have the same chance of leaving the stock. This means, for example, as in previous three-vintage models, all buildings in the early-stage sub-stock have the same chance of moving to the medium-stage sub-stock, regardless of their actual age and physical condition. Similarly, all buildings in the late-stage sub-stock have the same chance of leaving due to physical demolition or functional disuse, regardless of their age and physical condition. In practice, it is considered highly unlikely that a newly constructed building would be equally likely to be demolished or disused as an old building that already has been in use for 50 years. Intuitively, for a given stock consisting of buildings built at different times, the probability of buildings leaving the stock would be expected to be higher for older buildings than for younger buildings, suggesting a general trend of increasing risk for buildings in the stock over time. As an equivalent way of interpreting this logic, it is unrealistic to assume that a cohort of new buildings entering a stock would be in service for exactly the same time period, say, 50 or 100 years, and then leave the stock due to demolition or disuse simultaneously. Uncertainties associated with their lifetimes within the stock shall be taken into account appropriately.

Taking account of these concerns, it is necessary to disaggregate the aging process of buildings into a chain of a series of cascading sub-stocks, each of which represents a particular age group of buildings. Key to the aging chain structure is the extent of disaggregation. The question therefore is what the appropriate duration of each age group would be. As a sub-stock is used to group buildings in an age range, buildings within a sub-stock are considered homogenous. Therefore, the aging from this sub-stock to the next one is modelled as a first-order exponential delay process. To avoid having the undesirable perfect mixing effect, which is precisely the original purpose of applying an aging chain, the duration of each age group is set to be no longer than 1 year. Setting each age group to 1 year means that buildings do not reside in a sub-stock for longer than 1 year before shifting to the next sub-stock. Meanwhile, it would make little sense in practice to look at building age at a resolution level finer than 1 year, e.g. 1 month. Therefore, the duration of each age group is set to be 1 year. More critically, for this level of disaggregation to fully make sense, it is necessary to set the computational interval (dt), namely, the time step of the model, to be the same as the age group duration, i.e. 1 year. Technically, the computational interval could be finer than 1 year, however this would cause mixing within a sub-stock as long as the age group duration is larger than it, such as 1 year. Although the same solution can be applied to overcome the mixing issue, namely, by further disaggregating each sub-stock into 1/(computational interval) sub-stocks, this is not considered practically useful because: (a) building age and probability of being demolished/disused estimated at a resolution level finer than 1 year would not make much sense in reality; and (b) a significantly larger number of sub-stocks will be created, inevitably adding excessive details with little extra value and unnecessarily

increasing model complexity and computational cost.

This setup discretises the chronological aging process. The high level of granularity offers a detailed representation of sub-stocks characterised by heterogeneity with respect to factors affecting building lifetime (and associated energy properties, once additional layers are added to the model). It therefore enables the functionality of separately tracking the discretely aging process of buildings and experimenting policy interventions targeting buildings of specific age groups. For example, given a large stock consisting of residential buildings constructed over the past 40 years, a policy-maker may want to know how buildings constructed in 2010 have been performing in terms of energy consumption from 2011 to 2019, what the building stock in 2019 looks like in terms of its composition of buildings of different ages and the corresponding energy performance, what would be the possible trajectories of stock-wide average energy intensity from 2020 to 2030 if an energy efficiency retrofit programme targeting buildings older than 20 years is implemented in 2020, and so on.

Using subscripting techniques, the model structure is then re-formulated to improve representation and analytical convenience, while keeping the same underlying concept and capacity. As shown in Figure 7.2, the building stock can be viewed as a stack of multiple sub-stocks that are not explicitly represented but rather implicitly included. The number of the sub-stocks can be flexibly set, depending upon the possible maximum lifetime of buildings in the context being investigated. For any given year, the total stock of buildings in use is the sum of the age-specific sub-stocks. Whilst it is also likely that there might be additional inflows to the sub-stocks, e.g. reinjection of retrofitted buildings, they are not illustrated here for visual succinctness, but will be discussed in detail in later sections.
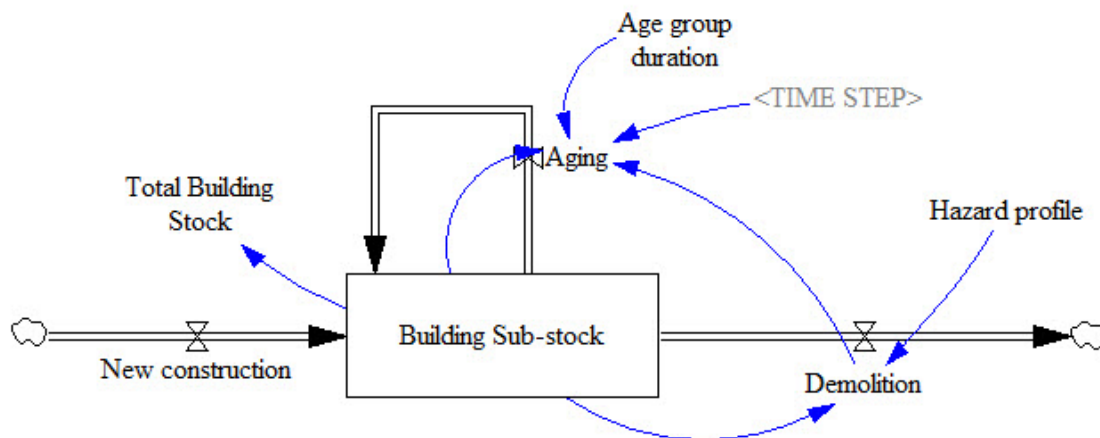

Figure 7.2: Reformulated aging chain structure

This model structure enables setting the age-specific risk (hazard rate) of building demolition based on available information and data, as opposed to previous models where the lifetime distribution of buildings is arbitrarily pre-defined and fixed. Introducing such flexibility in the model's functionality is significant because it allows context-specific variations to be taken into consideration. As demonstrated by Figure 7.3, for a given pulse input representing a cohort of new buildings put into use in 2019, the Erlang-distributed outflow of the 3-vintage model (mean 30 and standard deviation 17.3) can be moderately different from that of the disaggregated aging chain model. In the latter, the age-specific risk (hazard rate) may be derived from a certain form of building lifetime distribution with the same mean (30) and standard deviation (17.3), such as Lognormal, Weibull, etc. However, it should be noted that this is an extreme and rare scenario most in favour of the Erlang distribution derived from the 3-vintage model. The actual building lifetime distribution, which may be approximated by a Weibull, Lognormal or some other form of parametric distribution, can be significantly different from this pre-defined Erlang distribution, which consequently is a seriously distorted representation of reality. To illustrate this point, consider a much less extreme and more general scenario where the standard deviation of a Weibull or Lognormal distribution is different from that of the pre-defined distribution; in these cases, the difference in the shape of the demolition distribution as the outflow from the building stock is much more pronounced (Figure 7.4(a)). To further loosen the constraint by allowing a mean value different from the pre-defined distribution, the most general and common scenario is obtained, where the actual building lifetime distribution (approximated by a Weibull or Lognormal distribution) is significantly different from the pre-defined Erlang distribution, as shown by the difference in the shape of annual demolition in Figure 7.4(b). Inevitably such difference in stock aging dynamics, which can be very significant, will be propagated to stock energy performance, which in turn will have direct implications for policy analysis. As the stock size and composition are fundamental determinants of stock-level energy performance, an overly simplified model representation of lifetime distribution and aging process that deviates significantly from what is close to the reality is highly unlikely to generate reasonable modelling results and deliver insightful policy recommendations.

Figure 7.3: Comparison of outflow profile between the 3-vintage model based on an Erlang distribution and the disaggregated aging chain model based on a Lognormal or Weibull distribution of building lifetime. Same mean (30) and same standard deviation (17.3) are assumed.

(a)

Demolition (different mean, different SD)

(b)

Annual demolition: 3-vintage model (mean=30, SD=17.3) ——1——1——1——1——
Annual demolition: Lognormal (mean=50, SD=10) —2——2——2——2——2——2—
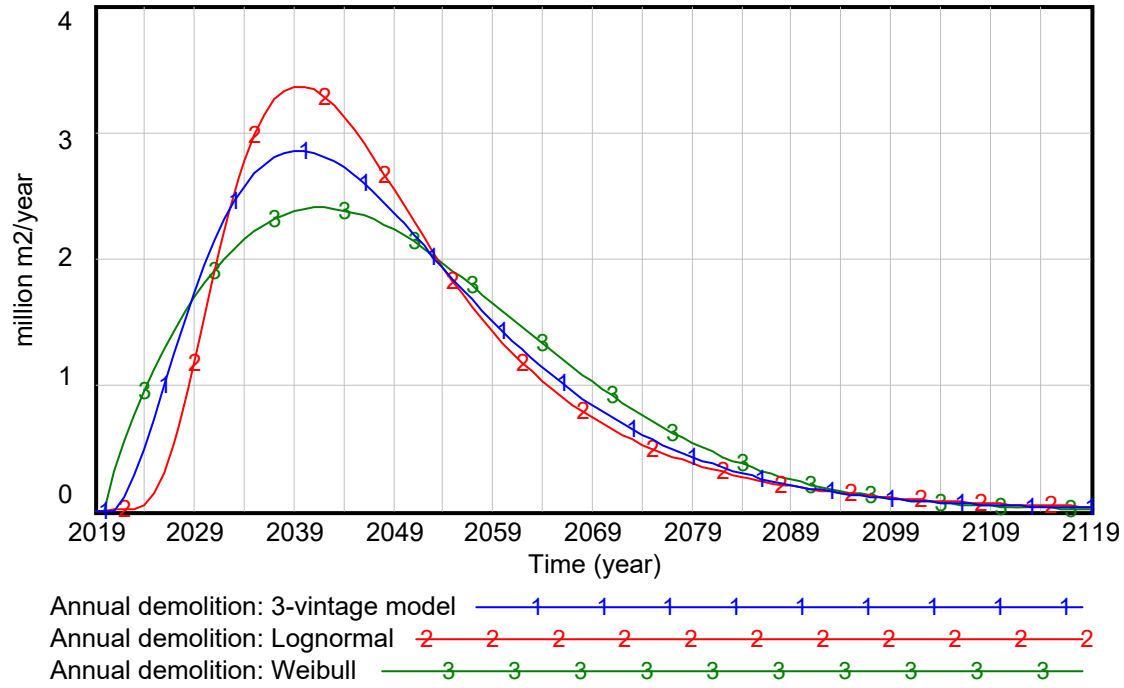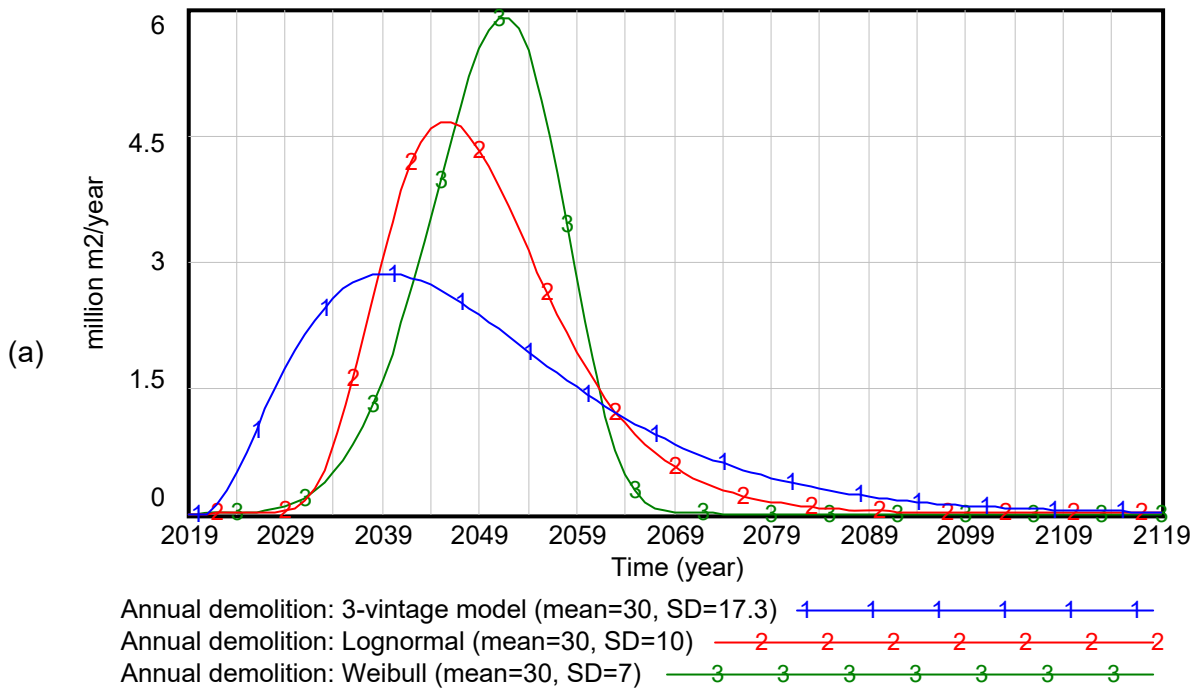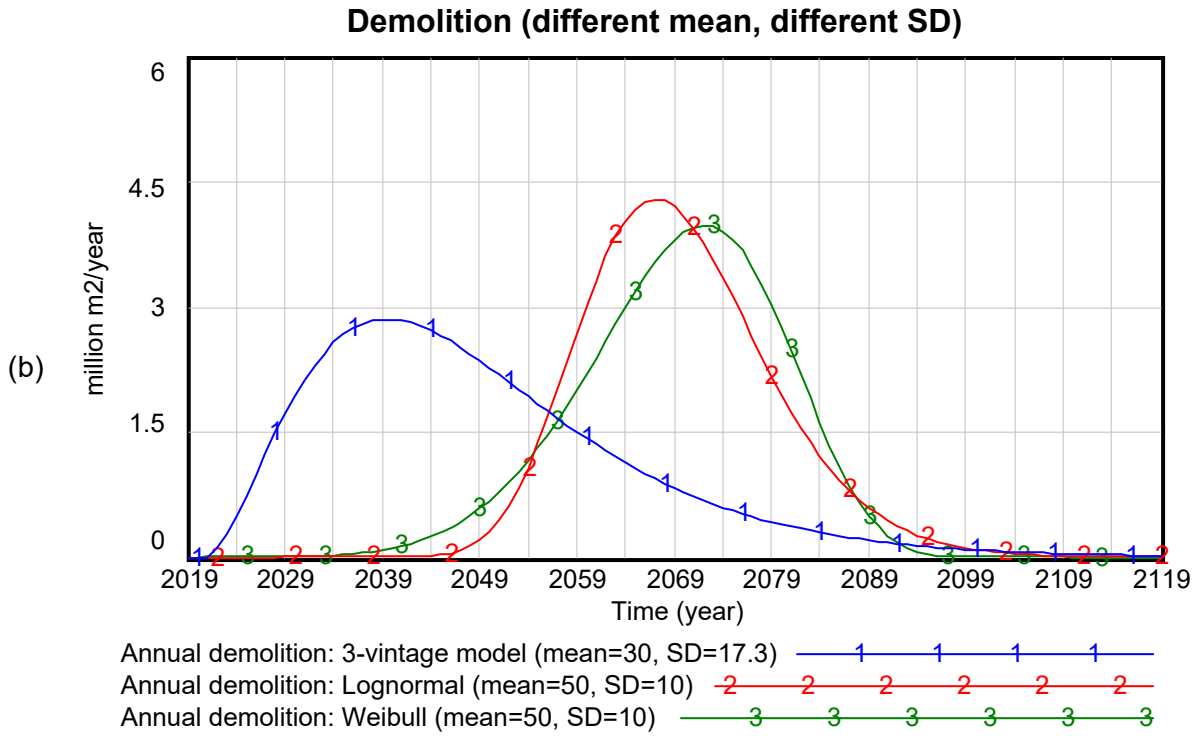Annual demolition: Weibull (mean=50, SD=10) ——3——3——3——3——3——3—

Figure 7.4: Comparison of outflow profile between the 3-vintage model based on an Erlang distribution and the disaggregated aging chain model based on a Lognormal or Weibull distribution of building lifetime. (a) Same mean (30) but different standard deviations; (b) different means and different standard deviations.

The outflow is determined by the age-specific hazard rate. Its shape reflects the lifetime distribution of the same cohort of buildings. Therefore, provided that sufficient empirical data on building lifetime can be obtained, such as through on-site survey targeting demolished buildings, the approximate lifetime distribution can be derived for use in the disaggregated aging chain model. Alternatively, when lifetime data is limited or unavailable, but data on annual total stock size and annual new construction is available, it is possible to calibrate the parameters specifying the lifetime distribution function, e.g. the shape and scale parameters of a Weibull distribution.

Thus, going from Figure 7.3 to Figure 7.4 (a) and further to Figure 7.4 (b), a progressive approach has been taken to illustrate the fundamental methodological limitation of those 3-vintage models and contrast it with the improved model in this chapter, which can overcome this limitation. The highly disaggregated structure of the improved model enables the representation of building lifetime distribution in a significantly more realistic manner than the previous 3-vintage models. It offers the functionality of calibrating the lifetime distribution (the shape of the curve) based on empirical data, whereas the previous models do not, because they pre-defined and fixed the lifetime distribution, such as an Erlang distribution.

In summary, in comparison with the 3-vintage first-order delay structure which pre-defines and fixes building lifetime distribution, the improved model setup provides both the high granularity and the flexibility necessary for calibrating the building lifetime distribution profile using empirical data.

7.3   Dynamics of retrofits for energy efficiency

The effect of adding new energy-efficient buildings will be limited when there is a very large stock of existing less efficient buildings, which creates inertia against stock-wide energy transition. This situation calls for energy-related retrofit of existing buildings. Depending upon the strategies taken, retrofit has the potential to significantly accelerate the process of transforming a building stock to attain a desired level of energy efficiency[5].

Energy retrofit can be explicitly modelled by adding an additional sub-stock "retrofitted building sub-stock", auxiliary variables and related feedback loops to the original aging chain (Figure 7.5). The inflow to this sub-stock is the amount of buildings at various ages that undergo retrofit, which is taken out from the original building sub-stock. In the retrofitted sub-stock, buildings continue their aging process while being subject to age-specific hazard rates. They differ from buildings in the original sub-stock in terms of their energy intensity levels as the result of retrofit. The age-specific retrofit rate per year is controlled by a default retrofit profile and a retrofit accelerator functioning as a multiplier to model various policy scenarios.

---

[5] This assumes that building operational characteristics and occupant behaviours do not vary significantly.
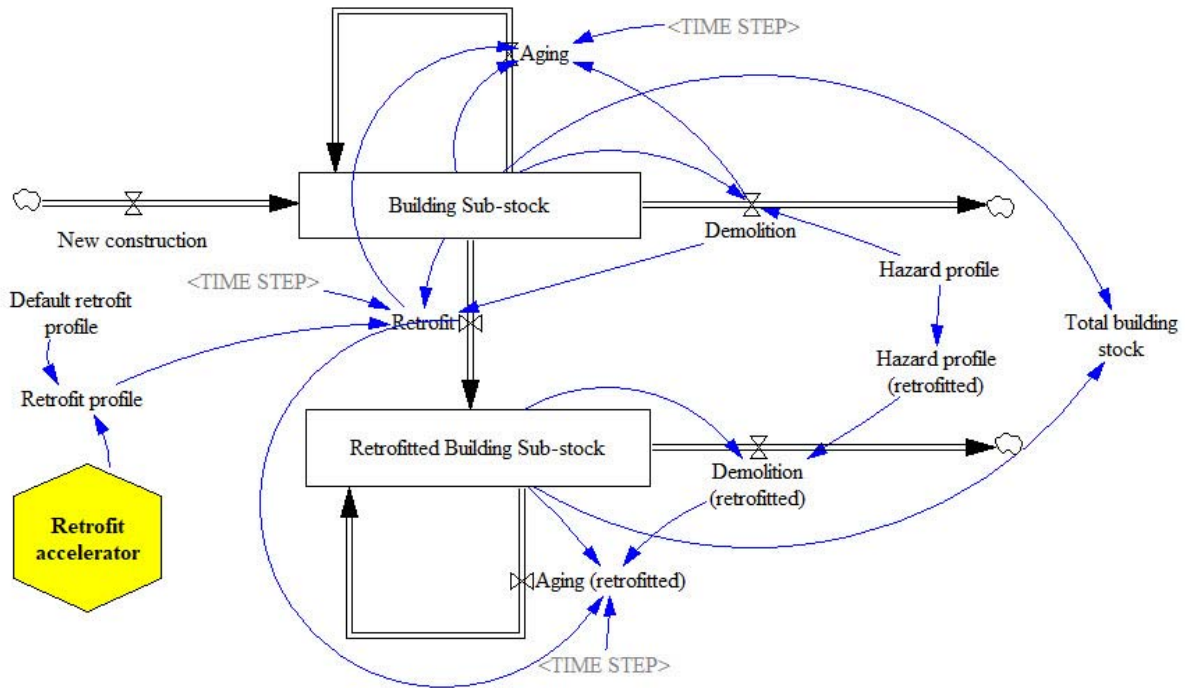
Figure 7.5: Interaction between main and dedicated sub-stocks of retrofit model

The energy demand reduction due to retrofit is represented by an additional outflow applied to the energy demand sub-stock of the original co-flow structure (Figure 7.6). This outflow is determined by the amount of retrofitted buildings and the energy intensity reduction achieved by retrofit. The latter is modelled as a percentage of the age-specific average energy intensity of existing buildings (including both retrofitted and unretrofitted buildings). The percentage is controlled by the variable "retrofit depth", representing the extent to which the energy intensity of existing buildings will be improved through a number of possible energy-related retrofit options in this context. It is fully recognised that in reality there exist a range of energy-related retrofit activities, with considerable variability and uncertainty over the achieved energy intensity reduction. As the purpose of this study is to develop a high-level generic model, the granularity at the level of specific retrofit activities is beyond the boundary. However, the model has the capability of taking account of the retrofit depth's variability. This can be done through converting the retrofit depth from a single value (e.g. 10%) to a distributional profile, which represents the share of a certain level of retrofit depth in all practically feasible levels of retrofit depth. For example, retrofit activities realising a depth of 5% to 10% accounts for 30%, retrofit activities realising a depth of 11% to 15% accounts for 40%, and so on. Such a profile will need to be established using empirical data collected from the specific context to which this generic model will be applied. In this chapter, the generic model uses a single value for retrofit depth just as an indicative value.
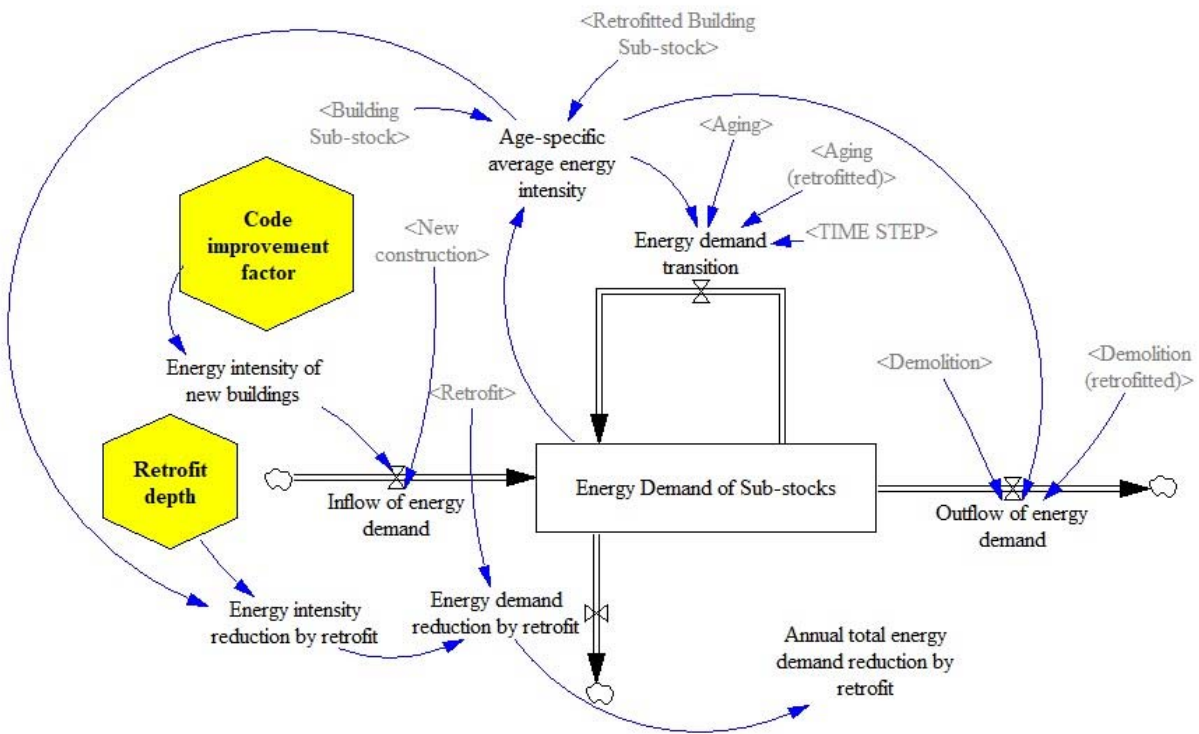
Figure 7.6: Dynamics of energy demand of retrofit model

So far, the model setup has assumed that a building will undergo at most one energy retrofit throughout its lifetime. The possibility that a building may be retrofitted two or more times is currently ruled out. This, however, is not necessarily consistent with real world behaviour, particularly in contexts where buildings are relatively long-lived. Sometimes for a large stock with a significant share of old buildings, strong policies may be designed and implemented to accelerate stock transformation by stimulating multiple rounds of retrofit that would not necessarily have been carried out otherwise. To accommodate the possibility of multiple retrofits, the model is now therefore extended by adding additional variables and functionalities.

Key to the multiple-retrofits model is the reinjection of retrofitted buildings back into the building sub-stock. Unlike the previous single-retrofit model, where retrofitted buildings stay in the retrofitted building sub-stock and undergo aging and demolition process, the retrofitted buildings in the multiple-retrofits model only stay in the retrofitted building sub-stock only for a certain period of time before being reinjected into the main building sub-stock, which is then a mix of non-retrofitted and retrofitted buildings. During the period in the dedicated retrofitted building sub-stock, the retrofitted buildings undergo an aging process as usual, and also continue to be subject to age-specific probabilities of being demolished/disused (Figure 7.7).
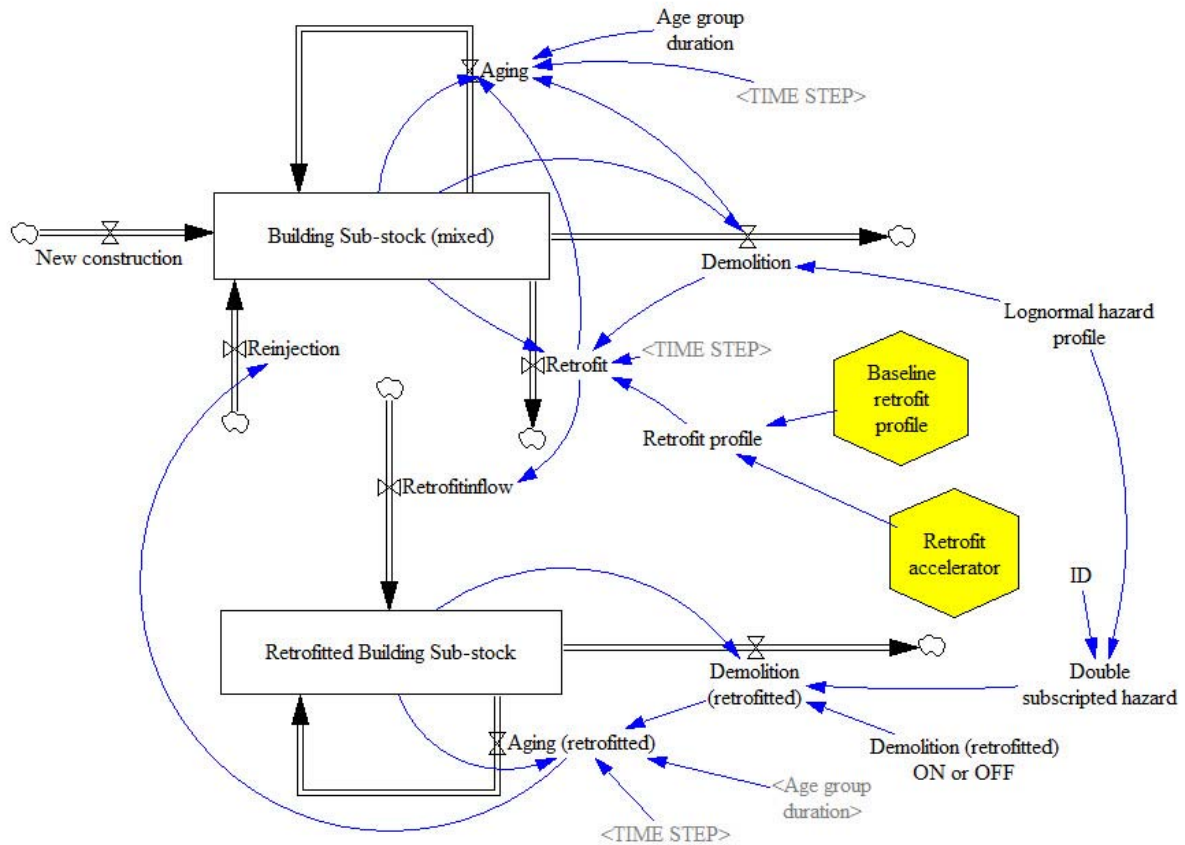
Figure 7.7: Interaction between main and dedicated sub-stocks of multiple-retrofits model

Here, the major purpose of having the dedicated sub-stock for retrofitted buildings is to take into account the fact that a newly retrofitted building is highly unlikely to be retrofitted for the same purpose again in the short term. This overcomes the issue of too-early retrofits found in previous models. Holding these retrofitted buildings in this sub-stock for a certain period prevents this situation from happening in the model. The retrofitted buildings in this dedicated sub-stock will continue to age and may possibly be removed due to demolition, depending upon age-specific hazard rates, but will not be retrofitted. The secondary purpose is to take into account the fact that a newly retrofitted building is much less likely to be demolished or become disused in the short term. Whilst in reality the possibility of being demolished or disused cannot be completely ruled out due to various factors, it would be reasonable to assume that newly retrofitted buildings are likely to be subject to lower hazard rates than other buildings of the same age which have not been recently retrofitted. This is intuitive because building retrofit involves not only technological analysis, but also economic evaluation which is more important in practice. The decision to retrofit or not has to be informed by cost and benefit analysis. A decision to retrofit would not have been made if the decision-maker had known there would not be a sufficiently

long remaining lifetime of a building to cover the payback period. An equivalent way of interpreting this logic is that, given a large sample size, newly retrofitted buildings are expected to have on average longer remaining lifetimes than non-retrofitted buildings with the same ages. In addition, sometimes an energy-related retrofit activity is carried out as part of a more general renovation activity such as structure and facade, which can result in building lifetime extension (Crawford et al. 2014) and a reduced hazard rate over the expected remaining lifetime of a building. The difference in hazard rate (demolition probabilities) between retrofitted and non-retrofitted buildings is accounted for in the model, as discussed below.

As a default setting, the "holding" period of the dedicated sub-stock, i.e. the interval between two retrofits, is set at 10 years. This means the dedicated sub-stock is a stack of 11 sub-stocks representing 1 year for completing the retrofit and the subsequent 10 years of having the benefits of improved energy efficiency while undergoing the aging process. The choice of a 10-year-period is indicative. The model allows the length of this period to be changed recognising the variation in different contexts and thus the need for adaptation. Under the default setting of a 10-year holding period, a retrofitted building enters into the dedicated sub-stock and starts to age for 10 years with respect to its original lifetime, provided that it will survive to the expiry of the holding period. Meanwhile, it also becomes "older" with respect to its post-retrofit age, e.g. 5 years after its retrofit. In a sense, this can be viewed as a double-aging process in the dedicated sub-stock. For example, by 2025, a 20-year-old building retrofitted in year 2020 will be both 25 years old and in the 5th year post retrofit. Provided that this particular building remains in use, when it leaves the dedicated sub-stock in 2030 it will be 30 years old and also 10 years post retrofit. To model this double-aging process, the model uses a double-subscripting method to denote a building in the dedicated sub-stock, i.e. year-after-construction and year-after-retrofit. This process can be illustrated using Figure 7.8.
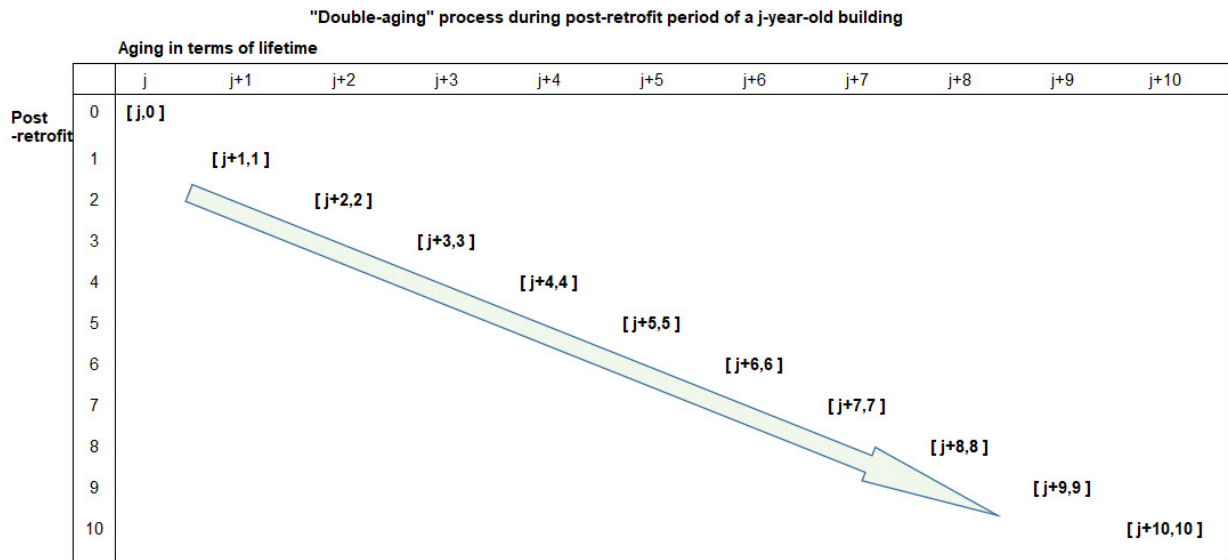
Figure 7.8: Illustration of "double-aging" process during post-retrofit period

As for the demolition, the default hazard profile is set to be the same as the one applied to the main sub-stock, e.g. a hazard profile derived from a parametric survival model estimated from empirical data. The variable "double-subscripted hazard" is numerically treated in such a way that it ensures, in the default scenario, that a t-year-old building that is retrofitted and thus enters into the dedicated sub-stock will have age-specific hazard rates for the next 10 years (holding period) as if it did not undergo retrofit and remained in the main sub-stock. In other words, the default setting assumes that a building's aging process and demolition profile are not changed, before and after its retrofit. What have changed are its property (energy performance) and its temporary status of not undergoing retrofit over the next 10 years while staying in the dedicated sub-stock. As discussed above, it would be reasonably expected that a newly retrofitted building will be subject to much lower risk of demolition or disuse, at least during the initial few years after its retrofit. The double-subscripted hazard variable can be adjusted to reflect this consideration, either arbitrarily or based on empirical evidence. The variable "Demolition (retrofitted) On/Off" serves as a switch, with "On" enabling the application of any profile of double-subscripted hazard, and "Off" representing an extreme scenario where no demolition/disuse will happen to a retrofitted building within the 10-year post-retrofit period. The default hazard profile of retrofitted buildings in the dedicated sub-stock is set to be the same as the one for the main sub-stock. In real applications, this profile can be flexibly set, for example, to a higher mean value as the result of retrofitted buildings' lifetimes being prolonged. The "Off" setting is therefore a special case of the flexible hazard profile of retrofitted buildings. In short, various settings can be made to the dedicated sub-stock to experiment with different policy scenarios and the resultant dynamics of retrofitted buildings and implications for energy performance.

Retrofitted buildings surviving to the expiry of the holding period are released and reinjected back into the main building sub-stock, where they get mixed with other buildings, including newly constructed buildings, old buildings which have never been retrofitted, and those which have already been retrofitted once or more. In the main sub-stock, buildings of the same age have the same chance of being retrofitted, regardless of whether or not they have already been retrofitted. A retrofit profile is applied to different age groups. The default setting takes a simple approach: the profile is arbitrarily exogenously defined to be time-invariant. The time-invariance means the retrofit rate applied to a specific age group of buildings is not a function of time, e.g. 10-year-old buildings in 2019 have the same retrofit rate as 10-year-old buildings in 2029. Depending upon modelling assumptions, the profile can be time-variant to reflect policy strengths in response to the trend of building stock energy performance. It may also be converted to an endogenously defined variable to enable the dynamic interplay between stock energy performance and policy interventions.

As afore-mentioned, the default setting of the holding period is fixed as 10 years. This is indicative, assuming a constant interval between two retrofits. In reality, retrofit intervals of buildings may vary due to a range of technological, economic and social factors. To recognise the uncertainty with respect to this parameter, a solution is to create multiple dedicated sub-stocks for retrofitted buildings and place them in parallel with the existing one. Each dedicated sub-stock is used to keep retrofitted buildings for a different holding period, e.g. a dedicated sub-stock with 12 vintages is for 11-year holding period, a dedicated sub-stock with 13 vintages is for 12-year holding period, and so on. Then the to-be-retrofitted buildings flowing into the original dedicated sub-stock can be distributed across these parallel dedicated sub-stocks, based on some distribution profile. For example, a total of 11 dedicated sub-stocks may be used to represent the range of 10-year to 20-year holding periods, with the first one having 11 vintages and the last one having 21 vintages. As an initial setting, the inflow into these sub-stocks may be distributed uniformly. When empirical data is available and sufficient, a distribution better describing the probability densities of various length of the holding period may be informed. Such a more sophisticated setup can be easily reduced back to the original default version by adjusting the distribution so that all to-be-retrofitted buildings will flow into the first dedicated sub-stock, namely the original one with 11 vintages (10-year holding period).
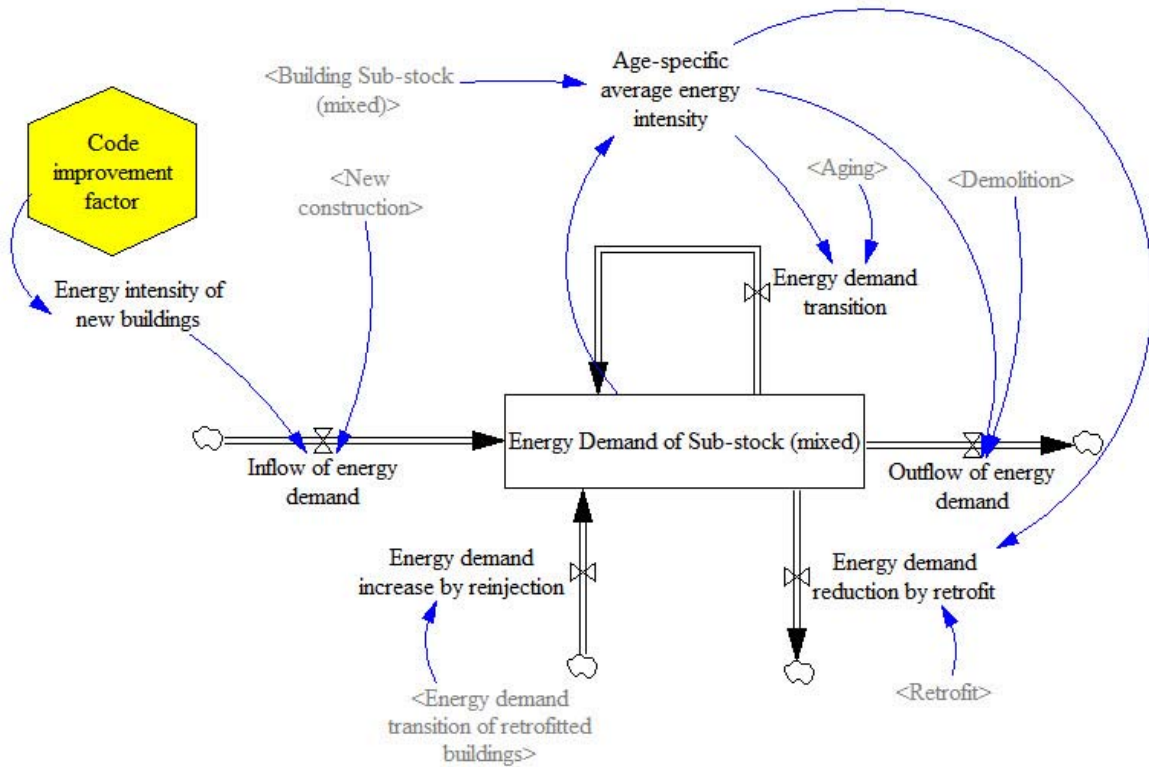
Figure 7.9: Dynamics of energy demand of main sub-stock of multiple-retrofits model

Similar to the settings for building stock, the (operational) energy demand of buildings is represented by using two sets of sub-stocks, with one for the main sub-stock and the other one for the sub-stock dedicated for retrofitted buildings experiencing the holding period. Compared to a regular co-flow setup, the energy demand of main sub-stock features an additional outflow of energy demand reduction due to outflow of buildings undergoing retrofit, and an additional inflow of energy demand increase due to reinjection of retrofitted buildings having survived the holding period (Figure 7.9). The outflow is determined by the amount of retrofitted buildings per year and the age-specific average energy intensity per year. It is useful to note that this outflow by itself is the sum of the outflows of energy demand reduction applicable to each of the age groups. As for the inflow, it is the total amount of energy demand of retrofitted buildings at all ages that survive their 10-year holding period and return to the main sub-stock of buildings. This inflow links the energy demand of main sub-stock with the energy demand of the sub-stock dedicated to retrofitted buildings, which has the typical structure of co-flow mirroring the structure of the sub-stock dedicated to retrofitted buildings themselves (Figure 7.10). This sub-stock is also double-subscripted to reflect the energy performance as a property of the retrofitted buildings experiencing the double-aging process. The inflowing energy demand into this sub-stock is a function of expected energy intensity of retrofitted buildings, which is a key target of policy interventions.
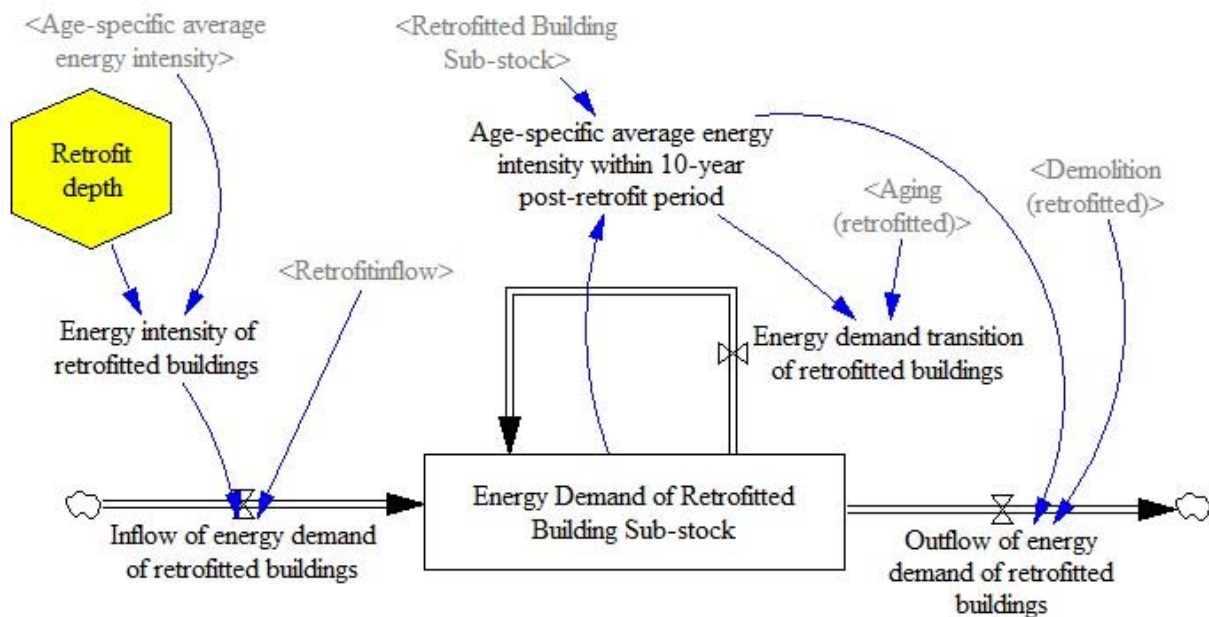
Figure 7.10: Dynamics of energy demand of dedicated sub-stock of multiple-retrofits model

As a simple approach, the default setting of the model is for the expected energy intensity of retrofitted buildings to be equal to the age-specific average energy intensity of existing buildings (including both retrofitted and unretrofitted buildings) minus the energy intensity reduction gained through retrofit. The gain is a percentage of the age-specific average energy intensity of existing buildings (including both retrofitted and unretrofitted buildings). The percentage, termed "retrofit depth", represents the extent to which the energy intensity of existing buildings will be improved relative to itself as a result of retrofit.

There are, of course, many factors contributing to the large variability and uncertainty with respect to energy intensity of new buildings in the future, technical potential and economic viability of retrofitting old buildings, depth of retrofit and associated costs, etc. These are context-specific factors and will need to be investigated in more detail when adapting and applying the model to a given context. The generic model presented here uses the variables "retrofit depth" and "code improvement" as simplified approximations of the impact of these factors.

The stock-wide average energy intensity of all buildings is obtained by dividing the total demand of all buildings, which is the sum of energy demand of the main sub-stock and that of the dedicated sub-stock, by the total floor area of all buildings consisting of buildings in the main stock (a mix of non-retrofitted and retrofitted buildings) and those in the dedicated sub-stock (retrofitted buildings only). The retrofit profile and retrofit depth have impacts on the stock-wide

average energy intensity and total energy demand. Meanwhile, in the default model setup, the dedicated sub-stock for retrofitted buildings is subject to the same hazard profile as the main sub-stock, although this may not be the case in practice. Newly retrofitted buildings are less likely to be demolished in the short term after the retrofit, as compared to buildings that are of the same age but not retrofitted. The "On" and "Off" setting of demolition profile for the dedicated sub-stock allows for exploration of its impact on the stock-wide average energy intensity under various scenarios.

7.4 Model limitations and potential extension

It is acknowledged that the model presented here, as in any models of buildings, energy and related sectors, has been developed based on various methodological assumptions to be a simplification of the dynamic complexity of real-world building stock evolution and energy performance characteristics. These assumptions lead inevitably to limitations inherent to the model that should be taken into account when applying the model. Extensions can be made to enhance the model's flexibility and applicability.

Firstly, in modelling the effect of retrofit, it is assumed that building operational characteristics and occupant behaviours do not vary significantly; this is a fairly common assumption explicitly or implicitly made by many building energy models. These variations may be incorporated into future modelling with empirical data and complementary modelling approach such as agent-based modelling.

Secondly, as the model's focus is on energy, it limits itself to those energy-related retrofits. However, it is acknowledged that sometimes general renovation activities that are not directly related to energy performance will have a direct impact on building lifetime. This resultant extension of building lifetime may have a long-term impact on the interplay between the demolition of old and inefficient buildings and the construction of new and efficient buildings which together decide the stock-level energy performance.

Thirdly, in the current version of the generic model, the retrofit depth is set as a single value. In reality there exist a range of energy-related retrofit activities and therefore many factors contributing to the variability and uncertainty with respect to retrofit depth. This can be taken into account through a very minor extension of the model which is to use a distribution profile to represent the share of a certain level of retrofit depth in all practically feasible retrofit depths. This extension will require empirical data.

Fourthly, the holding period of the dedicated substock of retrofitted buildings is set as a constant as an intended simplification. In reality, retrofit intervals may vary due to a range of technological, economic and social factors. To take this into account, additional structures can be easily added to the model to create multiple dedicated substocks in parallel with the existing ones as has been described. Each dedicated substock is used to keep retrofitted buildings for a different holding period. This setup enables a distribution of various holding periods, which needs to be informed by empirical data.

An overview of this stock turnover and multiple-retrofits model, which presents the dynamic interplay across variables, is given in Figure 7.11. This is presented as a simple generic version in order to highlight some key points (stock disaggregation and multiple retrofits) rather than a fully-fledged version, which could be used for real-world applications and policy analysis. To develop the latter, additional structures and variables still need to be added to the model. For example, exogenous drivers of new construction and feedback loops enabling dynamic interplays between new construction, aging of existing buildings, and demolition of old buildings reaching their end of lifetime could be incorporated in order to model future possible trends of stock evolution. In addition, the model boundary may be expanded to cover embodied energy consumption and carbon emissions incurred in producing building materials, construction, retrofit and demolition activities. Such an extension would enable a lifecycle perspective to be taken when evaluating building stock energy performance and carbon emissions.
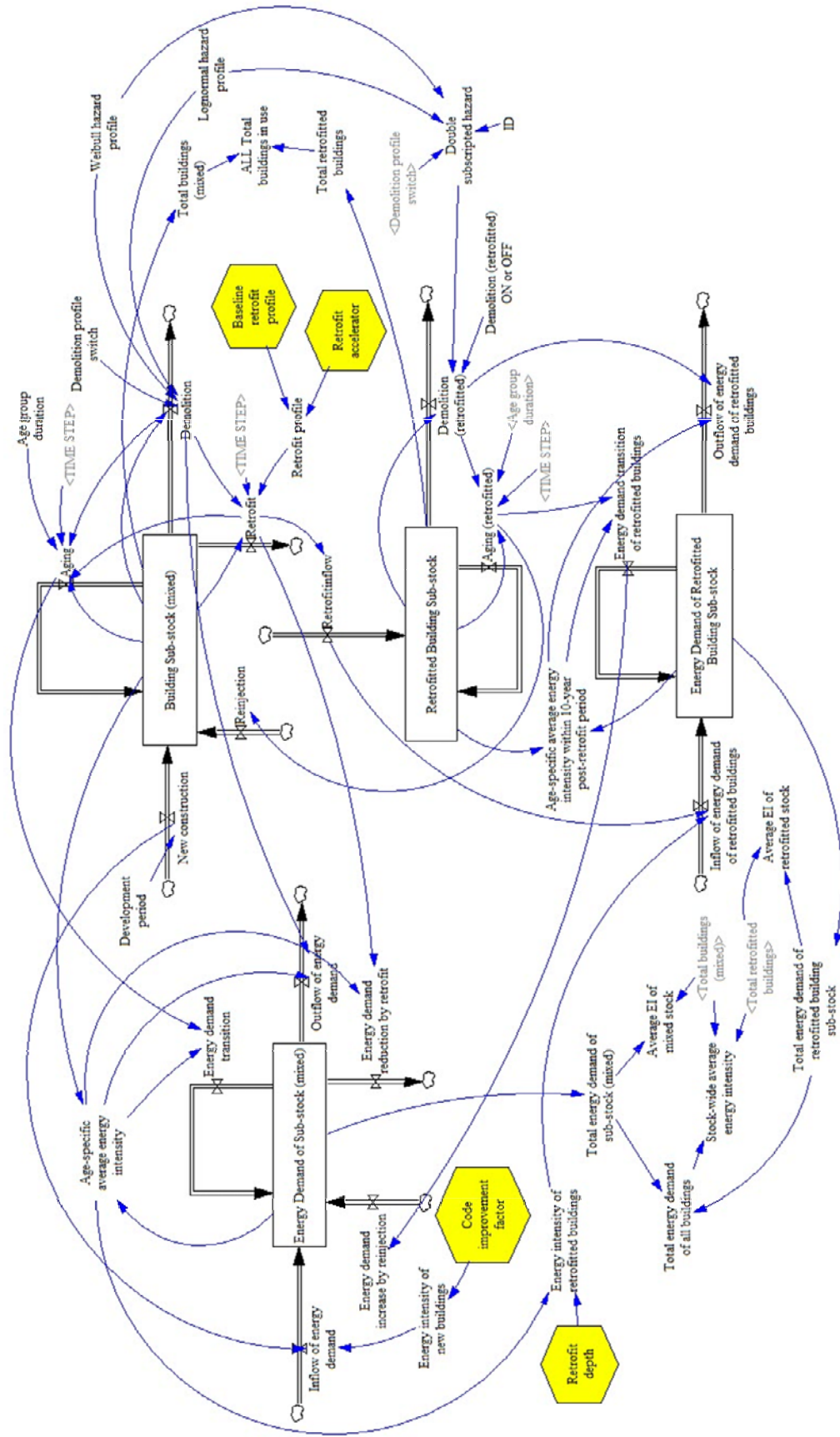
Figure 7.11: Full model of building stock energy model with multiple retrofits

7.5   Chapter summary

This chapter answers research question Q4. It develops an enhanced building stock operational energy model to address some of the fundamental structural and behavioural limitations found in previous applications of System Dynamics-based models. The model loosens the strong assumptions made by previous models, including perfect mixing in a first-order delay in a single stock model, and perfect mixing in each delay of a third-order delay in a three-vintage model. By disaggregating a building stock into age-specific sub-stocks, the model enables explicit representations of the uncertainties associated with age-specific risks of demolition. Greater structural flexibility is offered to accommodate various levels of data availability. Moreover, compared with previous models, the model avoids unreasonable situations where a building is allowed to undergo multiple rounds of retrofits within a very short period of time, or a building is demolished soon after being retrofitted.

The model is generic, transparent and therefore potentially applicable in a wide variety of contexts. Its flexibility enables adjustments to meet various requirements and settings. On the one hand, the model can be extended to accommodate increased granularity and enhanced level of sophistication, or expanded boundary of modelling. Structurally, with available empirical data, the sub-stocks of retrofitted buildings can be further divided to model various lengths of the holding period. Functionally, depending upon model purpose, additional structures and variables can be added to the model to enhance its utility, such as feedback loops linking demolition and new construction to model future stock growth, embodied energy and carbon due to production of building materials, building construction, retrofit and demolition activities, stock of existing heating technologies and possible future trends of technology mix to model carbon emissions of heating. On the other hand, sometimes building demolition is of less concern, e.g. the buildings are generally long-lived and/or the period of modelling and analysis is short relative to building lifetimes. In these circumstances, the model can be straightforwardly reduced to a three-vintage or single stock structure as found in previous studies. Similarly, the multiple retrofit dynamics can be easily reduced to single retrofit or no retrofit structure, but retain the ability of avoiding unrealistic modelling results of previous models. The reduced form version of the model will be useful when the interest is in modelling the general behavioural dynamic patterns of building stock and energy, rather than in detailed representation of model structures and variables for accurate numerical values of stock or sub-stock level performance indicators.

In summary, this model is well placed to be used as a stand-alone model or as part of a larger model looking at building stock-level energy in a variety of national or sectoral contexts. Its

transparency and flexibility will enable further extensions and improvements for greater capacity in wider applications for evaluating building energy policy interventions. For its application under this thesis, this model will be extended to have additional structures and variables and adapted to the specific context of Chinese urban residential stock. Details are presented in Chapter 8.

8

Future operational energy

8.1 Chapter introduction

This chapter is dedicated to modelling the future trajectories of the operational energy of the Chinese urban residential stock. The generic model developed in Chapter 7 is extended and adapted for operationalisation in Chinese urban context. The inputs to the model are the outputs from the probabilistic stock turnover model in Chapter 5 and data on energy intensity from various sources. Research question Q5 is answered.

8.2 Method operationalisation and data source

8.2.1 Geographical coverage

The geographical scope of this chapter (and also Chapter 9) is narrowed down from the entire territory of China to north China. Urban residential buildings in north China demand space heating during winter season, which is met by centralised heat supply systems dominated by fossil fuel fired thermal power plants.[6] This has significant impacts on energy use, carbon emissions, and

---

[6] In the context of centralised heating during winter season, north China refers specifically to a total of 16 provinces, autonomous regions, and municipalities, covering Beijing, Tianjin, Hebei, Shanxi, Inner Mongolia, Liaoning, Jilin, Heilongjiang, Shandong, Henan, Shaanxi, Gansu, Qinghai, Ningxia, Xinjiang, and parts of Sichuan.

environmental quality. In particular, due to space heating, the average operational energy intensity per m^2 in north China is much higher than that of the other regions, as well as the entire country as a whole. From the purpose of comparing embodied energy and operational energy, focusing on north China is a more 'conservative' approach as it may downplay the magnitude of embodied energy relative to higher operational energy. This way, the comparison will be biased in a good way, thereby providing a stronger argument about the importance of embodied energy and the necessity of a whole-life cycle perspective for building energy.

8.2.2   Stock turnover dynamics

To estimate stock operational energy, the generic model in Chapter 7 is extended to take into account the dynamic building stock evolution process in the future. The outputs from the probabilistic stock turnover model in Chapter 5 are used as inputs here. The initial year of the extended operational energy model is set to be 2018. From the outputs of the probabilistic stock turnover model, samples are drawn from the joint posterior predictive distribution of annual new construction, age-specific substocks, and age-specific hazard rates. Each sample corresponds to a particular combination of a time series of forecasted annual new construction from 2019 to 2070, a group of 101 age-specific substocks which form the total stock in 2018, and 101 age-specific hazard rates for substocks aged 0 to 100. This sample is then used to initialise the 2018 building stock of the extended operational energy model and drive its future evolution. Here a scale factor of 0.4 is applied to the sampled inputs of annual new construction and substocks in 2018, as historical statistics and THUBERC annual reports have shown that north China accounted for 40% of the total urban residential stock of China. This ratio is assumed to remain unchanged throughout the modelling period.

8.2.3   Heating energy

The operational energy consists of heating energy and non-heating energy, which are modelled separately. On heating energy, the average heating energy intensity in 2018 was 14.4 kgce/m^2 for existing urban heat supply systems (THUBERC 2020). These included old, inefficient boilers commonly found in small cities in many provinces. For new systems, the reference performance indicators of heating energy intensities, established by the Standard for Energy Consumption of Building (MOHURD 2016), are used to set values in the model. The term 'reference' is used because the standard is not yet mandatory, and the performance indicators are not time-bound. However, it is considered the most relevant reference because the standard for the first time establishes quantitative energy performance indicators that buildings are expected to achieve after being commissioned and put into use. Complementing the prevailing practice of prescriptive

design and ex-ante compliance, the standard emphasises performance-based and result-driven design and ex-post monitoring and evaluation of actual energy performance of buildings. Its indicators are determined based on actual building energy data and against the high-level development target of curbing economy-wide total energy consumption and carbon emissions. For heating in north China, the standard covers 14 provinces and two province-level municipalities. For each province/municipality, the indicator of heating energy intensity is categorised into a short-term baseline indicator and a medium- to long-term guiding indicator. The short-term baseline indicator reflects the reasonable heating energy intensity level based on the currently available technologies and prevailing practices, whereas the medium- to long-term guiding indicator is the desired target to be achieved by exploring and attaining the full potential of energy saving through continued policy interventions and technological advancement. Across the provinces and municipalities, the baseline indicators range from 6 to 11.4 kgce/m^2, and the guiding indicators range from 3 to 8 kgce/m^2. The mean values of the two categories are 8.62 kgce/m^2 and 5.16 kgce/m^2, respectively.

Based on the above indicators, the model for this chapter sets the average heating energy intensity of new buildings to linearly decrease from 8.62 kgce/m^2 in 2019 to 5.16 kgce/m^2 in 2040 and then remain at 5.16 kgce/m^2 from 2041onwards. For each year, a random component is applied to the average intensity to represent the uncertainty. The random component is assumed to be uniformly distributed, i.e. U(-2.5,2.5). The lower and upper bounds are set based on the interval lengths of the baseline indicators and the guiding indicators.

Heating energy related retrofit of existing buildings includes major measures taken to reduce the heating energy intensity, covering building envelope, heat source, and heat supply network. It is modelled as a function of the age-specific average heating energy intensity of substocks of a certain age, the heating energy intensity of new buildings, the retrofit depth, and the retrofit rate.

The heating energy intensity of new buildings is used as the benchmark against which the reduction of heating energy intensity achieved by a retrofit is determined. If the gap between the average heating energy intensity of an age-specific substock and the heating energy intensity of new buildings (denoted as "A") is larger than the average heating energy intensity of an age-specific substock multiplied with the retrofit depth (denoted as "B"), the reduction of heating energy intensity reduction is set to be equal to B. Otherwise, the reduction is set to be equal to A. This setting avoids the unrealistic situation where buildings already with very low heating energy intensity will keep being retrofitted further, or where the gap (A) is much larger than what can be realistically achieved through a retrofit.

For the retrofit depth, there is a dearth of empirical evidence in Chinese context, especially for residential buildings. A study on building energy retrofit activities in 28 member states of the EU from 2012 to 2016 found that energy savings per retrofit was 8.8% for residential buildings and 17.1% for non-residential buildings (Navigant 2019). Internationally, according to IEA's Energy Technology Perspectives, building energy retrofit was found to be typically less than a 10% to 15% energy intensity improvement (IEA 2017). A similar observation was reported by the global status report of the Global Alliance for Buildings and Construction (Global Alliance for Buildings and Construction et al. 2019). In this model, the retrofit depth is set to be 10%.

The retrofit rate is set to be 1%, namely, buildings that will be retrofitted per year are assumed to account for 1% of the total stock size. This assumption is based on several observations. Over the ten-year period from 2006 to 2015, the urban residential buildings in north China that were retrofitted for heating energy savings totalled to 0.99 billion m^2 (MOHURD 2012; MOHURD 2017). From 2016 to 2020, it was planned by MOHURD that an additional 0.5 billion m^2 would be retrofitted, i.e. 0.1 billion m^2 per year on average (MOHURD 2017; National Development and Reform Commission 2017). According to THUBERC (2020), the size of urban residential stock in north China was estimated to be 9.8 billion m^2 by end of 2018. These numbers suggest that, from 2006 to 2018, the annual retrofitted buildings were 99.2 million m^2 on average, which corresponded to a retrofit rate of 1% in 2018. The situation was similar in Europe. As found in (Navigant 2019), the annual retrofit rate of residential buildings in the EU was 1% for the period of 2012-2016. More internationally, the IEA noted that building retrofit rates were often much less than 1% of historical stock per year (IEA 2017).

8.2.4   Non-heating energy

Non-heating energy of urban residential buildings in north China consists of energy use by cooking, home appliances, lighting, water heating, and space cooling. The average non-heating energy intensity in 2018 was estimated to be 8.6 kgce/m^2 (THUBERC 2017; THUBERC 2020). In the future, the non-heating energy use of urban households in Chinese cities is expected to keep increasing as a result of continued improvement of living standards and increasing demand for amenities and comfort (IEA and THUBERC 2015). Over time, the trend is expected to plateau as the household energy demand will be satiated, similar to what has already been observed in some developed countries (Yu, Eom, Zhou, et al. 2014; THUBERC 2017; Xing et al. 2015; Clarke et al. 2018).

As established by the Standard for Energy Consumption of Building (MOHURD 2016), the medium- to long-term performance indicator of non-heating energy intensity of residential

buildings in north China is 9.8 kgce/m^2. This indicator is used by the model here for setting possible future values. It is assumed that the non-heating energy intensity of residential buildings in north China will reach its saturation in 2040. The saturated level is assumed to be normally distributed, with a mean value of 9.8, a standard deviation of 0.5, and bounded between 90% and 110% of the mean value. From 2018 to 2040, the intensity is assumed to increase linearly from 8.6kgce/m^2 in 2018 to a possible 2040 value of this normal distribution, and then remain constant from 2041 onwards.

It is useful to clarify that this setting does not consider the possible impact of the afore-mentioned building envelope retrofit on space cooling. Firstly, the electricity consumption by air conditioning for space cooling accounted for less than 8% of total non-heating energy in north China. Despite the possible increase of ownership and usage of air conditioners, over the medium to long term this share is expected to remain below 15% (THUBERC 2017). Secondly, building envelope plays a much different role in affecting space heating and cooling. Studies have found that thermal insulation and airtightness of building envelope have a significantly larger impact on heating energy use than cooling energy use (THUBERC 2017). In practice, improving building envelope performance makes little difference to cooling energy use of residential buildings (Li & Jiang 2006; Xie et al. 2012; Peng 2014). Therefore, electricity consumption for space cooling is not modelled separately as space heating, but implicitly modelled as an integral part of the non-heating energy in the model.

8.2.5 Uncertainty propagation

Through Monte Carlo simulations, the uncertainties associated with the above input variables are propagated through the emergent behaviour of the model to obtain the probability distribution of its outputs, such as stock-level total operational energy and stock-wide average operational energy intensity. The detailed results are presented in subsequent sections.

8.3 Results and discussion

8.3.1 Heating energy consumption

The modelling results of heating energy consumption of urban residential stock in north China is presented in Figure 8.1. Despite the strong increase of the stock size driven by increasing urban population and demand for housing, the heating energy consumption does not experience any significant rise or drop throughout the 40-year period of study. Starting from 2019, the mean value of heating energy consumption is found to increase continuously but marginally. Around 2034, it

reaches its peak value. The 95% credible interval is between 137.1 to 171.8 million tce. The mean value is 155.3 million tce, only 11% than the 2018 level of 139.9 million tce. For the same period, the stock size increases by 56%. This demonstrates that the expected increasingly stringent requirement on heating energy intensity of new buildings and persistent energy retrofit activities can effectively offset the stock expansion and curb the increase of heating energy consumption.
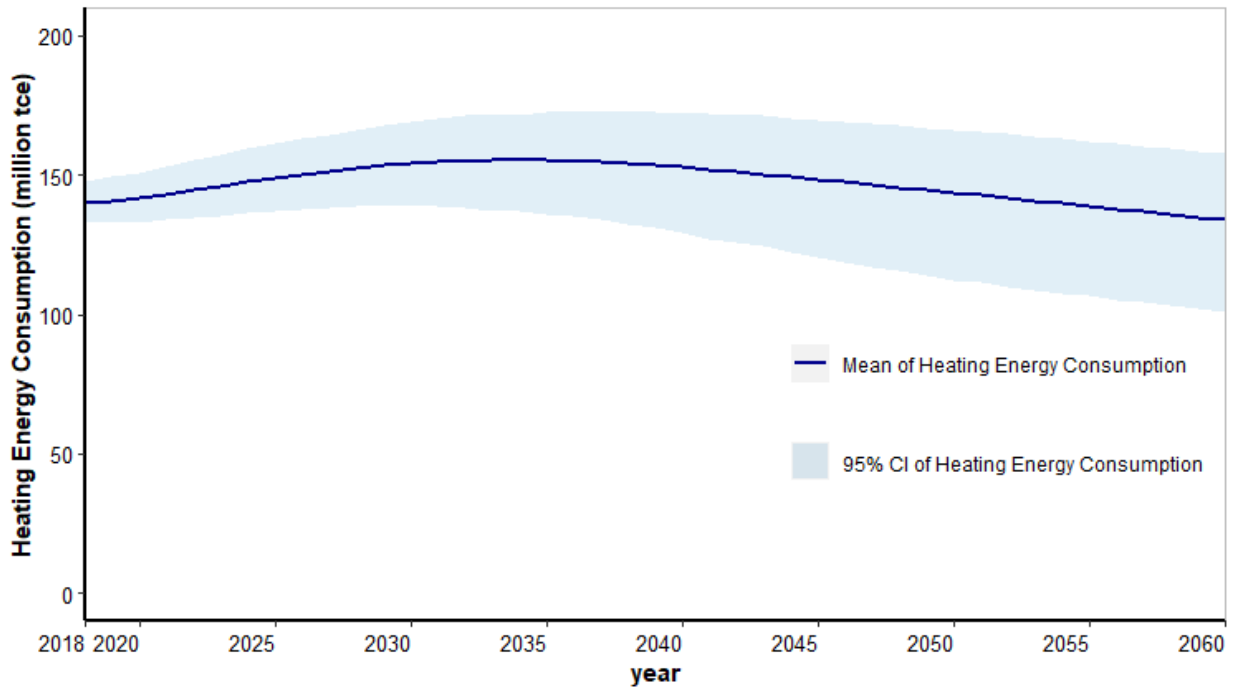

Figure 8.1: Heating energy consumption by urban residential stock in north China

From 2035 onwards, the residential stock keeps expanding, but at a gradually lower rate. By 2060, it approaches its peak value in 2065. During this period, the heating energy consumption firstly plateaus for several years following the peak and then starts to steadily decrease at a considerable rate. This is because the increasing amount of inefficient old buildings reaching the end of their lifetime are removed from the stock, in parallel with the construction of efficient new buildings. The heating energy consumption of these old buildings exceeds that of incoming new buildings. This gradual replenishment of the stock with new buildings helps to drive down the stock-wide heating energy consumption, which reaches 134 million tce by 2060, even 4.2% lower than the 2018 level.

Figure 8.2 shows the probability distribution of annual heating energy consumption in various years. This representation offers a further insight into the probability distribution of the heating energy per year, as the uncertainties associated with the stock size, annual new construction,

heating energy intensity of new and existing buildings, and retrofit activities are all captured and propagated through the emergent behaviours of the model outputs, namely, the dynamic evolution of the stock and the associated heating energy consumption.
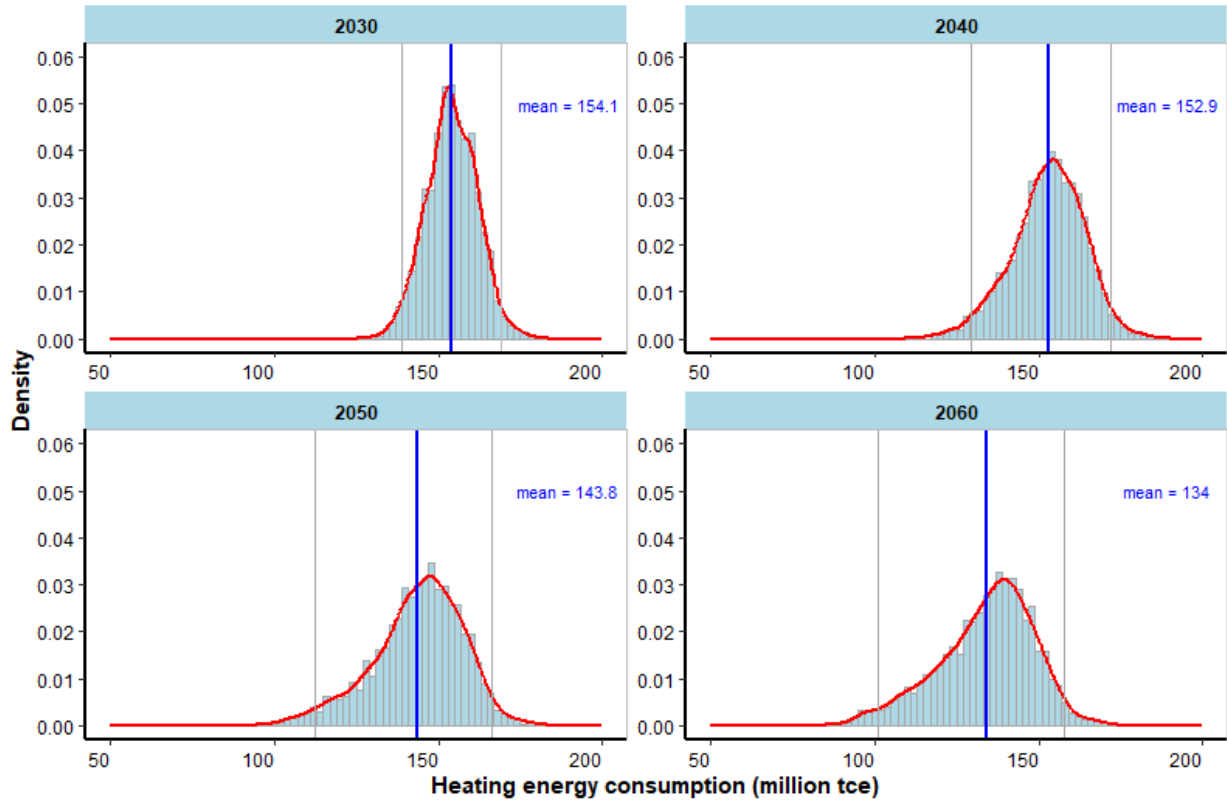

Figure 8.2: Distribution of heating energy consumption by urban residential stock in north China in selected years (2030, 2040, 2050, 2060)

The effect of heating energy efficiency improvement can be more clearly demonstrated by heating energy intensity trend. As shown in Figure 8.3, the incoming new buildings, which have a much lower average heating energy intensity than the existing stock, will effectively bring down the stock-wide average heating energy intensity. The energy retrofit of existing buildings also contributes to the improvement, but to a much less extent because of the ratio of retrofit, which is set to what is considered a practically feasible level. In general, the belt of credible interval and the curve of mean value show an overall trend similar to an exponential decay, characterised by a gradually reducing rate of decrease. This is because the combined effect of efficient new buildings and energy retrofit of existing buildings shrinks over time.
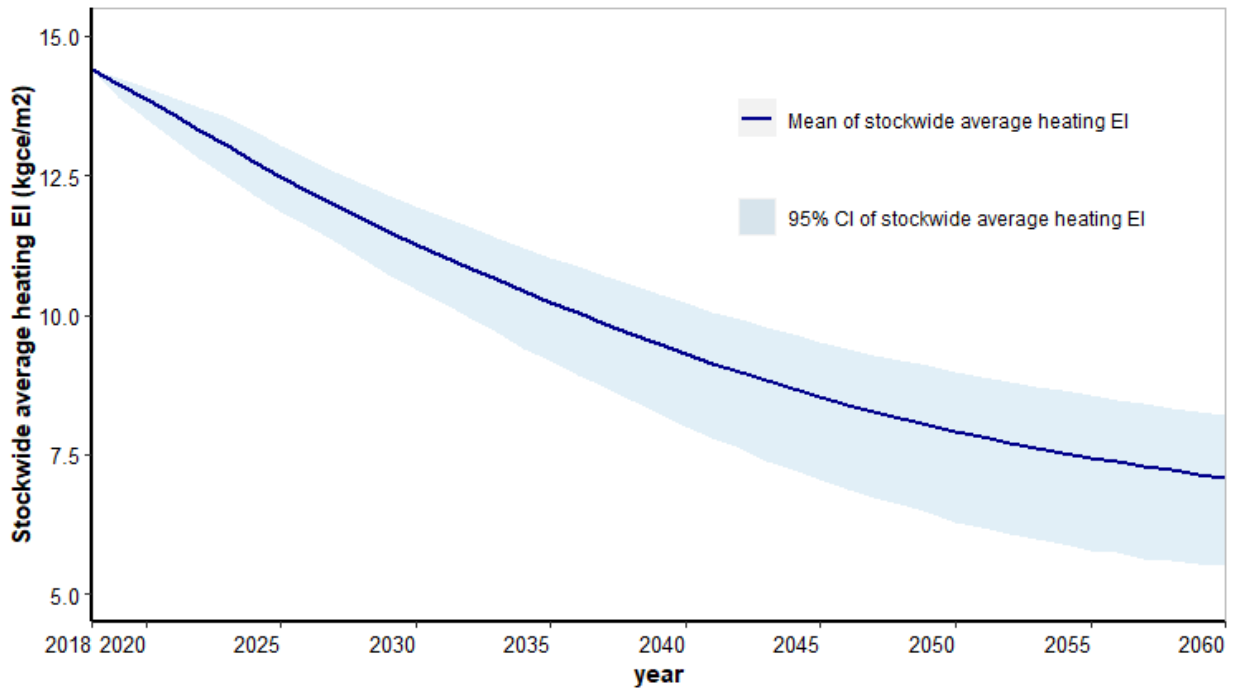
Figure 8.3: Stock-wide heating energy intensity

In the initial years, the annual incoming new buildings accounts for around 5 to 6% of the existing stock. This is a considerable level to potentially make some transformational impact on the stock. The average heating energy intensity of new buildings, which is expected to steadily decrease from 8.6 kgce/m^2 to 5.2 kgce/m^2 till 2040, is significantly lower than the average heating energy intensity of existing buildings in the stock, which is 14.4 kgce/m^2 in 2018. The continued injection of increasingly efficient new buildings into the stock, continued removal of inefficient old buildings from the stock, and continued energy retrofit of existing buildings in the stock collectively bring down the stock-wide average heating energy intensity. The mean value of stock-wide average heating energy intensity decreases to 12.5 kgce/m^2 in 2025 and further to 11.3 kgce/m^2 in 2030, respectively being 13% and 21% lower than the 2018 level.

Over time, the stock-wide average heating energy intensity decreases at a gradually slowing rate. This is due to several factors. First, with the accumulation of buildings in the stock, the ratio of annual incoming new buildings to the stock size keeps decreasing and therefore its impact on the stock diminishes gradually. Second, the gap between the stock-wide average heating energy intensity and the heating energy intensity of annual incoming new buildings keeps decreasing, resulting in less room for gains of energy savings from energy retrofit. Third, the demolished buildings are more energy-efficient than before. As a result, the removal of these buildings from the stock has less effect on reducing the total stock heating energy consumption and improving the stock-wide average heating energy intensity. From 2040 to 2060, the reduction in the mean

value of the stock-wide average heating energy intensity is 2.2 kgce/m^2, less than 50% of the reduction by 4.6 kgce/m^2 from 2020 to 2040. The probability distribution of the stock-wide average heating energy intensity is given in Figure 8.4.
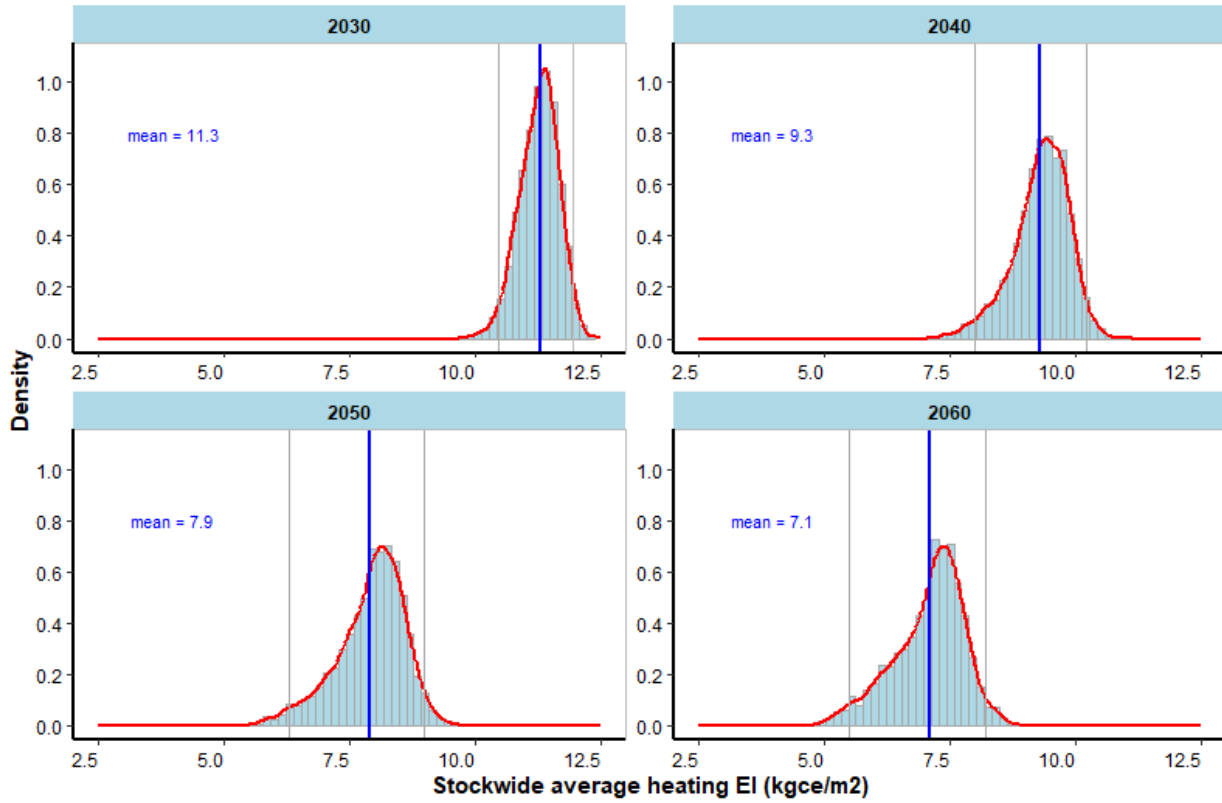

Figure 8.4: Distribution of stock-wide average heating energy intensity in selected years (2030, 2040, 2050, 2060)

8.3.2 Non-heating energy consumption

Figure 8.5 presents the forecasted trajectories of non-heating energy consumption of the urban residential stock in north China. From 2019 to 2040, a steady increase trend can be observed. The driving force of this increase is the combined effect of increasing urban population, increasing urban housing area per capita, and increasing ownership of appliance and the resultant demand for energy services of urban households. From 2041 onwards, the increase starts to decelerate gradually, due primarily to the expected satiation of household energy services demand. The substantially slow-downing growth of housing area per capita is also a contributing factor. This decelerating increase trend continues until 2065 when the peak is reached. This peaking largely coincides with the peaking of stock size, because the already satiated non-heating energy intensity no longer has any material impact on the trend change. The peaked non-heating energy consumption has a 95% credible interval of 165.3 to 208.2 million tce and a mean of 186.5 million

tce. Following the peaking, the non-heating energy consumption largely plateaus until 2070, when it starts to slowly go down. The probability distribution of the non-heating energy consumption is shown in Figure 8.6.
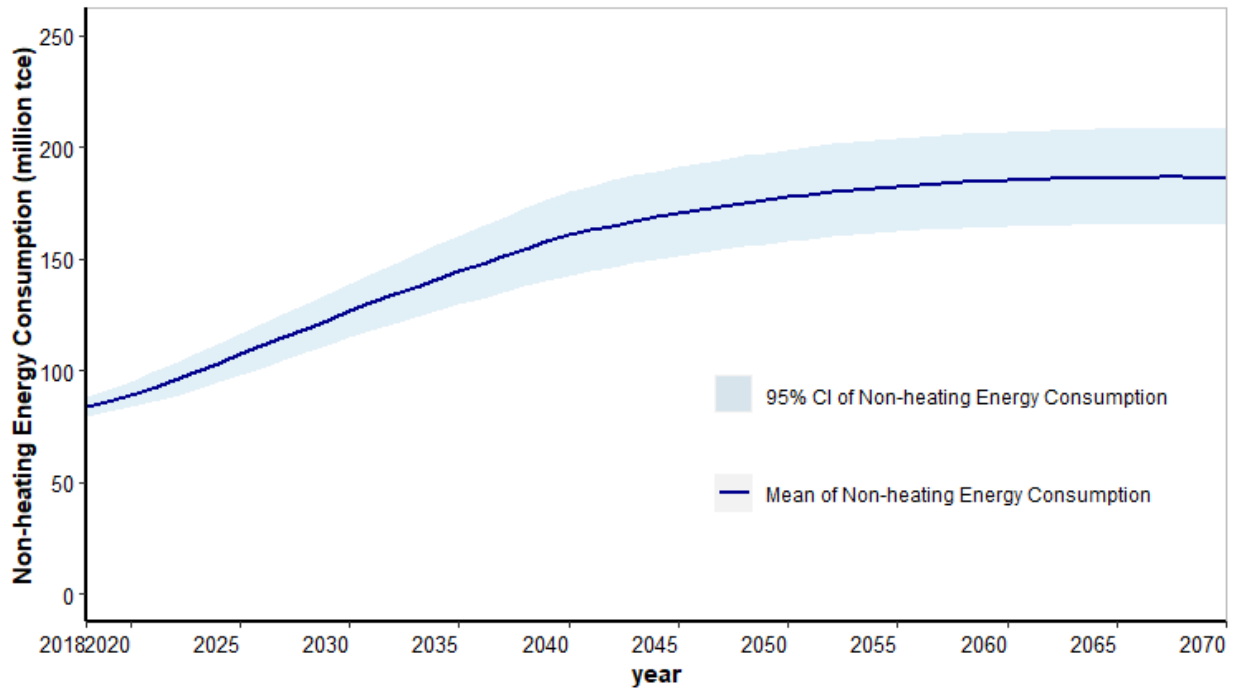

Figure 8.5: Non-heating energy consumption by urban residential stock in north China
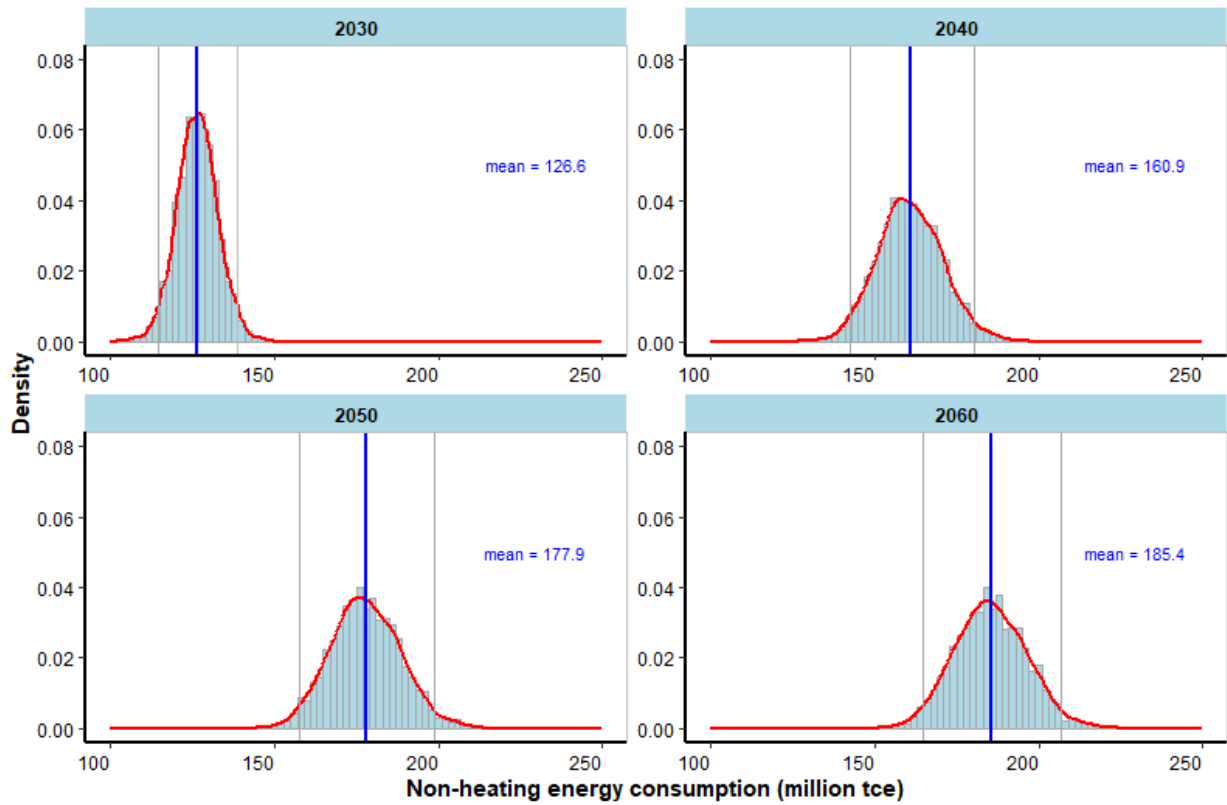
Figure 8.6: Distribution of non-heating energy consumption by urban residential stock in north
China in selected years (2030, 2040, 2050, 2060)

8.3.3 Total operational energy consumption

The sum of heating energy and non-heating energy gives the total operational energy of urban
residential stock in north China (Figure 8.7). Generally, the mean curve and the 95% credible
interval present a trend reflecting the combined effect of heating energy, which peaks early,
around 2034, and then declines steadily, and the non-heating energy, which peaks much later,
around 2065. For the first 20 years, the total operational energy keeps increasing as a largely
constant rate. From 2041, when the non-heating energy intensity of households is assumed to
reach its saturation, the increasing trend of total operational energy starts to slow down gradually.
Its peak is expected to be reached around 2051, when the 95% credible interval ranges from
280.3 million tce to 358.7 million tce and the mean value is 170 million tce. Following the peak,
the total operational energy largely plateaus for a few years until 2055, when it starts to slowly
decline. By 2060, its mean value reaches 318.8 million tce and its 95% credible interval ranges
from 276.2 to 356.8 million tce.
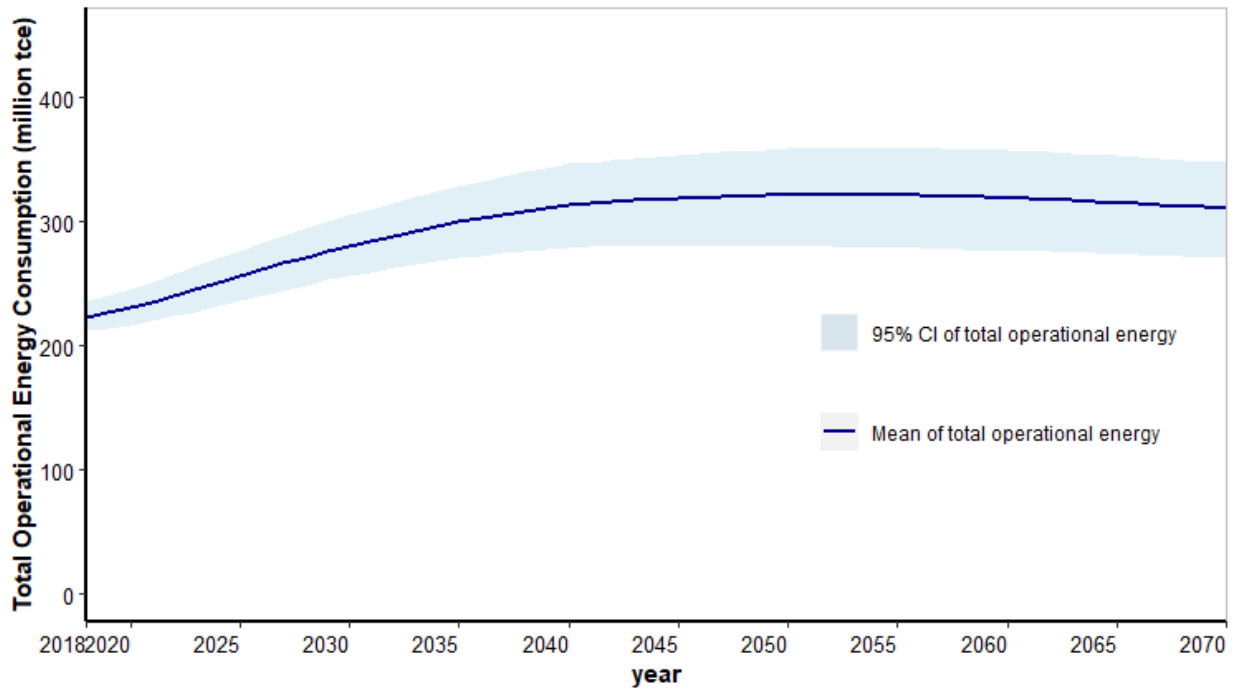
Figure 8.7: Total operational energy consumption by urban residential stock in north China

As shown in Figure 8.8, the distribution of total operational energy in typical years is less skewed and close to a bell shape. Compared to the distribution of heating energy or non-heating energy, the distribution is wider due to it being the sum of heating and non-heating energy. The probability distribution reflects the uncertainties associated with the stock turnover dynamics, total stock size, annual new construction, heating energy intensity of new and existing buildings, and non-heating energy intensity of new and existing buildings. These uncertainties are captured and propagated through the emergent behaviours of the model. In so doing, a further insight into the possible values of the total operational energy per year can be gained.

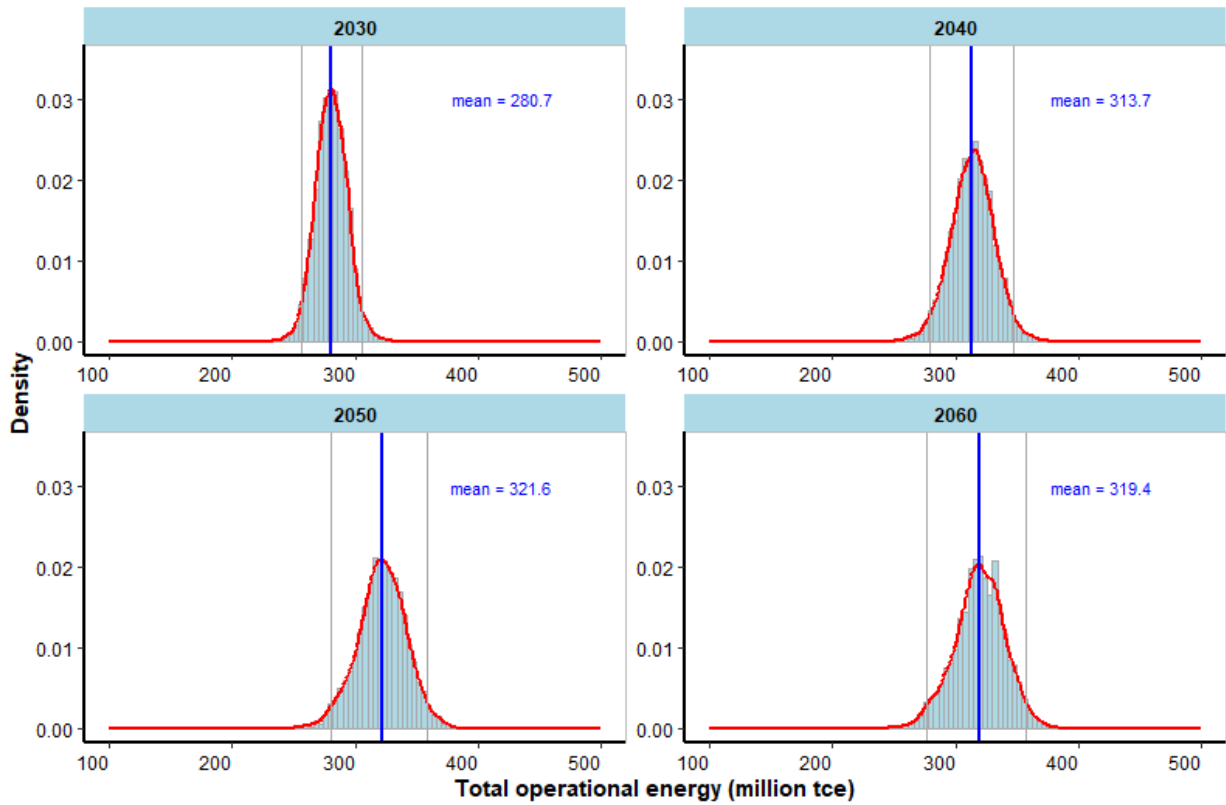Figure 8.8: Distribution of total operational energy consumption by urban residential stock in north China in selected years (2030, 2040, 2050, 2060)

It is useful to compare the results with previous studies. The Research Institute of Standards and Norms (RISN) under the Ministry of Housing and Urban-Rural Development forecasted that the total operational energy of the residential stock in north China, including heating and non-heating energy consumption, would peak around 2045 to 2050 (RISN 2016). In 2050, the estimate of RISN was 326 million tce. In their study on carbon emission and abatement potential outlook in China's building sector through 2050, Tan et al (2018) believed that the total energy consumption of Chinese buildings would not peak by 2050, but would continue to rise. Their estimate on the total operational energy of the residential stock in north China in 2050 was 305 million tce. Figure 8.9 shows a comparison amongst this study, RISN and Tan et al. The 95% credible interval of the 2050 forecast by this study is in the range of 280.7 and 358.7 million tce. The mean value is 321.7 million tce. The estimates by RISN (2016) and Tan et al. (2018) both fall into the 95% credible interval, with RISN located much closer to the mean value of this study.
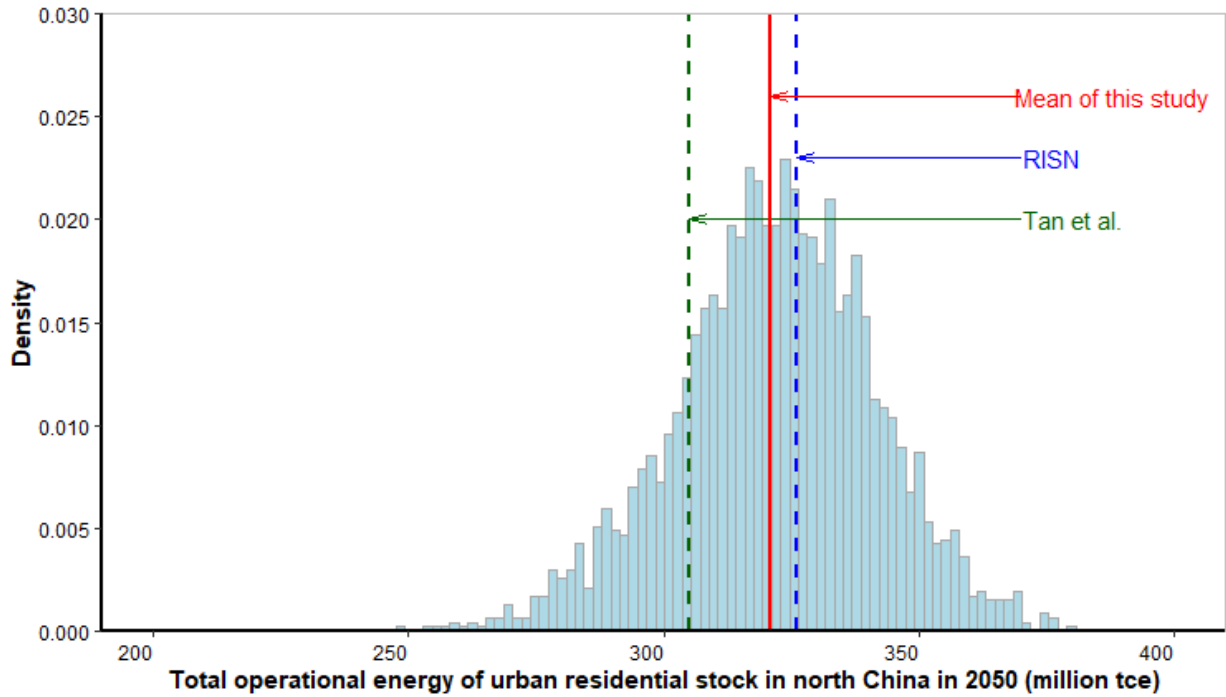
Figure 8.9: Forecasted total operational energy in 2050 – comparison with other studies

Using the empirical cumulative distribution function informed by the distribution in this figure, it can be calculated that the probability of the estimated total operational energy being higher than 305 million tce and lower than 326 million tce is 39.7%. This considerable probability demonstrates the large uncertainty associated with high-level point estimates by static scenario modelling. Compared to point estimates, the distribution of total energy obtained from dynamic scenario modelling through Monte Carlo simulation in this study provides a useful description of the uncertainty that allows policy-makers to avoid relying solely on point estimates and thereby make more informed decisions about policy measures.

Dividing the total operational energy by total stock size gives the stock-wide average operational energy intensity, as shown in Figure 8.10 and Figure 8.11. Similar to the heating energy intensity, the credible interval and mean curve show an overall trend largely following an exponential decay trend. Over time, the decline of the stock-wide total operational intensity slows down gradually. Compared to the heating energy intensity, the total operational energy intensity has a much less steep gradient, i.e. a slower declining rate. This is because the gradually increasing non-heating energy intensity keeps the total energy intensity high and partially offsets the effect of the rapidly declining heating energy intensity. From 2020 to 2050, the mean of the stock-wide average operational energy intensity drops by 22%, from 22.6 to $17.7 kgce/m^2$. In 2051, when the total operational energy of the stock is expected to reach its peak, the energy intensity will be in the

range of 15.8 to 19.1 kgce/m^2, with a mean of 17.6 kgce/m^2.

It is necessary to note that the stock-wide average operational energy intensity in this context applies to buildings in north China. This is different from the operational energy intensity presented in Table 6.2 in Chapter 6, which is the average of the entire Chinese residential stock covering all provinces and cities. In fact, the residential stock outside the boundary of north China accounts for 60% of the total floor area of the entire stock. There is no centralised heating for this region given the generally warm temperature during winter season. The energy intensity of households in this region is largely similar to the non-heating energy intensity of households in north China. Therefore, the average energy intensity across the entire residential stock is much lower than north China. For example, the 2018 average energy intensity across the entire residential stock, as presented in Table 6.2 in Chapter 6, is 15.5 kgce/m^2, approximately 32.6% lower than the mean of the average operational energy intensity of north China, 23 kgce/m^2, as shown in Figure 8.10.
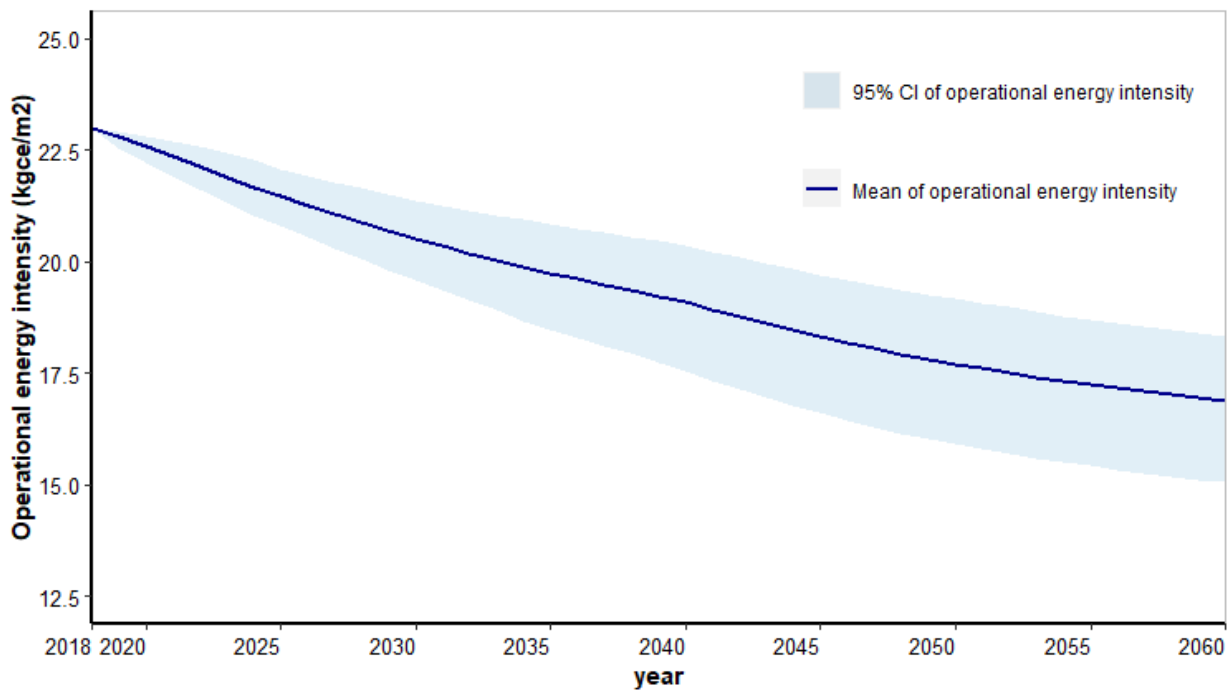
Figure 8.10: Stock-wide operational energy intensity
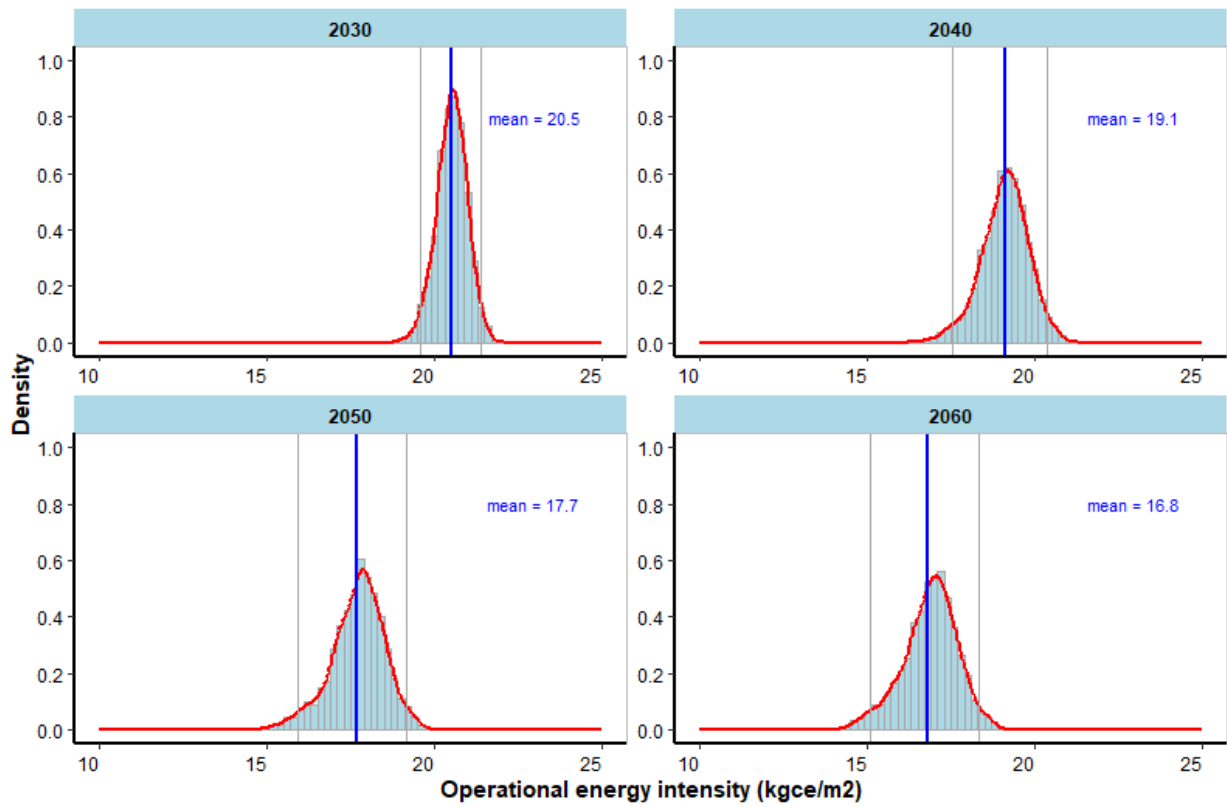
Figure 8.11: Distribution of stock-wide average operational energy intensity in selected years (2030, 2040, 2050, 2060)

8.4 Chapter summary

This chapter adapted and applied the generic System Dynamics model developed in Chapter 7 to forecast the future trend of operational energy of the residential stock in north China under the business-as-usual scenario. Key inputs to the adapted model include the outputs from the probabilistic stock turnover model presented in Chapter 5 and relevant energy intensity indicators specified in the Standard for Energy Consumption of Building issued by MOHURD. Heating energy and non-heating energy is forecasted separately and then aggregated to obtain the total operational energy. The future trend of energy intensity, as the key indicator of the collective effect of building energy efficiency policies and technologies, is also presented and discussed. These results help answer the research question Q5 and inform the calculation of whole-life energy consumption and scenario analysis in Chapter 9.

9

Whole-life energy under various policy scenarios

9.1 Chapter introduction

The embodied energy in Chapter 6 and operational energy in Chapter 8 make possible the modelling of future trajectories of the whole-life energy consumption. This chapter starts with a comparison between future embodied energy and operational energy at stock level and intensity level. It then proceeds to present and discuss the whole-life energy consumption under the business-as-usual (BAU) scenario. The BAU scenario is further compared with three policy scenarios, including extension of building lifetime (Policy A), acceleration of heating energy efficiency improvement (Policy B), and a combination of both (Policy C). The findings answer research question Q6.

9.2 Comparison between embodied energy and operational energy

In the preceding section 6.3.3, the estimated embodied energy of the entire Chinese residential stock over the historical period of 2010 to 2018 was compared with the operational energy of the stock. Its result provides clear evidence of the importance of embodied energy. In this section, the comparison is extended to the investigated future period of 2020 to 2060, with the focus on

the urban residential stock in north China. From the purpose of comparing embodied energy and operational energy, focusing on north China is a more 'conservative' approach as it may downplay the magnitude of embodied energy relative to operational energy. This way, the results will provide a stronger argument about the importance of embodied energy and the necessity of a whole-life cycle perspective for building energy.

9.2.1 Ratio of embodied energy to operational energy

As presented in preceding chapters, stock-level embodied energy (EE) and operational energy (OE) over the future decades has been forecasted in an integrated manner. This allows the comparison of EE and OE at the stock level with a comparability and robustness higher than the comparison for the historical period in Chapter 6, where EE is modelled by this thesis and OE refers to literature data. As the scope of this Chapter is limited to north China, the EE results in Chapter 6 are scaled down, from urban residential stock across the entire country to that in north China. The OE results in Chapter 8 are used directly for this comparison, as they are estimated based on the urban residential stock in north China.

As shown in Figure 9.1, the ratio of EE to OE from 2018 to 2070 is expected to remain largely stable year on year, with the mean curve in the narrow range of 17% to 25% for most of the period. In the first few years, the ratio increases steadily until 2022 when the mean value peaks at 0.271. From 2022 to 2026, the mean value large plateaus with a very slight decrease to 0.265. This trend coincides with the different increasing trends of EE and OE. From 2018 to 2026, the EE increases by 48%, whereas the OE increases only by 17%. The different increase rates result in the increasing and plateau trend of the ratio. From 2027 onwards, the ratio starts to decline, with a gradually decreasing rate. The shape of the credible interval and the mean curve resembles an exponential decay curve. Underlying this development is the modelled trend that the EE largely plateaus until 2034 and then starts to steadily decline at a very low rate, whereas the OE gradually increases to its peak around 2051, then largely plateaus until 2055 before it starts to decline slowly. By 2060, the mean of the ratio is expected to be 0.179, a small drop by 16% from the 2018 level.
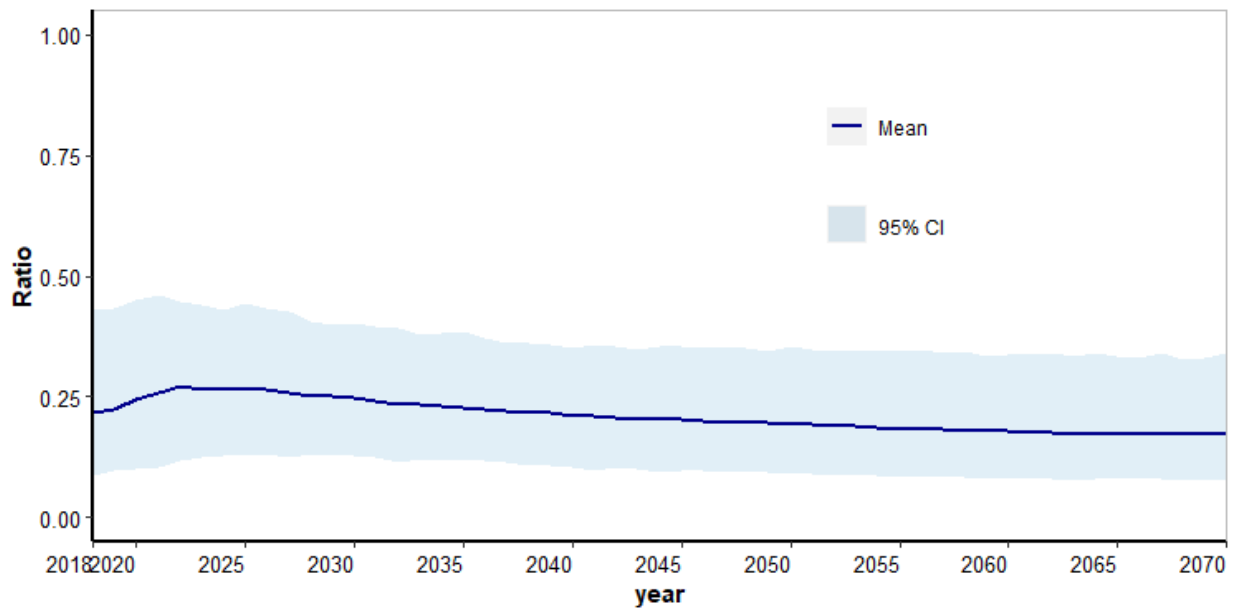
Figure 9.1: Future trend of ratio of EE of annual new buildings to annual OE of the urban
residential stock in north China

The distribution of the ratio in each year, as depicted by a histogram overlaid with a density curve, is largely bell-shaped, with some skewness (Figure 9.2). The distribution of the chosen typical years, including 2030, 2040, 2050, and 2060, has highly similar characteristics, except for the mean value which shifts slightly downwards over time. Throughout this period, the lowest value of the 5th percentile and highest value of the 95th percentile are 0.08 and 0.46 respectively. On the whole, the results with quantified uncertainties as presented in Figure 9.1 and Figure 9.2 provide strong evidence to substantiate the magnitude of embodied energy relative to operational energy in a mega-scale residential stock that keeps expanding.
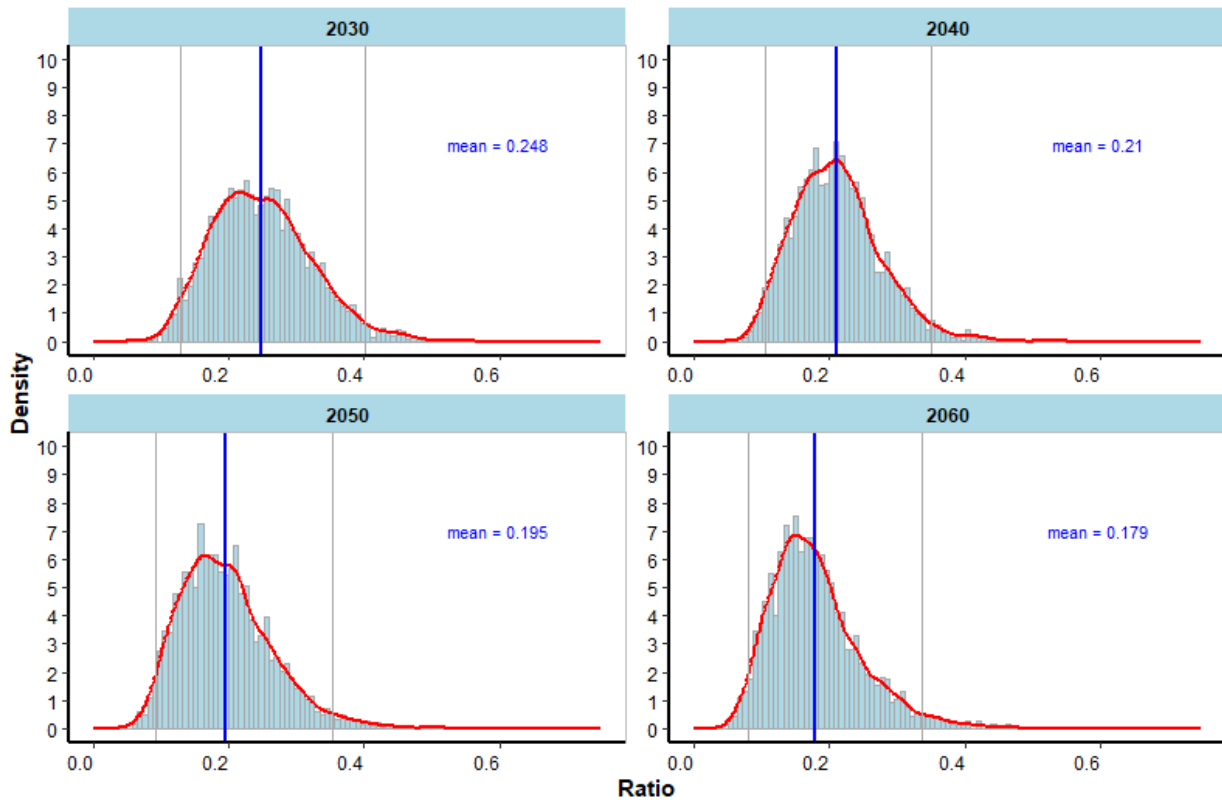
Figure 9.2: Distribution of ratio of EE of annual new buildings to annual EE of the urban residential stock in north China

It is necessary to clarify the ratio here is different from the EE-to-OE ratio for the historical period. The latter applies to the entire residential stock consisting of both north China and the other region, which accounts for 60% of total floor area and has no heating and therefore lower operational energy intensity. Therefore, scaling down the geographical coverage from whole country to the north region tends to increase the weightage of operational energy in whole-life energy. In other words, from entire country to north China, the EE and OE is scaled down disproportionately. As a result, the ratio of EE to OE for north China is brought down considerably. That is why the EE-to-OE ratio in 2018 is 0.31 for the entire residential stock across China, but 0.22 for that in north China. Hence, expanding the geographical coverage to the entire country will only further strengthen the argument for the magnitude of EE relative to OE.

9.2.2 Ratio of embodied energy intensity to operational energy intensity

Intensity provides a perspective that complements stock-level comparison. Figure 9.3 and Figure 9.4 show the ratio of embodied energy intensity (EEI) to the stock-wide operational energy intensity (OEI). The ratio steadily increases in a generally linear manner. From 2018 to 2060, its

mean value increases by 41%, from 4.6 to 6.5. This level is slightly lower than the ratio for the historical period of 2010 to 2018 in Table 6.2 in Chapter 6, for the same reason as explained in the preceding section.
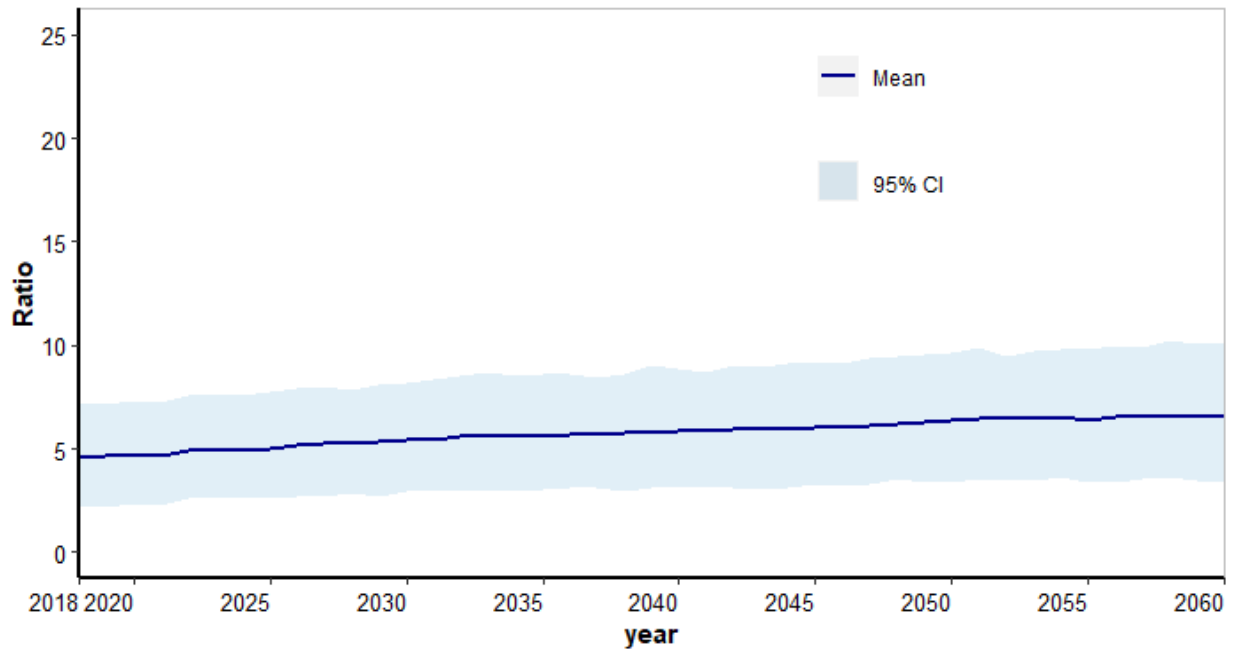
Figure 9.3: Future trend of ratio of EEI to stock-wide OEI of urban residential stock in north China
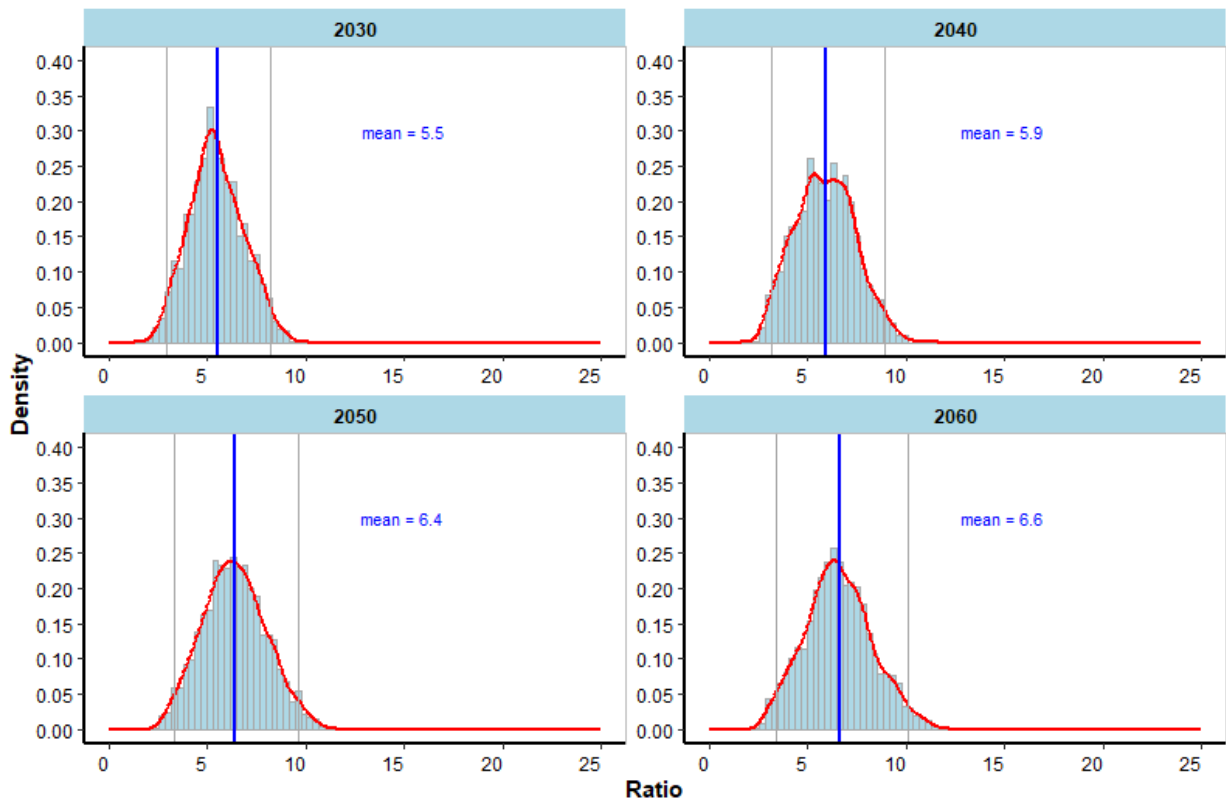
Figure 9.4: Distribution of ratio of EEI to stock-wide OEI of urban residential stock in north China

Probably a more telling indicator is the ratio of EEI to the OEI of new buildings. That is to compare the EEI of new buildings constructed in a given year with the OEI of the same cohort of new buildings (Figure 9.5). As opposed to the previous ratio, the older and less energy-efficient existing buildings in the stock are excluded from the comparison. As a result, the 95% credible interval and mean curve of the ratio shift upwards. Also, the shape of the credible interval and mean value is slightly bended. This is because the heating energy intensity component of the OEI of new buildings decreases more sharply than the stock-wide average heating energy intensity component of the stock-wide OEI. Throughout the modelled period, the ratio of EEI to the OEI of new buildings has its mean value increased from 6.2 to 7.5. By 2060, the 95% credible interval of this ratio is in the range of 3.8 to 11.7 (Figure 9.6).

Figure 9.5: Future trend of ratio of EEI to OEI of new buildings

Figure 9.6: Distribution of ratio of EEI to OEI of new buildings

9.3 Whole-life building stock energy performance

The whole-life energy consumption of the urban residential stock in north China is obtained by combining the embodied energy and the total operational energy (Figure 9.7). The 95% credible interval and the mean curve show a largely smooth increasing trend with a gradually decreasing rate. This trend is similar to that of the total operational energy be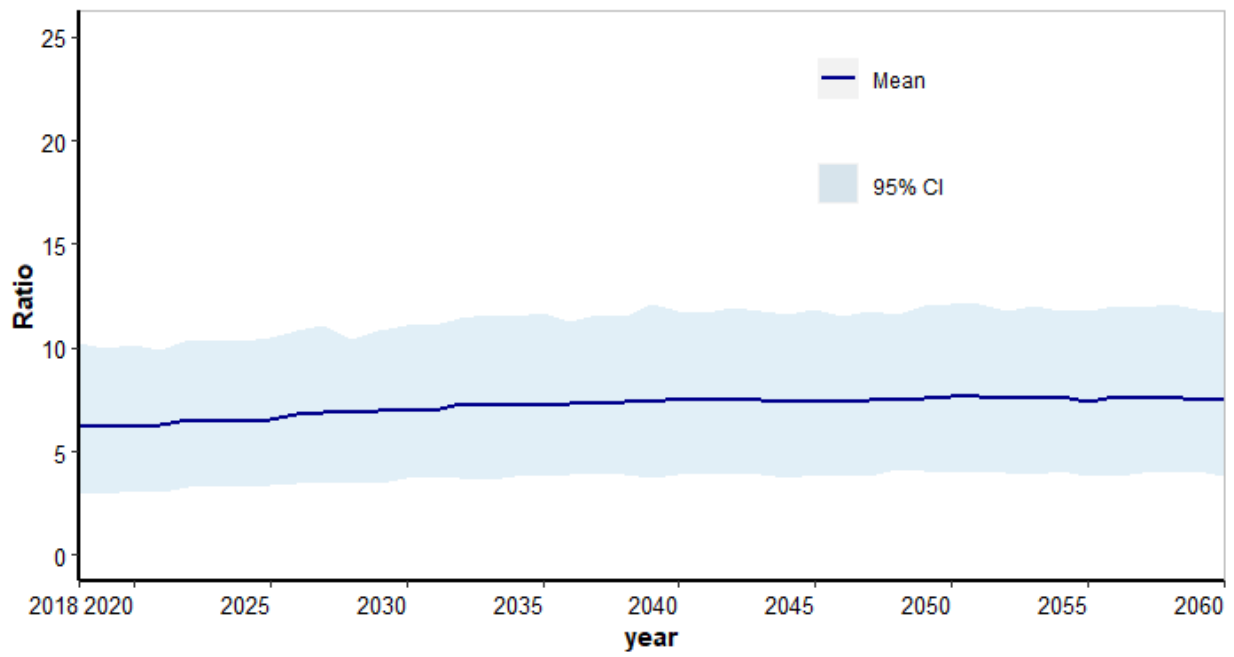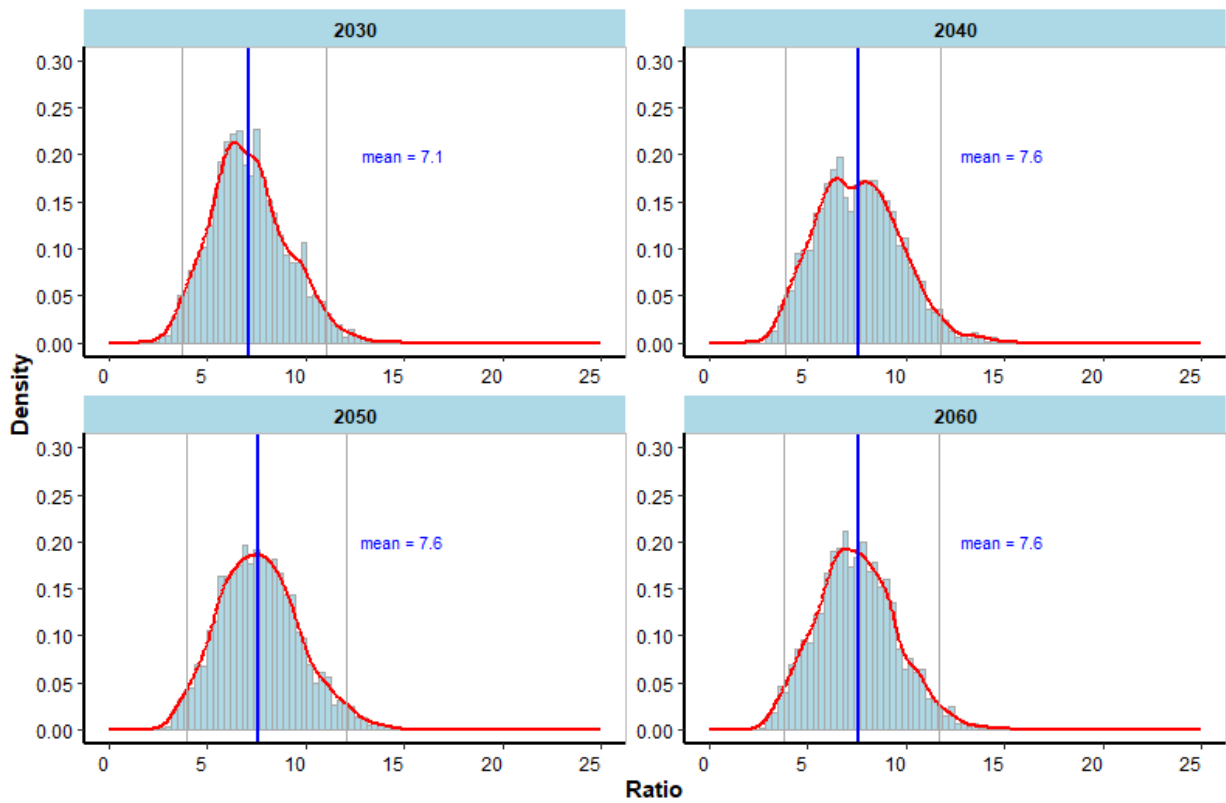cause the embodied energy, which has a largely stable overall trend and does not experience substantial variation, has limited effect on the whole-life energy trend other than shifting it upwards. Compared to the total operational energy, the 95% credible interval of the whole-life energy is wider, particularly in the first two decades, because it incorporates the uncertainties associated with the embodied energy.

Between 2018 and 2040, the mean value of the whole-life energy increases by 39%, from 271.6 million tce to 379.2 million tce. This is primarily driven by the total operational energy, which increases by 40% over the same period. The embodied energy, in contrast, varies very marginally during this period. From 2041, the credible interval and mean curve bend further downwards due to the slowing down increase rate, and starts to develop towards a plateau. This coincides with the expected saturation of non-heating energy intensity of households in 2040 and the slowly declining embodied energy after 2035. The whole-life energy largely plateaus from 2045 to 2051. Its mean values range within a very narrow band, from 383.3 to 383.7 million tce. The peak value of 383.7 million tce is reached in 2050, which is just one year ahead of the peak of the total operational energy. The 95% credible interval for the peak year ranges from 338.9 to 432.6 million tce. From 2051 onwards, the whole-life energy starts to decline gradually. By 2060, its mean value decreases to 375.7 million tce, with a 95% credible interval between 333.6 and 420.9 million tce.
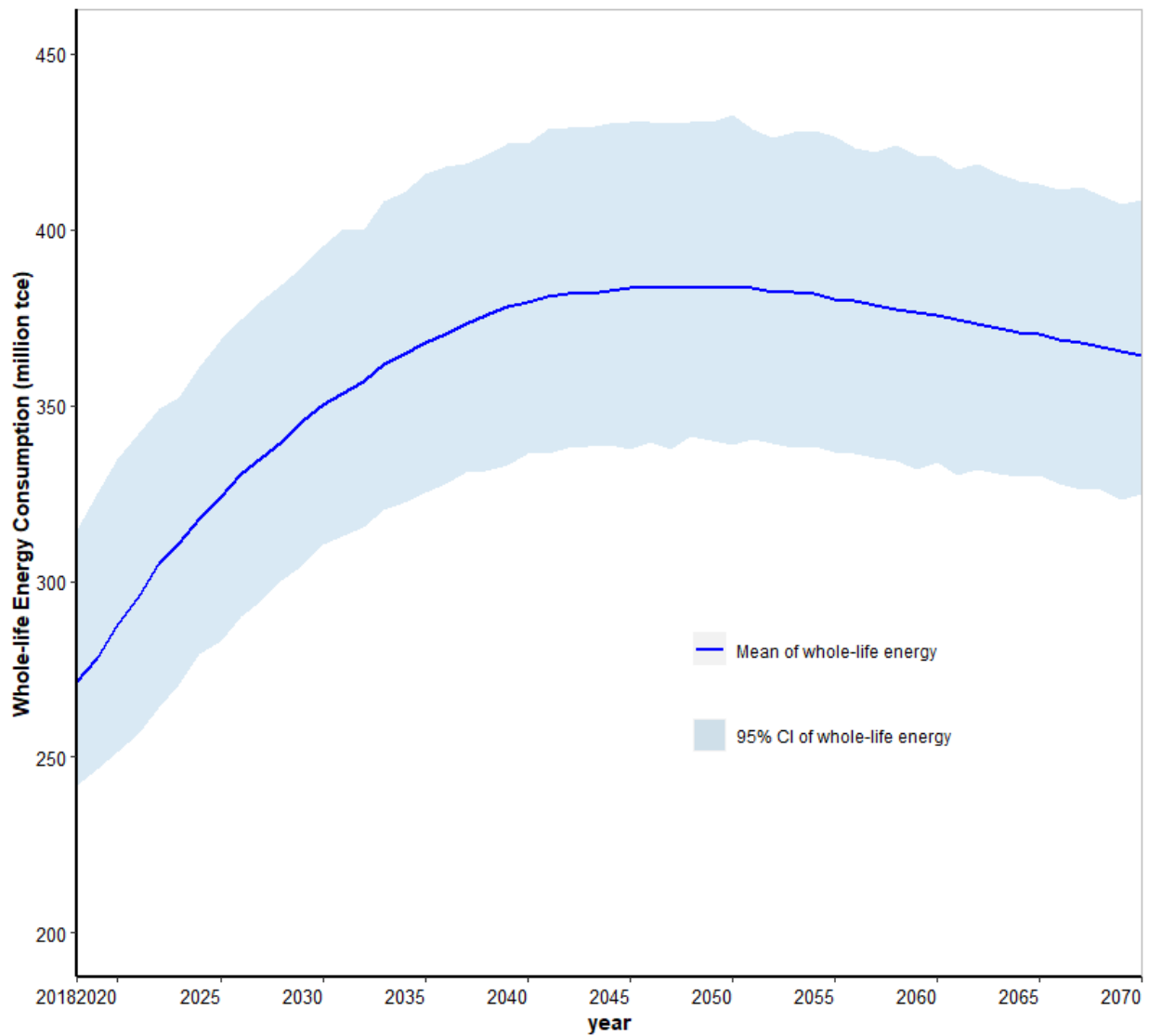
Figure 9.7: Future trend of whole-life energy of the urban residential stock in north China

As shown in Figure 9.8, the distribution of whole-life energy in typical years is highly close to a bell-shaped normal distribution, with little skewness. This is as expected because the distribution of the whole-life energy, as the high-level output from the emergent behaviour of the model, captures all uncertainties associated with the key input variables.
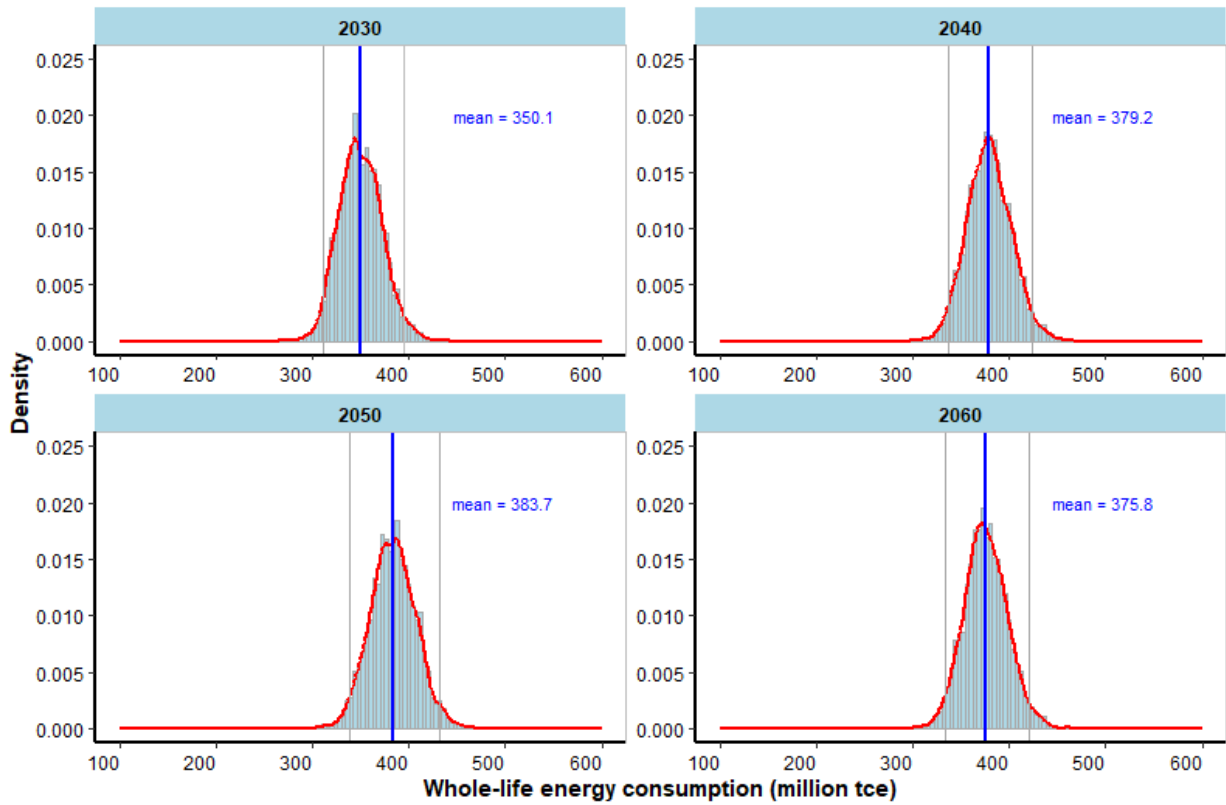
Figure 9.8: Distribution of whole-life energy of the urban residential stock in north China

9.4 Scenario analysis on effects of policy instruments

9.4.1 Policy A: Extension of building lifetime

The first policy whose impact on whole-life energy of the stock is explored here is the progressive building lifetime extension from 2021 to 2040. This is the same policy scenario as in Chapter 6 where the impact of extending building lifetime on the embodied energy of annual new buildings is investigated. Extending building lifetime is expected to have double-sided effects. On the one hand, extending lifetime of existing buildings means less new buildings are needed to be constructed to meet the incremental housing demand. The demand for building materials and construction activities is therefore reduced. Consequently, the embodied energy of annual new buildings can be substantially reduced, as already quantitatively ascertained in Chapter 6. On the other hand, as new buildings (and urban centralised heating systems) are expected to be more energy-efficient due to increasingly stringent regulations, a reduced rate of annual new buildings means a slower turnover of the building stock. The less efficient older buildings would be kept in the stock for longer and the construction and operation of more efficient new buildings would be delayed. That is, the stock would be more prone to the risk of operational energy "lock-in". It therefore is useful to explore the possible stock-level whole-life energy resulting from the

interplay between the two effects. The probabilistic model setup of this study enables the quantification of the probability that this policy would lead to a stock-level whole-life energy lower than the business-as-usual (BAU) scenario discussed in preceding sections.

As shown in Figure 9.9, the Policy A scenario has a largely similar trend to the BAU scenario. For the first few years, the two scenarios overlap completely. The gradual lifetime extension is set to take place from 2021. Its effect starts to unfold from 2022 and becomes increasingly evident over time. The whole-life energy under the Policy A scenario increases slower than the BAU, with its 95% credible interval and mean curve gradually diverging from the BAU over time. During this period, the positive effect of reduced embodied energy would prevail over the negative effect of delayed construction and operation of efficient new buildings. When the lifetime extension ends in 2040, the divergence reaches its maximum at 7.2 million tce on average. This is a large amount of energy saving - it significantly exceeds the 2015 total provincial building operational energy consumption of several provinces of China, such as Ningxia (4.3 million tce), Qinghai (4 million tce), and Hainan (3.3 million tce) (Cai et al. 2020).

From 2041 onwards, the divergence between the two scenarios gradually shrinks due to two factors. First, the declining trend of the embodied energy under the Policy A scenario decelerates as the lifetime extension ends. Second, the slower stock turnover during the lifetime extension period keeps the stock-wide average operational energy intensity higher than the BAU. Its effect remains after the lifetime extension ends. The stock-level total operational energy is kept higher than the BAU. The combined effect is a weakened momentum of curbing the whole-life energy. As the two scenarios develop towards convergence, the Policy A scenario reaches its peak in 2050, when its mean value is 379.9 million tce and 95% credible interval ranges from 338.4 to 422.6 million tce. This peaking time is the same as the BAU. The gap between the two peaks in 2050 is 3.7 million tce on average, approximately 49% below the 2040 level. Different from the BAU scenario, the Policy A scenario does not have a plateau period around its peak. Its peak is followed by a steady decrease trend largely in parallel with that of the BAU. The average gap between the two scenario remains generally stable, varying in a relatively narrow range between 2.8 to 3.3 million tce.
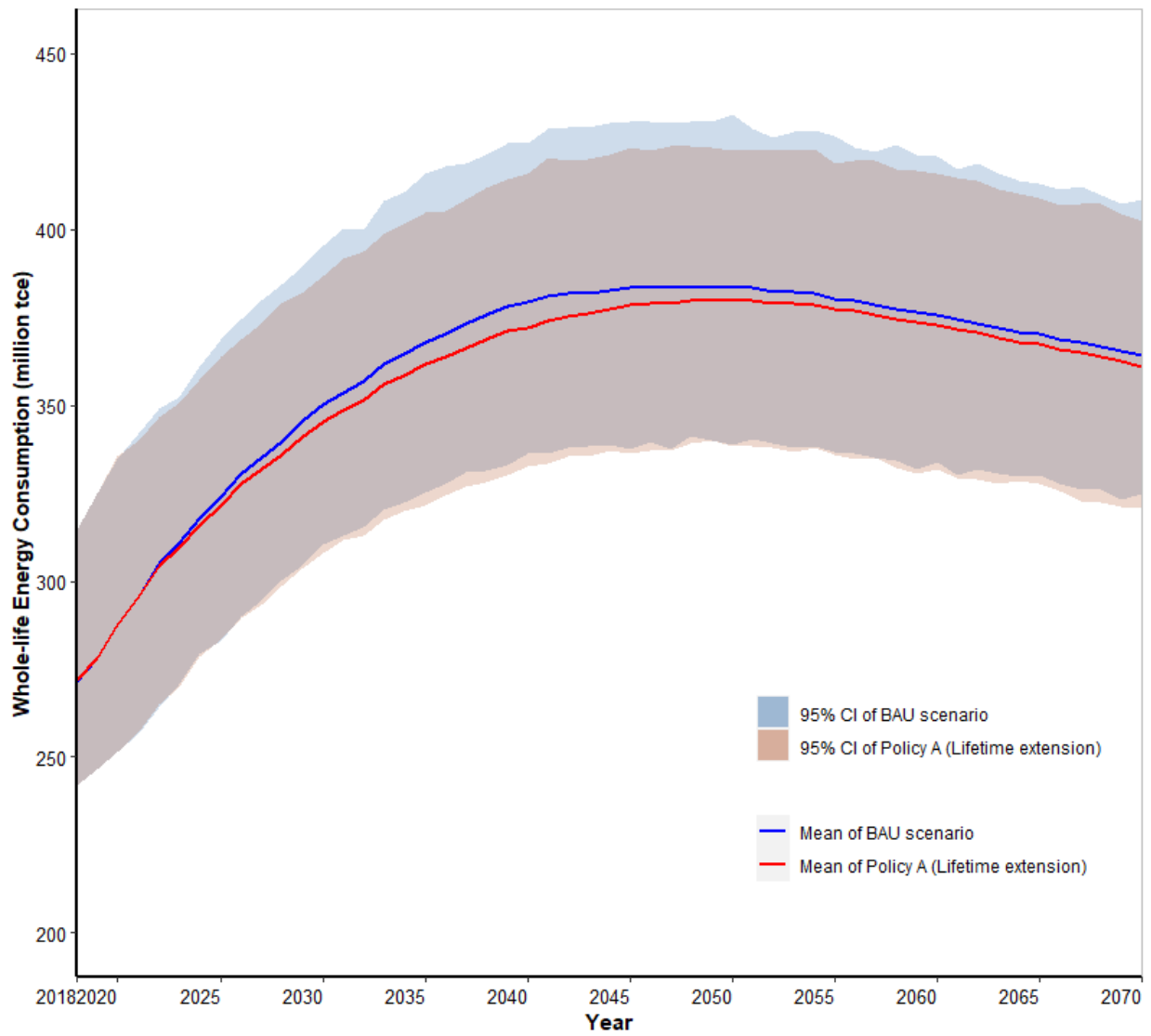
Figure 9.9: Future trend of whole-life energy: BAU vs Policy A
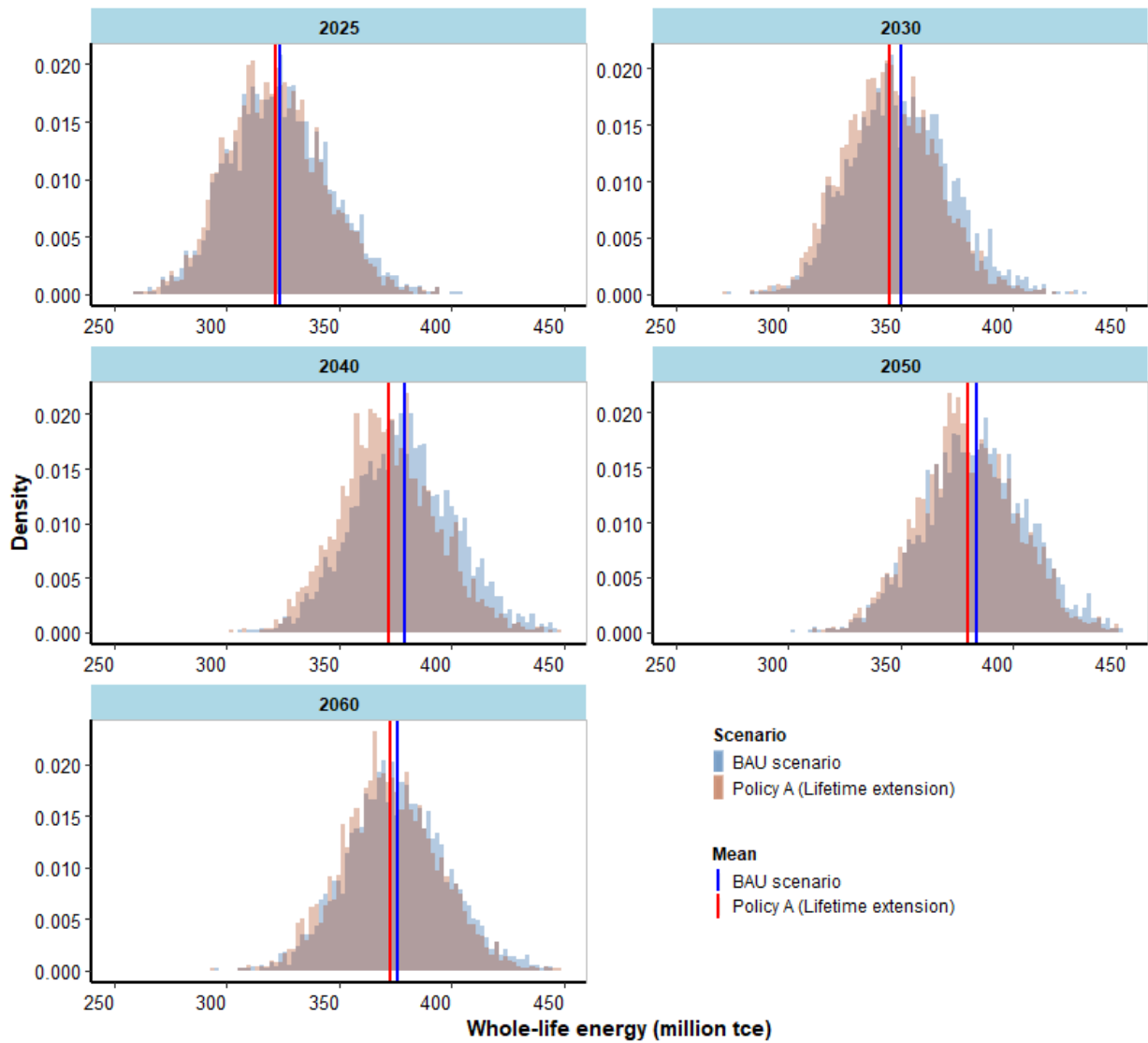
Figure 9.10: Distribution whole-life energy in 2030, 2040, 2050 and 2060: BAU vs Policy A

As expected, the distribution of the two scenarios in typical years shows a generally symmetrical bell shape with little skewness (Figure 9.10). The difference between the two scenarios is most discernible in 2040 and least in 2025. The visually largely overlapped distribution makes it necessary to develop a further insight into the difference between the two scenarios so as to ascertain the extent to which Policy A could potentially improve the whole-life energy performance.

First, the difference is represented using an explicit distribution, which provides a visual inspection on how Policy A could influence the whole-life energy relative to the BAU scenario (Figure 9.11). The shaded area of the distribution represents the situation where Policy A would not reduce the whole-life energy, but instead lead it to a higher level. As expected, the shaded area for each typical year is substantially smaller than non-shaded area, suggesting that Policy

A would be more likely to bring down the whole-life energy from the BAU level than otherwise. The mean values correspond to the gap between the two scenarios' mean values previously discussed.

Second, using the empirical CDFs derived from the difference distribution, the effectiveness of Policy A is quantitatively evaluated in Figure 9.12. The intersection points of the CDF and the vertical line of zero value represent the probabilities by which the whole-life energy under the BAU scenario is lower than that under the Policy A scenario. The probability is found to be consistently below 0.5 for each year. This means a negative difference between the BAU and Policy A scenario is less probable to occur than a positive one. Put differently, these results point to the argument that Policy A is expected to be able to reduce the whole-life energy from the BAU level by a probability of 0.77 in 2030, 0.7 in 2040, 0.57 in 2050, and 0.55 in 2060, respectively.
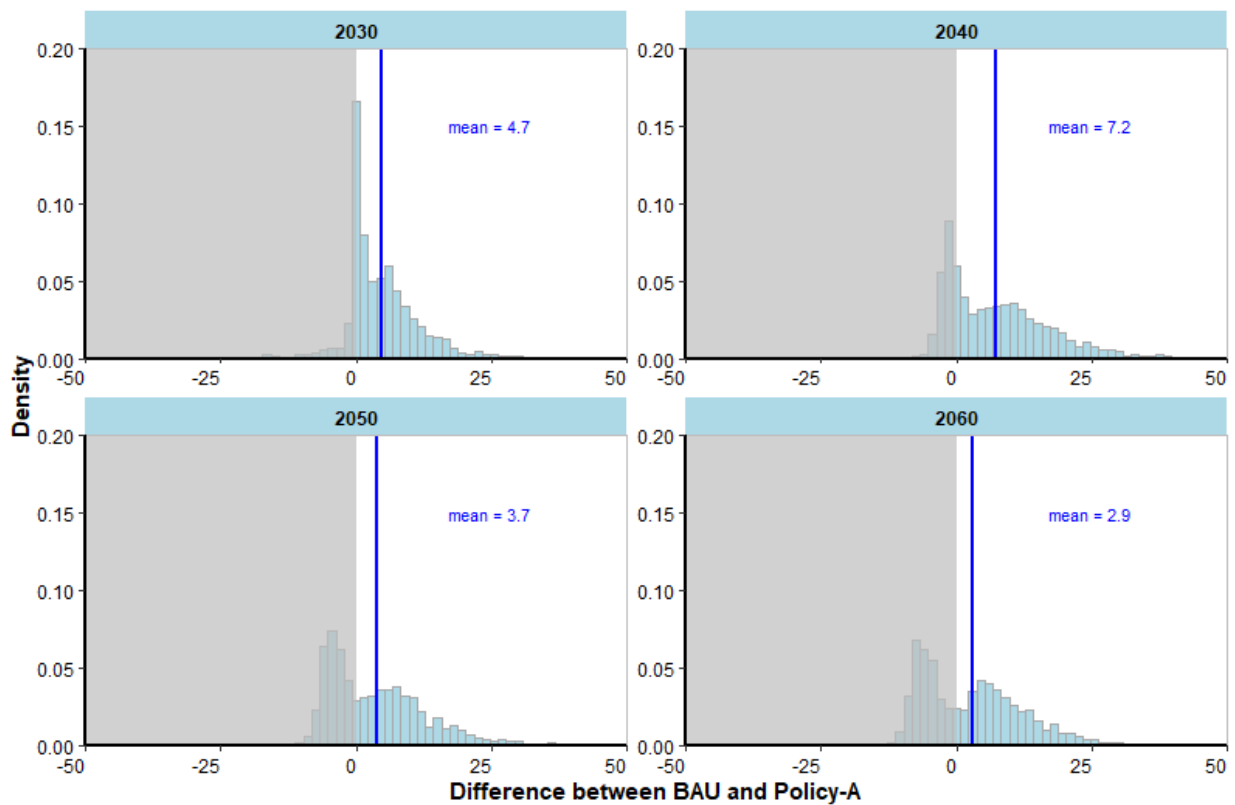
Figure 9.11: Distribution of whole-life energy difference between BAU and Policy A in 2030, 2040, 2050 and 2060
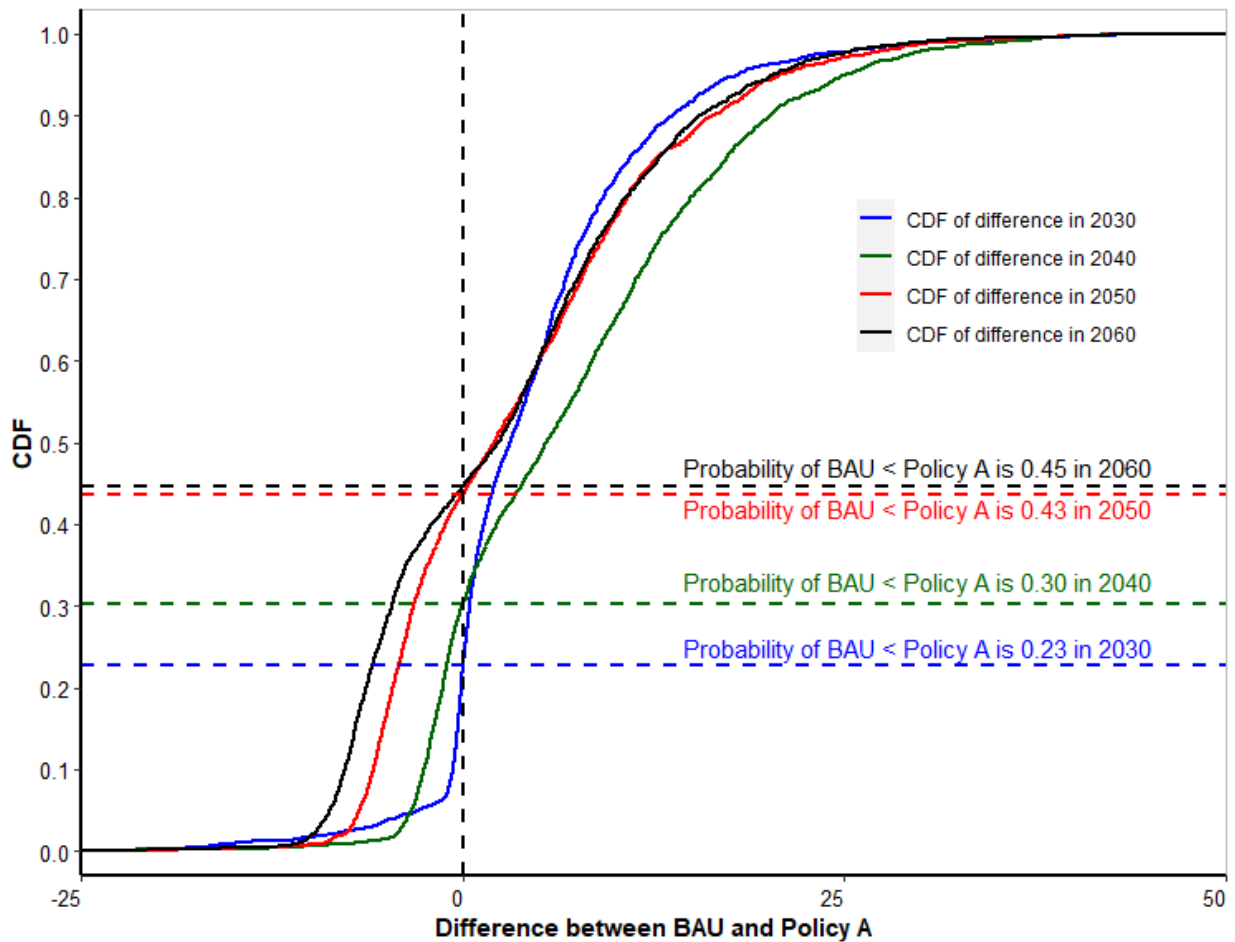
Figure 9.12: CDF of whole-life energy difference between BAU and Policy A in 2030, 2040,
2050 and 2060

9.4.2   Policy B: Accelerate energy efficiency of new buildings

Policy B targets the improvement of heating energy efficiency of new buildings. Compared to the
BAU, Policy B brings forward the timeline of heating energy intensity of new buildings decreasing
to the 'guiding' target established by the Standard for Energy Consumption of Buildings issued
by MOHURD in 2016. This timeline is 2040 under the BAU scenario and reset to be 2030 under
Policy B scenario. This new timeline accelerates the heating energy efficiency improvement of
new buildings, as well as the residential stock which is constantly replenished with new buildings.
All other settings of the mode remain unchanged.
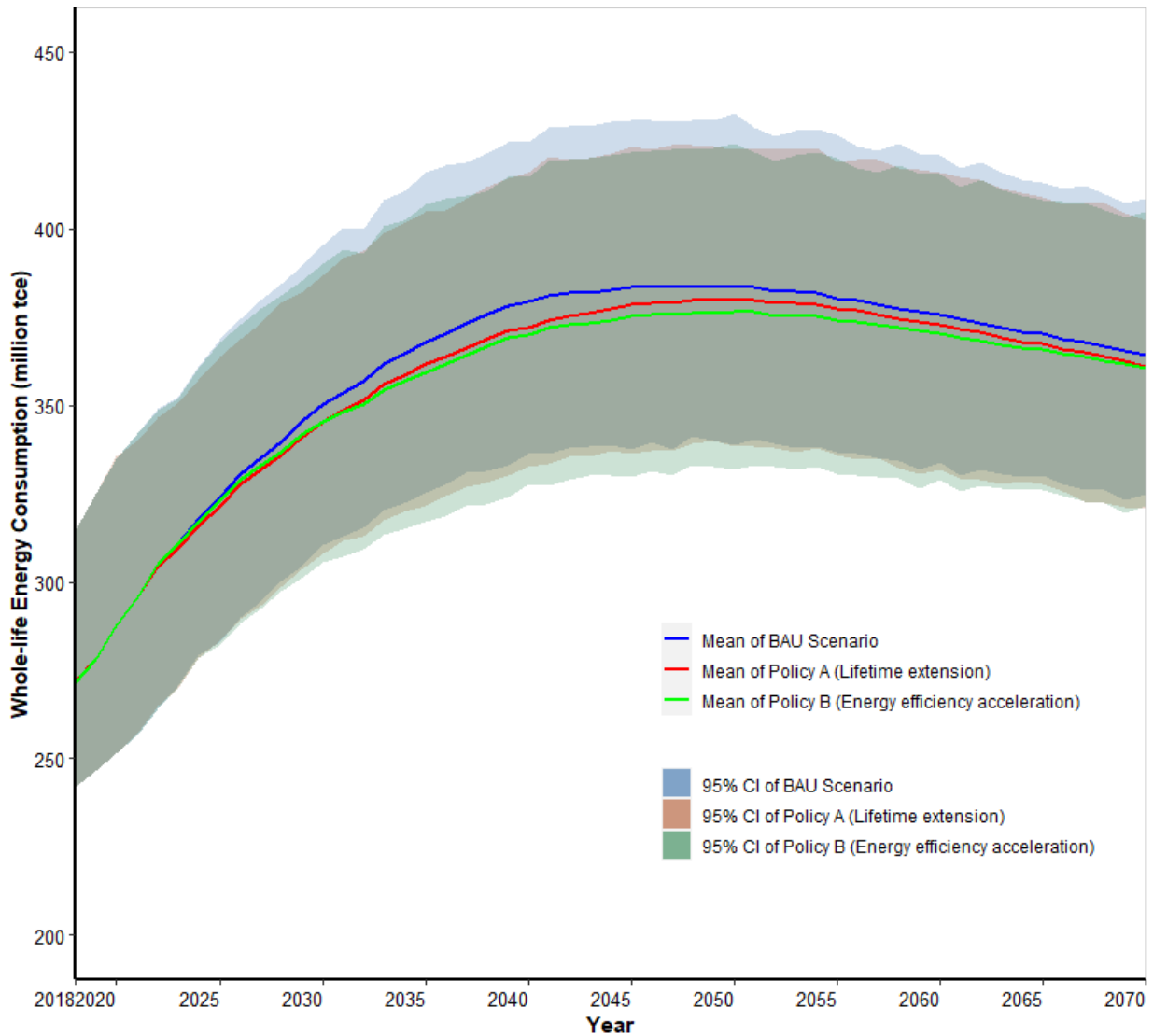
Figure 9.13: Future trend of whole-life energy: BAU, Policy A and Policy B

The future trend of whole-life energy under BAU and Policy B is shown in Figure 9.13. Policy A is also presented for comparison purpose. Under both the BAU and Policy B scenarios, the heating energy intensity of new buildings is set to decrease from 2021. Thus, in the first few years there is no difference between the two scenarios. From 2022 onwards, Policy B starts to diverge from the BAU steadily as in the case of Policy A. As the 'guiding' target of heating energy intensity is reached in 2030, all new buildings entering the stock from 2031 onwards are operated at this high efficiency level. Compared to the BAU scenario, this accelerated energy intensity reduction under Policy B generates additional benefits to the stock-wide average energy intensity in three ways. First, from 2021 to 2030, the heating energy intensity of new buildings decreases at a higher rate than the BAU. The entry of these buildings into the stock helps to bring down the

stock-wide average heating energy intensity to a larger extent than BAU during this period. Second, the realisation of the 'guiding' target 10 years ahead of the BAU means that the stock replenishment from 2031 to 2040 is with new buildings more efficient than those under the BAU. Third, the accelerated reduction of heating energy intensity of buildings helps to increase the energy savings of retrofit, which uses the heating energy intensity of new building as the benchmark against which retrofit is conducted.

Over time, the divergence between BAU and Policy B keeps increasing. It maximises in 2039, when the difference of the two mean values is 9.3 million tce. After that, the divergence shrinks slowly, and the mean curve of Policy B gradually approaches that of BAU. This is on account of several factors. First, new buildings under the BAU scenario start to be at the 'guiding' heating energy intensity level from 2040 onwards, meaning that Policy B no longer prevails over BAU in terms of heating energy intensity of incoming new buildings. That is, from 2040 onwards, the incoming new buildings have the same impact on the stock energy performance under both scenarios. Second, as the result of a late realisation of the 'guiding' heating energy intensity, the demolished older buildings under the BAU have higher energy intensities than Policy B. Their exit from the stock therefore has a stronger positive impact on reducing stock-wide average energy intensity under BAU, as compared to Policy B. Third, owing to the accelerated energy intensity reduction from 2021 to 2030, the stock-wide average energy intensity under Policy B is brought down to a level considerably lower than the BAU. This difference is large enough to offset the other two factors and keep the stock-wide heating energy consumption under Policy B lower than BAU throughout the modelled period.

The peak of whole-life energy under Policy B is reached in 2050, the same year as the BAU. Its mean value at peak is 376.5 million tce, which is 7.2 million tce lower than the BAU. This gap is almost twice that of the peak gap between the BAU and Policy A. Similar to the BAU, the Policy B scenario also has a plateau around its peak. The credible intervals and mean values in 2048, 2049 and 2051 differ very marginally from the peak in 2050. Following the plateau, the whole-life energy under Policy B scenario gradually declines. Its declining trend is slightly less steep than the BAU, due to the fact the demolished buildings exiting the stock have lower energy intensities under Policy B scenario. Despite that the two scenarios' declining trajectories slowly approach each other, the gap between the two mean values remains considerable. In 2060, the gap is 5.3 million tce.

It should be noted that Policy B does not involve any intervention on the volume of incoming new buildings. The embodied energy remains the same under the two scenarios. Therefore, the difference in whole-life energy between BAU and Policy B is attributable solely to operational

energy as discussed above.
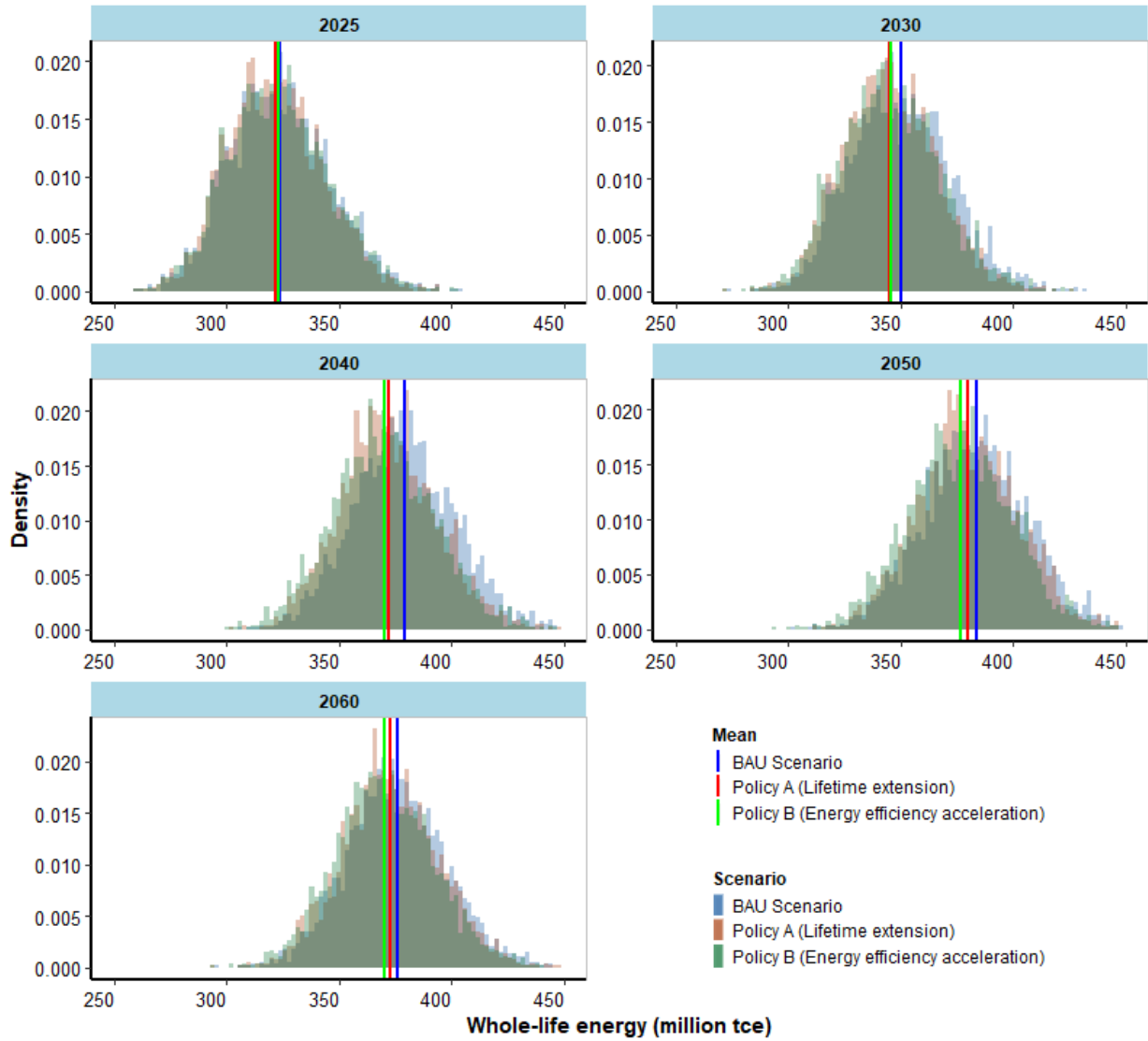
Figure 9.14: Distribution of whole-life energy in 2030, 2040, 2050 and 2060: BAU, Policy A and Policy B

As shown in Figure 9.14, the distribution of Policy B in typical years is very similar that of the BAU or Policy A. It is a largely bell-shaped distribution with little skewness. Taking the same approach as in the case of Policy A, the difference between BAU and Policy B is further investigated through a distribution (Figure 9.15) and a CDF (Figure 9.16). Clearly and understandably, the probability of the BAU being lower than Policy B is zero. It therefore is reasonable to claim that Policy B, which is about accelerating the heating energy efficiency improvement of new buildings, can effectively reduce the whole-life energy from the BAU level.
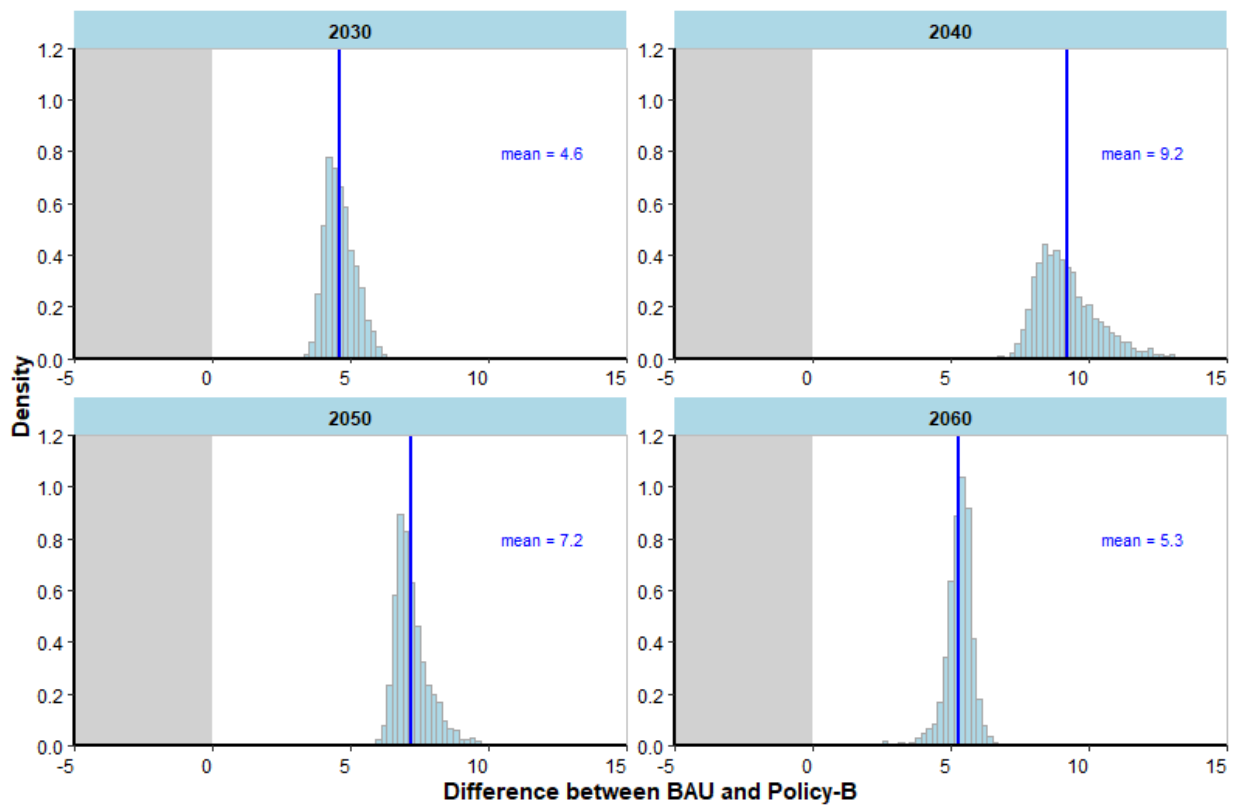
Figure 9.15: Distribution of whole-life energy difference between BAU and Policy B scenario in 2030, 2040, 2050 and 2060
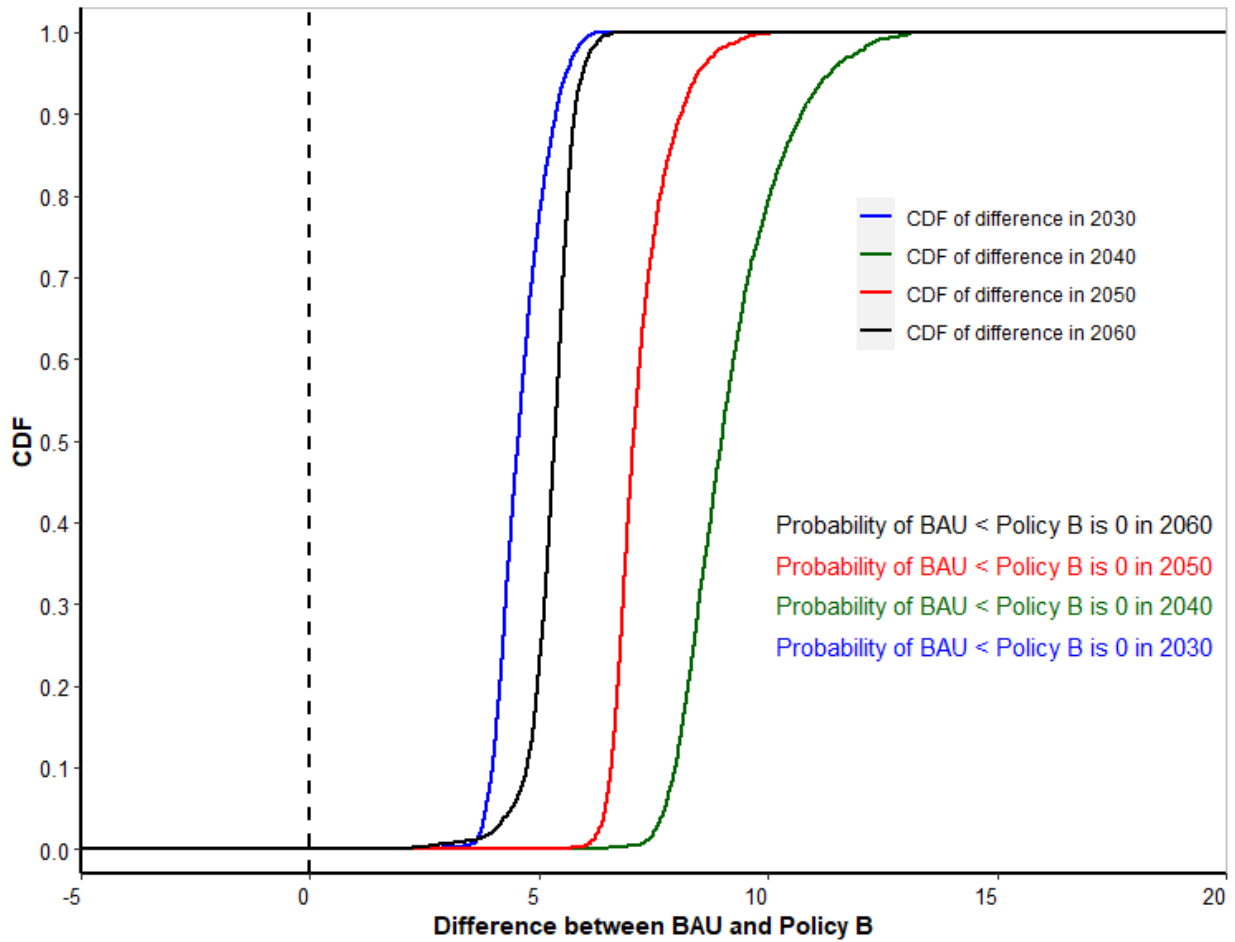
Figure 9.16: CDF of whole-life energy difference between BAU and Policy B scenario in 2030, 2040, 2050 and 2060

9.4.3   Comparison of Policy A with Policy B

The preceding sections show that both Policy A and Policy B are likely to have material impacts on the stock-wide whole-life energy. Policy A aims to extend the average lifetime of buildings in the stock through various regulatory, economic and technical means, whereas Policy B focuses specifically on reducing heating energy intensity of new buildings through improving heat generation and supply system and building envelope performance. In a way, they are different routes to the same goal, which is to curb the increase of whole-life energy. Comparing these two routes will provide further insights into their relative effectiveness and relevant policy implications.
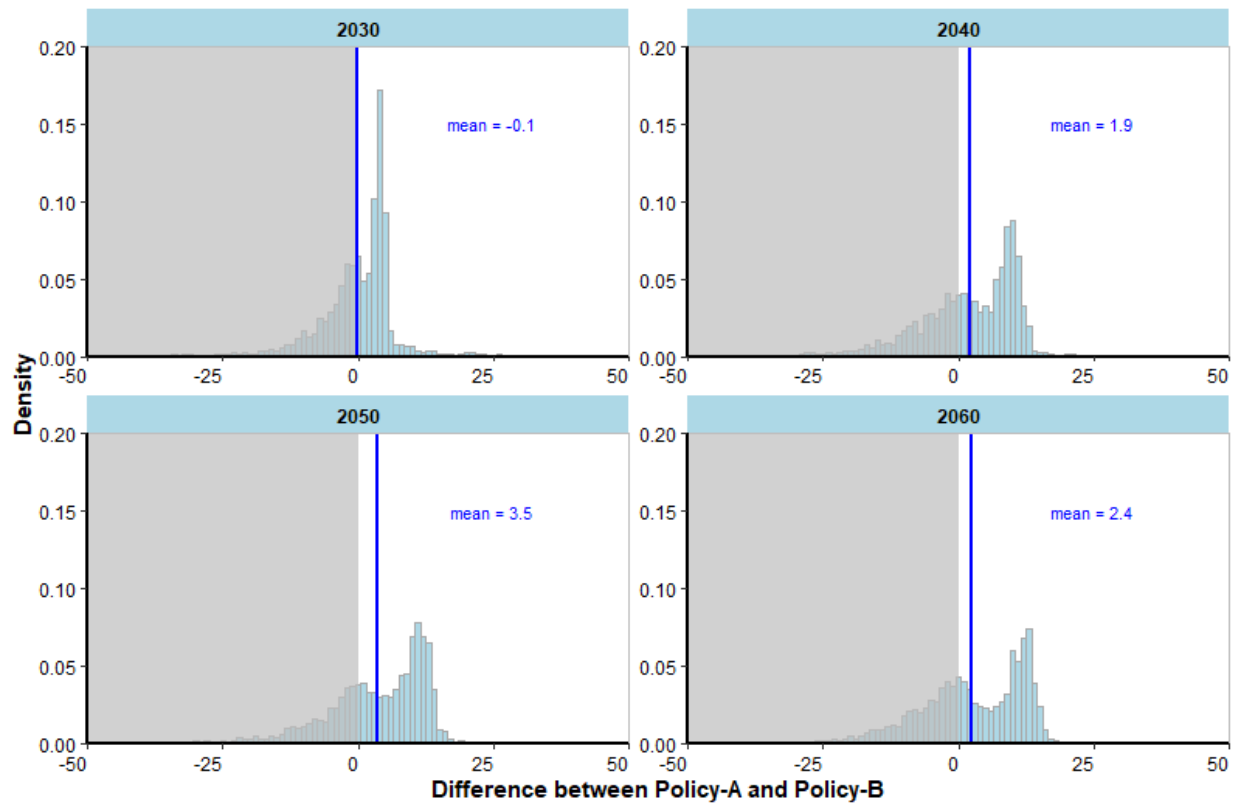
Figure 9.17: Distribution of whole-life energy difference between Policy A and Policy B in 2030, 2040, 2050 and 2060
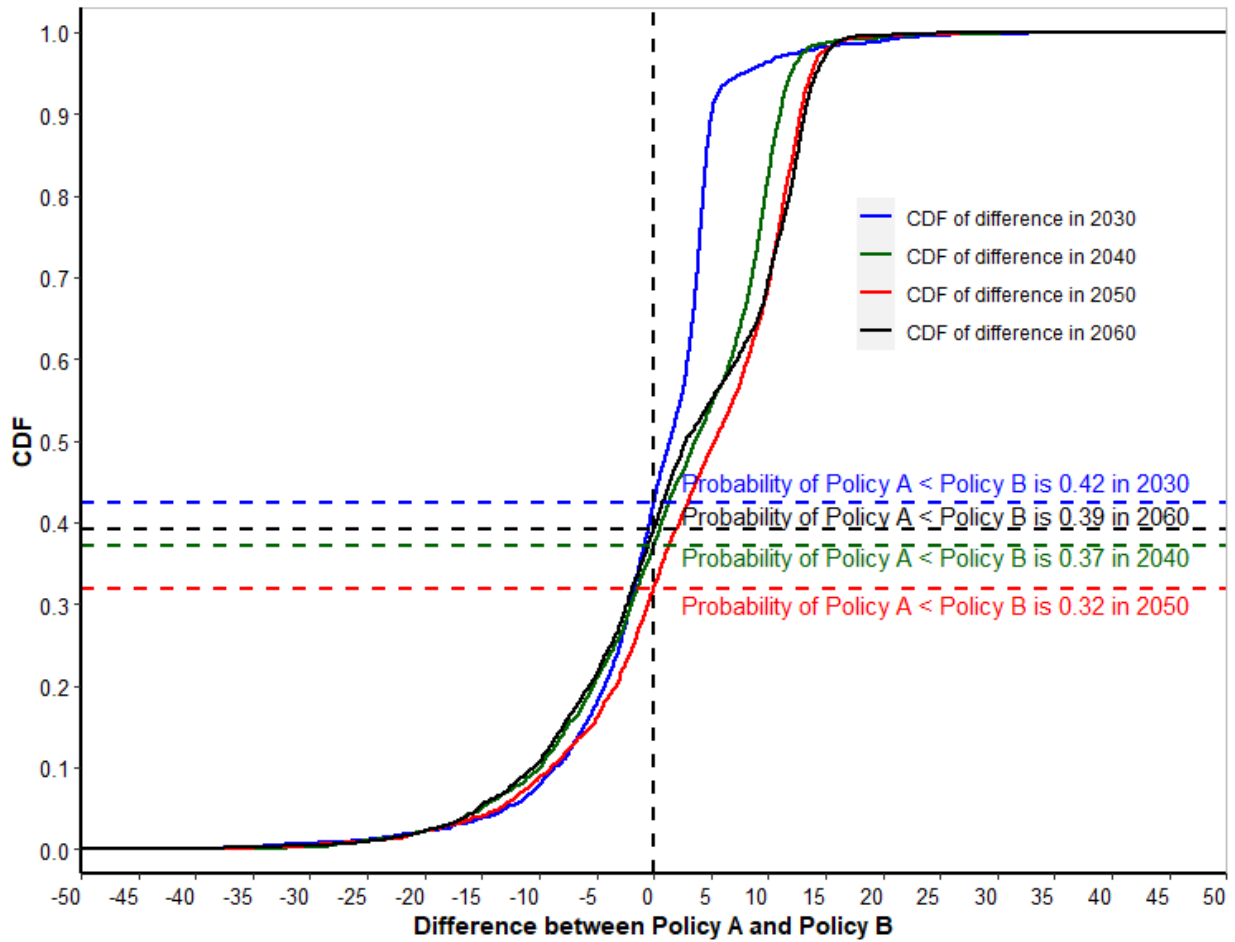
Figure 9.18: CDF of whole-life energy difference between Policy A and Policy B in 2030, 2040,
2050 and 2060

As a general observation, the two scenarios follow largely similar trajectories. The 95% credible intervals and mean curves overlap for the most part until 2032, when the difference starts to become gradually discernible and the gap between the mean values exceeds 1 million tce (Figure 9.13 and Figure 9.14). This is a very marginal amount, accounting for approximately 0.3% of the whole-life energy under either scenario. From 2033 onwards, the two scenarios gradually diverge. The maximum gap between the two mean curves is 3.6 million tce, reached in 2049. After that, the two mean curves gradually decline towards convergence. The gap reduces to 2.4 million tce in 2060 and further to 0.7 million tce in 2070.

The distribution of the difference between the two scenarios in each typical year has a considerable share in the shaded area (Figure 9.17). This means there is a considerable probability of Policy A having a stock-level whole-life energy lower than Policy B. Specifically, the probability is 0.42 in 2030, 0.37 in 2040, 0.32 in 2050 and 0.39 in 2060 (Figure 9.18). These

numbers prove that extending building lifetime as a stand-alone policy instrument has a considerable probability of reducing stock-level whole-life energy consumption more effectively than applying stringent regulations and technological measures to improve heating system and building envelope performance.

This observation is not against the previous findings that the probability for Policy B to reduce whole-life energy from BAU is 1 whereas this probability is considerably lower for Policy A. In fact, it is fully consistent with them. Mathematically, the difference between Policy A and Policy B is equal to the difference between BAU and Policy B (Figure 9.15) minus the difference between BAU and Policy A (Figure 9.11). Whilst the whole-life energy under Policy B is always below BAU under all possibilities, the difference is narrowly distributed around its mean in each year. In contrast, the difference between Policy A and BAU is more broadly distributed, spreading over a much larger range. Therefore, the difference between the Policy A and Policy B has a considerable probability of being negative, as shown in Figure 9.17.

It is not the intention of this comparison to ascertain whether one policy would outperform another one. In fact, it would not be appropriate to overinterpret the comparison and generalise the findings, because the settings of the hypothetical scenarios are largely arbitrary. Under the current setting, it is more probable for the whole-life energy under Policy B to be lower than under Policy A. This may well be reversed based on adjusted settings that extend lifetime more aggressively and reduce heating energy intensity more conservatively. More fundamentally, the implications of these policies go well beyond energy per se in practice. Extending building lifetime is a highly complex and challenging task in reality. As discussed earlier in this thesis, Chinese buildings are short-lived, in spite of the established standard stipulating a design lifetime of 50 years. Addressing this issue has to take a systematic approach to a wide range of factors. Those directly relating to buildings include quality of building materials, enforcement of design regulations and standards, improvement of construction techniques and practices, maintenance and renovation of building structural components, etc. Other factors such as urbanisation process, city expansion, urban planning, land acquisition and resettlement are not directly related to quality of buildings but have significant high-level impacts on how buildings will be constructed, operated, renovated and demolished. In a broader sense, there are very strong inherent links of construction and demolition of buildings with urban land utilisation, development of real estate sector, tax revenue of local governments, etc. The socioeconomic costs and benefits are significant and far-reaching. All these are fundamental determinants of the feasibility and implementability of potential policies address building lifetime.

Similarly, accelerating the improvement of heating energy intensity in practice requires a system

approach to addressing institutional, regulatory, technological, financial and social challenges. Developing new centralised heat supply systems and upgrading existing ones for improved energy efficiency and environmental performance require significant investments. State-owned heating companies need stronger government support through fiscal subsidies and preferential taxation. More active private sector participation in developing and operating heating systems should be incentivised through effective policy measures, such as various types of public-private-partnerships (PPPs). Moreover, apart from heat supply systems, achieving reduction in heating energy intensity depends heavily upon the demand side. Thermal insulation properties of building envelope need to be further improved through more stringent building design standards and acceptance codes. The compliance enforcement in practice is key. Equally important, if not more, is the heat metering and billing mechanism through which heat consumption by household is regulated to avoid overheating and heat waste. The envisaged transition, from the fixed fee based on household floor area to variable fee based on actual heat consumption, needs to be enforced in an effective and efficient manner, with social impacts duly taken into consideration.

9.4.4   Policy C: Combination of policies A and B

As Policy A and Policy B are not mutually exclusive, but largely complementary, in practice there is the possibility to implement them in parallel to attain more energy-saving potentials. In the model, this is defined as Policy C, which combines Policy A on extending the lifetime of new and existing buildings and Policy B on accelerating the improvement of heating energy efficiency of new buildings.

Figure 9.19 shows the trend of whole-life energy under Policy C, in comparison with the BAU, Policy A and Policy B scenarios. As expected, Policy C keeps the whole-life energy considerably lower than the other scenarios throughout the investigated period. From 2022, the effect of Policy C starts to become evident, as its mean curve diverges gradually from the other three curves. Policy C tends to be more effective than Policy A and B because it avails of the benefits of both lifetime extension and acceleration of heating energy efficiency improvement. From 2025 to 2030, against the BAU scenario, Policy C is expected to achieve a cumulative energy saving of 36.7 million tce on average. As an indication of the magnitude of this saving, the total operational energy consumption of all residential, commercial and public buildings in Beijing was 32 million in 2015. With the most developed service sector in China, Beijing has the most energy-consuming stock of buildings than any other cities in China. In fact, its building energy consumption in 2015 was higher than 23 of the total 31 provinces across China.
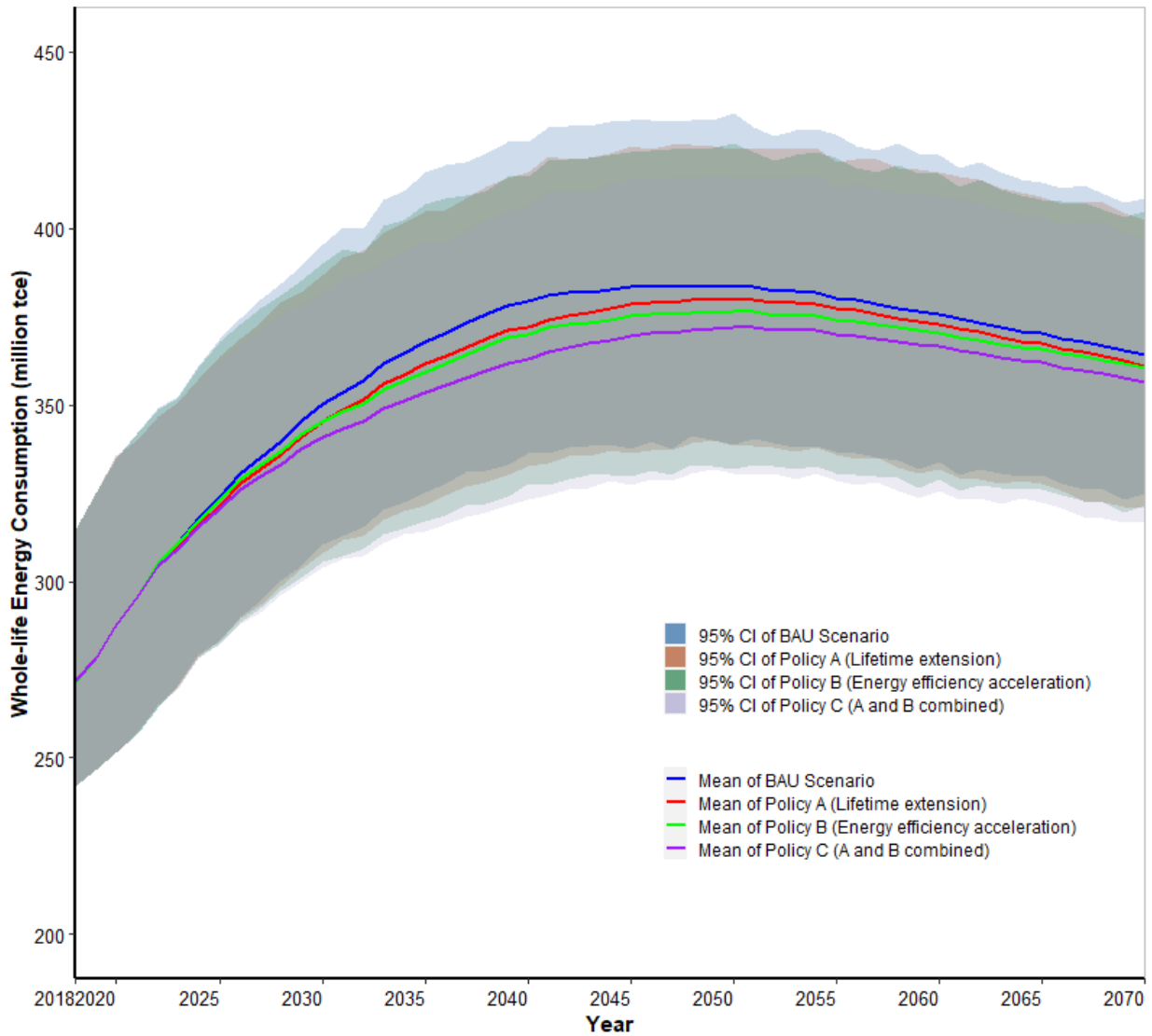
Figure 9.19: Future trend of whole-life energy: BAU, Policy A, Policy B and Policy C

From 2031 to 2040, although both BAU and Policy C keep an increasing trend, the divergence between them gradually enlarges. The divergence maximises in 2040, when Policy C achieves the largest annual saving, which amounts to 16.4 million tce. This is approximately 75% of the total operational energy of all buildings in Shanghai in 2015. From 2041 onwards, Policy C keeps its momentum of growth, whereas the BAU starts to quickly approach its plateau period. This results in a reducing difference between the two scenarios, as shown by their mean curves gradually approaching each other. Same as the BAU as well as Policy A and Policy B, Policy C reaches its peak in 2050. Its mean value in 2050 is 371.8 million tce and 95% credible interval ranges from 330.4 to 414.7 million tce. The difference between the mean curves of Policy C and BAU in this year is 11.8 million tce, which is 218% higher than Policy A and 64% higher than Policy B. Compared to the 2015 provincial data, this annual energy saving achieved by Policy C

in 2050 exceeds the annual building operational energy consumption in 9 provinces, such as Anhui, Fujian, Jiangxi, Guangxi, etc. Compared to BAU which largely plateaus from 2045 to 2051, Policy C has a plateau period three years later. From 2049 to 2053, its mean value largely levels off, varying narrowly from 371.4 to 371.8 million tce. Following the plateau, Policy C starts to decline gradually. By 2060, its mean value decreases to 366.5 million tce and its 95% credible interval ranges between 325.8 and 409.3 million tce. In this process, the declining trends of Policy C and the BAU are similar, resulting in a largely consistent gap between the two mean curves.
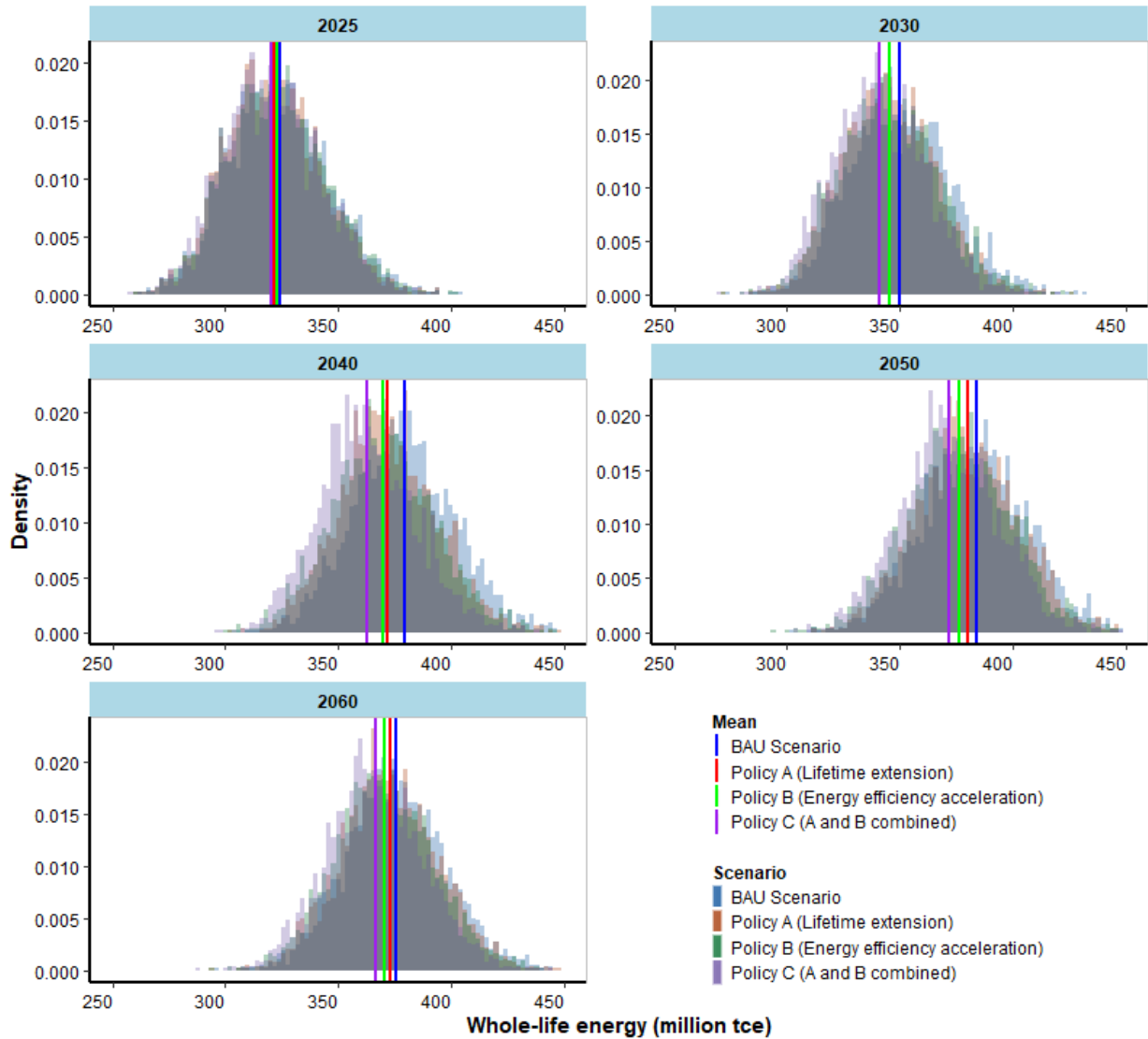
Figure 9.20: Distribution of whole-life energy in 2030, 2040, 2050 and 2060: BAU, Policy A, Policy B and Policy C

Figure 9.20 shows the distribution of Policy C in typical years, in comparison with the other three scenarios. As expected, the distribution of Policy C is largely bell-shaped, with little skewness.

The difference between Policy C and the others is evident. It is useful to clarify that the energy saving effect of Policy A is not a linear combination of the separate effects of Policy A and Policy B. In fact, it does not make sense to simply add together the two separate effects. In reality, it is not possible to implement Policy A and Policy B separately over the same period of time, as they target the same building stock. Instead, they have to be implemented in parallel. Therefore, the effect of Policy C is the result of modelling both Policy A and Policy B in an integrated manner. It captures all the endogenous dynamics of heating operational energy intensities of age-specific building substocks and the stock-wide average heating operational energy intensity, amid the time-varying building lifetime distribution. To partially illustrate this point, Table 9.1 compares effect of Policy C with the sum of the separate effects of Policy A and B. The mean values in selected years are used as the indicators.

Table 9.1: Comparison between energy saving by Policy C and the sum of energy savings by Policy A and B in typical years

Comparison Year	Annual energy saving by Policy C	Sum of annual energy savings by Policy A and Policy B
2030	9.1	9.3
2035	14.3	14.6
2040	16.4	16.4
2045	13.8	13.2
2050	11.8	10.9
2055	10.2	9.2
2060	9.2	8.1
2065	8.4	7.4
2070	7.8	6.9

As in previous sections, the difference between BAU and Policy C is investigated through a distribution (Figure 9.21) and a CDF (Figure 9.22). Most of the distribution is located in the non-shaded area. This indicates that Policy C would be more likely to be an effective policy measure than otherwise. This is confirmed by the CDFs showing that the probabilities of Policy C resulting in a stock-level whole-life energy consumption lower than BAU would be 0.96 in 2030, 1 in 2040, 0.99 in 2050 and 0.82 in 2060. While the probabilities are high, the possibility of Policy C increasing the stock-level whole-life energy consumption from the BAU level cannot be ruled out entirely. For example, in 2030 this probability is 0.04. This is because extending lifetime has a

mixed effect. The reduction of annual embodied energy is coupled with less aggressive improvement of stock-wide heating energy intensity improvement. Implementing this policy alone does not necessarily achieve reduction in whole-life energy consumption, but instead may lead to a situation where the whole-life energy consumption would exceed the BAU. The probability of such a situation occurring is not negligible, as found in the section for Policy A. For example, this probability is 0.23 in 2030. Under Policy C, the negative part of this mixed effect, i.e. slowed-down turnover of building stock and less aggressive heating energy intensity improvement, is largely (but not entirely) offset by the positive effect of accelerating heating energy efficiency improvement.
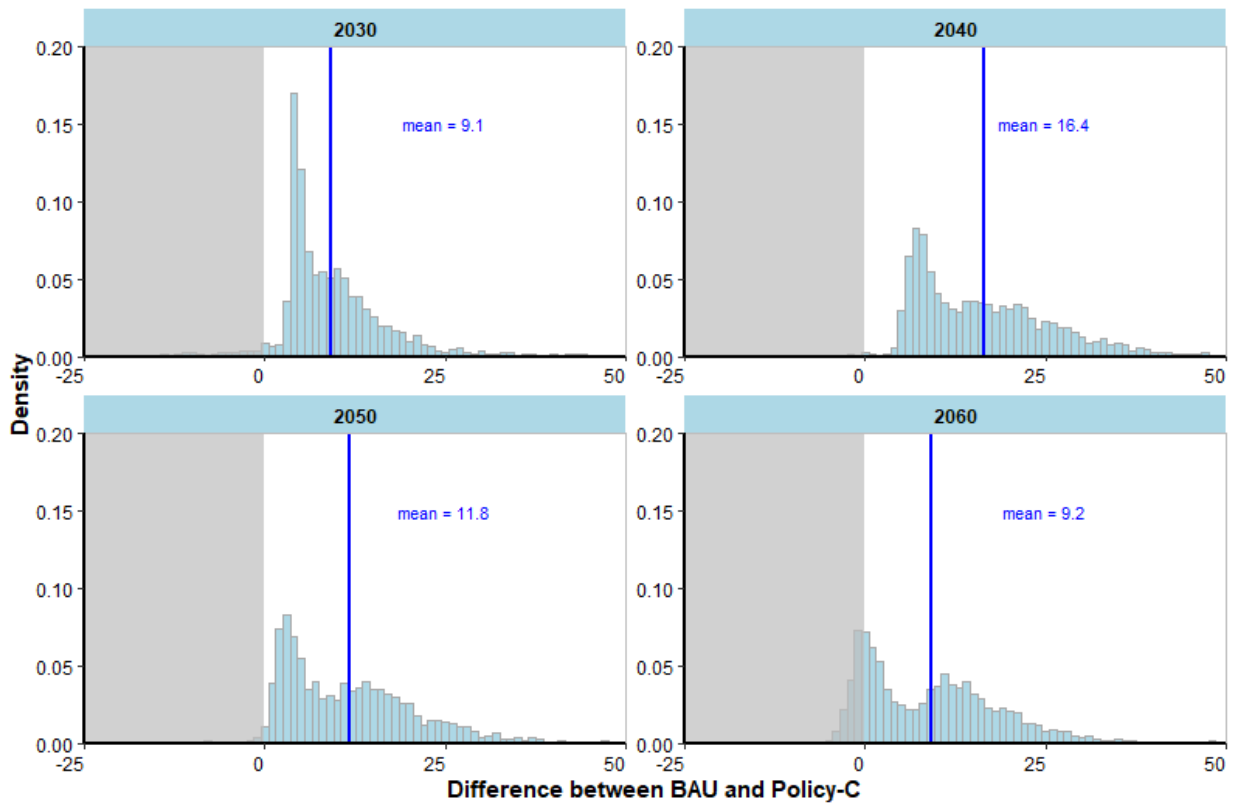
Figure 9.21: Distribution of whole-life energy difference between BAU and Policy C in 2030, 2040, 2050 and 2060
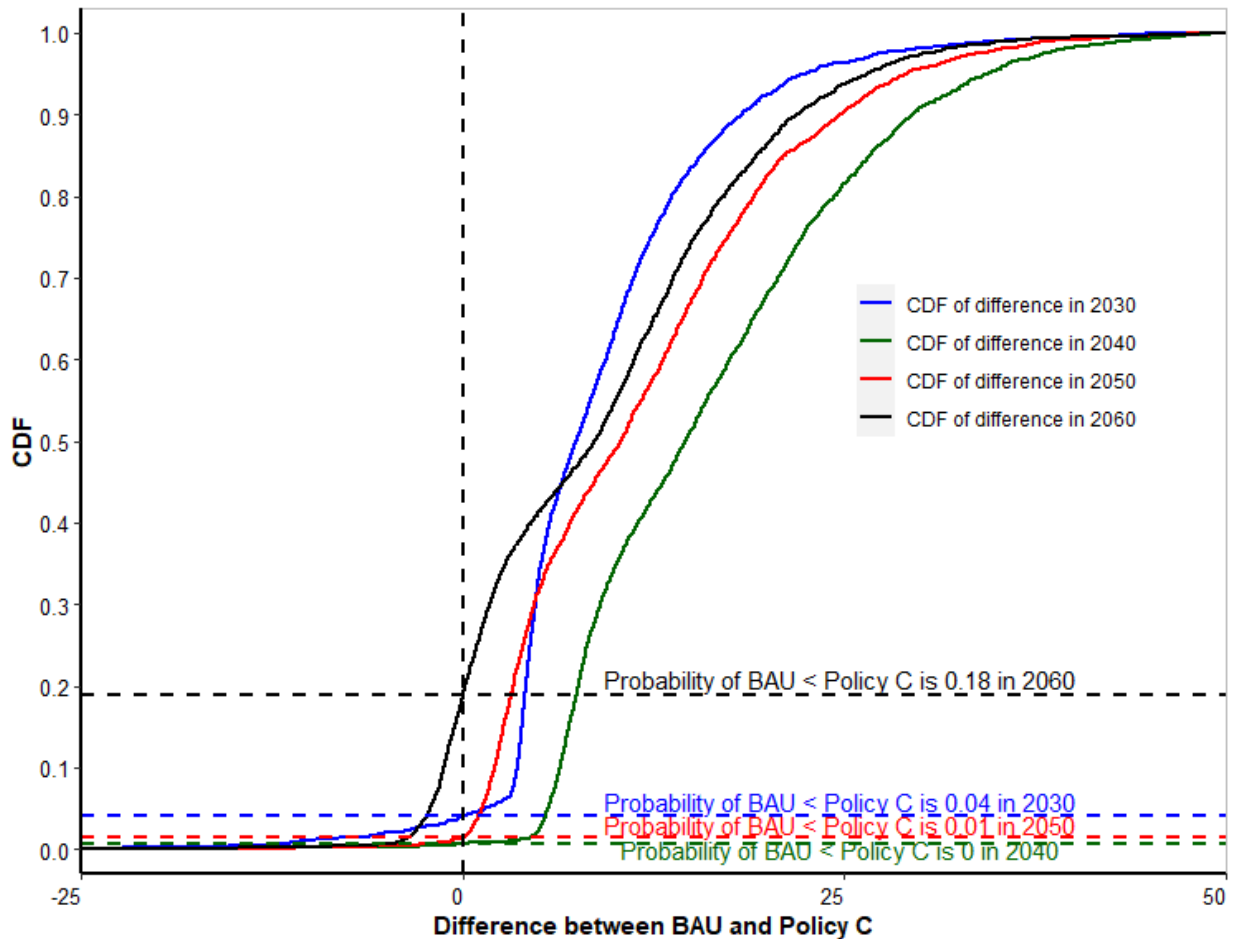
Figure 9.22: CDF of whole-life energy difference between BAU and Policy C in 2030, 2040, 2050 and 2060

9.5   Chapter summary

This chapter builds on preceding chapters and presents the modelling results of whole-life energy consumption of the urban residential stock in north China. It firstly compares EE and OE at stock level and intensity level. The results demonstrate the magnitude of EE relative to OE and support the argument that a whole-life perspective should be taken to address building energy consumption. Second, it presents the possible trajectories of the whole-life energy consumption of the urban residential stock in north China up to 2070. The whole-life energy is expected to peak around 2050, with a 95% credible interval of 338.9 to 432.6 million tce and a mean value of 383.7 million tce. Third, two policy scenarios are explored, including Policy A on extension of building lifetime and Policy B on acceleration of heating energy efficiency improvement. The results show that Policy A has the potential of reducing whole-life energy from the BAU scenario by considerable probabilities, whereas the probabilities under Policy B are always 1. However, the extent of potential reduction under the two scenarios differs substantially. Comparing the two policies further reveal that there is a considerable probability of Policy A leading to a whole-life

energy lower than Policy B. Last, Policy C, which integrates Policy A and Policy B, is modelled. As an effective measure, Policy C can achieve a cumulative energy saving of 35.7 million tce over the period of 2025 to 2030, which is a significant amount exceeding the provincial total building operational energy in 24 provinces in 2015. Under Policy C, the whole-life energy will peak in 2050, with a 95% credible interval between 330.4 and 414.7 million tce and a mean value of 371.8 million tce. In summary, this chapter answers research question Q6 and completes the planned research work of this thesis.

10
Conclusion

10.1 Chapter introduction

As the concluding section of this thesis, this chapter summarises the key findings and highlights its main contributions to the domain knowledge and methodological approach for research in a broader context. A series of policy recommendations are presented, with a view towards informing policies targeting the transformation of the Chinese buildings and construction sector towards greater energy efficiency and low-carbon development. This is followed by a discussion of the limitations inherent to modelling and data analysis of the thesis and how they may be addressed. Finally, future work that can build on and take forward the presented methods and findings is identified.

10.2 Key findings and contributions

10.2.1 Key findings and answers to research questions

This thesis formulates six research questions to guide the research design, model development and result analysis. The findings in chapters 4 to 9 provide answers to six specific questions.

Q1: How to model building stock turnover dynamics? What was the average lifetime of

Chinese urban residential buildings, and how did the residential stock evolve over the recent historical period since 2007?

Chapter 4 develops a residential stock turnover model using a System Dynamics approach. The model applies survival analysis to represent building lifecycle, from being newly constructed to being eventually demolished. Demolition is modelled as a stochastic process based on a hazard function derived from a Weibull distribution representing the uncertainties associated with building lifetime. Using historical data starting with 1978, the first year official building stock statistics are available, the Weibull distribution's shape and scale parameters are calibrated. The specified Weibull distribution had a mean value of 34.1 years, which represents the average building lifetime. This result adds to the very limited scientific evidence to substantiate the general observation that urban residential buildings in China have an average lifetime much shorter than the design lifetime of 50 years. In the absence of official statistics on building lifetime, this model of stock turnover dynamics can provide a useful method to assist policymakers in characterising existing buildings at the national, provincial and municipal levels. Based on annual new construction and the calibrated lifetime distribution, the total stock size of urban residential buildings is estimated to have increased from 17.8 billion m^2 in 2010 to 23.7 billion m^2 in 2017.

Q2: How can the building stock model be extended to forecast possible future trajectories of Chinese residential stock evolution over the medium to long term?

Chapter 5 builds on and significantly extends the stock turnover model in Chapter 4 to forecast future trajectories of the urban residential stock evolution. It turns the System Dynamics based model into a probabilistic one in a Bayesian framework. The probabilistic stock turnover model is then operationalised by separately investigating five candidate parametric survival models (Weibull, Lognormal, Loglogistic, Gamma, Gumbel) to represent the uncertainties associated with building lifetime. For each survival model, stock turnover is simulated through Markov Chain Monte Carlo methods to obtain the posterior predictive distribution of total historical stock and the marginal likelihood used to estimate the posterior model probability. Bayesian Model Averaging is applied to create a model ensemble to combine model-specific predictions of the historical stock evolution pathway based on model probabilities. By extending the model structure and incorporating variables relating to possible trends in urbanisation and demand for per capita floor area, future stock turnover dynamics through 2100 are forecasted using each survival model and then combined through model averaging. Using this novel approach, this chapter generates forecasts of total stock, age-specific sub-stocks, annual new construction and annual demolition, with their uncertainties fully characterised by their posterior predictive distributions. These results and the modelling approach are a major contribution of this thesis.

Q3: What are the possible future trajectories of annual embodied energy of urban residential stock in China over the medium to long term?

Based on the forecasted annual new construction and its posterior predictive distribution, **Chapter 6** estimates the embodied energy of new construction in a probabilistic manner. Empirical data of building material intensities are fitted to probability distribution functions, with the joint distribution of steel and cement intensities captured using a copula function. Energy intensities of material production, building construction and demolition are modelled using Bayesian non-linear regression. The uncertainties of these input variables, as well as the forecasted annual new construction, are propagated through to model embodied energy of new construction using Monte Carlo simulation. According to this approach, embodied energy of Chinese urban residential buildings is likely to peak around 2027, with a 95% credible interval ranging from 87 to 283 million tce and a mean of 170 million tce. Even after the peak, embodied energy is expected to remain high at around 150 million tce per year. Some obvious methods of reducing this energy cost in the future include reducing annual construction, or reducing material energy intensity, either through reducing the energy intensity of key materials, or moving to using materials with lower embodied energy. A further route explored in this chapter is to increase building lifetime, which, as found in Chapter 4, is very short in the current Chinese urban context. Gradually increasing this lifetime will reduce total embodied energy by 20% (31.8 million tce) by 2040.

Q4: How can existing system dynamics models of building stock operational energy be improved, for better representation of stock turnover dynamics and energy retrofit of buildings and for integration with modelling of embodied energy?

In parallel with embodied energy, it is necessary to model operational energy of the Chinese urban residential stock so as to obtain the whole-life energy consumption. This therefore entails the development of a building stock operational energy model that can be fully integrated with the System Dynamics model for building stock turnover dynamics, based on which embodied energy is estimated. It therefore makes most sense to develop a System Dynamics model for operational energy, as presented in **Chapter 7**. The developed model substantially extends the stock turnover model by adding a number of variables and causal loops relating to energy intensities of new buildings and existing buildings, energy-related retrofit depth and profile of existing buildings, and stock-level energy consumption. The model loosens the strong assumptions made by previous models in literature, such as perfect mixing in a first-order delay (exponential distribution) in a single stock model, perfect mixing in each delay of a third-order

delay (Erlang distribution) in a 3-vintage model, etc. It offers great structural flexibility that can accommodate various level of data availability. A salient feature of this model is that it avoids the unrealistic situations found in previous models, e.g. a building undergoes multiple rounds of retrofits within a very short period of time, or a building is demolished soon after its retrofit. Structurally and variable-wise, the generic model presented here is flexible, enabling adjustments to meet various application requirements.

Q5: What are the possible future trajectories of annual operational energy of urban residential stock in China over the medium to long term?

Chapter 8 adapts the generic building stock operational energy model presented in Chapter 7 to the Chinese urban context. Instead of considering the entire urban residential stock in China, this chapter focuses on the urban residential stock in north China, where centralised heat supply during winter season accounts for a substantial share of total building operational energy consumption and leads to significant environmental impacts. The model applies a scale factor to the age-specific sub-stocks and annual new construction obtained from the probabilistic stock turnover dynamics model in Chapter 5 to serve as input values for driving the residential stock development. Relevant energy intensity indicators specified in the Standard for Energy Consumption of Building issued by MOHURD are used to define possible trends of heating energy intensity and non-heating-related energy intensity. The results show that the heating energy consumption of urban residential buildings in north China is likely to peak around 2034 and then decrease steadily. As for non-heating-related energy consumption, the peaking will occur much later, around 2063, due to continued increase in appliance ownership and demand for energy driven by improving household living standards. In aggregate, the total operational energy consumption of urban residential buildings in north China will peak around 2051, with a 95% credible interval ranging from 280.4 to 358.7 million tce and a mean of 321.9 million tce.

Q6: What are the possible future trajectories of whole-life (embodied + operational) energy of urban residential stock in China over the medium to long term? How would they vary under different policy scenarios?

Based on the results from preceding chapters and additional modelling, **Chapter 9** investigates the possible trajectories of whole-life energy consumption of urban residential stock in China under various policy scenarios. Embodied energy (EE) is compared with operational energy (OE) to demonstrate the magnitude of EE relative to OE. At the stock level, the ratio of EE to OE remains above 0.18 from 2018 to 2060. At the intensity level, the ratio of embodied energy intensity (EEI) to stock-wide operational energy intensity (OEI) increases from 4.6 in 2018 to 6.5

in 2060. For the same period, the ratio of EEI to OEI of new buildings increases from 6.2 to 7.5. These results support the argument that a whole-life perspective should be taken to address building energy consumption. Possible trajectories up to 2070 are forecasted for the whole-life energy consumption of the urban residential stock in north China. The peak is expected to be reached around 2050, with a 95% credible interval of 338.9 to 432.6 million tce and a mean value of 383.7 million tce. Further modelling is conducted to explore the effects of various policy measures, including Policy A on extension of building lifetime, Policy B on acceleration of heating energy efficiency improvement, and Policy C that combines Policies A and B. The results show that Policy A has the potential of reducing whole-life energy from the BAU scenario by considerable probabilities, whereas the probabilities under Policy B are always 1. However, the possible amounts of potential reduction under the two scenarios differ substantially, as evidenced by the contrasting characteristics of the distributions of their annual energy savings from the BAU. Comparing the two policies further reveals that there is a considerable probability of Policy A being able to achieve more reduction of the whole-life energy than Policy B. Policy C integrates Policy A and Policy B by capturing all the endogenous dynamics of heating operational energy intensities of age-specific building substocks and the stock-wide average heating operational energy intensity, amid the time-varying building lifetime distribution. Over the period of 2025 to 2030, Policy C can achieve a cumulative energy saving of 35.7 million tce, exceeding the sum of provincial building operational energy of 24 out of the total 31 provinces of mainland China in 2015. Under Policy C, the whole-life energy will peak in 2050, with a 95% credible interval between 330.4 and 414.7 million tce and a mean value of 371.8 million tce.

10.2.2 Contributions to domain knowledge and methodology

By answering the research questions above, this thesis makes a number of important contributions to the literature. The contributions feature some innovative and first-of-a-kind attempts across several areas, as listed below.

(1)   As one of the very few attempts looking into building lifetime in China, this thesis estimates lifetime and associated uncertainties through a dynamic stock turnover model. The findings add to the very limited scientific evidence to substantiate the widely quoted anecdotal claim that Chinese urban residential buildings are generally short-lived.[7]

---

[7] It is expected that the lifetime of urban residential buildings in Chinese cities will generally become longer, as the result of more reasonable planning and implementation of urban renewal and expansion, more stringent design standards and effective enforcement, higher quality of building materials, improved construction techniques and practices, and adequate maintenance and renovation. The lifetime distribution presented in this thesis is estimated using data from the specific historical period of 1978 to 2006. When

(2)   This thesis models the stock turnover dynamics and forecasts the future development trends of Chinese urban residential stock using a Bayesian framework for the first time, in which the uncertainties associated with survival models and parameters are captured and quantified. This is a major contribution of this thesis.

(3)   As a first-of-its-kind attempt, this thesis estimates the historical and future trends of annual embodied energy of Chinese urban residential stock in a probabilistic manner. The results provide a valuable addition to this under-researched area.

(4)   Future trends in whole-life energy consumption of Chinese urban residential stock are modelled for the first time by integrating stock turnover dynamics, embodied energy, and operational energy. This will also facilitate further work to quantify whole-life carbon emissions of the stock, which is of strategic relevance to China's announced climate targets of peaking its economy-wide carbon emissions by 2030 and achieving carbon neutrality by 2060.

Underpinning the contributions to the domain knowledge are the models developed by this thesis. These innovative models contribute a valuable addition to the development of methodological approaches for further research on building stock energy in a broader context.

(a)   The probabilistic building stock turnover model, developed in Chapter 5 using System Dynamics and Bayesian Model Averaging, contributes an innovative methodological approach to the general field of modelling building stock dynamics. The model's generality, flexibility and transparency make it potentially applicable to a wide variety of geographical contexts. It is particularly relevant and useful to countries experiencing rapid urbanisation and massive construction, such as developing countries in South and Southeast Asia (World Bank 2015; Ellis & Roberts 2016; ASEAN Secretariat 2018). Addressing building energy and carbon emissions has been emphasized as a key climate change mitigation strategy in the Nationally Determined Contributions (NDCs) of these countries (IEA and UNEP 2018; UNFCCC 2020). Correspondingly, building energy is also amongst the focus areas on the development agenda of multilateral and bilateral donor agencies providing loans, grants and technical assistance to these countries. The modelling approach and its application in the Chinese context as elaborated in this thesis provides a useful reference for these countries and donor agencies to take stock of their existing buildings, forecast possible stock evolution pathways and evaluate stock-level energy consumption and carbon emissions under

---

additional, more recent data becomes available, the model and its results can be updated to more precisely characterise the lifetime uncertainties of Chinese urban residential buildings.

different policy and intervention scenarios.

(b)   The generic System Dynamics model for operational energy of building stock, developed in Chapter 7, is well placed to be used as a stand-alone model or as part of a larger model looking at building stock-level operational energy in a variety of national or sectoral contexts. Its flexibility and transparency enable adjustments to meet various requirements and settings. The model can be extended to accommodate increased granularity and enhanced level of sophistication, or expanded boundary of modelling. Structurally, with available empirical data, the sub-stocks of retrofitted buildings can be further divided to model various lengths of the holding period post energy efficiency retrofit. Functionally, additional structures and variables can be added to the model to enhance its utility, such as stock of existing heating technologies and possible future trends of technology mix to model carbon emissions of heating. Sometimes building demolition is of less concern, e.g. when buildings are generally long-lived and/or the period of modelling and analysis is short relative to building lifetimes. In these circumstances, the model can be straightforwardly reduced to a three-vintage or single stock structure as found in literature. Similarly, the multiple retrofit dynamics can be easily reduced to single retrofit or no retrofit structure but retain the ability of avoiding unrealistic modelling results found in literature.

10.3 Policy implications

Clearly, new construction in China involves significant annual embodied energy so it is essential to address the issue in order to reduce national carbon emissions. This embodied energy, as has been shown, comes from the high energy intensity of common building materials, a high construction rate, and the high material intensity of that construction.

The energy intensities of producing steel, cement, aluminium, glass, and other building materials have progressively declined as a result of technological advances and sectoral policy mandates over past decades. Going forward, the potential for further improvement is expected to be limited, unless disruptive technologies and policies become available. Therefore, annual new construction, and material intensities of that construction will remain essential determinants to have major impacts on the embodied energy of Chinese building stock.

Whilst annual new construction serves to meet incremental housing demand, the real estate sector is subject to high risk of speculation and disorderly rapid expansion, which has resulted in

massive construction and destruction, over-supply of housing, high vacancy rate and excessive urban sprawl (Chivakul et al. 2015; Glaeser et al. 2017). These issues should be addressed through strong macro-level regulation and control, and effective market-based instruments in order to support the healthy growth of the housing market. Amongst the wide range of economic, social and environment benefits of strengthened housing regulations will be an effectively contained new construction scale, with reduced materials consumption and associated embodied energy.

Meanwhile, new buildings are becoming gradually more material intensive due to the observed transition of building structural types preferred by designers and developers. To counter this trend, quantitative design standards and performance indicators for material intensities should be established to facilitate performance benchmarking of new buildings. A phased approach may be taken. At the initial stage, this may involve updating existing standards for green buildings, such as the *Code for Green Design of Civil Buildings* (MOHURD 2010) and the *Assessment Standard for Green Building* (MOHURD 2019a). For example, the 2019 standard's section on material conservation and green materials may be updated to explicitly include quantitative material intensity indicators in the rating. The implementation of the updated standards could potentially be supported by additional administrative and/or financial incentives for developers and homebuyers. Over time, mandatory requirements should be introduced and enforced in pilot cities and gradually rolled out more widely.

To date, the lack of data has been a constraint on evidence-informed policymaking. Beyond existing statistics on annual new construction, it is suggested that building-related statistics are expanded to cover city-wide residential stock size, which can then be aggregated to the provincial and national levels. Floor area and age of individual buildings are valuable information to obtain, possibly on a sampling basis if comprehensive data is practically difficult. Given the governance structure and administrative systems in the Chinese urban context, this is a practically feasible task and municipal authorities should take initiatives to implement it. A comprehensive and transparent database can provide the much-needed evidence to energy and climate policies on buildings. The same consideration applies to data on building material intensity. It is worthwhile exploring the feasibility of considering material intensities at the design and approval stages of property development.

It is expected that buildings will become progressively more energy efficient and 'greener' over time. The *Standard for Energy Consumption of Building* issued by MOHURD in 2016 sends a strong signal of the envisaged transition of the design and evaluation of operational energy. Instead of focusing only on prescriptive design and *ex-ante* compliance, an increasing emphasis

is being placed on performance-based and result-driven design and *ex-post* evaluation of actual energy performance (MOHURD 2016). Meanwhile, it is unlikely that embodied energy intensity of new buildings would decline substantially over the short to medium term. Rather, over that timeframe, it is more likely to increase. In fact, it has been found that the desired operational performance of green buildings was often obtained at the cost of much higher embodied energy than conventional buildings (Zhao et al. 2014). With new buildings becoming more operationally efficient, the capital cost of embodied energy and carbon will be more significant and should be fully taken into consideration in the decision-making process for sustainable design, construction and use of buildings.

An important and less obvious route to reducing annual embodied energy and whole-life energy has been explored in this thesis – increasing the lifetime of buildings. This approach also demonstrated the importance of ensuring that operational and embodied energy should be addressed in an integrated manner. While extending the lifetime of existing buildings will reduce embodied energy, in so doing, less efficient older buildings would be kept in the stock for longer and the construction and operation of more efficient new buildings (assuming operational standards continue to improve) would be delayed. The stock-level average operational energy efficiency would therefore not be as desirable as what otherwise would have been the case. Conversely, accelerated demolition of older inefficient buildings may be desirable from the perspective of stock-level operational energy performance, but will incur higher embodied energy for new buildings that otherwise would not have been built. Moreover, accelerating demolition is much less likely to be implemented in practice due to its social and economic implications on housing provision. These trade-offs across stock-level embodied and operational energy should be adequately recognised and analysed when designing future strategies and policies for buildings. As demonstrated in Chapter 9, the combination of policy measures on extending building lifetime and accelerating heating energy efficiency improvement can achieve a significant amount of energy saving. It is therefore strongly recommended that a whole-life perspective should be taken towards building energy, which could offer a small but important step in achieving China's overarching climate target of carbon neutrality by 2060.

10.4 Research limitations

This thesis, like any model-based approach, is subject to some inherent limitations.

Firstly, the stock turnover model treats the urban areas of China as a whole, without further disaggregation into provinces. Geographically, there exist substantial differences amongst provinces in population size, economic and social development, and climatic conditions. These

factors are likely to have some impact on building lifetime and stock turnover dynamics at the regional, provincial and local levels. For example, the average lifetime of the residential stock in a coastal megacity in the east may differ considerably from that of a small underdeveloped city in the hinterland. Similarly, due to limited availability of empirical data, the model only considers the longitudinal variation in building lifetime profile in Chapter 6 and Chapter 9 where lifetime extension is explicitly modelled as a policy scenario. It is possible that buildings built in the 1980s and 2000s might have experienced (and are currently experiencing) rather different dynamics of use, renovation and demolition due to changing technological, economic and social factors. However, further investigation into the geographical and longitudinal variations would require significant collective efforts for data collection involving a wide range of stakeholders, which are beyond the scope of this thesis. Notwithstanding this limitation, I believe that extending the stock turnover model to a probabilistic one and adopting a Bayesian Model Averaging approach in Chapter 5 have adequately taken into account the uncertainties based on limited available data and therefore have, to a large extent, offset the potentially adverse effects of the above limitation. The Bayesian modelling offers ample potential for representing a wide range of eventualities regarding the survival of the existing urban residential building stock as well as the future evolution of the building stock.

Secondly, as mentioned in Chapter 6, the generic model for stock operational energy, as in any models of buildings, energy and related sectors, has been developed based on methodological assumptions to be a simplification of the dynamic complexity of real-world building stock energy performance characteristics. For example, the model sets the retrofit depth as a constant, whereas in reality there exist various energy-related retrofit activities and therefore various factors contributing to the variability and uncertainty with respect to retrofit depth. Similarly, the interval between two retrofits is set as a constant as an intended simplification due to data constraint. This is more of an engineering intuition, which may not be the case in reality due to technological, economic and social factors. With adequate empirical data, the practical variations of retrofit depth and interval can be accounted for through model extension enabled by its structural and functional flexibility and adaptability.

Finally, the material intensity data is from 150 urban residential buildings across different cities in China. This is a small sample size, given the scope of this thesis. However, this is the best publicly available database that this thesis has access to. If additional data becomes available, the fitting of the marginal distributions of the material intensities as well as their interdependence structure can be easily updated to re-calculate the embodied energy. It is also acknowledged that the scope of embodied energy calculation only covers some of the building lifecycle stages and some of the materials, and the construction sector is taken as a whole to estimate the energy intensity

of construction and demolition. These can be improved in future research.

10.5 Recommendations for future research

The above-mentioned limitations are possible aspects that could be further researched, provided adequate additional data can be collected and made available. Meanwhile, the models and findings of this thesis prepare a solid foundation for exploring the following research topics relating to buildings or beyond, given their great relevance to China's climate targets featuring emissions peaking by 2030 and carbon neutrality by 2060.

Embodied energy and carbon. The embodied energy part of the model may be further improved by expanding scope and increasing the level of detailedness of the calculations. The overall model and its results of this thesis lay the groundwork for estimating embodied carbon. Forecasting future trends in energy-related embodied carbon due to energy use in building material production entails insights into possible structural changes of production process and technological advancement that would lead to changes to shares of energy types, as well as energy savings. In parallel, process emissions from material production and future trends need to be investigated.

Operational carbon. For space heating of urban residential buildings, CO_2 emissions are mainly produced by heat sources, which are dominated by coal-fired co-generation, coal-fired boilers, and gas-fired boilers at various scales (IEA and THUBERC 2015; THUBERC 2019a). There also exist a small but gradually increasing share of less polluting heating systems such as geothermal energy, electricity (heat pumps of various types, solar power, the otherwise-curtailed wind power), biomass and biogas, industrial waste heat recovery, etc (National Development and Reform Commission 2017). Driven by policies and plans on clean heating, the heating generation mix is expected to keep evolving towards decreasing energy and carbon intensities. These dynamics have to be modelled in an effort to forecast CO_2 emissions from space heating. For non-heating energy use in residential buildings, CO_2 emissions are caused primarily by electricity for appliances, lighting, air-conditioning, and electricity and gas for water heating and cooking (THUBERC 2017). Thus, to estimate CO_2 emissions, it is important to project the respective shares of gas and electricity in future non-heating energy use of urban residential buildings.

Commercial and public buildings. As an integral part of China's total building stock, commercial and public buildings was 12.3 billion m^2 in 2017, approximately 51% of the size of urban residential buildings. Operationally, commercial and public buildings consumed 293 million tce in 2017, whereas urban residential buildings consumed 226 million tce. Its high energy

intensity suggests large potential of improving energy efficiency of both new and existing commercial and public buildings through various measures (Hou et al. 2016). On embodied energy, commercial buildings use more materials per m^2 and incur higher embodied energy than residential buildings (Zhao et al. 2014). With minor adjustments to its structure and variables, the model developed in this thesis can be extended to commercial and public buildings. It would be interesting to explore whether the stock of commercial and public buildings experiences turnover dynamics similar to that of residential buildings and explore effective and efficient strategies to decelerate the increase of its energy use, both embodied and operational.

Power grid emission factor. As electricity is a key source of energy used in building material production, building construction and building operation, power grid emission factors are needed to calculate embodied and operational carbon emissions, which in turn will require additional data. Whilst officially published power grid emission factors can be used for recent historical period, future trends in electricity grid emission factors will have to be projected to be able to forecast embodied and/or operational carbon emissions over the medium to long term. This is a challenging task as the forecasting will involve holistic and in-depth modelling of the dynamics of national electricity demand, generation capacity mix, fuel mix, technological advancement, policies on power sector decarbonisation, etc. While being well beyond the scope of studies focusing on building sector, this has a direct and substantial impact on quantification of embodied and operational carbon emissions of buildings.

Bibliography

Abeysundara, U.G.Y., Babel, S. & Gheewala, S., 2009. A matrix in life cycle perspective for selecting sustainable materials for buildings in Sri Lanka. *Building and Environment*, 44(5), pp.997–1004. Available at: https://doi.org/10.1016/j.buildenv.2008.07.005.

Abeysundra, U.G.Y. et al., 2007. Environmental, economic and social analysis of materials for doors and windows in Sri Lanka. *Building and Environment*, 42(5), pp.2141–2149. Available at: https://doi.org/10.1016/j.buildenv.2006.04.005.

Aden, N., Qin, Y. & Fridley, D., 2010. *Lifecycle Assessment of Beijing- Area Building Energy Use and Emissions: Summary Findings and Policy Applications*, Available at: https://china.lbl.gov/publications/lifecycle-assessment-beijing-area.

Aksözen, M. et al., 2016. Mortality analysis of an urban building stock. *Building Research & Information*, 45(3), pp.1–19. Available at: http://www.tandfonline.com/doi/abs/10.1080/09613218.2016.1152531.

Allison, P., 2010. *Survival Analysis Using SAS: A Practical Guide*, SAS Institute.

Anuradha, I.G.N., Perera, B.A.K.S. & Ekanayake, B.J., 2019. Significance of whole life embodied energy and embodied carbon of wall materials compared to their initial/maintenance costs. *International Journal of Construction Management*. Available at: https://doi.org/10.1080/15623599.2019.1683690.

ASEAN Secretariat, 2018. *ASEAN Sustainable Urbanisation Strategy*, Jakarta, Indonesia. Available at: https://asean.org/storage/2018/11/ASEAN-Sustainable-Urbanisation-Strategy-ASUS.pdf.

Asia Green Real Estate, 2019. *Housing Policies in China – How the "Visible Hand" Guides the Housing Market*, Available at: https://www.asiagreen.com/images/easyblog_articles/124/190929_Asia-Insights_Housing-Policies-in-Chin_20191002-122606_1.pdf.

Asian Development Bank, 2013. *Strategic Options for Urbanization in the People's Republic of China - Key Findings*, Manila, Philippines. Available at: https://www.adb.org/sites/default/files/publication/30397/options-urbanization-prc-findings.pdf.

Aye, L. et al., 2012. Life cycle greenhouse gas emissions and energy analysis of prefabricated reusable building modules. *Energy and Buildings*, 47, pp.159–168. Available at: https://doi.org/10.1016/j.enbuild.2011.11.049.

Bajaj, A. & Wrycza, S., 2009. *Systems Analysis and Design for Advanced Modeling Methods: Best Practices*, Information Science Reference.

Bansal, D., Singh, R. & Sawhney, R.L., 2014. Effect of construction materials on embodied energy and cost of buildings - A case study of residential houses in India up to 60 m2 of plinth area. *Energy and Buildings*, 69, pp.260–266. Available at: https://doi.org/10.1016/j.enbuild.2013.11.006.

Birgisdottir, H. et al., 2017. IEA EBC annex 57 "evaluation of embodied energy and CO2eq for building construction." *Energy and Buildings*, 154, pp.72–80. Available at: http://dx.doi.org/10.1016/j.enbuild.2017.08.030.

Bohne, R.A. et al., 2006. Estimation of the Service Life of Residential Buildings, and Building

Components, in Norway. In *Towards The City Surface Of Tomorrow*. pp. 29–33. Available at: https://www.academia.edu/27632589/Estimation_of_the_Service_Life_of_Residential_ Buildings_and_Building_Components_in_Norway.

Bribián, I., Capilla, A. & Usón, A., 2011. Life cycle assessment of building materials: comparative analysis of energy and environmental impacts and evaluation of the eco-efficiency improvement potential. *Building and Environment*, 46(5), pp.1130–1140. Available at: https://doi.org/10.1016/j.buildenv.2010.12.002.

Broun, R. & Menzies, G.F., 2011. Life Cycle Energy and Environmental Analysis of Partition Wall Systems in the UK. *Procedia Engineering*, 21, pp.864–873. Available at: https://doi.org/10.1016/j.proeng.2011.11.2088.

Brown, N.W.O., Olsson, S. & Malmqvist, T., 2014. Embodied greenhouse gas emissions from refurbishment of residential building stock to achieve a 50% operational energy reduction. *Building and Environment*, 79, pp.46–56. Available at: https://doi.org/10.1016/j.buildenv.2014.04.018.

Burnham, K.P. & Anderson, D.R., 2002. *Model Selection and Multimodel Inference: A Practical Information-Theoretic Approach*, Springer, New York, NY.

CABEE, 2018. *China Building Energy Consumption Research Report 2018*, Available at: https://www.cabee.org/site/content/22960.html.

Cabeza, L.F. et al., 2013. Affordable construction towards sustainable buildings: review on embodied energy in building materials. *Current Opinion in Environmental Sustainability*, 5(2), pp.229–236. Available at: https://doi.org/10.1016/j.cosust.2013.05.005.

Cabeza, L.F. et al., 2021. Embodied energy and embodied carbon of structural building materials: Worldwide progress and barriers through literature map analysis. *Energy and Buildings*, 231. Available at: https://doi.org/10.1016/j.enbuild.2020.110612.

Cai, W. et al., 2020. Calculation and analysis of provincial building energy consumption in China [in Chinese]. *HV&AC*, 50(2). Available at: http://www.hvacjournal.cn/Item/9273.aspx.

Cai, W. et al., 2015. Short-Lived Buildings in China: Impacts on Water, Energy, and Carbon Emissions. *Environmental Science and Technology*, 49(24), pp.13921–13928. Available at: http://pubs.acs.org/doi/full/10.1021/acs.est.5b02333%0A.

Cao, Z. et al., 2016. Toward a better practice for estimating the CO2 emission factors of cement production: An experience from China. *Journal of Cleaner Production*, 139, pp.527–539. Available at: https://doi.org/10.1016/j.jclepro.2016.08.070.

CEN, 2012. *EN 15978: Sustainability of Construction Works - Assessment of Environmental Performance of Buildings - Calculation Method*,

Center for Industrial Energy Efficiency, 2014. *Progress report on industrial energy conservation in China [in Chinese]*, Available at: https://www.efchina.org/Reports-zh/reports-20140701-zh.

Chalmers, P., 2014. *Climate Change: Implications for Buildings. Key Findings from the Intergovernmental Panel on Climate Change Fifth Assessment Report*, Available at: http://www.cisl.cam.ac.uk/business-action/low-carbon-transformation/ipcc-climate-science-business-briefings/pdfs/briefings/IPCC_AR5__Implications_for_Buildings__Briefing__WEB_EN.pdf.

Chastas, P., Theodosiou, T. & Bikas, D., 2016. Embodied energy in residential buildings-towards the nearly zero energy building: A literature review. *Building and Environment*, 105, pp.267–282. Available at: http://dx.doi.org/10.1016/j.buildenv.2016.05.040.

Chau, C.K. et al., 2017. Assessment of CO_2 Emissions Reduction in High-Rise Concrete Office Buildings Using Different Material-Use Options. In *Handbook of Low Carbon Concrete*. Elsevier, pp. 39–61. Available at: https://doi.org/10.1016/B978-0-12-804524-4.00003-8.

Chen, J. et al., 2017. An empirical study on the CO_2 emissions in the Chinese construction industry. *Journal of Cleaner Production*, 168, pp.645–654. Available at: http://dx.doi.org/10.1016/j.jclepro.2017.09.072.

Chen, T.., Burnett, J. & Chau, C.., 2001. Analysis of embodied energy use in the residential building of Hong Kong. *Energy*, 26(4), pp.323–340. Available at: https://doi.org/10.1016/S0360-5442(01)00006-8.

Chen, T.Y., Burnett, J. & Chau, C.K., 2001. Analysis of embodied energy use in the residential building of Hong Kong. *Energy*, 26(4), pp.323–340. Available at: https://doi.org/10.1016/S0360-5442(01)00006-8.

China Daily, 2010. Short-lived buildings create huge waste. Available at: http://www.chinadaily.com.cn/china/2010-04-06/content_9687545.htm [Accessed January 19, 2021].

China Iron and Steel Industry Association, 2019. *China iron and steel industry Thirteenth Five-Year coal cap mid-term evaluation and later-term outlook [in Chinese]*, Available at: http://coalcap.nrdc.cn/Public/uploads/pdf/1559097268757375782.pdf.

Chivakul, M. et al., 2015. *Understanding Residential Real Estate in China*, Available at: https://www.imf.org/en/Publications/WP/Issues/2016/12/31/Understanding-Residential-Real-Estate-in-China-42873.

Clarke, L. et al., 2018. Effects of long-term climate change on global building energy expenditures. *Energy Economics*, 72, pp.667–677. Available at: https://doi.org/10.1016/j.eneco.2018.01.003.

Cole, R.J., 1999. Energy and greenhouse gas emissions associated with the construction of alternative structural systems. *Building and Environment*, 34(3), p.335. Available at: https://doi.org/10.1016/S0360-1323(98)00020-1.

Crawford, K. et al., 2014. *Demolition or Refurbishment of Social Housing?*, Available at: http://www.engineering.ucl.ac.uk/engineering-exchange/files/2014/10/Report-Refurbishment-Demolition-Social-Housing.pdf.

Crawford, R.H. et al., 2016. Evaluating the life cycle energy benefits of energy efficiency regulations for buildings. *Renewable and Sustainable Energy Reviews*, 63, pp.435–451. Available at: http://dx.doi.org/10.1016/j.rser.2016.05.061.

Crawford, R.H. et al., 2006. Life-cycle energy analysis of building integrated photovoltaic systems (BiPVs) with heat recovery unit. *Renewable and Sustainable Energy Reviews*, 10(6), pp.559–575. Available at: https://doi.org/10.1016/j.rser.2004.11.005.

Crawford, R.H. & Treloar, G.J., 2003. Validation of the use of Australian input-output data for building embodied energy simulation. In *Proceedings of the Eighth International Building Performance Simulation Association Conference on Building Simulation: For better Building Design*. Available at: http://www.inive.org/members_area/medias/pdf/Inive%5CIBPSA%5CUFSC881.pdf.

Crawley, M.J., 2013. *The R Book* Second., Wiley.

Delignette-Muller, M.L. & Dutang, C., 2015. fitdistrplus: An R package for fitting distributions. *Journal of Statistical Software*, 64(4), pp.1–34. Available at: https://www.jstatsoft.org/index.php/jss/article/view/v064i04/v64i04.pdf.

Delmastro, C., Lavagno, E. & Mutani, G., 2015. Chinese residential energy demand: Scenarios to 2030 and policies implication. *Energy and Buildings*, 89, pp.49–60. Available

at: https://www.sciencedirect.com/science/article/pii/S0378778814010536.

Devi, P.L. & Palaniappan, S., 2014. A case study on life cycle energy use of residential building in Southern India. *Energy and Buildings*, 80, pp.247–259. Available at: http://dx.doi.org/10.1016/j.enbuild.2014.05.034.

Ding, N. et al., 2012. Environment impact analysis of primary aluminum and recycled aluminum. *Procedia Engineering*, 27, pp.465–474. Available at: https://doi.org/10.1016/j.proeng.2011.12.475.

Dixit, M.K., 2017a. Embodied energy analysis of building materials: An improved IO-based hybrid method using sectoral disaggregation. *Energy*, 124, pp.46–58. Available at: https://doi.org/10.1016/j.energy.2017.02.047.

Dixit, M.K., 2017b. Life cycle embodied energy analysis of residential buildings: A review of literature to investigate embodied energy parameters. *Renewable and Sustainable Energy Reviews*, 79, pp.390–413. Available at: http://dx.doi.org/10.1016/j.rser.2017.05.051.

Dixit, M.K., 2019. Life cycle recurrent embodied energy calculation of buildings: A review. *Journal of Cleaner Production*, 209, pp.731–754. Available at: https://doi.org/10.1016/j.jclepro.2018.10.230.

Dodoo, A. & Gustavsson, L., 2013. Life cycle primary energy use and carbon footprint of wood-frame conventional and passive houses with biomass-based energy supply. *Applied Energy*, 112, pp.834–842. Available at: https://doi.org/10.1016/j.apenergy.2013.04.008.

Eberlein, R.L. & Thompson, J.P., 2013. Precise modeling of aging populations. *System Dynamics Review*, 29(2), pp.87–101. Available at: https://doi.org/10.1002/sdr.1497.

Eberlein, R.L., Thompson, J.P. & Matchar, D.B., 2012. Chronological Aging in Continuous Time. In *Proceedings of the 30th International Conference of the System Dynamics Society, St. Gallen, Switzerland, 2012*. Available at: https://www.systemdynamics.org/assets/conferences/2012/proceed/papers/P1064.pdf.

Ellis, P. & Roberts, M., 2016. *Leveraging Urbanization in South Asia: Managing Spatial Transformation for Prosperity and Livability*, Washington, DC: World Bank Publications. Available at: https://elibrary.worldbank.org/doi/pdf/10.1596/978-1-4648-0662-9.

Emmanuel, R., 2004. Estimating the environmental suitability of wall materials: preliminary results from Sri Lanka. *Building and Environment*, 39(10), pp.1253–1261. Available at: https://doi.org/10.1016/j.buildenv.2004.02.012.

Energy Research Institute/Lawrence Berkeley National Laboratory/Rocky Mountain Institute, 2019. *Reinventing Fire: China – A Roadmap for China's Revolution in Energy Consumption and Production to 2050*, Available at: https://rmi.org/insight/reinventing-fire-china/.

Eom, J. et al., 2012. China's building energy demand: Long-term implications from a detailed assessment. *Energy*, 46(1), pp.405–419. Available at: http://www.sciencedirect.com/science/article/pii/S0360544212006214.

ERI, 2014. *A study on low-carbon building scenarios and policy roadmaps in China [in Chinese]*, Available at: http://www.efchina.org/Reports-zh/reports-20140706-zh.

Fadali, M.S. & Visioli, A., 2013. *Digital Control Engineering: Analysis and Design* Second edi., Academic Press.

Fawley, B.W. & Wen, Y., 2013. The Great Chinese Housing Boom. *Economic Synopses*, (13). Available at: http://research.stlouisfed.org/publications/es/article/9774.

Fazeli, R. & Davidsdottir, B., 2015. Energy Modeling of Danish Housing Stock Using System Dynamics. In *Proceedings of the 33rd International Conference of the System Dynamics*

Society, Cambridge, Massachusetts, USA, 2015. Available at: http://www.systemdynamics.org/conferences/2015/papers/P1384.pdf.

Fazeli, R. & Davidsdottir, B., 2017. Energy performance of dwelling stock in Iceland: System dynamics approach. *Journal of Cleaner Production*, 167, pp.1345–1353. Available at: https://doi.org/10.1016/j.jclepro.2017.05.009.

Forbes, C. et al., 2011. *Statistical Distributions (Fourth Edition)*, John Wiley & Sons, Inc., Hoboken, New Jersey.

Forrester, J.W., 1961. *Industrial Dynamics*, MIT Press.

Forrester, J.W., 1958. Industrial dynamics: a major breakthrough for decision makers. *Harvard Business Review*, 36(4).

Forrester, J.W., 2007. System dynamics - a personal view of the first fifty years. *System Dynamics Review*, 23(2–3). Available at: http://onlinelibrary.wiley.com/doi/10.1002/sdr.382/epdf.

Forrester, J.W., 1969. *Urban Dynamics*, MIT Press.

Fragoso, T.M., Bertoli, W. & Louzada, F., 2018. Bayesian Model Averaging: A Systematic Review and Conceptual Classification. *International Statistical Review*, 86(1), pp.1–28. Available at: https://onlinelibrary.wiley.com/doi/epdf/10.1111/insr.12243.

Fridley, D. et al., 2012. *China Energy and Emissions Paths to 2030 (2nd edition)*, Available at: https://eaei.lbl.gov/sites/default/files/lbl-4866e-rite-modelaugust2012.pdf.

Fridley, D., Zheng, N. & Zhou, N., 2008. *Estimating Total Energy Consumption and Emissions of China's Commercial and Office Buildings*, Available at: https://china.lbl.gov/sites/all/files/lbl-248e-commercial-buildingmarch-2008.pdf.

Frühwirth-Schnatter, S., 2004. Estimating marginal likelihoods for mixture and Markov switching models using bridge sampling techniques. *The Econometrics Journal*, 7(1), pp.143–167. Available at: https://academic.oup.com/ectj/article/7/1/143/5073348.

Gan, V.J.L., Chan, C.M., et al., 2017. A comparative analysis of embodied carbon in high-rise buildings regarding different design parameters. *Journal of Cleaner Production*, 161, pp.663–675. Available at: https://doi.org/10.1016/j.jclepro.2017.05.156.

Gan, V.J.L., Cheng, J.C.P., et al., 2017. Developing a CO2-e accounting method for quantification and analysis of embodied carbon in high-rise buildings. *Journal of Cleaner Production*, 141, pp.825–836. Available at: http://dx.doi.org/10.1016/j.jclepro.2016.09.126.

Gelman, A. et al., 2014. *Bayesian Data Analysis, Third Edition*, Chapman and Hall/CRC.

Gibbons, J.M. et al., 2008. Applying Bayesian Model Averaging to mechanistic models: An example and comparison of methods. *Environmental Modelling and Software*, 23(8), pp.973–985. Available at: https://www.sciencedirect.com/science/article/pii/S1364815207002241.

Giordano, R. et al., 2017. Embodied Energy Versus Operational Energy in a Nearly Zero Energy Building Case Study. *Energy Procedia*, 111, pp.367–376. Available at: https://doi.org/10.1016/j.egypro.2017.03.198.

Glaeser, E. et al., 2017. A real estate boom with Chinese characteristics. *Journal of Economic Perspectives*, 31(1), pp.93–116. Available at: https://doi.org/10.1257/jep.31.1.93.

Global Alliance for Buildings and Construction and UNEP, 2020. *2020 Global Status Report for Buildings and Construction: Towards a Zero-emission, Efficient and Resilient Buildings and Construction Sector*, Nairobi. Available at: https://globalabc.org/sites/default/files/inline-files/2020 Buildings GSR_FULL REPORT.pdf.

Global Alliance for Buildings and Construction, IEA & UNEP, 2019. *2019 Global status report for buildings and construction: Towards a zero-emission, efficient and resilient buildings and construction sector*, Available at: https://www.worldgbc.org/sites/default/files/2019 Global Status Report for Buildings and Construction.pdf.

Global Buildings Performance Network, 2019. China: the world's largest single market in new construction. Available at: http://130.226.56.250/our-blog/china-worlds-largest-single-market-new-construction.

Goggins, J., Keane, T. & Kelly, A., 2010. The assessment of embodied energy in typical reinforced concrete building structures in Ireland. *Energy and Buildings*, 42(5), pp.735–744. Available at: https://doi.org/10.1016/j.enbuild.2009.11.013.

Gronau, Q.F. et al., 2017. A tutorial on bridge sampling. *Journal of Mathematical Psychology*, 81, pp.80–97. Available at: https://www.sciencedirect.com/science/article/pii/S0022249617300640.

Gronau, Q.F. & Singmann, H., 2018. bridgesampling: Bridge Sampling for Marginal Likelihoods and Bayes Factors. Available at: https://cran.r-project.org/web/packages/bridgesampling/index.html.

Gronau, Q.F., Singmann, H. & Wagenmakers, E.-J., 2018. bridgesampling: An R Package for Estimating Normalizing Constants. Available at: http://arxiv.org/abs/1710.08162.

Gu, D. et al., 2007. Comparison between construction and operation energy consumption of buildings [in Chinese]. *HV&AC*, 37(5). Available at: https://www.cnki.com.cn/Article/CJFDTotal-NTKT200705013.htm.

Gu, L., 2009. *Studies on the environmental impact of the building industry in China based on the life cycle assessment*. Tsinghua University.

Guan, D. et al., 2018. Structural decline in China's CO2 emissions through transitions in industry and energy systems. *Nature Geoscience*, 11(8), pp.551–555. Available at: http://dx.doi.org/10.1038/s41561-018-0161-1.

Guerrero, C.N., Schwarz, P. & Slinger, J.H., 2016. A recent overview of the integration of System Dynamics and Agent-based Modelling and Simulation. In *Proceedings of the 34th International Conference of the System Dynamics Society*. pp. 1–13. Available at: http://repository.tudelft.nl/islandora/object/uuid%3Af16c5dca-e0f0-41cf-a777-c19069c3aa6a.

Guo, H. & Wang, Q., 2018. Construction Energy Consumption of Building Industry in Shanghai. *Building Energy Efficiency*, 46(331), pp.1–5. Available at: http://www.cnki.com.cn/Article/CJFDTotal-FCYY201809035.htm.

Gustavsson, L. & Sathre, R., 2006. Variability in energy and carbon dioxide balances of wood and concrete building materials. *Building and Environment*, 41(7), pp.940–951. Available at: https://doi.org/10.1016/j.buildenv.2005.04.008.

Hacker, J.N. et al., 2008. Embodied and operational carbon dioxide emissions from housing: A case study on the effects of thermal mass and climate change. *Energy and Buildings*, 40(3), pp.375–384. Available at: https://doi.org/10.1016/j.enbuild.2007.03.005.

Hall, L.M.H. & Buckley, A.R., 2016. A review of energy systems models in the UK: Prevalent usage and categorisation. *Applied Energy*, 169, pp.607–628. Available at: http://www.sciencedirect.com/science/article/pii/S0306261916301672.

Hamada, M.S. et al., 2008. *Bayesian Reliability*, Springer-Verlag New York. Available at: http://link.springer.com/10.1007/978-0-387-77950-8.

Han, M.Y. et al., 2013. Embodied energy consumption of building construction engineering: Case study in E-town, Beijing. *Energy and Buildings*, 64, pp.62–72. Available at: http://dx.doi.org/10.1016/j.enbuild.2013.04.006.

Hao, J. et al., 2020. Carbon emission reduction in prefabrication construction during materialization stage: A BIM-based life-cycle assessment approach. *Science of the Total Environment*, 723. Available at: https://doi.org/10.1016/j.scitotenv.2020.137870.

Harris, D.J., 1999. A quantitative approach to the assessment of the environmental impact of building materials. *Building and Environment*, 34(6), pp.751–758. Available at: https://doi.org/10.1016/S0360-1323(98)00058-4.

Hartig, F., Minunno, F. & Paul, S., 2018. BayesianTools: General-Purpose MCMC and SMC Samplers and Tools for Bayesian Statistics. Available at: https://github.com/florianhartig/BayesianTools.

He, K., Wang, L. & Li, X., 2020. Review of the energy consumption and production structure of China's steel industry: Current situation and future development. *Metals*, 10(3). Available at: https://doi.org/10.3390/met10030302.

Heeren, N. & Fishman, T., 2019. A database seed for a community-driven material intensity research platform. *Scientific Data*, 6(1). Available at: https://doi.org/10.1038/s41597-019-0021-x.

Herbst, A. et al., 2012. Introduction to Energy Systems Modelling. *Swiss Journal of Economics and Statistics*, 148(2), pp.111–135. Available at: https://link.springer.com/content/pdf/10.1007%2FBF03399363.pdf.

Hermann, A. et al., 2013. *Buildings Energy Efficiency in China, Germany, and the United States*, Available at: http://climatepolicyinitiative.org/wp-content/uploads/2013/04/Buildings-Energy-Efficiency-in-China-Germany-and-the-United-States.pdf.

Hoeting, J.A. et al., 1999. Bayesian Model Averaging: A Tutorial. *Statistical Science*, 14(4), pp.382–417. Available at: https://projecteuclid.org/euclid.ss/1009212519.

Hoeting, J.A., 2002. Methodology for Bayesian model averaging: an update. In *Proceedings of invited paper presentations, International Biometric Conference*. Freiburg, Germany, pp. 231–240. Available at: https://www.stat.colostate.edu//~jah/papers/ibcbma.pdf.

Hofert, M. et al., 2018. *Elements of Copula Modeling with R*, Springer. Available at: https://doi.org/10.1007/978-3-319-89635-9.

Hong, J., Shen, G.Q., Li, C.Z., et al., 2018. An integrated framework for embodied energy quantification of buildings in China: A multi-regional perspective. *Resources, Conservation and Recycling*, 138, pp.183–193. Available at: https://doi.org/10.1016/j.resconrec.2018.06.016.

Hong, J., Shen, G.Q. & Tang, M., 2018. Current approaches for embodied carbon assessment of buildings in China: An overview. In F. Pomponi, C. De Wolf, & A. Moncaster, eds. *Embodied Carbon in Buildings: Measurement, Management, and Mitigation*. Springer International Publishing, pp. 417–442.

Hong, L. et al., 2016. Building stock dynamics and its impacts on materials and energy demand in China. *Energy Policy*, 94, pp.47–55. Available at: https://www.sciencedirect.com/science/article/pii/S0301421516301276.

Hong, L. et al., 2014. Modeling China's Building Floor-Area Growth and the Implications for Building Materials and Energy Demand. In *2014 ACEEE Summer Study on Energy Efficiency in Buildings*. pp. 146–157. Available at: https://aceee.org/files/proceedings/2014/data/papers/10-230.pdf.

Hou, J. et al., 2016. Comparative study of commercial building energy-efficiency retrofit policies in four pilot cities in China. *Energy Policy*, 88, pp.204–215. Available at: tps://doi.org/10.1016/j.enpol.2015.10.016.

Hu, M., 2019. Building impact assessment—A combined life cycle assessment and multi-

criteria decision analysis framework. *Resources, Conservation and Recycling*, 150. Available at: https://doi.org/10.1016/j.resconrec.2019.104410.

Hu, M., Bergsdal, H., et al., 2010. Dynamics of urban and rural housing stocks in China. *Building Research and Information*, 38(3), pp.301–317. Available at: https://www.tandfonline.com/doi/abs/10.1080/09613211003729988.

Hu, M., Pauliuk, S., et al., 2010. Iron and steel in Chinese residential buildings: A dynamic analysis. *Resources, Conservation and Recycling*, 54(9), pp.591–600. Available at: https://www.sciencedirect.com/science/article/pii/S0921344909002407.

Hu, M., Voet, E. van der & Huppes, G., 2010. Dynamic Material Flow Analysis for Strategic Construction and Demolition Waste Management in Beijing. *Journal of Industrial Ecology*, 14(3), pp.440–456. Available at: https://onlinelibrary.wiley.com/doi/full/10.1111/j.1530-9290.2010.00245.x.

Huang, T. et al., 2013. Materials demand and environmental impact of buildings construction and demolition in China based on dynamic material flow analysis. *Resources, Conservation and Recycling*, 72, pp.91–101. Available at: https://www.sciencedirect.com/science/article/pii/S0921344912002273.

Huang, W., 2006. Speech at the meeting of "She Hui Zhu Yi Xin Nong Cun Jian She" ["Building new countryside of the socialist society"]. Available at: http://www.mohurd.gov.cn/jsbfld/200612/t20061225_165486.html [Accessed March 16, 2019].

Huo, T. et al., 2018. China's energy consumption in the building sector: A Statistical Yearbook-Energy Balance Sheet based splitting method. *Journal of Cleaner Production*, 185, pp.665–679. Available at: https://doi.org/10.1016/j.jclepro.2018.02.283.

Huo, T., Ren, H. & Cai, W., 2019. Estimating urban residential building-related energy consumption and energy intensity in China based on improved building stock turnover model. *Science of the Total Environment*, 650, pp.427–437. Available at: https://doi.org/10.1016/j.scitotenv.2018.09.008.

IEA, 2019a. Buildings sector energy intensity in selected regions in the Sustainable Development Scenario, 2000-2030. Available at: https://www.iea.org/data-and-statistics/charts/buildings-sector-energy-intensity-in-selected-regions-in-the-sustainable-development-scenario-2000-2030 [Accessed May 21, 2020].

IEA, 2015. *Energy Technology Perspectives 2015 - Mobilising Innovation to Accelerate Climate Action*, Available at: http://www.iea.org/etp/etp2015/.

IEA, 2017. *Energy Technology Perspectives 2017 - Catalysing Energy Technology Transformations*, Available at: http://www.iea.org/etp/etp2017/.

IEA, 2020a. *Energy Technology Perspectives 2020*, Paris. Available at: https://www.iea.org/reports/energy-technology-perspectives-2020.

IEA, 2020b. Estimated global buildings construction in the Sustainable Development Scenario, 2018-2030. Available at: https://www.iea.org/data-and-statistics/charts/estimated-global-buildings-construction-in-the-sustainable-development-scenario-2018-2030 [Accessed May 21, 2020].

IEA, 2020c. Tracking Buildings. Available at: https://www.iea.org/reports/tracking-buildings [Accessed January 19, 2021].

IEA, 2013a. *Transition to Sustainable Buildings: Strategies and Opportunities to 2050*, Available at: http://www.iea.org/publications/freepublications/publication/Building2013_free.pdf.

IEA, 2013b. *Transition to Sustainable Buildings - Strategies and opportunities to 2050*, Available at: https://www.oecd-ilibrary.org/energy/transition-to-sustainable-

buildings_9789264202955-en.

IEA, 2019b. *World Energy Outlook 2019*, Available at: https://www-oecd-ilibrary-org.ezp.lib.cam.ac.uk/energy/world-energy-outlook-2019_caf32f3b-en.

IEA and THUBERC, 2015. *Partner Country Series - Building Energy Use in China: Transforming Construction and Influencing Consumption to 2050*, Available at: https://www.iea.org/reports/partner-country-series-energy-use-in-the-chinese-building-sector.

IEA and UNEP, 2018. *2018 Global Status Report - Towards a zero-emission, efficient and resilient buildings and construction sector*, Available at: https://www.unenvironment.org/resources/report/global-status-report-2018.

International Electrotechnical Commission, 2015. *IEC 60050-192:2015 International electrotechnical vocabulary - Part 192: Dependability*, Available at: http://www.electropedia.org/iev/iev.nsf/display?openform&ievref=192-01-24.

Ionides, E.L., 2008. Truncated importance sampling. *Journal of Computational and Graphical Statistics*, 17(2), pp.295–311. Available at: https://www.tandfonline.com/doi/abs/10.1198/106186008X320456.

IPCC, 2014. *Buildings. In: Climate Change 2014: Mitigation of Climate Change. Contribution of Working Group III to the Fifth Assessment Report of the Intergovernmental Panel on Climate Change*, Available at: https://www.ipcc.ch/pdf/assessment-report/ar5/wg3/ipcc_wg3_ar5_chapter9.pdf.

Jackman, S., 2009. *Bayesian Analysis for the Social Sciences*, Wiley.

Johnstone, I.M., 2001. Energy and mass flows of housing: Estimating mortality. *Building and Environment*, 36(1), pp.43–51. Available at: http://www.sciencedirect.com/science/article/pii/S0360132399000669.

Karlsson, J.F. & Moshfegh, B., 2007. A comprehensive investigation of a low-energy building in Sweden. *Renewable Energy*, 32(11), pp.1830–1841. Available at: https://doi.org/10.1016/j.renene.2006.10.009.

Kavgic, M. et al., 2010. A review of bottom-up building stock models for energy consumption in the residential sector. *Building and Environment*, 45(7), pp.1683–1697. Available at: http://www.sciencedirect.com/science/article/pii/S0360132310000338.

Kejun, J. et al., 2021. Transition of the Chinese Economy in the Face of Deep Greenhouse Gas Emissions Cuts in the Future. *Asian Economic Policy Review*, 16(1), pp.142–162. Available at: https://doi.org/10.1111/aepr.12330.

Kelly, R.A. et al., 2013. Selecting among five common modelling approaches for integrated environmental assessment and management. *Environmental Modelling and Software*, 47, pp.159–181. Available at: https://doi.org/10.1016/j.envsoft.2013.05.005.

Killiches, M., Kraus, D. & Czado, C., 2017. Examination and visualisation of the simplifying assumption for vine copulas in three dimensions. *Australian and New Zealand Journal of Statistics*, 59(1), pp.95–117.

Kleemann, M., 2016. Misconceptions regarding the self-attenuation of residential energy retrofitting policies? – Validation via disaggregation. In *Proceedings of the 34th International Conference of the System Dynamics Society, Delft, Netherlands, 2016*. Available at: https://www.systemdynamics.org/assets/conferences/2016/proceed/papers/P1245.pdf.

Kleinbaum, D.G. & Klein, M., 2012. *Survival Analysis: A Self-Learning Text*, Springer-Verlag New York.

Koezjakov, A. et al., 2018. The relationship between operational energy demand and

embodied energy in Dutch residential buildings. *Energy and Buildings*, 165, pp.233–245. Available at: https://doi.org/10.1016/j.enbuild.2018.01.036.

Kyriakidis, A. et al., 2018. Thermal performance and embodied energy of standard and retrofitted wall systems encountered in Southern Europe. *Energy*, 161, pp.1016–1027. Available at: https://doi.org/10.1016/j.energy.2018.07.124.

Laner, D., Rechberger, H. & Astrup, T., 2014. Systematic Evaluation of Uncertainty in Material Flow Analysis. *Journal of Industrial Ecology*, 18(6), pp.859–870.

LBNL, 2017. China 2050 Demand Resources Energy Analysis Model (DREAM). Available at: https://china.lbl.gov/dream.

Li, B. et al., 2020. Feasibility assessment of the carbon emissions peak in China's construction industry: Factor decomposition and peak forecast. *Science of the Total Environment*, 706. Available at: https://doi.org/10.1016/j.scitotenv.2019.135716.

Li, D.Z. et al., 2013. A methodology for estimating the life-cycle carbon efficiency of a residential building. *Building and Environment*, 59, pp.448–455. Available at: http://dx.doi.org/10.1016/j.buildenv.2012.09.012.

Li, G. & Shi, J., 2010. Application of Bayesian model averaging in modeling long-term wind speed distributions. *Renewable Energy*, 35(6), pp.1192–1202. Available at: https://www.sciencedirect.com/science/article/pii/S096014810900398X.

Li, X. et al., 2014. An assessment framework for analyzing the embodied carbon impacts of residential buildings in China. *Energy and Buildings*, 85, pp.400–409. Available at: http://dx.doi.org/10.1016/j.enbuild.2014.09.051.

Li, X. & Xu, D., 2013. Clarification of misled statistic data: overestimated per-capita housing area. *China Economic Journal*, 6(2–3), pp.134–151. Available at: https://www.tandfonline.com/doi/abs/10.1080/17538963.2013.860681.

Li, Z. & Jiang, Y., 2006. Characteristics of cooling load and energy consumption of air conditioning in residential buildings in Beijing [in Chinese]. *HV&AC*, 36(8).

Liang, W., 2014. Is the per capita urban residential floor area in China 33 m2 or 18 m2? Available at: http://www.cssn.cn/preview/zt/19364/19369/201403/t20140313_1027648.shtml [Accessed May 22, 2019].

Lin, L. et al., 2015. Analysis on China building construction energy and CO2 emissions [in Chinese]. *China Energy*, 37(3). Available at: http://www.cnki.com.cn/Article/CJFDTotal-ZGLN201503005.htm.

Liu, H., Yang, F. & Xu, Y., 2013. Analysis on urban housing in China based on 2010 population census [in Chinese]. *Journal of Tsinghua University (Philosophy and Social Sciences)*, 6(28), pp.138–147. Available at: http://www.cre.tsinghua.edu.cn/publish/cre/9553/20150709/51111436450299533.pdf.

Liu, T. & Hu, D., 2006. Environmental Impact of Residential Building Construction in Beijing (1949-2003)-Assessing the Construction Materials' Environmental Impact by LCA. *Journal of the Graduate School of the Chinese Academy of Sciences*, 23(2), p.231–241.(In Chinese). Available at: http://journal.ucas.ac.cn/CN/article/downloadArticleFile.do?attachType=PDF&id=9682.

Liu, X., 2012. *Survival Analysis: Models and Applications*, Wiley.

Lopes, M.A.R., Antunes, C.H. & Martins, N., 2012. Energy behaviours as promoters of energy efficiency: A 21st century review. *Renewable and Sustainable Energy Reviews*, 16(6), pp.4095–4104. Available at: http://www.sciencedirect.com/science/article/pii/S1364032112002171.

Lucon, O. et al., 2014. Buildings. In O. Edenhofer et al., eds. *Mitigation of Climate Change. Contribution of Working Group III to the Fifth Assessment Report of the Intergovernmental Panel on Climate Change*. Cambridge, United Kingdom: Cambridge University Press. Available at: https://www.ipcc.ch/site/assets/uploads/2018/02/ipcc_wg3_ar5_chapter9.pdf.

Lyneis, J., 2000. System dynamics for market forecasting and structural analysis. *System Dynamics Review*, 16(1). Available at: http://onlinelibrary.wiley.com/doi/10.1002/(SICI)1099-1727(200021)16:1%3C3::AID-SDR183%3E3.0.CO;2-5/epdf.

Lyneis, J., 1998. System Dynamics In Business Forecasting: A Case Study of the Commercial Jet Aircraft Industry. In *The 16th International Conference of The System Dynamics Society*. Available at: http://www.systemdynamics.org/conferences/1998/PROCEED/00089.PDF.

Lyneis, J.M. & Ford, D.N., 2007. System dynamics applied to project management: a survey, assessment, and directions for future research. *System Dynamics Review*, 23(2–3). Available at: http://onlinelibrary.wiley.com/doi/10.1002/sdr.377/epdf.

Mahdavi, A. & Doppelbauer, E.-M., 2010. A performance comparison of passive and low-energy buildings. *Energy and Buildings*, 42(8), pp.1314–1319. Available at: https://doi.org/10.1016/j.enbuild.2010.02.025.

Mallapaty, S., 2020. How China could be carbon neutral by mid-century. Available at: https://media.nature.com/original/magazine-assets/d41586-020-02927-9/d41586-020-02927-9.pdf.

Malmqvist, T. et al., 2018. Design and construction strategies for reducing embodied impacts from buildings – Case study analysis. *Energy and Buildings*, 166, pp.35–47. Available at: https://doi.org/10.1016/j.enbuild.2018.01.033.

May, B. et al., 2012. Cradle-to-gate inventory of wood production from Australian softwood plantations and native hardwood forests: Embodied energy, water use and other inputs. *Forest Ecology and Management*, 264, pp.37–50. Available at: https://doi.org/10.1016/j.foreco.2011.09.016.

McLaren, C. & Stapenhurst, C., 2015. *ONS Methodology Working Paper Series No 3: A note on distributions used when calculating estimates of consumption of fixed capital*, Available at: http://webarchive.nationalarchives.gov.uk/20160111030849/http://www.ons.gov.uk/ons/guide-method/method-quality/specific/gss-methodology-series/ons-working-paper-series/index.html.

McNeil, A.J., Embrechts, P. & Frey, R., 2015. *Quantitative Risk Management: Concepts, Techniques and Tools*, Princeton University Press.

McNeil, M.A. et al., 2016. Energy efficiency outlook in China's urban buildings sector through 2030. *Energy Policy*, 97, pp.532–539. Available at: http://www.sciencedirect.com/science/article/pii/S0301421516303949.

Meadows, D. & Robinson, J., 1985. *The Electronic Oracle: Computer Models and Social Decisions*, Chichester: Wiley.

Meng, X.-L. & Wong, H.W., 1996. Simulating ratios of normalizing constants via a simple identity: A theoretical exploration. *Statistica Sinica*, 6(4), pp.831–860. Available at: https://pdfs.semanticscholar.org/6a40/18c9c2927d702d85257c34130b1204fa7584.pdf.

Miatto, A., Schandl, H. & Tanikawa, H., 2017. How important are realistic building lifespan assumptions for material stock and demolition waste accounts? *Resources, Conservation and Recycling*, 122, pp.143–154. Available at: https://www.sciencedirect.com/science/article/pii/S0921344917300265.

MIIT, 2016. Implementation Guidelines on Green Manufacturing (2016-2020). Available at: http://www.miit.gov.cn/n1146285/n1146352/n3054355/n3057542/n5920352/c5253469/content.html.

MIIT and MOHURD, 2015. Action plan for promoting green building materials production and application. Available at: http://www.scio.gov.cn/32344/32345/33969/35217/xgzc35223/Document/1492872/1492872.htm.

Minunno, R. et al., 2021. Investigating the embodied energy and carbon of buildings: A systematic literature review and meta-analysis of life cycle assessments. *Renewable and Sustainable Energy Reviews*, 143. Available at: https://doi.org/10.1016/j.rser.2021.110935.

MIT, 1997. *Building a System Dynamics Model Part 1: Conceptualization*, Available at: https://ocw.mit.edu/courses/sloan-school-of-management/15-988-system-dynamics-self-study-fall-1998-spring-1999/readings/building.pdf.

Mithraratne, N. & Vale, B., 2004. Life cycle analysis model for New Zealand houses. *Building and Environment*, 39(4), pp.483–492. Available at: https://doi.org/10.1016/j.buildenv.2003.09.008.

MOHURD, 2019a. *Assessment Standard for Green Building (GB/T 50378-2019)*, Beijing: China Architecture and Building Press.

MOHURD, 2010. *Code for Green Design of Civil Buildings (JGJ/T 229-2010)*, Beijing: China Architecture and Building Press.

MOHURD, 2012. *Special Plan for Building Energy Efficiency during the 12th Five-Year Plan (2011-2015)*, Available at: http://www.gov.cn/zwgk/2012-05/31/content_2149889.htm.

MOHURD, 2019b. *Standard for Building Carbon Emission calculation (GB/T 51366-2019)*, Available at: http://www.mohurd.gov.cn/wjfb/201905/t20190530_240723.html.

MOHURD, 2016. *Standard for energy consumption of building*, Beijing: China Architecture and Building Press.

MOHURD, 2017. *The 13th Five-Year Plan for Building Energy Conservation and Green Building Development*, Available at: http://www.mohurd.gov.cn/wjfb/201703/W020170314100832.pdf.

Moncaster, A.M. et al., 2018. Why method matters: Temporal, spatial and physical variations in LCA and their impact on choice of structural system. *Energy and Buildings*, 173, pp.389–398. Available at: https://doi.org/10.1016/j.enbuild.2018.05.039.

Moncaster, A.M. et al., 2019. Widening understanding of low embodied impact buildings: Results and recommendations from 80 multi-national quantitative and qualitative case studies. *Journal of Cleaner Production*, 235, pp.378–393. Available at: https://doi.org/10.1016/j.jclepro.2019.06.233.

Moncaster, A.M. & Song, J.Y., 2012. A comparative review of existing data and methodologies for calculating embodied energy and carbon of buildings. *International Journal of Sustainable Building Technology and Urban Development*, 3(1), pp.26–36. Available at: https://doi.org/10.1080/2093761X.2012.673915.

Morini, A.A., Ribeiro, M.J. & Hotza, D., 2019. Early-stage materials selection based on embodied energy and carbon footprint. *Materials and Design*, 178. Available at: https://doi.org/10.1016/j.matdes.2019.107861.

Müller, D.B., 2006. Stock dynamics for forecasting material flows — Case study for housing in The Netherlands. *Ecological Economics*, 59(1). Available at: http://www.sciencedirect.com/science/article/pii/S092180090500460X.

Müller, M.O. & Ulli-Beer, S., 2012. How can the Diffusion of Energy-Efficient Renovations be Accelerated? Policy Implications from a System Dynamics Modeling Study. In *Proceedings of the 30th International Conference of the System Dynamics Society, St. Gallen, Switzerland, 2012*. Available at: https://www.systemdynamics.org/assets/conferences/2012/proceed/papers/P1357.pdf.

Müller, M.O. & Ulli-Beer, S., 2010. Policy Analysis for the Transformation of Switzerland's Stock of Buildings. A Small Model Approach. In *Proceedings of the 28th International Conference of the System Dynamics Society, Seoul, Korea, 2010*. Available at: https://www.systemdynamics.org/assets/conferences/2010/proceed/papers/P1172.pdf.

Nachtrieb, R. et al., 2017. *CERC-BEE Impact Model*, Available at: http://eta-publications.lbl.gov/sites/default/files/2016-cercbee-impact-model.pdf.

Nagler, T. et al., 2019. *VineCopula: Statistical inference of vine copulas*, Available at: https://cran.r-project.org/web/packages/VineCopula/VineCopula.pdf.

National Bureau of Statistics, 2017. *China Energy Statistical Yearbook 2017*, Beijing: China Statistics Press.

National Bureau of Statistics, 2007. *China Statistical Yearbook 2007*, China Statistics Press.

National Bureau of Statistics, 2018. *China Statistical Yearbook 2018*, China Statistics Press.

National Bureau of Statistics, 2019. *China Statistical Yearbook 2019*, China Statistics Press.

National Center for Climate Change Strategy and International Cooperation, 2018. *Pathway and policy analysis to China's deep decarbonization [in Chinese]*, Available at: http://www.ncsc.org.cn/yjcg/zlyj/201804/P020180920508767376089.docx.

National Development and Reform Commission, 2017. *Clean Winter Heating Plan for North China (2017-2021)*, Available at: http://www.gov.cn/xinwen/2017-12/20/content_5248855.htm.

Navigant, 2019. *Comprehensive study of building energy renovation activities and the uptake of nearly zero-energy buildings in the EU Final report*, Available at: https://op.europa.eu/en/publication-detail/-/publication/97d6a4ca-5847-11ea-8b81-01aa75ed71a1.

NDRC, 2015. *Enhanced Actions on Climate Change: China's Intended Nationally Determined Contributions*, Available at: http://www4.unfccc.int/ndcregistry/PublishedDocuments/China First/China%27s First NDC Submission.pdf.

NDRC, 2004. *Medium and Long-Term Plan for Energy Conservation [in Chinese]*,

NDRC and MIIT, 2016. Notice on implementing tiered electricity tariff policy for the cement industry [in Chinese]. Available at: http://www.gov.cn/xinwen/2016-01/21/content_5035069.htm.

NDRC and MIIT, 2013. Notice on implementing tiered electricity tariff policy for the electrolytic aluminium industry [in Chinese]. Available at: http://www.gov.cn/zwgk/2013-12/26/content_2554621.htm.

NRDC, 2019. *China cement industry Thirteenth Five-Year coal cap mid-term evaluation and later-term outlook [in Chinese]*, Available at: http://coalcap.nrdc.cn/Public/uploads/pdf/155909711066054821.pdf.

OECD, 2001. *Measuring capital: OECD manual: measurement of capital stocks, consumption of fixed capital and capital services*, Available at: https://www.oecd.org/std/na/1876369.pdf.

OECD, 2009. *Measuring Capital: OECD manual 2009*, Available at: https://www.oecd.org/std/productivity-stats/43734711.pdf.

Onat, N.C., Egilmez, G. & Tatari, O., 2014. Towards greening the U.S. residential building stock: A system dynamics approach. *Building and Environment*, 78, pp.68–80. Available at: http://www.sciencedirect.com/science/article/pii/S0360132314000900.

Osgood, N. & Liu, J., 2013. Bayesian Parameter Estimation of System Dynamics Models Using Markov Chain Monte Carlo Methods : An Informal Introduction. In *The 31st International Conference of the System Dynamics Society*. pp. 1–19. Available at: https://www.systemdynamics.org/assets/conferences/2013/proceed/papers/P1391.pdf.

Osgood, N.D. & Liu, J., 2015. Combining Markov Chain Monte Carlo Approaches and Dynamic Modeling. In H. Rahmandad, R. Oliva, & N. Osgood, eds. *Analytical Methods for Dynamic Modelers*. Cambridge, Massachusetts: MIT Press.

Pacheco-Torgal, F., Faria, J. & Jalali, S., 2012. Embodied energy versus operational energy. Showing the shortcomings of the energy performance building directive (EPBD). *Materials Science Forum*, 730, pp.587–591. Available at: https://www.scientific.net/MSF.730-732.587.

Pajor, A., 2017. Estimating the marginal likelihood using the arithmetic mean identity. *Bayesian Analysis*, 12(1), pp.261–287. Available at: https://projecteuclid.org/download/pdfview_1/euclid.ba/1459772735.

Palisade, 2016. *Risk Analysis and Simulation Add-In for Microsoft® Excel*, Available at: https://www.palisade.com/downloads/documentation/75/EN/RISK7_EN.pdf.

Peng, C. et al., 2015. Building energy use in China: Ceiling and scenario. *Energy and Buildings*, 102, pp.307–316. Available at: http://dx.doi.org/10.1016/j.enbuild.2015.05.049.

Peng, C., 2014. *Research on roadmap for China building energy conservation based on total amount control*. Tsinghua University.

Peng, C., Yan, D. & Jiang, Y., 2013. China Road Map for Building Energy Conservation. In D. Stolten & V. Scherer, eds. *Transition to Renewable Energy Systems*. Wiley-VCH Verlag GmbH & Co. KGaA, pp. 891–911.

Pomponi, F. & Moncaster, A., 2016. Embodied carbon mitigation and reduction in the built environment – What does the evidence say? *Journal of Environmental Management*, 181, pp.687–700. Available at: http://dx.doi.org/10.1016/j.jenvman.2016.08.036.

Pomponi, F. & Moncaster, A., 2018. Scrutinising embodied carbon in buildings: The next performance gap made manifest. *Renewable and Sustainable Energy Reviews*, 81, pp.2431–2442. Available at: https://www.sciencedirect.com/science/article/pii/S136403211730998X.

Praseeda, K.I., Reddy, B.V.V. & Mani, M., 2015. Embodied energy assessment of building materials in India using process and input-output analysis. *Energy and Buildings*, 86, pp.677–686. Available at: https://doi.org/10.1016/j.enbuild.2014.10.042.

Qudrat-Ullah, H., 2013. *Energy Policy Modeling in the 21st Century*, Springer-Verlag New York.

Qudrat-Ullah, H., 2016. *The Physics of Stocks and Flows of Energy Systems: Applications in Energy Policy*, Springer International Publishing.

R Core Team, 2019. R: A language and environment for statistical computing. Available at: https://www.r-project.org.

Ramesh, T., Prakash, R. & Shukla, K.K., 2012. Life cycle energy analysis of a residential building with different envelopes and climates in Indian context. *Applied Energy*, 89(1), pp.193–202. Available at: https://doi.org/10.1016/j.apenergy.2011.05.054.

Rasmussen, F.N. et al., 2018. Analysing methodological choices in calculations of embodied energy and GHG emissions from buildings. *Energy and Buildings*, 158, pp.1487–1498. Available at: https://doi.org/10.1016/j.enbuild.2017.11.013.

Rawlinson, S. & Weight, D., 2007. Sustainability: Embodied Carbon. *Building*, (41).

ReliaSoft, 2018. Introduction to Life Data Analysis. In *Life Data Analysis Reference Book*. Available at: http://reliawiki.com/index.php/Introduction_to_Life_Data_Analysis.

Ren, Z., Xiong, C. & Bai, X., 2019. Urban housing in China: surplus or shortage? [in Chinese]. Available at: http://m.zqrb.cn/house/hangyedongtai/2019-02-18/A1550447505753.html [Accessed May 22, 2019].

Richardson, G.P., 2001. System dynamics. In *Encyclopedia of Operations Research and Management Science*. Springer Science & Business Media B.V., pp. 807–810.

Richardson, G.P., 2011. The Basic Elements of System Dynamics. In R. A. Meyers, ed. *Complex Systems in Finance and Econometrics*. New York : Springer, pp. 856–862.

Rinne, H., 2008. *The Weibull Distribution: A Handbook*, Chapman and Hall/CRC.

RISN, 2016. *Top-level design for building energy efficiency under new urbanisation in China*, Available at: https://www.efchina.org/Reports-zh/report-cbp-20150112-2-zh.

Rogelj, J. et al., 2018. *Mitigation Pathways Compatible with 1.5°C in the Context of Sustainable Development. In: Global Warming of 1.5°C. An IPCC Special Report on the impacts of global warming of 1.5°C above pre-industrial levels and related global greenhouse gas emission pathw*, Available at: https://www.ipcc.ch/site/assets/uploads/sites/2/2019/02/SR15_Chapter2_Low_Res.pdf.

Roh, S. et al., 2019. Probabilistic analysis of major construction materials in the life cycle embodied environmental cost of Korean apartment buildings. *Sustainability (Switzerland)*, 11(3). Available at: https://doi.org/10.3390/su11030846.

Rossi, B., Marique, A.-F. & Reiter, S., 2012. Life-cycle assessment of residential buildings in three different European locations, case study. *Building and Environment*, 51, pp.402–407. Available at: https://doi.org/10.1016/j.buildenv.2011.11.002.

Saeed, K., 2003. Articulating developmental problems for policy intervention: A system dynamics modeling approach. *Simulation and Gaming*, 34(3). Available at: http://journals.sagepub.com/doi/pdf/10.1177/1046878103255792.

Schmidt, S., Jäger, T. & Karl, U., 2012. The Transition of the Residential Heat Market in Germany - A System Dynamics Approach. In *Proceedings of the 30th International Conference of the System Dynamics Society, St. Gallen, Switzerland, 2012*. Available at: https://www.systemdynamics.org/conferences/2012/proceed/papers/P1120.pdf.

Schmidt, T., 2007. Coping with Copulas. In J. Rank, ed. *Copulas: From Theory to Application in Finance*. Risk Books.

Schöniger, A. et al., 2014. Model selection on solid ground: Rigorous comparison of nine ways to evaluate Bayesian model evidence. *Water Resources Research*, 50(12), pp.9484–9513. Available at: https://agupubs.onlinelibrary.wiley.com/doi/epdf/10.1002/2014WR016062.

Scrieciu, S., Rezai, A. & Mechler, R., 2013. On the economic foundations of green growth discourses: The case of climate change mitigation and macroeconomic dynamics in economic modeling. *Wiley Interdisciplinary Reviews: Energy and Environment*, 2(3), pp.251–268. Available at: https://onlinelibrary.wiley.com/doi/abs/10.1002/wene.57.

Seo, S., Foliente, G. & Ren, Z., 2018. Energy and GHG reductions considering embodied impacts of retrofitting existing dwelling stock in Greater Melbourne. *Journal of Cleaner Production*, 170, pp.1288–1304. Available at: https://doi.org/10.1016/j.jclepro.2017.09.206.

Shen, X., 2013. Has the per capita urban residential floor area in China exceeded 32 m2? The biggest lie of Chinese livelihood. *Tencent Housing*. Available at:

https://house.qq.com/bside/31.htm [Accessed May 22, 2019].

Shepherd, S. & Emberger, G., 2010. Introduction to the special issue: system dynamics and transportation. *System Dynamics Review*, 26(3). Available at: http://onlinelibrary.wiley.com/doi/10.1002/sdr.454/epdf.

Shi, F. et al., 2012. Toward a low carbon-dematerialization society: Measuring the materials demand and co 2 emissions of building and transport infrastructure construction in China. *Journal of Industrial Ecology*, 16(4), pp.493–505. Available at: https://onlinelibrary.wiley.com/doi/full/10.1111/j.1530-9290.2012.00523.x.

Shi, J., Chen, W. & Yin, X., 2016. Modelling building's decarbonization with application of China TIMES model. *Applied Energy*, 162, pp.1303–1312. Available at: https://www.sciencedirect.com/science/article/pii/S0306261915008144.

Shukla, A.K., Yadav, S.K. & Tiwari, V., 2015. Linear Models for S-Shaped Growth Curves. *Journal of Statistics Applications and Probability*, 117(1), pp.113–117. Available at: http://www.naturalspublishing.com/files/published/96sp961dj2687j.pdf.

Soetaert, K., Petzoldr, T. & Setzer, R., 2010. Solving differential equations in R: Package deSolve. *Journal of Statistical Software*, 33(9), pp.1–25. Available at: https://www.jstatsoft.org/article/view/v033i09.

Soetaert, K. & Petzoldt, T., 2010a. Inverse Modelling, Sensitivity and Monte Carlo Analysis in R Using Package FME. *Journal of Statistical Software*, 33(3). Available at: https://www.jstatsoft.org/article/view/v033i03.

Soetaert, K. & Petzoldt, T., 2010b. Inverse Modelling, Sensitivity and Monte Carlo Analysis in R Using Package FME. *Journal of Statistical Software*, 33(3), pp.1–28. Available at: https://www.jstatsoft.org/article/view/v033i03.

Stephan, A., Crawford, R.H. & De Myttenaere, K., 2012. Towards a comprehensive life cycle energy analysis framework for residential buildings. *Energy and Buildings*, 55, pp.592–600. Available at: http://dx.doi.org/10.1016/j.enbuild.2012.09.008.

Sterman, J.D., 2000. *Business Dynamics: Systems Thinking and Modeling for a Complex World*, Boston, MA: Irwin McGraw-Hill.

Struben, J., Sterman, J. & Keith, D., 2015. Parameter Estimation Through Maximum Likelihood and Bootstrapping Methods. In H. Rahmandad, R. Oliva, & N. Osgood, eds. *Analytical Methods for Dynamic Modelers*. Cambridge, Massachusetts: MIT Press.

Su, X. et al., 2020. Embodied and operational energy and carbon emissions of passive building in HSCW zone in China: A case study. *Energy and Buildings*, 222. Available at: https://doi.org/10.1016/j.enbuild.2020.110090.

Su, X. & Zhang, X., 2016. A detailed analysis of the embodied energy and carbon emissions of steel-construction residential buildings in China. *Energy and Buildings*, 119, pp.323–330. Available at: http://dx.doi.org/10.1016/j.enbuild.2016.03.070.

Swan, L.G. & Ugursal, V.I., 2009. Modeling of end-use energy consumption in the residential sector: A review of modeling techniques. *Renewable and Sustainable Energy Reviews*, 13(8), pp.1819–1835. Available at: http://www.sciencedirect.com/science/article/pii/S1364032108001949.

Sweetser, A., 1999. A Comparison of System Dynamics (SD) and Discrete Event Simulation (DES). In *Proceedings of 17th International Conference of the System Dynamics Society*. Available at: https://www.systemdynamics.org/conferences/1999/PAPERS/PARA78.PDF.

Swinerd, C. & McNaught, K.R., 2012. Design classes for hybrid simulations involving agent-based and system dynamics models. *Simulation Modelling Practice and Theory*, 25, pp.118–133. Available at: http://www.sciencedirect.com/science/article/pii/S1569190X1100147X.

Tan, X. et al., 2018. Carbon emission and abatement potential outlook in China's building sector through 2050. *Energy Policy*, 118, pp.429–439. Available at: https://doi.org/10.1016/j.enpol.2018.03.072.

Tedeschi, L.O., Nicholson, C.F. & Rich, E., 2011. Using System Dynamics modelling approach to develop management tools for animal production with emphasis on small ruminants. *Small Ruminant Research*, 98(1–3). Available at: http://www.sciencedirect.com/science/article/pii/S0921448811001015.

Thomas, S., 2015. *Energy Efficiency Policies for Buildings*, Available at: http://www.bigee.net/media/filer_public/2015/02/06/bigee_broschuere_energy_efficiency_policy_in_buildings.pdf.

Thormark, C., 2002. A low energy building in a life cycle—its embodied energy, energy need for operation and recycling potential. *Building and Environment*, 37(4), pp.429–435. Available at: http://www.sciencedirect.com/science/article/pii/S0360132301000336.

THUBERC, 2012. *2012 Annual Report on China Building Energy Efficiency*, China Architecture & Building Press.

THUBERC, 2013. *2013 Annual Report on China Building Energy Efficiency*, China Architecture & Building Press.

THUBERC, 2014. *2014 Annual Report on China Building Energy Efficiency*, China Architecture & Building Press.

THUBERC, 2015. *2015 Annual Report on China Building Energy Efficiency*, China Architecture & Building Press.

THUBERC, 2016. *2016 Annual Report on China Building Energy Efficiency*, Beijing: China Architecture & Building Press.

THUBERC, 2017. *2017 Annual Report on China Building Energy Efficiency*, Beijing: China Architecture & Building Press.

THUBERC, 2018. *2018 Annual Report on China Building Energy Efficiency*, Beijing: China Architecture & Building Press.

THUBERC, 2019a. *2019 Annual Report on China Building Energy Efficiency*, Beijing: China Architecture & Building Press.

THUBERC, 2020. *2020 Annual Report on China Building Energy Efficiency*, Beijing: China Architecture & Building Press.

THUBERC, 2019b. *China Building Energy Use 2018*, Available at: https://berc.bestchina.org/Files/CBEU2018.pdf.

Tjørve, K.M.C. & Tjørve, E., 2017. The use of Gompertz models in growth analyses, and new Gompertz-model approach: An addition to the Unified-Richards family. *PLoS ONE*, 12(6). Available at: https://journals.plos.org/plosone/article?id=10.1371/journal.pone.0178691.

Trappey, C. V. & Wu, H.Y., 2008. An evaluation of the time-varying extended logistic, simple logistic, and Gompertz models for forecasting short product lifecycles. *Advanced Engineering Informatics*, 22(4), pp.421–430. Available at: https://www.sciencedirect.com/science/article/pii/S1474034608000372.

UNDP, 2016. *Sustainable Urbanisation Strategy: UNDP's Support to Sustainable, Inclusive and Resilient Cities in the Developing World*, Available at: http://www.undp.org/content/dam/undp/library/Sustainable Development/Urbanization/UNDP_Urban-Strategy.pdf.

UNFCCC, 2020. NDC Registry (Interim). Available at: https://www4.unfccc.int/sites/NDCStaging/Pages/All.aspx [Accessed May 25, 2020].

United Nations Population Division, 2017. *World Population Prospects: The 2017 Revision*, Available at: https://population.un.org/wpp/Publications/Files/WPP2017_Volume-I_Comprehensive-Tables.pdf.

United Nations Population Division, 2014. *World Urbanization Prospects: The 2014 Revision*, Available at: https://esa.un.org/unpd/wup/CD-ROM/.

Upton, B. et al., 2008. The greenhouse gas and energy impacts of using wood instead of alternatives in residential construction in the United States. *Biomass and Bioenergy*, 32(1), pp.1–10. Available at: https://doi.org/10.1016/j.biombioe.2007.07.001.

Urge-Vorsatz, D. et al., 2012. *Best Practice Policies for Low Energy and Carbon Buildings: A Scenario Analysis*, Available at: http://www.gbpn.org/sites/default/files/08.CEU Technical Report copy_0.pdf.

Urge-Vorsatz, D. et al., 2013. Energy use in buildings in a long-term perspective. *Current Opinion in Environmental Sustainability*, 5(2), pp.141–151. Available at: http://www.sciencedirect.com/science/article/pii/S1877343513000468?via%3Dihub.

Utama, A. & Gheewala, S.H., 2009. Indonesian residential high rise buildings: A life cycle energy assessment. *Energy and Buildings*, 41(11), pp.1263–1268. Available at: https://doi.org/10.1016/j.enbuild.2009.07.025.

Venkatarama Reddy, B.. & Jagadish, K.., 2003. Embodied energy of common and alternative building materials and technologies. *Energy and Buildings*, 35(2), pp.129–137. Available at: https://doi.org/10.1016/S0378-7788(01)00141-4.

Vennix, J.A.M., 1999. Group model-building: tackling messy problems. *System Dynamics Review*, 15(4). Available at: http://onlinelibrary.wiley.com/doi/10.1002/(SICI)1099-1727(199924)15:4%3C379::AID-SDR179%3E3.0.CO;2-E/epdf.

Vennix, J.A.M., 1996. *Group Model Building: Facilitating Team Leaning Using System Dynamics*, Chichester: John Wiley.

Ventana Systems Inc., 2019. Vensim Software. Available at: https://vensim.com/vensim-software/.

Verbeeck, G. & Hens, H., 2010a. Life cycle inventory of buildings: A calculation method. *Building and Environment*, 45(4), pp.1037–1041. Available at: https://doi.org/10.1016/j.buildenv.2009.10.012.

Verbeeck, G. & Hens, H., 2010b. Life cycle inventory of buildings: A contribution analysis. *Building and Environment*, 45(4), pp.964–967. Available at: https://doi.org/10.1016/j.buildenv.2009.10.003.

Voïta, T., 2018. *The Power of China's Energy Efficiency Policies*, Available at: https://www.ifri.org/sites/default/files/atoms/files/voita_power_china_2018.pdf.

van Vuuren, D.P. et al., 2009. Comparison of top-down and bottom-up estimates of sectoral and regional greenhouse gas emission reduction potentials. *Energy Policy*, 37(12), pp.5125–5139. Available at: https://www.sciencedirect.com/science/article/pii/S0301421509005394.

Wang, C., Yang, Y. & Zhang, J., 2015. China's sectoral strategies in energy conservation and carbon mitigation. *Climate Policy*, 15, pp.60–80. Available at: https://doi.org/10.1080/14693062.2015.1050346.

Wang, Q., 2001. 2001 Energy Data [in Chinese]. *Energy Policy Research [in Chinese]*, (1), pp.1–104. Available at: http://www.cqvip.com/qikan/Detail.aspx?gch=95070A&years=2001&num=01.

Wang, Q., 2013. *2013 Energy Data [in Chinese]*, Beijing. Available at: https://www.efchina.org/Attachments/Report/reports-20131212-zh/reports-20131212-zh.

Wang, Q., 2016. *2016 Energy Data [in Chinese]*, Beijing. Available at: https://www.efchina.org/Reports-zh/report-lceg-20200413-4-zh.

Wang, Q., 2018. *2018 Energy Data [in Chinese]*, Beijing. Available at: https://www.efchina.org/Reports-zh/report-lceg-20200413-2-zh.

Wang, Q., 2019. *2019 Energy Data [in Chinese]*, Beijing. Available at: https://www.efchina.org/Reports-zh/report-lceg-20200413-zh.

Wang, Q., 2014. *Suggestions to the reform of China energy statistics [in Chinese]*, Available at: http://nrdc.cn/Public/uploads/2017-01-11/5875c66525271.pdf.

Wang, Y.B. et al., 2018. A new Monte Carlo method for estimating marginal likelihoods. *Bayesian Analysis*, 13(2), pp.311–333. Available at: https://projecteuclid.org/download/pdfview_1/euclid.ba/1488250818.

Wilson, E. et al., 2016. A High-Granularity Approach To Modeling Energy Consumption and Savings Potential in the U . S . Residential Building Stock. In *ASHRAE and IBPSA-USA SimBuild 2016 Building Performance Modeling Conference*. Available at: https://www.ashrae.org/File Library/docLib/Events/Simbuild2016/Papers/C053.pdf.

World Bank, 2015. *East Asia's Changing Urban Landscape: Measuring a Decade of Spatial Growth. Urban Development Series*, Washington, DC. Available at: https://openknowledge.worldbank.org/handle/10986/21159.

World Bank, 2014. *Urban China: Toward Efficient, Inclusive and Sustainable Urbanization*, Washington, DC. Available at: https://openknowledge.worldbank.org/handle/10986/18865.

World Green Building Council, 2019. *Bringing embodied carbon upfront: coordinated action for the building and construction sector to tackle embodied carbon.*, Available at: https://www.worldgbc.org/sites/default/files/WorldGBC_Bringing_Embodied_Carbon_Up front.pdf.

Xie, W. et al., 2011. Improving marginal likelihood estimation for bayesian phylogenetic model selection. *Systematic Biology*, 60(2), pp.150–160. Available at: https://www.ncbi.nlm.nih.gov/pmc/articles/PMC3038348/pdf/syq085.pdf.

Xie, Z., Sun, L. & Yang, F., 2012. The influence of window heat transfer coefficient on heating and air conditioning energy consumption of a typical residential building [in Chinese]. *Building Energy & Environment*, 31(6).

Xing, R. et al., 2015. An impact assessment of sustainable technologies for the Chinese urban residential sector at provincial level. *Environmental Research Letters*, 10(6). Available at: https://doi.org/10.1088/1748-9326/10/6/065001.

Xu, D. & Liu, Y., 2018. *Understanding China's Overcapacity*, Singapore: Springer Singapore.

Yan, Y. et al., 2017. Investigation on CO2 emissions from flat glass production in China [in Chinese]. *Acta Scientiae Circumstantiae*, 37(8). Available at: http://www.actasc.cn/hjkxxb/ch/reader/view_abstract.aspx?file_no=20160924004&flag=1.

Yan, Y., 2011. *Life Cycle Assessment on Energy Consumption and CO2 Emission of Buildings in Zhejiang Province*. Zhejiang University.

Yang, T. et al., 2017. CO2 emissions in China's building sector through 2050: A scenario analysis based on a bottom-up model. *Energy*, 128, pp.208–223. Available at: https://www.sciencedirect.com/science/article/pii/S0360544217304814.

Yang, W. & Kohler, N., 2008. Simulation of the evolution of the Chinese building and infrastructure stock. *Building Research & Information*, 36(1), pp.1–19. Available at: http://www.tandfonline.com/doi/abs/10.1080/09613210701702883.

Yang, X. et al., 2018. Building-information-modeling enabled life cycle assessment, a case study on carbon footprint accounting for a residential building in China. *Journal of Cleaner Production*, 183, pp.729–743. Available at: https://doi.org/10.1016/j.jclepro.2018.02.070.

Yu, H. & Li, G., 1999. *Construction project investment estimation handbook*, Beijing: China Architecture & Building Press.

Yu, S., Eom, J., Evans, M., et al., 2014. A long-term, integrated impact assessment of alternative building energy code scenarios in China. *Energy Policy*, 67, pp.626–639. Available at: http://www.sciencedirect.com/science/article/pii/S0301421513011166.

Yu, S. et al., 2020. *Five strategies to achieve China's 2060 carbon neutrality goal*, Available at: https://cgs.umd.edu/sites/default/files/2020-09/5 Strategies_China 2060_english.pdf.

Yu, S., Eom, J., Zhou, Y., et al., 2014. Scenarios of building energy demand for China with a detailed regional representation. *Energy*, 67, pp.284–297. Available at: http://www.sciencedirect.com/science/article/pii/S036054421400005X.

Yu, S., Evans, M. & Shi, Q., 2015. *Analysis of the chinese market for building energy efficiency*, Available at: https://www.pnnl.gov/main/publications/external/technical_reports/PNNL-22761.pdf.

Yücel, G., 2013. Extent of inertia caused by the existing building stock against an energy transition in the Netherlands. *Energy and Buildings*, 56, pp.134–145. Available at: https://doi.org/10.1016/j.enbuild.2012.09.022.

Zaiontz, C., 2018. Weibull Distribution. Available at: http://www.real-statistics.com/other-key-distributions/weibull-distribution/ [Accessed March 31, 2018].

Zeitz, A., Griffin, C.T. & Dusicka, P., 2019. Comparing the embodied carbon and energy of a mass timber structure system to typical steel and concrete alternatives for parking garages. *Energy and Buildings*, 199, pp.126–133. Available at: https://doi.org/10.1016/j.enbuild.2019.06.047.

Zhang, L. & Singh, V.P., 2019. *Copulas and their Applications in Water Resources Engineering*, Cambridge University Press. Available at: https://doi-org.ezp.lib.cam.ac.uk/10.1017/9781108565103.

Zhang, W. & Yang, J., 2015. Forecasting natural gas consumption in China by Bayesian Model Averaging. *Energy Reports*, 1, pp.216–220. Available at: https://www.sciencedirect.com/science/article/pii/S2352484715000347.

Zhang, X. & Wang, F., 2017. Analysis of embodied carbon in the building life cycle considering the temporal perspectives of emissions: A case study in China. *Energy and Buildings*, 155, pp.404–413. Available at: http://dx.doi.org/10.1016/j.enbuild.2017.09.049.

Zhang, X. & Wang, F., 2016. Assessment of embodied carbon emissions for building construction in China: Comparative case studies using alternative methods. *Energy and Buildings*, 130, pp.330–340. Available at: http://dx.doi.org/10.1016/j.enbuild.2016.08.080.

Zhang, X. & Wang, F., 2015. Life-cycle assessment and control measures for carbon emissions of typical buildings in China. *Building and Environment*, 86, pp.89–97. Available at: http://dx.doi.org/10.1016/j.buildenv.2015.01.003.

Zhang, Y. et al., 2015. China's energy consumption in the building sector: A life cycle approach. *Energy and Buildings*, 94, pp.240–251. Available at: http://dx.doi.org/10.1016/j.enbuild.2015.03.011.

Zhang, Y. et al., 2019. Modelling of energy consumption and carbon emission from the building construction sector in China, a process-based LCA approach. *Energy Policy*, 134. Available at: https://doi.org/10.1016/j.enpol.2019.110949.

Zhao, P. et al., 2014. *Materials assessment and selection system for green buildings*, China

Building Materials Press.

Zhong, P., 2005. *Study of building life-cycle energy use and relevant environmental impacts [in Chinese]*. Sichuan University.

Zhou, N. et al., 2011. *China's Energy and Carbon Emissions Outlook to 2050*, Available at: https://china.lbl.gov/sites/all/files/lbl-4472e-energy-2050april-2011.pdf.

Zhou, N. et al., 2013. China's energy and emissions outlook to 2050: Perspectives from bottom-up energy end-use model. *Energy Policy*, 53, pp.51–62. Available at: http://www.sciencedirect.com/science/article/pii/S0301421512008476.

Zhou, N. et al., 2014. Cost-Effective Options for Transforming the Chinese Building Sector. In *ACEEE Summer Study on Energy Efficiency in Buildings*. The American Council for an Energy-Efficient Economy, pp. 367–377. Available at: http://aceee.org/files/proceedings/2014/data/papers/3-472.pdf.

Zhou, N. et al., 2007. *Energy Use in China: Sectoral Trends and Future Outlook*, Available at: https://china.lbl.gov/sites/all/files/lbl-61904-sectoral-energy-trendjan-2007.pdf.

Zhou, N. et al., 2016. Policy Roadmap to 50 % Energy Reduction in Chinese Buildings by 2050. In *ACEEE Summer Study on Energy Efficiency in Buildings*. Available at: http://aceee.org/files/proceedings/2016/data/papers/9_1132.pdf.

Zhou, N., Mcneil, M. & Levine, M., 2012. Assessment of building energy-saving policies and programs in China during the 11th Five-Year Plan. *Energy Efficiency*, 5(1), pp.51–64. Available at: https://link.springer.com/article/10.1007%2Fs12053-011-9111-0.

Zhou, S. et al., 2021. Research on low-carbon energy transformation of China necessary to achieve the Paris agreement goals: A global perspective. *Energy Economics*, 95. Available at: https://doi.org/10.1016/j.eneco.2021.105137.

Zhou, W. et al., 2019. Estimating lifetimes and stock turnover dynamics of urban residential buildings in China. *Sustainability (Switzerland)*, 11(13). Available at: https://doi.org/10.3390/su11133720.

Zhou, W. et al., 2020. Forecasting urban residential stock turnover dynamics using system dynamics and Bayesian model averaging. *Applied Energy*, 275. Available at: https://doi.org/10.1016/j.apenergy.2020.115388.

Zhu, W. et al., 2020. Analysis of the embodied carbon dioxide in the building sector: A case of China. *Journal of Cleaner Production*, 269. Available at: https://doi.org/10.1016/j.jclepro.2020.122438.

Zhu, W. et al., 2019. Assessing the effects of technological progress on energy efficiency in the construction industry: A case of China. *Journal of Cleaner Production*, 238. Available at: https://doi.org/10.1016/j.jclepro.2019.117908.